Fakultät für Medizin

III. Medizinische Klinik und Poliklinik - Hämatologische Forschung

The role of Wnt5a in hematopoiesis and leukemia

Christina Schreck

Vollständiger Abdruck der von der Fakultät für Medizin der Technischen Universität München zur Erlangung des akademischen Grades eines

Doktors der Naturwissenschaften (Dr. rer. nat.)

genehmigten Dissertation.

Vorsitzender: Univ.-Prof. Dr. J. Ruland

Prüfer der Dissertation:

1. apl. Prof. dr R. A. J. Oostendorp
2. Univ.-Prof. A. Schnieke, Ph.D.

Die Dissertation wurde am 26.06.2014 bei der Technischen Universität München eingereicht und durch die Fakultät für Medizin der Technischen Universität München am 19.11.2014 angenommen.

meiner Familie

Table of contents

1. Introduction

1.1. Hematopoietic development

1.1.1. Early hematopoiesis

During mouse ontogeny, hematopoiesis develops in several distinct anatomical environments. The first hematopoietic cells can be detected at embryonic day 7.5 (E7.5) in the yolk sac. At this early stage of development the hematopoietic cells are organized in “blood islands”, which also contain blood vessels. These blood vessels are believed to originate from primitive hemangioblasts, which are capable of producing both hematopoietic and endothelial cells. After the emergence of primitive hematopoiesis in the yolk sac, the circulation of the cells starts at embryonic day 8.5 (E8.5) [1]. The first definitive HSC that can regenerate hematopoiesis in adult recipients can be detected in the aorta-gonads-mesonephros (AGM) region from E10.5 [2]. More hematopoietic cells can be found at this stage of development in placenta, vitelline and umbilical arteries. After embryonic day 11.5 (E11.5), the fetal liver becomes a major hematopoietic organ. At this stage HSC self-renew to expand in numbers, but also undergo strong differentiation to increase the number of hematopoietic progenitors [3]. At embryonic day 16.5, HSCs start to migrate into bone marrow. Between three and four weeks after the birth, HSCs switch their active, proliferative cellular state to a more quiescent cellular state. Throughout adulthood, the main function of HSCs is to maintain hemostasis and to rapidly activate when environmental cues require a regenerative rersponse [4].

1.1.2. The adult mouse hematopoietic hierarchy

The adult HSC is determined by its ability to self-renew, proliferate and give rise to all blood cell types. As such, the HSCs are at the top of a hierarchical system in which each layer of progeny cells gains specific functions. Description and characterization of hematopoietic subsets of cells helps to understand the complex process of proliferation, differentiation as well as regeneration. The standard manner to follow this process of differentiation from HSCs throughout the hierarchy uses the technique of flow cytometry and fluorescently labelled monoclonal antibodies.

The earliest long-term repopulating (LT-)HSCs, are included in a population we designate as LSKs, which do not express markers of mature blood cells (lineage-negative (**L**in-)), but express both Lymphocyte antigen 6A-2/6E-1 (Ly-6A/E, **S**CA-1) and CD117 (**K**IT) (Figure 1) [5]. Furthermore, detailed studies have demonstrated that this population of cells does not express hematopoietic progenitor cell antigen CD34

[6], fetal liver kinase 2/Fms-like tyrosine kinase3 (FLK-2/FLT-3) [7] or CD48 antigen, but express signalling lymphocytic activation molecule CD150 and the endothelial protein C receptor (CD201) [5-10]. In addition, amongst the $CD34^-$ LSK cells only the $CD150^{high}$ cells have the potential of multilineage reconstitution in secondary recipient mice [11]. Thus, it is now possible to isolate single LT-HSCs ($CD34^-$ $CD48^-$ $CD135^-$ $CD150^{high}$ $CD201^+$ LSK) and interrogate their repopulating ability.

Single-cell transplantation studies have revealed that HSCs are not a homogenous population of cells, but demonstrated a remarkable heterogeneity amongst single HSCs. Several subtypes of HSCs were identified on the basis of engraftment patterns and kinetics, which distinguish between lymphoid deficient α-HSCs and balanced (lymphoid and myeloid biased) β-HSCs as well as self-renewal lacking, myeloid-deficient γ+δ-HSCs [12-13]. The exact lineage relations between these populations is, as yet, unresolved, but downstream in the hematopoietic hierarchy, progenitor cells are characterised by a gain of CD48 (SLAMF2), and CD34, and at the same time a functional loss of multipotency and commitment to only certain lineages can be observed. Committed hematopoietic cells progressively mature to lymphoid and myeloid lineages [14]. However, the hierarchic path from stem cell to mature blood cell is by no means linear. For instance, Yamamoto *et al*. found long term repopulating myeloid restricted progenitors within the phenotypically defined LT-HSC compartment [15]. In this thesis, the different HSCs and progenitor populations have been defined as shown in Figure 1.

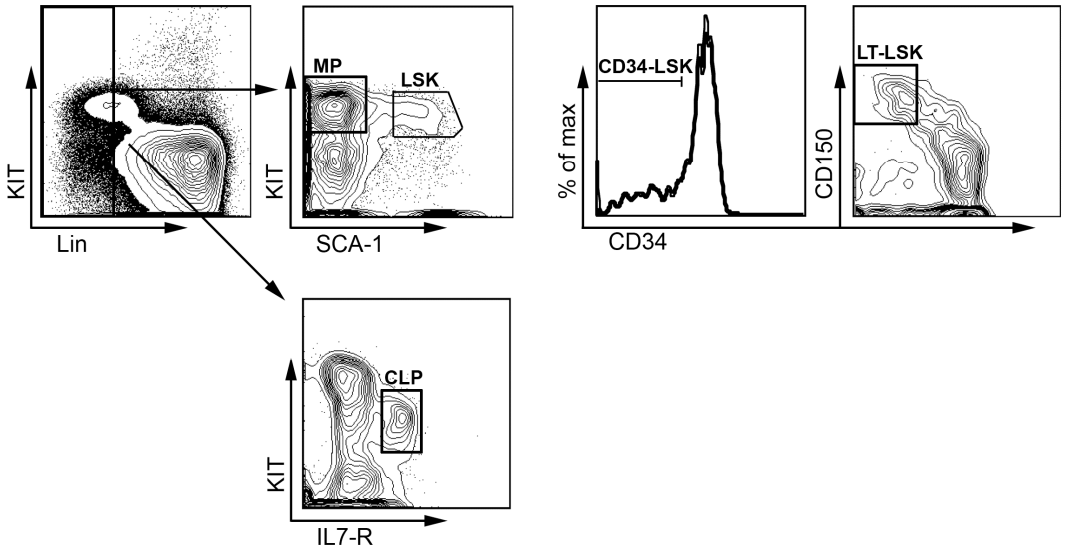

Figure 1. Flow cytometry to define subpopulations of early hematopoietic cells. This combined scheme with the cell markers described by the laboratories of I. Weissman and H. Nakauchi allows the dissection of the early cell types in the hematopoietic hierarchy [6, 16-18].

Taken together, the blood cell system is a hierarchical stem cell system, in which the HSC self-renews and/or differentiates. The changes of the composition of the hematopoietic hierarchy can be followed using combinations of cell surface markers, which make the blood cell system ideal for studying hierarchical stem cell systems.

1.2. The hematopoietic stem cell niche

Based on two decades of study on the Spleen colony-forming cells, Schofield proposed that stem cells were localized and regulated in an anatomical compartment, which he termed the “niche” [19]. This microenvironment regulates maintenance of HSCs and controls their self-renewal, survival, differentiation and proliferation [17, 20-22]. Many investigators currently describe two main types of niches: the endosteal niche, where HSCs reside close to osteoblasts (OBs) of trabecular bone and the vascular niche, where stem cells remain close to sinusoid endothelium [23-25]. Using real-time live imaging a small fraction of HSC was localized close to OBs in endosteal surface shortly after intravenous injection [26-27], demonstrating the endosteal niche as dominantly chemoattractive.

Several groups described cell types thought to be involved in niche formation, that are localized closer to the endosteal or vascular regions. **S**pindle-shaped **N**-cadherin$^+$ CD45$^-$ **o**steoblasts (SNO) [25], stromal cell-derived factor 1 (SDF-1, **C**XCL-12 **a**bundant **r**eticular cells (CAR) [28], **i**mmature early B-cell factor2$^+$ (**E**BF-2$^+$) **o**steoblasts (IEO) [29], leptin receptor (LEP-R$^+$) stromal cells [30] and Nestin$^+$ multipotent stroma cells [31], which interestingly all express the HSC attracting chemokine CXCL-12. Also, non-myelating Schwann cells [32] and subpopulations of mesenchymal cell types characterized by the expression of vascular cell adhesion protein 1 (VCAM-1) [33], platelet-derived growth factor subunit A receptor (PDGFRA) [34], activated leukocyte cell adhesion molecule (ALCAM, CD166) and SCA-1, Thy-1 membrane glycoprotein (THY-1, CD90), endoglin or Enpep [35] are suggested to play a role in regulation of HSCs. Nakamura *et al.* elucidated the influence of platelet endothelial cell adhesion molecule (PECAM-1, CD31), glycophorin A (TER-119), CD45, ALCAM and SCA-1: CD31$^-$/TER-119$^-$/CD45$^-$/ALCAM$^+$/SCA-1$^-$ mesenchymal stromal cells (MSC) reconstitute LT-status of HSCs by upregulation of homing and cytokine related genes (Figure 2). Osteoblasts expressing SCA-1 but not ALCAM were suggested to regulate HSCs over cell adhesion [36]. Chan *et al.* recently described three different subpopulations of stromal cells expressing THY-1, endoglin or Enpep. While *in vitro* THY-1$^+$ or endoglin$^+$ cells promote differentiation, Enpep$^+$ cells exhibited the potential to maintain HSC self-renewal [35]. Morikawa *et al.* isolated PDGFRA$^+$/SCA-1$^+$/CD45$^-$/TER-119$^-$ MSCs from murine bone marrow. Transplantation experiments exhibited

osteogenic and adipogenic differentiation potential and also differentiation into hematopoietic niche cells [34]. In Frenette`s group PDGFRA and CD51 were shown as markers of Nestin^{+} MSC in the human system [37].

Whether the endosteal and vascular niches are truly different still needs to be established. Despite the dominant chemotactic activity of the endosteal region, the majority of HSCs reside within the vascular niche [38]. In addition, OB-deficient mouse models did not show any changes in LTR-HSC G0/G1 state or function [39]. Also loss of N-cadherin, a molecule described specifically on endosteal cells, does not influence HSC maintenance and hematopoiesis [40]. Endothelial cells expressing CD31 are able to restore hematopoiesis after lethal irradiation and positively influence long-term reconstitution [41-42]. These findings show that both niche types function as niches for HSC maintenance. The initial view that the endosteal region preferably houses dormant cells, still holds true, since only endothelial cells of vascular niche express the adhesion molecule E-selectin and loss of E-selectin results in increased HSC quiescence. This points to the role of vascular niche in ensuring the regulation of proliferation and differentiation [40, 43-44]. Thus, cells isolated from both endosteal and vascular regions of the marrow may support LT-HSC activity in culture and localize to same areas as HSCs, and although it is well possible that different niche cells maintain different HSC subpopulations, this issue requires further investigation.

1.3. Niche-dependent signals which regulate hematopoiesis

Dormant HSCs remain quiescent and divide about five times per lifespan [4]. This population comprises the majority of multilineage long-term self-renewal activity. The dormant HSC is activated by response to bone marrow injury, such as that simulated by G-CSF activation and return to dormancy after re-establishment of homeostasis [4]. Other stimuli that activate dormant HSCs include IFNA [45] and As_2O_3 [46]. The several signalling molecules from the niche and HSC interact in order to keep or to re-establish homeostasis. One of the first niche factors described to influence HSC function, is stem cell factor (SCF), the ligand of Kit tyrosine kinase receptor. SCF is expressed in both membrane-bound as well as secreted forms of protein. Whereas SCF mutant mice ("steel" SI/SI^{d}mice) show niche-deficient maintenance of HSCs [47], the mutated kit signalling in Kit$^{W/Wv}$ mutant mice leads to the reduction of the number of functional HSCs [48-49]. By conditional deletion of SCF in different niche cells, it could be shown that HSCs get lost when SCF is deleted from both endothelial cells and leptin receptor-expressing perivascular stromal cells [30]. Another secreted factor with an established function in HSC regulation is the above-mentioned chemokine CXCL-12 that is expressed on stromal cells and guide HSCs to their niche in the bone marrow [50].

Mice deficient for *Cxcl-12* and its receptor C-X-C chemokine receptor type 4 (*Cxcr-4*) show defects in B-lymphopoiesis and myelopoiesis [51]; [52-53]. A similar phenotype could be found in HSCs of nuclear factor, erythroid derived 2, like 2 (*Nfe2l2, Nrf2*) knock-out mice. Recently, NRF2 was shown to bind directly to *Cxcr-4* promoter and activate its expression. By analyzing *Nrf2* knockout mice, Tsai *et al*, 2013 [54] showed that *Nrf2* deficient HSCs did not express CXCR-4, resulting in loss of self-renewal and hyperproliferation. Another molecule known to regulate expression of CXCR-4 is the serin/threonin kinase PIM-1. The *Pim1* knockout mice show no large defects in hematopoiesis [55], possibly due to remained low level expression of CXCR-4, which may possibly suffice to uphold HSC function.

Other studies have identified several apparently unconnected secreted factors, such as bone morphogenetic protein 4 (BMP-4) [56], Dickkopf-related protein 1 (Dkk-1) [57], pleiotrophin (PTN) [58], secreted frizzled-related protein 1 (sFRP-1) [59] and thrombopoietin (THPO) [60] as critical regulators of HSC behaviour by analyzing genetic models. In most of these models, the level of these proteins affects the proportion of HSCs residing in the G0 phase of the cell cycle. These studies confirm the view that the main function of secreted factors in the niche is to maintain HSCs in the G0 of the cell cycle.

In addition to these factors which maintain HSCs through extrinsic regulation, some niche-intrinsic mesenchymal factors have been uncovered, which are important for production of stromal signals required to maintain HSC quiescence, such as EBF-2 [29]. EBF-2 is the signalling mediator of SH2-domain-containing inositol 5'-phosphatase-1 (SHIP) [61] and the retinoblastoma protein (RB) [62]. In addition, while the ribonuclease type III DICER-1 [63] was shown to reduce the ability of the niche to maintain HSC, Moesin-ezrin-radixin-like protein/Neurofibromin-2 (MERLIN) was shown to promote the ability of the niche to maintain HSCs suggesting these factors are involved in managing the extrinsic regulation of HSC dormancy.

An additional class of mediators shown by several investigators to modulate HSC numbers and quality are members of Wnt signalling. The nuclear factor of activated T cells (NF-AT), which is involved in non-canonical Wnt signalling (further described below), was found to negatively regulate osteoblast differentiation and bone formation. OB-specific NF-AT activity mediates early B lymphopoiesis, possibly by regulating *Vcam1* expression on osteoblasts [64]. Moreover, the well characterized Wnt molecule Wnt5a is reported to function as mesenchymal regulatory factor by influencing recruitment, maintenance, and differentiation of MSCs and enhancing osteogenesis *ex vivo* [65]. The Wnt signalling pathway may form a possible interface in niche-mediated

regulation of normal and malignant hematopoiesis. In figure 2, an overview is given of the interplay between HSCs and niche molecules involved in HSC regulation.

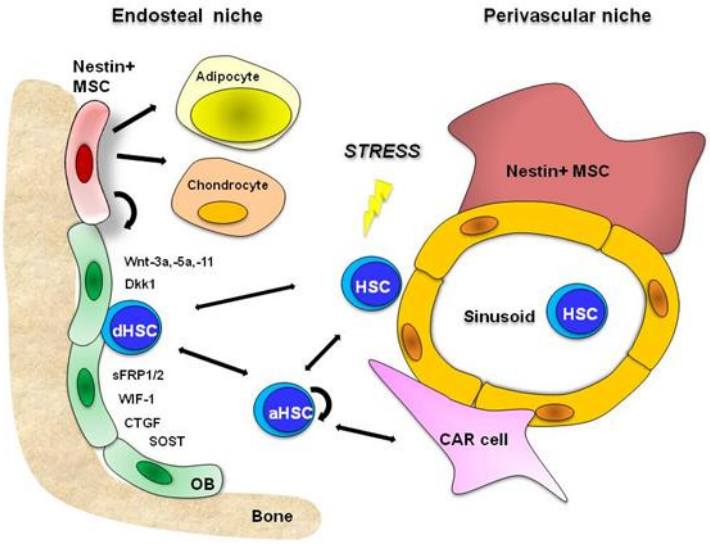

Figure 2. Members of Wnt signalling pathway in a model of endosteal and perivascular niche. Mesenchymal stem cells (MSCs) can differentiate into osteoblasts (OBs), adipocytes and chondrocytes. In endosteal region OBs and Nestin+ MSCs maintain HSCs in a dormant state (dHSC). Factors of Wnt signalling, including Wnt ligands Wnt3a, 5a, 11 and Wnt inhibitors Dkk-1, sFRP-1, -2, CTGF, SOST and WIF-1 regulate HSC quiescence. Dormant HSCs are activated (aHSC) by response to hematopoietic stress like wounding, infection, irradiation or leukemia. CAR cells are components of perivascular niche promoting self-renewal of active HSCs. Model adapted from Ehninger et al., 2011 [18, 66].

1.4. Wnt signalling

The Wnt genes encode a large family of secreted molecules, which are known to play an important role in embryonic development and transduce signals through their receptors, Frizzled and Dishevelled [67]; [68]. Wnt signalling was reported to be essential for blood cell production and plays also a role in HSC fate determinations. In culture systems it could be shown that Wnt proteins, like Wnt1, Wnt5a or Wnt10b can stimulate cell expansion [69-70]. Furthermore, its deregulation may promote the development of leukemia.

Wnt signalling is roughly separated into canonical and non-canonical pathways. The canonical pathway mainly signals through beta-catenin *via* activation of beta-catenin-transcription complex. Non-canonical Wnt signalling is diverse and involves calcium-dependent and -independent pathways as well as Rho-type GTPases, MAP kinases and nuclear factors like NF-AT. The non-canonical pathway in particular is involved in

shaping the niche architecture through its involvement in skeletogenesis and mesenchymal differentiation.

1.4.1. The canonical Wnt signalling

Some of the Wnt factors, such as Wnt1 and Wnt3a, are the most common canonical stimulators. In absence of canonical Wnt ligands, beta-catenin remains bound in a protein complex with Axin: the APC complex. Further, the complex contains the upstream protein kinase GSK-3 beta, which phosphorylates beta-catenin, thus rendering it susceptible for ubiquitination by the $SCF^{\beta TRCP}$ E3 ligase and subsequent proteasomal degradation. Binding of Wnt ligands to frizzled (Fz) receptors and its co-receptors low-density lipoprotein receptor-related protein 5 and 6 (LRP-5 and LRP-6) causes Dishevelled phosphorylation and disruption of the Axin complex. This allows the stabilization of catenin, as it is no longer phosphorylated by GSK-3 beta , and facilitates nuclear translocation of beta-catenin, which then binds to TCF/LEF transcription factors, resulting in transcriptional activation of several Wnt target genes including *Myc, osteopontin (Spp1), suppressor of cytokine signalling 2 (Socs2), P2Y purinoceptor 14 (P2ry14) and cyclin-D1 (Ccnd1)* [71], [72]. Canonical and/or non-canonical Wnt pathways might be activated by Wnts dependent on the receptor analog. Fz function can be involved in both Wnt pathways. There are ten mammalian Fz proteins that are seven-transmembrane (7TM) receptors and have large extracellular N-terminal cysteine-rich domains (CRD) [73]. Its hydrophobic binding surface interacts with a lipid on the Wnt ligands [74]. LRP5/6 is specifically required in canonical Wnt signalling by building a Wnt/Fz/LRP5/6 complex. However, some investigators suggest that LRP6 antagonizes non-canonical Wnt signalling *in vivo* by competing for Wnt ligands [75-76]. Recently, a new protein family has been linked to Wnt/canonical signalling activation and regulation. The R-spondin (Rspo1-4) proteins can also bind to LRP-6, and therefore, activate the beta-catenin-dependent pathway independent of Wnt-Frizzled interactions [77].

The involvement of the canonical Wnt signalling in hematopoiesis was investigated amongst others by Reya and her group [78], where they found, that overexpression of activated beta-catenin expands the pool of hematopoietic stem and progenitor cells and increases *in vivo* repopulation capacity over increased expression of HoxB4 and Notch1. However, conditional deletion of beta-catenin or both beta-catenin and γ-catenin does not affect HSCs [79-81]. The canonical signal Wnt3a was also found to be crucial for hematopoiesis and is highly expressed by hematopoietic cells. The homozygous mutants of *Wnt3a* lack caudal somites, have a disrupted notochord, fail to

form a tail bud and die prenatally around E12.5 [82]. The fetal liver of *Wnt3a* knockout embryos shows a reduced number of HSC and progenitor cells [83]. Furthermore, Wnt3a induces proliferation and inhibits differentiation in co-cultures of marrow cells only in the presence of stromal cells, indicating the requirement of niche cells in canonical Wnt signalling in hematopoiesis [67]. In addition, Fleming et al. could show that inhibition of beta-catenin dependent canonical Wnt signalling in osteoblasts leads to inhibition of Wnt signalling in HSCs, followed by increased cell cycling and decline in regenerative function after transplantation of HSCs [57].

1.4.2. The non-canonical Wnt signalling

Wnt5a and Wnt11 are the main activators of non-canonical Wnt pathways, which have been reported to be involved in diverse processes such as embryogenesis, cell movement, and cell division [84]. Perhaps the most basic role this pathway regulates is the planar cell polarity (PCP) pathway, which governs asymmetric cell division and asymmetric distribution of proteins within the cell. This pathway is stimulated through Fzd3, Fzd6, ROR2 and Dishevelled and downstream activation of Jun-N-terminal kinase (JNK), mitogen-activated protein kinase 8 (MAPK8) and small G proteins, like RAC and RHO, Rho GTPases CDC42 and the Rock1 RHO-associated kinase [84]. A second pathway activated through non-canonical Wnt signalling involves heterotrimeric GTP-binding proteins, which mobilize phospholipase C (PLC) and phosphodiesterase (PDE), and a further release of Ca^{2+} cations from intracellular sources. Besides the frizzled receptors, ROR1/2 receptors can also bind some Wnt factors and activate non-canonical signalling through release of Ca^{2+}. Calcium release activates Calcium/calmodulin-dependent kinase-II (CaMK-II) and protein kinase C (PKC). This pathway diverges and can activate the aforementioned NF-AT-pathway, or the TAK1/NLK pathway which both lead to transcriptional activation. NLK was shown to negatively regulate beta-catenin dependant wnt signalling over phosphorylation of TCF/LEF, inhibiting the binding of beta-catenin/TCF/LEF complex to DNA for transcriptional activation of its target genes [85] [86] or in neurons, overexpression of NLK suppressed the beta-catenin/LEF binding [87].

1.4.3. The Wingless-type MMTV integration site family member (*Wnt5a*)

Wingless-type MMTV integration site family, member 5a (***Wnt5a***) has a molecular weight of ~45kDa. Human Wnt5a maps to chromosome 3, while mouse Wnt5a is located on chromosome 14. It is now known that *Wnt5a* is conserved in a wide range of species from Caenorhabditis elegans to humans [88]. Wnt5a was first isolated from

E9.5 fetal cDNA as Gavin and coworkers [89] searched for novel Wnt-1-related genes with a developmental role. The group designated four novel Wnt clones Wnt4, Wnt5a, Wnt6 and Wnt7a that all contained a single, long open reading frame with conservation of all cysteine residues, a noticeable feature of the Wnt family. *Wnt5a* transcripts were detected throughout the embryo at several distinct sites of accumulation, including the CNS, the limb, facial processes and the posterior region of the fetus. In adult mice, Wnt5a is expressed in brain at a very low level, as well as in lung, kidney heart and Spleen [89].

In general, Wnt proteins have a highly conserved distribution of cysteine residues. The proteins are post-translationally palmitoylated on a conserved cysteine and palmitoylation enhances the hydrophobicity of the protein and contributes to their membrane association. As a consequence of the resulting insolubility, it is difficult to isolate Wnt proteins in an active form. Enzymatic removal of the palmitate or mutations of the modified cysteine resulted in loss of activity, indicating the importance of the lipid for signalling [90-91].

Wnt5a as a secreted molecule can be purified from conditioned medium and is glycosylated. Although the types of glycans are still unclear, possible glycosylation sites might be Asn114, Asn120, Asn311 and Asn325 [92]. The state of glycosylation is important for secretion of Wnt5a. Additionally, it is known, that Wnt5a protein is modified with palmitate at Cys104, which is necessary for its binding to the receptor [88, 93]. Wnt5a as secreted molecule has various receptors. Wnt5a signalling is mediated by binding to several Fz receptors (Fz2, Fz3, Fz4, Fz5, Fz6, Fz7, Fz8, Fmi) [88]. In hematopoiesis, it was shown that Flamingo (Fmi) and Frizzled 8 (Fz8) are overexpressed in long-term HSCs (LT-HSCs) compared to short-term HSCs (ST-HSCs) [94]. Recently, ROR2 tyrosine kinase receptor and the putative pseudokinase RYK[95], that belong to the receptor tyrosine kinases (RTK) family have been shown to bind to Wnt5a. Signalling through these receptors antagonizes canonical Wnt/beta-catenin signalling [96], probably through stimulation of the calcium-dependent signalling. Thus in hematopoiesis, inhibition of RYK, blocked the ability of Wnt5a to induce HSC quiescence and enhance short-term and long-term hematopoietic repopulation [97].

In cell culture systems, one has thought long that HSCs could only be maintained in direct contact with stromal cells. We found that secretion of Wnt5a by stromal cells enables HSC maintenance and removes this requirement of direct HSC-stromal cell contact [98]. In addition, we recently showed that Wnt5a triggers Ca^{2+} influx in the cytoplasm and activates the calcium-sensitive transcription factor NF-ATc in these cells

over CaMK-II signalling. This finding indicates that HSCs can respond to environmental Wnt5a [99]. Though, the precise mode of the action of Wnt5a has not been elucidated. In 1999, Yamaguchi and co-workers, created *Wnt5a*-deficient mice by functionally inactivating Wnt5a by disrupting the gene in exon 2, at codon 31 of the Wnt5a protein. The homozygous loss of *Wnt5a* led to perinatal lethality. The homozygotes showed gross morphological defects in outgrowing tissues: truncated snout, mandibles and tung, a shortened A-P axis and a loss of the tail [100]. First experiments with *Wnt5a* conditional knockout mice showed that Wnt5a is required for crypt regeneration after injury in mice [101].

In hematopoiesis, in contrast to canonical ligands Wnt3a and Wnt10b that are only expressed in HSCs, Wnt5a is expressed in both hematopoietic and niche cells, where Wnt5a is particularly highly expressed in stromal cells [69, 102] and in osteoblast-lineage cells [103]. Evidence from literature reports indicated that Wnt5a and its receptor ROR2 in particular are key players in HSC-niche regulation. For instance, it was shown that Wnt5a-ROR2 signalling is relevant for the balance between OB-lineage cells and bone-remodelling osteoclast precursors: if non-canonical Wnt signalling is active, osteoclastogenesis is enhanced [103]. Nemeth and coworkers showed that highly enriched HSCs cultured with SCF, FLT-3L and Wnt5a could engraft significantly better than cells cultured without Wnt5a [104]. Furthermore, as stated above, we identified Wnt5a as the soluble factor in co-culture of human HSCs with the EL08-1D2 stromal cell line responsible for the maintenance of true long-term repopulating HSCs in non-contact cultures [98].

Due to the complexity of parallel pathways in non-canonical Wnt-signalling, the precise mechanisms of action are still unclear. Interestingly, there appears to be cross-talk between the CXCL-12-stimulated CXCR-4 signalling and non-canonical Wnt signals, since it has been found in T cells that Wnt5a and protein kinase C signals are required for CXCL-12-mediated homing of T cells to their niche [105]. Also in a collaborative study performed as part of this thesis, we recently showed that although Wnt5a expression is hardly detected in LT-HSCs of 10 weeks old mice, it is upregulated during aging and its expression may in part be responsible for the poor engraftment ability of aged stem cells [106]. In addition, it was shown that cell division control protein 42 (CDC42) activity determines polarized expression of surface proteins in aged LT-HSCs, and we were able to show that Wnt5a is responsible for stem cell aging through increasing CDC42 activity and regulating cellular polarity [107].

1.4.4. Wnt inhibitors

The Wnt signalling pathway includes a complex network of Wnt-inhibitors which fine-tune responses to Wnts. The inhibitors may bind the Wnt-mediators themselves (secreted frizzled-related proteins (sFRPs), dickkopf homologues (Dkks)), others may disrupt the assembly of the Frizzled signalosome (Kremen, connective tissue growth factor (CTGF), and Sclerostin (SOST)). Depending on the context of Frizzled (Fz) receptors, some “inhibitors”, like sFRP-1, may directly bind to Fz and modulate Wnt signalling in that way [108].

The secreted frizzled-related proteins **sFRP-1** and **sFRP-2** directly bind Wnt-molecules and, thus, regulate the interaction of Wnts with both canonical and non-canonical Fz receptors [109]. *Sfrp1* and *Sfrp2* double mutants have been shown to activate the non-canonical Wnt/PCP pathway in embryonic stem cells and interestingly the phenotype of these double mutants is closely related to phenotype of *Wnt5a*$^{-/-}$ mice [110]. Although the redundancy of sFRP-1 and sFRP-2 was demonstrated during mouse embryogenesis [111-113], it seems not to persist in adult hematogenesis. Nakajima *et al.* revealed the expression of sFRP-1 and sFRP-2 in osteoblasts and their differential regulation of HSC homeostasis. For sFRP-1 our group previously showed, that sFRP-1 is required for HSC self-renewal and HSC maintenance in an extrinsic manner [59]. Number and potentially altered function of hematopoietic cells in *Sfrp2* knockout mice have not been published so far, but sFRP-2 is highly secreted by mineralized osteoblasts in endosteal niche [114] [115] and is suggested to inhibit differentiation of HSC by enhancing self renewal [116]. Stimulation of LT-HSC with sFRP-2 *in vitro* results in an increased HSC engraftment in serial transplantation experiments in contrast to sFRP-1 lending support to the idea the functions of sFRP-1 and sFRP-2 in steady state hematopoiesis or under stress conditions may not be redundant [116].

Dkk-1, a member of the Dickkopf (Dkk) family of Wnt inhibitors, binds to the Wnt co-receptor LRP-5/6 in combination with a Kremen receptor leading to the internalization of the complex. While *Dkk1* is expressed in LT-HSCs [59], it is also expressed in osteoblasts and can extrinsically influence Wnt signalling through the microenvironment and consequently regulate HSC number and regenerative function after transplantation [57] [117-118].

WIF-1, a member of Wnt inhibitory factor (WIF) family proteins that bind to Wnt ligands directly and consequently block both canonical and non-canonical Wnt signalling, like sFRP-1 [119]. In contrast to sFRP-1, WIF-1 is lacking a cystein-rich domain and NTR domain resulting in disability in binding to frizzled receptors [120]. Schaniel *et al.*[121] analysed *Col2.3-Wif1* transgenic (*Wif*1Tg) mice in which *Wif1* is overexpressed in

osteoblasts. While there is no effect in bone architecture, the percentages of LT-HSC are increased.

1.5. The role of the niche in leukemogenesis

Malignant transformed leukemic stem cells (LSCs) share many of the characteristics with normal HSC, but in contrast, LSCs from many types of leukemia show defective differentiation [122]. Several examples are now known, in which it has been shown that leukemic cells alter niche function and *vice versa*.

Here, two different mechanisms are highlighted by which the niche may be involved in leukemia development and maintenance. Recently, Lutzny et al. demonstrated that chronic lymphatic leukemic (CLL) cells “hijack” the niche and alter its function. In CLL, a direct cell-cell interaction induces strong changes in stromal cell gene and protein expression, such as expression of protein kinase C beta type II (*PkcbII*/ PKC-BII). The expression of this PKC isoform improves CLL cell survival through stromal nuclear factor NF-kappa-B signalling, showing that leukemia-induced alterations in stromal cell signalling may promote survival of leukemic cells [123].

Another example of a leukemia-modulated and possibly “hijacked” niche was demonstrated in a mouse model of BCR/ABL- and nuclear core complex 98 / homeobox protein-A9 (Nup98/HoxA9) -positive AML, in which the number and function of OB and osteoprogenitors was severely decreased. In BCR/ABL transgenic mice, which display myeloproliferative neoplasia (MPN), OBs are displaced from the niche to the marrow cavity and increased in number. The osteoblastic cells were shown to be remodelled to leukemic LSC-supporting myelofibrotic cells with decreased osteogenic markers such as Col-1a1, VCAM-1, and integrin alpha 11 and an increase in inflammatory molecules [124].

However, primary alterations in the niche, which may cause secondary proliferative disorder, can lead to malignant transformation as well. The first example of such a niche-dependent defect was reported in *Ikba*$^{-/-}$ *(Nfkba*$^{-/-}$*)* mice, where a myeloproliferative disease developed with increasing Notch signalling in myelocytes [125]. Similar niche-dependant proliferative diseases were found in mice deficient in E3 ubiquitin-protein ligase *Mib1,* retinoblastoma associated protein *Rb1* and retinoic acid receptor gamma *Rarg* [126]. Interestingly, in recently published pre-osteoblast-specific knockout of the ribonuclease *Dicer1,* in a small number of cases myelodysplasia progresses into leukemic development. In addition, pre-osteoblastic knockout of the *Sbds* gene, which is down-regulated in Dicer-1-lacking stromal cells, shows very similar

features, demonstrating that primary disruption of molecules required to maintain HSC quiescence, increase the chance of malignant transformation [63].

These studies show that malignant alterations in hematopoietic cells may modulate niche cells to promote hematopoietic malignancy, and *vice versa*: alterations in niche cells promote the emergence of malignant cells. We and others have shown that dysregulation of Wnt signalling in the niche impairs HSC function [57, 59]. Furthermore, in AML, the Wnt/beta-catenin pathway seems to be required for LSC self-renewal. Moreover, HoxA9/Meis1 fusion oncogene was shown to reactivate Wnt/beta-catenin pathway in GMP, resulting in AML [127]. CML is characterized by a chronic phase and a blast crisis. Beta-catenin is required for the progression from the chronic phase into blast crisis [128]. In addition, like in experimentally HoxA9/Meis1-induced AML, activation of beta-catenin also contributes to malignant transformation of GMP in CML [129]. It is however unknown through which mechanisms beta-catenin-signalling is upregulated in (pre-) malignant cells. One mechanism to activate Wnt signals would be down-regulation of Wnt inhibitors that are expressed in niche and in HSCs [59]. Indeed, promoter regions of Wnt antagonists are frequently methylated and inactive in cancer cells. In MDS, promoter methylation of the *Sfrp* and *Dkk* families has been proposed to be prognostic markers of progression into AML [130]. In CLL, *Dkk1*, *Sfrp1* and Cadherin-1 (*Cdh1*) are the most heavily methylated and, thus, silenced genes [131-132]. In AML, 61% of patients show aberrant Wnt inhibitor promoter hypermethylation. Interestingly, the type of oncogenic fusion gene expressed was associated with silencing of distinct inhibitors: *Dkk1* hypermethylation correlated with putative polycomb group protein ASXL1 mutations and *Sfrp1* hypermethylation was associated with Runx1/Runx1T1 (AML1-ETO, t(8:21)) [133] of which it is a direct repressional target [134]. Thus, myelodysplastic and leukemic cells show a general epigenetic silencing of Wnt inhibitor expression. In these diseases, it has so far not been established whether silencing of Wnt inhibitors contributes to upregulation of canonical Wnt signalling. In addition, the expression of inhibitors in the leukemic niche has, so far, not been investigated and, since upregulated beta-catenin expression improves the ability of niche cells to maintain HSCs [135], it would be of interest, whether the presence of leukemic cells alters expression of Wnt antagonists in niche cells.

Parts of this introduction have already been published [18].

1.6. Aim of this study and overview of the experimental approach

The overview of the literature shows that in studies aimed at understanding regulatory mechanisms of the blood cell system, most knowledge has accumulated about the blood cells themselves. However, environmental non-hematopoietic cells which regulate HSC dormancy, self-renewal, and possibly also HSC differentiation are largely unexplored.

There are several methods to investigate the role of communication between the HSCs and their niche. Considering that Wnt5a is overexpressed in stromal cells maintaining HSCs [98] and that it has been described to inhibit HSC expansion [104], we decided to study mice with modified expression of Wnt5a: heterozygous *Wnt5a* knockout mice (*Wnt5a*$^{+/-}$)[100]. Using such mouse models, one can analyse the influence of one single signal from the hematopoietic cells and their niche. Also of importance, genetic models allow the study of steady-state hematopoiesis. All other techniques to investigate hematopoiesis and HSCs *in vivo* (transplantation, 5-FU, BrdU, etc.) are associated with stress signalling. By transplantation assay one can additionally test the self-renewal and differentiation potential of HSCs *in vivo*. Signals regulating self-renewal and differentiation are delivered by a combination of HSC intrinsic signals and extrinsic signals from the microenvironment, which consists of stromal cells, endothelial cells and the hematopoietic cells. Dysregulation of either HSC intrinsic or extrinsic microenvironmental signals may ultimately result in leukemia [62]. In order to study the effect of the microenvironment on HSC behaviour, more than 100 cell lines were generated from murine midgestion embryonic tissues [136]. In former studies, two embryo-derived stromal cell lines: UG26-1B6 and EL08-1D2 were generated, which maintain HSCs in culture [136-137]. UG26-1B6 stromal cell line was able to maintain HSCs without direct contact [115], whereas EL08-1D2 stromal cells were only able to maintain HSCs in non-contact co-culture experiments, if HSCs were highly purified. This finding suggests that EL08-1D2 may expand mature cell types, which decrease HSC maintenance. In comparisons between the two supportive cell lines, gene expression analysis [138] revealed Wnt5a as soluble factor, which is underrepresented in EL08-1D2, when compared to UG26-1B6 cell line. In fact, co-culture experiments showed that EL08-1D2 did not maintain repopulating HSCs in the Lin$^-$ population, whereas, addition of Wnt5a could rescue the maintenance of HSCs in co-culture of EL08-1D2 [98].

Until now, HSCs have not been characterized and analysed in mice deficient in Wnt5a expression, so far. In hematopoiesis, Wnt5a is expressed in both fetal liver and bone marrow cells, especially in B220$^+$ B cells, and was reported to upregulate B cell

proliferation in a cell-autonomous manner and has been proposed to have oncogenic function [139]. Wnt5a is mainly expressed in stromal cells [69, 102], particularly in cells of the osteogenic lineage and also, at very low levels, in LT-HSCs [99]. Recently it was shown that Wnt5a-ROR2 signalling is relevant for the balance between OB-lineage cells and osteoclast precursors. If Wnt5a/ROR2-stimulated non-canonical Wnt signalling is active, osteoclastogenesis is enhanced [103]. Thus, Wnt5a might be important for the interactions between HSCs and their niche with regard to maintenance and proliferation.

Prior to this thesis, Nemeth *et al.* showed that highly enriched HSCs cultured with SCF, FLT-3L and Wnt5a could engraft significantly better than cells cultured without Wnt5a [104]. Furthermore, Wnt5a was detected as the soluble factor in co-culture of human HSCs with the EL08-1D2 stromal cell line in non-contact cultures, which is responsible for the maintenance of true long-term repopulating HSCs [98]. Interestingly, there appears to be cross-talk between the CXCL-12-stimulated CXCR-4 signalling and non-canonical Wnt signals, since it has been found in T cells that Wnt5a and protein kinase C signals are required for CXCL-12-mediated homing of T cells to their niche [105].

The available literature reports suggest a critical role of the non-canonical Wnt regulator Wnt5a in microenviromental control of HSCs. Nevertheless, the influence of Wnt5a expressed by the microenvironment on HSCs has not yet been investigated *in vivo*.

The aim of the thesis was therefore to analyse the effects of decreased levels of Wnt5a in the bone marrow niche on HSC function and maintenance *in vivo*, as well as analysing underlying molecular pathways, particularly the balance between canonical and non-canonical signalling. Furthermore, since the role of niche alterations in leukemogenesis is becoming increasingly clear, we wanted to explore the role of Wnt5a signalling in the niche during leukemogenesis and its influence on leukemic stem cells. Additionally, we want to further characterize the role of Wnt5a in shaping the niche cell compartment itself in steady state hematopoiesis and leukemia.

In order to reach these goals, we analysed *Wnt5a* heterozygous knockout mice, created by Dr. Yamaguchi *et al.* in 1999 [100], mentioned above, in case of hematopoiesis and leukemia. We investigated the involvement of Wnt5a *in vivo* on HSC maintenance under steady-state conditions, intrinsically (in the HSCs) and extrinsically (through external microenvironmental signals), by transplantation assays and analysed the development of leukemic stem cells in a *Wnt5a*-deficient microenvironment.

2. Materials

2.1. General material

Table 1: Materials

Materials	Manufacturers
Blood lancets Supra	megro GmbH & Co KG, Wesel, Germany
Cell Culture Flasks Cellstar125 ml/250 ml/550 ml	Greiner Bio-One GmbH, Frickenhausen, Germany
Cell Culture Dish, 10 mm, growth enhanced treated	Corning Inc., Corning, U.S.A.
Cell Culture Dish, 10 cm, growth-enhanced treated	TPP Techno Plastic Products AG, Trasadlingen, Schweiz
Cell Culture Plates Cellstar 6/12/24/48/96 Well	Greiner Bio-One GmbH, Frickenhausen, Germany
Cryogenic vial, 2 ml	Corning Inc., Corning, U.S.A.
Disposable bags	Carl Roth, Karlsruhe, Germany
Disposable UV cuvettes	Brand GmbH & Co KG, Wertheim, Germany
Filter Vacuum driven disposable bottle top filter Steritop	Millipore Co., Billerica, U.S.A.
Filters 0.45/30/70/100 µl	BD FalconTM, BD Biosciences, Heidelberg, Germany
Filter tips TipOne 10/100/200/1000 µl	Starlab, Hamburg, Germany
Hamilton Syringe; Gastight; 1710	Hamilton, Bonaduz, Switzerland
Hamilton Needle; 6/pk	Hamilton, Bonaduz, Switzerland
MACS LS cell separation columns	Miltenyi Biotec, Bergisch Gladbach, Germany
MicroAmp® Fast 96-Well Reaction Plate with Barcode	Applied Biosystems, Foster City, U.S.A.
Microcentrifuge safe-lock tubes, 1.5/2 ml	Eppendorf AG, Hamburg, Germany
Monoject, blunt cannula needles	Kendall Healthcare, Mansfield, U.S.A.
Needles, 100 Sterican, 27 Gauge	B. Braun Melsungen AG, Melsungen, Germany
Petri dish with vants 10 mm	Greiner Bio-One GmbH, Frickenhausen, Germany
Poly-L-lysine-coated glass slides	Thermo Fisher Scientific Inc., Waltham, U.S.A.
Polypropylene centrifuge tubes 15/50 ml	Greiner Bio-One GmbH, Frickenhausen, Germany
Serological Pipets	BD FalconTM, BD Biosciences, Heidelberg, Germany
S-Monovette Blood Collection System	Sarstedt AG & Co., Nümbrecht, Germany

Syringes, U-40 Insulin, Omnifix, 1 ml	B. Braun Melsungen AG, Melsungen, Germany
Syringes with Needle, Sub-Q, 1 ml	BD, Franklin Lakes, U.S.A.
Syringes single-use omnifix 3/5/10/20/30 ml	B. Braun Melsungen AG, Melsungen, Germany

2.2. Instruments and Equipment

Table 2: Instruments and equipment

Type of device	Name	Manufacturer
Animal Blood Counter	Counter Scil Vet AbcTM	Scil vet academy, Viernheim, Germany
Cell incubator	Hera Cell 240	Heraeus Instruments, Hanau, Germany
Cell sorter	MoFlo High Speed	Beckman Coulter, US
Centrifuge	Megafuge 3.0 RS, Multifuge 3S	Heraeus Instruments, Hanau, Germany
Counting chamber	Neubauer-improved	Paul Marienfeld GmbH, Lauda Königshofen, Germany
Flow cytometer	CyAn ADP LxP8	Beckman Coulter Inc., U.S.A.
Fluorescent microscope	Leica DM RBE	Leica, Wetzlar, Germany
Ice machine	S.-No:061244	Ziegra Eismaschinen, Isernhagen, Germany
Laminar flow hood	ANTAES 48/72	BIOHIT, Germany
Linear accelerator	Mevatron KD2	Siemens, Erlangen, Germany
Microscope	Axiovert 25	Carl Zeiss, Jena, Germany
NanoDrop	ND-1000 UV/Vis-spectrophotometer	NanoDrop Technologies, Wilmington, DE, U.S.A.
Precision scales	PLJ 2100-2M	Kern & Sohn GmbH, Balingen, Germany
QuadroMACS Separator	MACS	Miltenyi Biotec, Bergisch Gladbach, Germany
Real-Time PCR System	StepOne	Applied Biosystems, Foster City, U.S.A.
Spectrophotometer	SmartSpec Plus	Bio-Rad, Philadelphia, U.S.A.
Thermal Cycler	PTC 100 Peltier	Bio-Rad, Philadelphia, U.S.A.
Thermomixer	comfort	Eppendorf AG, Hamburg, Germany
Vortex	IKA MS1 minishaker	Werke & Co., Staufen im Breisgau, Germany
Water bath	SUB	Grant Instruments Ltd.,

		Cambridgeshire, UK
Radiation Unit	Gulmay	Gulmay, Suwanee, U.S.A

2.3. Chemical and biological reagents

Table 3: reagents

Reagents	Manufacturer
Agar	Sigma-Aldrich, Taufkirchen, Germany
Albumin Fraction V; ≥98%, bovine (BSA)	Carl Roth, Karlsruhe, Germany
Ampicillin	Sigma-Aldrich, Taufkirchen, Germany
Baytril (Enrofloxacin); 2,5%	Bayer AG, Leverkusen, Germany
Ciprofloxacin	Fresenius Kabi, Bad Homburg, Germany
Collagenase Type 1	Worthington Biochemical Corp, Lakewood, NY, U.S.A
Dimethyl sulfoxid (DMSO)	SERVA Electrophoresis GmbH, Heidelberg, Germany
Ethanol, 99,8%	AppliChem, Darmstadt, Germany
Ethidium bromide, 1% solution	Carl Roth, Karlsruhe, Germany
Fetal calf serum (FCS)	PAA, Cölbe, Germany
Formalin solution 10%	Sigma-Aldrich, Taufkirchen, Germany
Gelatin	Sigma-Aldrich, Taufkirchen, Germany
HBSS	Invitrogen, Darmstadt, Germany
HEPES	Invitrogen, Darmstadt, Germany
Horse serum (HS)	BioWhittaker, Vallensbaek, Denmark
Isolfluran 100%	Abbott Laboratories, Abbott Park, Illinois, U.S.A.
Isopropanol	Sigma-Aldrich, Taufkirchen, Germany
Lipofectamine 2000	Invitrogen, Darmstadt, Germany
mIL3, mIL6, mSCF	R&D Systems, Wiesbaden, Germany
Penicillin/Streptomycin	Invitrogen, Darmstadt, Germany

Peptone	Carl Roth, Karlsruhe, Germany
Polybrene	Sigma-Aldrich, Taufkirchen, Germany
Propidium-Jodid (PI)	Invitrogen, Darmstadt, Germany
Triton X-100	Carl Roth, Karlsruhe, Germany
Trypan blue	Invitrogen, Darmstadt, Germany
Trypsin 10x	Invitrogen, Darmstadt, Germany
Türk`s solution	Merck KGaA, Darmstadt, Germany
UltraPure DNase/RNase-Free Distilled Water	Invitrogen, Darmstadt, Germany
β-Mercapto-ethanol	Invitrogen, Darmstadt, Germany
5-FU, 5-Fluoruracil	Ribosepharm, Munich, Germany

2.4. Buffers and media

Table 4: Home-made buffers, solutions and media

Name	Ingredients
FACS buffer (500 ml)	500 ml DPBS 0.5% BSA
Gelatin solution (1%, 500 ml)	5 g Gelatin powder 500 ml deionized H_2O
HF2+ buffer (100 ml)	100 ml HBSS (10x) 20 ml FCS 10 ml HEPES 10 ml Penicillin/Streptomycin 860 ml deionized H_2O
CLM (cell loading medium)	50 ml HBSS 500 µl FCS 1 mM $CaCl_2$ 1 nM $MgCl_2$
BBMM	325 ml IMDM (1x)

	150 ml FCS 25 ml BSA 5 ml L-Glutamin 2.5 Penicillin/Streptomycin (100x) 1 ml β-Mercaptoethanol (50mM)
Blocking buffer for Immunofluorescence	1 ml FCS 30 µl Triton-X 30 ml PBS
LB medium	6 g Peptone 3 g Yeast extract 1.5 g NaCl Ampicillin (50 µg/ml) 300 ml deionized H_2O
Long term culture medium (500 ml)	400 ml Alpha MEM 75 ml FCS 25 ml Horse Serum (HS) Inositol (1:1000) Folic acid (1:1000) 5 ml Penicillin/Streptomycin 100 µl β-Mercaptoethanol
Phoenix Eco culture medium	500 ml DMEM 50 ml FCS
Stroma medium (500 ml)	400 ml α-MEM 75 ml FCS 25 ml Horse Serum (HS)
MSC medium (500 ml)	444,5 ml α-MEM 50 ml FCS 5 ml Penicillin/Streptomycin (1:100) 0.5 ml β-Mercaptoethanol (1:1000)

Adipogenic induction medium	α-MEM plus GlutaMAX Human recombinant insulin (10 µg/ml) 3-isobutyl-1-methylxanthine (IBMX) (0.5mM) Dexamethasone (1 µM) 20% FCS Ciprobay antibiotic (1:200)
Adipogenic maintenance medium	α-MEM plus GlutaMAX Human recombinant insulin (10 µg/ml) 20% FCS Ciprobay antibiotic (1:200)
Oil Red O Stock solution	0.5 g Oil Red O 100 ml Isopropanol
Osteogenic differentiation media	α-MEM plus GlutaMAX Ascorbic acid-2-phosphat (0.05 mM) β-glycerolphosphat (10 mM) Dexamethasone (100 nM) Human recombinant insulin (10 µg/ml) 20% heat-inactivated FCS Ciprobay antibiotic (1:200)
Silver Nitrate solution	1 g $AgNO_3$ 20 ml deionized H_2O.
Sodium Carbonate solution	5 g Na_2CO_3 200 µl Formaldehyde (37%) 100 ml deionized H_2O

Table 5: Commercial buffers and media

Name	Ingredients
ACK Lysing buffer	Invitrogen, Darmstadt, Germany
α-MEM	Invitrogen, Darmstadt, Germany

DMEM	Invitrogen, Darmstadt, Germany
Dulbecco´s PBS (DPBS)	PAA, Cölbe, Germany
MethoCult M3434	Stemcell Technologies, Vancouver, Canada
Opti-MEM	Invitrogen, Darmstadt, Germany
0.5% Trypsin-EDTA (10x)	Invitrogen, Darmstadt, Germany

Table 6: Kits

Name	Ingredients
APC/Fitc BrdU Flow Kit	BD Pharmingen, San Diego, CA, U.S.A.
Lineage cell depletion kit	Miltenyi Biotec, Bergisch Gladbach, Germany
Power SYBR Green PCR Master Mix	Applied Biosystems, Foster City, CA, U.S.A.
QuantiTect Reverse Transcription Kit	Quiagen Inc, Hilden, Germany
RNeasy Micro Kit	Quiagen Inc, Hilden, Germany
DNA extraction Kit	Quiagen Inc, Hilden, Germany
MaxiPrep Kit	Quiagen Inc, Hilden, Germany

2.5. Antibodies

Table 7: Primary antibodies for Flow cytometry

Antigen	Clone	Fluorochrome	Volume/ $1*10^6$ cells	Manufacturer
CD4	GK1.5	PE-Cy5	1 µl	ebioscience, San Diego, CA, U.S.A.
CD8a	53-6.7	PE-Cy5	1 µl	ebioscience, San Diego, CA, U.S.A.
CD11b	M1/70	APC-eFluor®780	1 µl	ebioscience, San Diego, CA, U.S.A.
CD16/32	93	PE	1 µl	ebioscience, San Diego, CA, U.S.A.
CD34	RAM34	FITC; eFluor®647	2 µl	ebioscience, San Diego, CA, U.S.A.
CD45.1	A20	PE; FITC; eFluor450®	1 µl	ebioscience, San Diego, CA, U.S.A.
CD45.2	104	FITC; PE	1 µl	ebioscience, San Diego, CA, U.S.A.

Cd45r (B220)	RA3-6B2	PE-Cy7	1 µl	ebioscience, San Diego, CA, U.S.A.
CD117 (KIT)	2B8	PE; APC	3 µl	ebioscience, San Diego, CA, U.S.A.
CD127 (IL7-R)	A7R34	APC; PE	2 µl	ebioscience, San Diego, CA, U.S.A.
CD150	9D1	APC; PE	2 µl	ebioscience, San Diego, CA, U.S.A.
Gr-1(Ly-6G)	RB6-8C5	eFluor450®	1 µl	ebioscience, San Diego, CA, U.S.A.
SCA-1	D7	PE-Cy7	3 µl	ebioscience, San Diego, CA, U.S.A.
TER119	TER-119	eFluor450®	1 µl	ebioscience, San Diego, CA, U.S.A.
CD31	390	APC; FITC	2 µl	ebioscience, San Diego, CA, U.S.A. BD Pharmingen, San Diego, CA, U.S.A.
CD51	RMV-7	PE	2 µl	ebioscience, San Diego, CA, U.S.A.
ALCAM	eBioAlc 48	PE	2 µl	ebioscience, San Diego, CA, U.S.A.
Biotinylated anti-mouse Gr-1(Ly-6G)	RB6-8C5		0.2 µl	ebioscience, San Diego, CA, U.S.A.
Biotinylated anti-mouse B220	RA3-6B2		0.2 µl	ebioscience, San Diego, CA, U.S.A.
Biotinylated anti-mouse CD3e	145-2C11		0.2 µl	ebioscience, San Diego, CA, U.S.A.
Biotinylated anti-mouse TER-119	TER-119		0.2 µl	ebioscience, San Diego, CA, U.S.A.
Biotinylated anti-mouse CD11b	M1/70		0.2 µl	ebioscience, San Diego, CA, U.S.A.

Table 8: Secondary antibodies for Flow cytometry

Reagent	Conjugate	Volume/1*10^6 cells	Manufacturer
Streptavidin	eFluor450®; PE-Cy5.5	0.5µl	Invitrogen, Darmstadt, Germany

Table 9: Antibodies for Immunofluorescence (IF)

Product	Species	Dilution	Manufacturer
Anti-Cyclin-D1	rabbit	1:25	Cell Sign. Techn., U.S.A.
Anti-phospho-Smad2 (Ser465/467)/Smad3 (Ser423/425)	rabbit	1:200	Cell Sign. Techn., U.S.A.
Anti-beta-catenin	rabbit	1:100	Cell Sign. Techn., U.S.A.
Anti-phospho-beta-catenin (Ser33/37/Thr41)	rabbit	1:100	Cell Sign. Techn., U.S.A.
Anti-GSK-3 beta (Ser9)	rabbit	1:200	Cell Sign. Techn., U.S.A.
Anti-Fbxw7	rabbit	1:200	Aviva Systems Biology, Corp., San Diego, CA, U.S.A.
Anti-phospho-GSK-3 beta (Ser9)	rabbit	1:200	Cell Sign. Techn., U.S.A.
Anti-CaMK-II	rabbit	1:200	Cell Sign. Techn., U.S.A.
Anti-Phospho-CaMK-II (Thr286)	rabbit	1:200	Cell Sign. Techn., U.S.A.
Anti-C/EBPα	rabbit	1:200	Cell Sign. Techn., U.S.A.
Anti-ROR2	rabbit	1:200	Cell Sign. Techn., U.S.A.
Anti-PLCβ3	rabbit	1:200	Cell Sign. Techn., U.S.A.
Anti-DVL2	rabbit	1:200	Cell Sign. Techn., U.S.A.
Anti-NF-ATc1	mouse	1:50	Santa Cruz Biotechnology, Inc., U.S.A.
Anti-NLK	rabbit	1:50	Santa Cruz Biotechnology, Inc., U.S.A.
Anti-PU.1	rabbit	1:200	Cell Sign. Techn., U.S.A.
Anti-GATA-1	rabbit	1:200	Cell Sign. Techn., U.S.A.
Anti-PPARγ	rabbit	1:200	Cell Sign. Techn., U.S.A.
Anti-p53	rabbit	1:50	Santa Cruz Biotechnology, Inc., U.S.A.

Table 10: Secondary antibodies for Immunofluorescence

Reagent	Species	Manufacturer
AlexaFluor®488	rabbit	Invitrogen, Darmstadt, Germany
Anti-Alexa Fluor®488	rabbit	Invitrogen, Darmstadt, Germany
Alexa Fluor®488	goat	Invitrogen, Darmstadt, Germany
AlexaFluor®546	goat	Invitrogen, Darmstadt, Germany

2.6. Primers for PCR and qRT-PCR

Table 11: Primers for qRT-PCR (SYBR Green-based detection) and PCR

Name	Sequence (5'-3')
Gorasp2-F	CACTGGGTTCCCTGTACCAC
Gorasp2-R	GATGCGACTCACAGAGACCA
Rpl13a-F	CCCTCCACCCTATGACAAGA
Rpl13a-R	TTCTCCTCCAGAGTGGCTGT
Rpl39-F	ATTCCTCCGCCATCGTGCGCG
Rpl39-R	TCCGGATCCACTGAGGAATAGGGCG
qPCR Wnt5a-F2	AGGAGTTCGTGGACGCTAGA
qPCR Wnt5a-R2	GCCGCGCTATCATACTTCTC
mWnt5aWT-F	GAGGAGAAGCGCAGTCAATC
mWnt5aWT-R	CATCTCAACAAGGGCCTCAT
mWnt5amut-F	GCCAGAGGCCACTTGTGTAG

2.7. Expression Vectors

Table 12: Expression Vectors for leukemia assays

Name	laboratory
MIG	Kindly provided by Bubnoff group [140]
pMIG-p185(BCR/ABL)	Kindly provided by Bubnoff group [140]

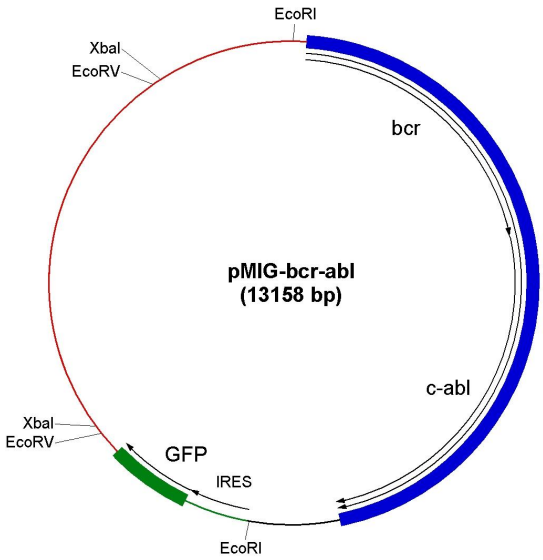

Figure 3. Vector map of pMIGp185 BCR/ABL plasmid. The MIG vector is derived from murine stem cell virus (MSCV) and contains the genes encoding the green fluorescent protein (GFP), Ampicillin resistance (AMP), internal ribosomal entry side (IRES) and the fusion oncogene p185 BCR/ABL [140]; The control vector MIG contains GFP, AMP and IRES;

2.8. Cell line

Table 13: Retroviral cell line

Name	Factory
Phoenix™ ecotropic helper-free retroviral producer cells	G Nolan, Stanford, USA

2.9. Mice

Table 14: Mice strains

Name	Factory
C57BL/6.J	Harlan Laboratories, Rossdorf, Germany
129S2/SvHsd	Harlan Laboratories, Rossdorf, Germany
B6;129S7-Wnt5atm1Amc/J mice	The Jackson Laboratory, Maine, USA
B6;129S2-Wnt5atm1Amc/J mice	The Jackson Laboratory, Maine, USA (backcrossed)
B6/SJL (Ly5.1)	Taconic Europe, Ry, Denmark
129S2 × C57BL/6.J	Breeding in Zentrum für Präklinische Forschung (ZPF)
129S2 × Ly5.1	Breeding in Zentrum für Präklinische Forschung (ZPF)

Mice were kept in microisolators under SPF conditions according to FELASA recommendations in ZPF.

3. Methods

3.1. Mice and Genotyping

Wnt5a$^{+/-}$ mice were bred on a 129 × C57BL/6.J (129B6) background [100]. The mice were constantly backcrossed to 129 x C57BL/6 for all experiments. Age- and sex-matched *Wnt5a* $^{+/+}$ (WT) littermate mice were used as controls in all experiments. Mice were kept in microisolators under SPF conditions according to FELASA recommendations. *Wnt5a* heterozygous (HE) and wild type (WT) mice were distinguished from one another by means of the polymerase chain reaction (PCR) (Figure 4). Either small pieces of the ear (from ear clipping) or the tail were used as samples. The tissue samples were incubated over night in lysis buffer (100 mM Tris/HCl), 1 % Tween 20, with freshly added 200 µg/ml Proteinase K at 50 °C with constantly shaking in order to decompose the tissue. The next day, the Proteinase K was inactivated by incubation of the samples at 95 °C for 5 min. After that, the samples were centrifuged at 15 000 g for 2 min and the supernatant or purified DNA was used for PCR analysis. DNA purification was performed with DNA extraction Kit following manufacturers' descriptions.

PCR Mastermix:

10 µl peqGOLD PCR Master Mix Y

1 µl Primer: mWnt5aWT-F

1 µl Primer: mWnt5aWT-R

1 µl Primer: mWnt5amut-F

1 µl DMSO

0.5 µl $MgCl_2$

0.5 µl gDNA template

5 µl H_2O

20 µl final volume

The samples were run in a PTC 100 Peltier Thermal Cycler

Program:

94 °C	3 min		
94 °C	30 s	}	35 cycles
51.7 °C	1 min		
72 °C	1 min		
72 °C	2 min		
4 °C	hold		

5 µl of loading buffer (30 % glycerol with Orange G) were added to the samples. After loading the samples on a 1.5 % agarose gel made with NaB buffer (0.01 M di-sodium tetraborate) and ethidium bromide (0.5 µg/ml), the gel was run with 180 V and analysed with BioRad Gel-Doc XR Imaging System.

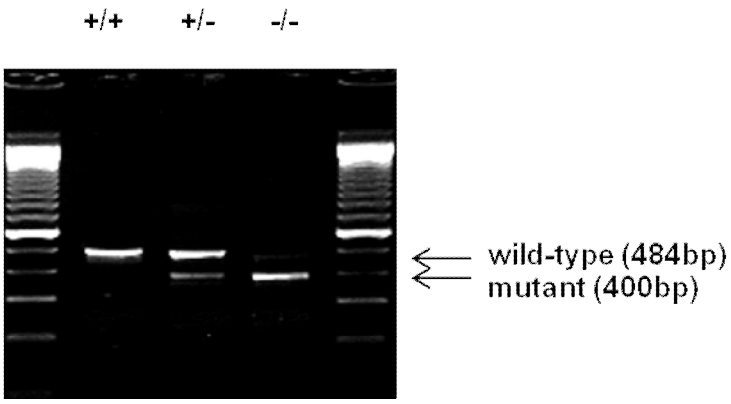

Figure 4. Genotyping of *Wnt5a* knockout mice. Mouse DNA loaded on a 1.5% agarose gel. 100bp ladder was used to distinguish the size of the bands. WT DNA shows a 484bp fragment, *Wnt5a*$^{-/-}$ DNA shows a 400bp mutant band and *Wnt5a*$^{+/-}$ DNA displays both bands.

3.2. Preparation of murine tissues

In this project, we studied murine aorta-gonad-mesonephros region (AGM), fetal liver (FL), bone marrow (BM), stromal niche cells, Spleen (Sp) and peripheral blood (PB).

To obtain embryonic tissues for the analysis of hematopoietic cells or culturing primary stroma, adult male mice were bred with two females in the late afternoon. On the following morning the females were checked for the presence of a vaginal plug. The time point of plug existence was considered as embryonic day 0 (E0). Pregnant females were sacrificed on E 10.5 for isolation of AGM and on E14.5 for isolation of fetal liver. The uteri were removed and by using fine forceps and scissors, the embryo

was transferred out of the uterus into culture dishes containing HF2+ buffer. The dissection needles were used to cut the trunk of the embryo from the tail and head. The tail was needed for genotyping. The ventral dermis was removed and the liver could be dissected cleanly and transferred to culture dishes containing HF2+ buffer at 4 °C. For AGM isolation, the somites and neural tube, located along the dorsal side of the embryo, were removed without injuring the dorsal aorta. Then, the trunk of the embryo was turned, so that the ventral side is facing upwards and the AGM region is visible. By setting the needles under the AGM region, remaining somites were removed. AGM region was further transferred to 6 well dishes, cut with scalpel and cultured in stroma medium to receive primary AGM stroma for co-cultures with hematopoietic cells. Fetal liver was squeezed and subsequently filtered through 70 µm cell strainer, digested with DNase and further analysed for hematopoietic cell population by flow cytometry.

For the BM analysis, the four long bones (femurs and tibia) of both hind legs were dissected and BM was flushed with a total of 10 ml HF2+ buffer. The cell suspension was homogenized, filtered through a 30 µm filter and used for analysis.

For stromal niche cell isolation, flushed four long bones were crushed with mortar and pestle. Bone chips were washed once in HF2+ buffer to release the loosely adherent BM cells and several times in PBS until the chips were white. Endosteal stromal cells were released from the hematopoietic-depleted bone chips by digestion with 3 mg/ml type I collagenase and 15 µg/ml DNAse dissolved in PBS for 1 hour at 37 °C at 110 rpm. This stromal fraction was used in all subsequent analyses of endosteal populations.

For the analysis of Spleen, the organs were squeezed and subsequently filtered through a 70 µm filter, homogenized, again filtered through a 30 µm filter and used for analysis.

Peripheral blood was obtained by punctuating the facial vein (mouse: during experiment) or was directly sampled from the heart (mouse: end of experiment). The blood was collected in EDTA-coated vials. Blood samples were mixed with 5 ml ACK lysing buffer and incubated on ice for 15 min, in order to lyse erythrocytes. The samples were centrifuged at 500 g for 5 min and the pellet was resuspended in HF2+ buffer.

3.3. Flow cytometry staining

For staining of surface markers, the cells were resuspended in 100 µl staining buffer with primary antibodies. For whole bone marrow stains, we generally used $2x10^6$ for mature population stains, and $6x10^6$ for staining of progenitors and HSCs. Used antibodies are listed in Table 7. The cells were incubated with the antibodies for 15 min at 4 °C and after that, washed with staining buffer. In some staining, a secondary antibody was added (diluted in staining buffer, see Table 8). Finally the stained cells were resuspendend in staining buffer with 1 µg/ml propidium iodide and analysed on CyAn ADP Lx P8.

For sorting of several cell populations, the cells were stained as described above, and sorted on MoFlo High Speed cell sorter.

3.4. Calcium flux

Lin^- $SCA\text{-}1^+$ KIT^+ (LSK) cells were sorted out of ten pooled 10-week-old male C57BL/6 mice. The sorted cells were suspended in 1 ml Cell Loading Medium (CLM) in a 15-ml tube. The cells were loaded with indo-1 AM (Molecular Probes I-1203, final concentration 0.25 µM) for 45 min at 37 °C in the dark. After loading, the cells were washed twice with CLM. The indo-1 cells were then resuspended in 1 ml CLM again and stored in the dark at room temperature for 1 h. Before flow cytometric analysis, the cells were equilibrated at 37 °C in the dark for 30 min. The cells were analysed by flow cytometry. An aliquot of the untreated cells was run to establish the baseline fluorescence of the indo-1-loaded cells. In one sample, ionomycin was used as positive control for Ca^{2+} release (1 µg/ml final concentration). After a few minutes a calcium chelator, EGTA, was added during acquisition, and served as negative (Ca^{2+} low) control (8 mM final concentration). The response to Wnt5a was measured by adding murine recombinant Wnt5a to a final concentration of 300 ng, 1 min after start of the measurement. Seven minutes after the first Wnt5a addition, a second, higher concentration of Wnt5a was added (700 ng/ml). To determine the calcium response to addition of Wnt5a, indo-1-loaded LSKs were analysed relative to a time parameter, and the change in fluorescence ratio over time can be related to changes in activation or stimulation by some agonist that will elicit a calcium influx. For visualization of this influx, the change in ratio of indo-1-bound Ca^{2+} (420 nm) and free indo-1 (510 nm) was depicted against the time after start of the measurement.

3.5. Immunocytofluorescence staining

For Immunocytofluorescence staining, LSK, MP, CLP and B-cell populations were sorted out of four pooled 8-10-week-old male mice per experiment and a total of 500 - 1000 cells were spotted on poly L-Lysin coated slides. After incubation for 30 min at 4°C, the cells were fixed with 4% paraformaldehyde for 5 min and subsequently blocked with blocking buffer for 30 min at room temperature. Cells were stained overnight at 4° C in humid chamber with primary antibody diluted in blocking buffer. The next day, the cells were washed with blocking buffer and stained overnight at 4 °C in humid chamber with secondary antibody. After this step, the cells were washed twice with blocking buffer and once with PBS. The cells were counterstained with SlowFadeGold with DAPI (4.6-diamino-2-phenylindole dihydrochloride) at room temperature. After one week desiccation at room temperature in the dark, the fluorescence was measured. Fluorescence digital images were taken using constant settings on a Leica DM RBE fluorescent microscope using AxioVision software (Carl Zeiss). For each particular sample, images at 100 fold magnification of 30 to 40 randomly captured cells were taken. Fluorescence digital images were then analysed using the digital image processing software ImageJ (NIH). The mean fluorescence intensity (average intensity of pixels per cell) was determined. Background correction was performed by determining the signal intensity of the pixels around the perimeter of the area being quantified. These background signals were then subtracted from specific signals caused by antibody staining. To compare measurements from separate experiments, they were additionally normalized to the mean of a set of control samples and expressed as fold changes in relation to the control samples. For comparison of means of different groups, a two-tailed *t*-test assuming equal variances was used. A *P* value less than 0.05 was considered to be statistically significant.

3.6. Colony forming assay

Colony forming assay is a functional cellular assay to quantify multi-potential progenitors and lineage-restricted progenitors of the erythroid (BFU-E), granulocytic, monocyte-macrophage, and megakaryocyte-myelopoietic pathways (CFU-GM and CFU-GEMM) as well as a subset of mouse pre-B lymphoid cells. When cultured in a suitable semi-solid matrix, individual progenitors, called colony-forming cells (CFCs), proliferate to form discrete cell clusters or colonies. This assay shows that on a clonal level. For colony forming assay, BM cells ($2.5x10^4$) or co-cultures initiated with $1x10^4$ Lin- cells were cultivated in methylcellulose on 3.5 mm dishes for ten days at 37 ° and

5% CO_2. Colonies formed, were distinguished into *GM, GEMM and BFU-E*, and counted under the microscope (Figure 5).

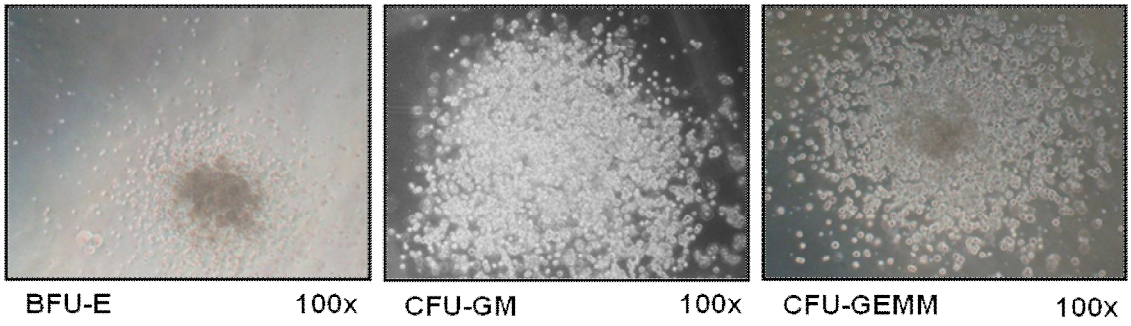

Figure 5. Colony-forming cells: Examples of colonies. Erythroid (BFU-E), granulocytic, monocyte-macrophage, and megakaryocyte-myelopoietic cells (CFU-GM and CFU-GEMM).

3.7. Gene expression analysis

In order to detect gene expression in hematopoietic tissues, analysis from different hematopoietic cell populations was performed. We isolated the following cell populations: LSKs, MPs, CLPs, B-cells, T-cells, granulocytes and monocytes using cell sorting. UG26-1B6 stroma cell line was used as murine stromal tissue. The cells were sorted into HF2+ buffer and the RNA was either directly isolated or the cell pellet was frozen at -80 °C.

RNA isolation was performed using the RNeasy Mini Kit according to the manufacturer´s instructions. Sorted cell population were pelleted and resuspended in RLT buffer containing guanidine-thiocyanate lysing the cells and inactivating RNases. Subsequently the samples were homogenized by QIAshredder spin columns. The homogenized samples were mixed with ethanol to optimize binding conditions and loaded on RNeasy Mini spin columns where the RNA binds to the silica-based membrane. Contaminants were washed away by the use of the wash buffers RW1 and RPE and finally, the total RNA was eluted under low-salt conditions.

Subsequent reverse transcription was carried out. RNA was transcribed to cDNA by the use of the QuantiTect Reverse Transcription Kit:

12 µl H_20 + 1 µg RNA

2 µl gDNA Wipeout Buffer, 7x

The mixture was incubated for 2 min at 42 °C.

1 µl Quantiscript Reverse Transcriptase

4 µl Quantiscript RT Buffer, 5x

1 µl RT Primer Mix

The mixture was incubated for 15 min at 42 °C, followed by 3 min at 95 °C.

The cDNA was stored at -20 °C or real time PCR (RT-PCR) was carried out.

Real time PCR was used to determine the expression levels of *Wnt5a* in hematopoietic cell population. Real time PCR allows monitoring the progress of PCR as it occurs and can therefore detect and quantify cDNA. In this study, the SYBR Green system was used to detect PCR products. The samples were diluted after reverse transcription (Stroma 1:8; mature hematopoietic cells 1:6, stem and progenitor cells 1:4). In order to examine the optimal conditions, a mixture of the different stromal cell lines was used as standard. The standards were serially diluted and used for every primer to determine the amplification rate per cycle. Gorasp2 [141] and Rpl13a [142] were used as housekeeping genes for normalization.

10 µl Power SYBR Green PCR Master Mix

1 µl Primer (forward and reverse each 10 µM)

1 µl template

8 µl H_2O

The RT-PCR was operated on Applied Biosystem Step One Plus Real-Time PCR System.

Program:

50 °C 2 min

95 °C 5 min

95 °C 15 s
58 °C 20 s } 40 cycles
72 °C 30 s

3.8. Co-cultures of Lin- cells with primary AGM stroma

Lineage-depleted bone marrow cells (Lin^-) were co-cultured with 30 Gy irradiated confluently (80 %) grown aorta-gonade-mesonephros (AGM) stromal cells. The lineage negative fraction (Lin^-) was negatively selected from flushed bone marrow according to the manufacturers' instructions. In brief, bone marrow cells were first incubated with a mixture of primary biotinylated antibodies against CD3, B220, CD11b, Gr-1 and

TER119 and subsequently with streptavidin-conjugated magnetic Micro Beads. The labelled cells were run through columns in a magnetic field. Cells coated with Micro Beads were restrained in the column, the Lin^-, unlabelled cells, run through the column. 10000 Lin^- cells were plated on the confluent and irradiated stromal cells in a 3 cm dish. The cells were cultured in stroma medium for one and for two weeks and CFU assay was carried out like described in Chapter 3.5.

3.9. MSC differentiation

To test whether sorted mesenchymal populations show the capacity for multipotent differentiation *in vitro*, cultured non-hematopoietic cell populations were tested for their ability to differentiate into mesenchymal lineages. For this reason the endosteum-associated BM stromal cells were sorted for MSCs (TER119/CD45/$CD31^-$/$SCA\text{-}1^+$), and OBCs (TER119/CD45/$CD31^-$/$ALCAM^+$/$SCA\text{-}1^-$) from whole BM mixed up with BM from collagenase-treated crushed bones of *Wnt5a*$^{+/-}$ mice and their WT littermates (Figure 6). In previous work [143-145] three main differentiation pathways of the mesenchymal cells are determined *in vitro* and *in vivo*. *In vitro*, MSCs should have the potential to differentiate into adipogenic, chondrogenic and osteogenic lineage.

In this thesis the differentiation potential of mouse BM-MSCs was tested. We looked for differences in adipogenic and osteogenic differentiation potential of *Wnt5a*$^{+/-}$ BM-MSCs and their WT littermate BM-MSCs. Differentiation was induced after the MSCs have grown to a confluent monolayer. OBCs were cultured and spontaneous differentiation was monitored.

Adipogenic differentiation

Adipogenic differentiation was performed following the protocol of Pittenger *et al*. [145]. The adipogenic differentiation procedure consists of a cycled process by changing induction medium with maintenance medium. When cells were a confluent monolayer, the cell culture medium was removed and replaced by induction medium. After three days, the induction medium was removed and replaced by maintenance medium for two days. This process was repeated three times. Finally, the cells were incubated for one week in maintenance media.

Histological detection of adipogenic differentiation

After 20 days (three times induction/maintenance), adipogenic differentiation is visible by expansion of the cytoplasmatic lumen and appearance of fatty vesicles of different

sizes. For coloration of the lipid vesicles, Oil Red O staining was performed. Oil Red O is incorporated in the fatty vesicles and appears red.

To prepare Oil Red O staining solution, six parts of Oil Red O stock solution were diluted with four parts distilled water. The solution should be mixed well and incubated for 24 h at room temperature. The next day, prior using, the solution was filtered to remove unsolved particles.

After removing the maintenance medium, the MSCs were washed carefully with 1xPBS and fixed with 2% paraformaldehyd (PFA) in 1xPBS for 30 min at 4 °C. After fixation, PFA was discarded and the cells were incubated with Oil Red O staining solution for 30 min at room temperature. Finally, the cells were washed several times with distilled water. The staining is stable for a few days.

Osteogenic differentiation

Osteogenic differentiated cells will change their morphological appearance into cuboidal phenotype and will deposit calcium, which can be detected by staining of mineralized osteogenic membrane. To detect this calcium deposition, the von Kossa procedure was used. The induction of the osteogenic differentiation was performed as described at Jaiswal *et al.* [146].

After formation of a confluent monolayer culture, MSC culture medium was replaced by osteogenic differentiation medium and renewed every third day for a total of three weeks. Calcium accumulations will appear which are visible as dense brown-coloured areas in the culture. The mineralized matrix of osteogenic differentiated cells was visualized by von Kossa staining.

Histological detection of osteogenic differentiated cells with von Kossa staining

Calcium deposits at the membrane of osteogenic differentiated cells can be detected by von Kossa staining. Here, calcium salts (phosphate, carbonate) of the mineralized matrix are revealed by substitution to metallic cations from silver nitrate. The silver nitrate is visualized after reduction to metallic silver (black). This black staining indicates the mineralization of the bone matrix.

After removing the medium, the MSCs were washed carefully with 1xPBS and fixed with ice-cold methanol for 20 min at 4 °C. After fixation, the cells were washed, covered with silver nitrate and incubated for 30 min at room temperature in the dark. The silver nitrate was binding to the calcium and marked the osteogenic differentiated cells. The reaction was stopped by washing several times with 1xPBS after removing the silver nitrate. Finally, sodium carbonate was added. After 5-10 min, the silver nitrate was

reduced and black staining appeared. The cells were stored in distilled water for photography.

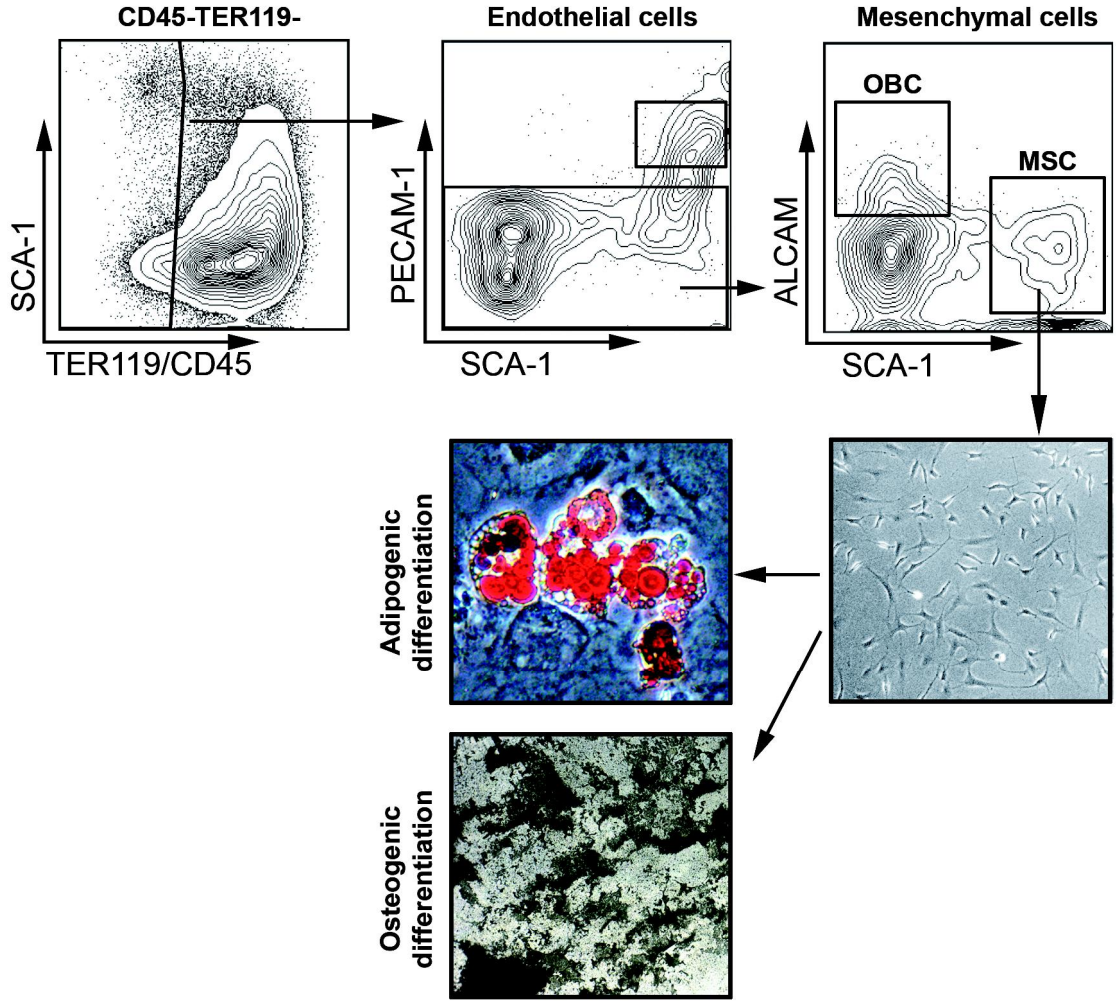

Figure 6. BM niche components. (A) Representative FACS profile of ALCAM and SCA-1 expression in CD45$^-$ CD31$^-$ TER119$^-$ cells in BM cells mixed with the bone-associated fraction (cells isolated from bone fragments using collagenase treatment). CD45$^-$ TER119$^-$ cells were gated and characterized as endothelial cells by CD31 expression; OBCs are characterized as CD31$^-$ SCA-1$^-$ ALCAM$^+$ cells, and MSCs as CD31$^-$ SCA-1$^+$ ALCAM^{med} cells [36]. MSCs were sorted, cultured and adipogenic and osteogenic differentiation was induced [18].

3.10. Transplantation assay

Since regeneration of tissues *in vivo* is one of the required properties of somatic stem cells, transplantation assays are required to determine donor-derived blood cell regeneration and for studying HSC function *in vivo* in mice. Deficiencies and other alterations in HSC function can be detected and quantified using this assay. Throughout this thesis, the CD45 congenic system (CD45.1 and CD45.2) was used to distinguish donor-derived cells from recipient cells.

Adult transplantation assay was used for intrinsic/extrinsic transplantations: eight-to ten-week- old lethally irradiated recipient mice (9 Gy) received donor cells via intravenous injection in the tail vain (i.v.).

Newborn transplantation assay were used for primary extrinsic transplantation assays (Chapter 4.6.) and leukemic approaches (Chapter 4.7.) instead of adult mice of the mouse strain B6;129S2-Wnt5atm1Amc/J. These adult mice died after lethal irradiation and following BM transplantation, because of *staphylococcus* infection. The newborn pups of the same mouse strain, survived irradiation and consequent BM transplantation.

The newborn pubs can be transplanted right after birth (P1), until the fourth day after birth (P4) for transplantation assay. The pubs were carefully separated from the parents for irradiation. P1 to P4 pups were irradiated with 4.5 Gy and got donor cells via intra-hepatic (i.h.) injection. Hamilton syringes were used to inject the cells in a final volume of 20 µl into the fetal liver of the embryo. The newborn mice were carefully put back in the mothers' cage and received antibiotics (1mg/ml Borgal) via the mothers' milk for a total of three weeks.

Also adult mice received 1 mg/ml Borgal for three weeks after transplantation through the drinking water. Peripheral blood was analysed five and ten weeks after transplantation by flow cytometry. 16 weeks after transplantation, mice were sacrificed and BM, Spleen, and peripheral blood (PB) were analysed by flow cytometry. Sorted BM cells were also used as donor cells for further transplantations. Mice were counted positive with ≥ 1 % myeloid and 1 % lymphoid donor engraftment.

In leukemia models, $1x10^5$ GFP^+ BM cells, expressing BCR/ABL oncogene, were injected into newborn pups. GFP expression system was used to detect injected oncogene-expressing cells. Mice were sacrificed when severe disease pattern was discovered.

3.11. Homing assay

The homing assay was carried out in order to investigate the ability of HSC to migrate to and enter their niche in the BM *in vivo*. This microenvironment regulates maintenance of HSCs and controls their self-renewal, survival, differentiation and proliferation [17, 20-22]. In the following assay, the role of Wnt5a in the BM niche was investigated in terms of homing of BM cells.

In Chapter 4.6.2., for steady-state homing assay, 1.25x10^6 Lin^- Ly5.1/Ly5.2 BM cells were injected into lethally irradiated *Wnt5a*$^{+/-}$ recipients and their WT littermates (Ly5.2). For extrinsic homing assay, WT cells that migrated to WT and *Wnt5a*$^{+/-}$ microenvironment in primary transplantation, were sorted out after 16 weeks and 1000 LSKs together with 30 000 MP cells were injected (i.v.) into secondary WT (C57BL/6.J) recipients. In leukemic homing approaches, we injected 800 000 BCR/ABL expressing 5-FU treated BM cells into WT and *Wnt5a*$^{+/-}$ mice.

After 16 h the mice were sacrificed and the BM harvested. The homing ability of the WT cells was measured by analysing the BM engraftment by flow cytometry.

3.12. Phoenix helper-free retrovirus producer cell line cultivation

The cell line is based on the 293T cell line (a human embryonic kidney line transformed with adenovirus E1a and carrying a temperature sensitive T antigen co-selected with neomycin). The phoenix cell line was created by placing constructs capable of producing gag-pol and envelope proteins for ecotropic viruses into 293T cells. The cell line is highly transfectable. Prior to transfection, phoenix cells were selected with selective medium (DMEM +10% FCS+ 0.3 mg/ml hygromycinB and 2 µg/ml diphtheria toxin). The gag-pol introduction can be selected by hygromycin selection, the envelope introduction by diphtheria toxin selection. Daily, supernatant was discarded (removing dead cells) and cells were maintained in a concentration of 0.5-1 x10^6 cells per ml fresh selective medium. Selection was continued until no more cells died due to gag-pol env deficiency (5-6 days). After that passage zero (p0) phoenix cells were rescued with phoenix medium (DMEM + 10% FCS), maintained in a concentration of 0.5-1 x10^6 cells/ml and expanded to p5 to p10 which are the appropriate passages for transfection.

3.13. Retroviral transfection with p185 (BCR/ABL) and infection of BM cells

To isolate high quantities of plasmid DNA competent Escherichia coli bacteria were transformed by heat-shock with MIG empty vector control and MIG-p185BCR/ABL vector [140] containing an ampicillin resistance gene (Amp) and a gene encoding green fluorescence protein (GFP) cultured 16 h in liquid LB-medium with 100 µg/ml ampicillin. After that, Maxiprep was performed following manufacturer's instructions.

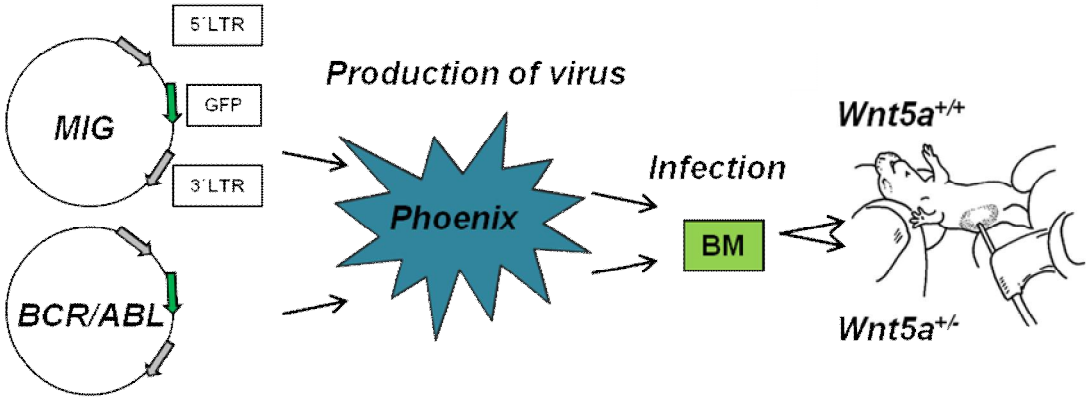

Figure 7. Experimental set-up.

Phoenix ecotropic helper-free retroviral producer cells were grown in Phoenix medium. Retroviruses were generated by transient transfection of Phoenix producer cells with p185BCR/ABL and MIG control retroviral construct using Lipofectamine 2000 according to the manufacturer's recommendations. Transfection efficiency of Phoenix cells was tested by flow cytometry analysis for GFP-expression.

Bone marrow infection, transplantation and animal studies

Bone marrow cells from male B6 donor mice were collected 4 days after treatment with 150 mg/kg 5-FU. Cells were suspended in BBMM containing growth factors (rmIL-3 10 ng/ml, rmIL-6 10 ng/ml, rmSCF 50 ng/ml) and prestimulated for 24 h. BM cells were transduced with viral supernatants by spin infection four times every 12 h (90 min, 32°C, 2400 rpm). The cells were harvested 12 h after the last spin infection, washed with PBS, resuspended in HF2+ buffer and MIG-BCR/ABL infected cells were tested for GFP expression by FACS analysis. Lethally irradiated newborn pubs were transplanted intra-hepatically with 100 000 GFP^+ BM cells (Figure 7).

3.14. Statistics

For statistical analysis unpaired and paired Student´s t-test were used where appropriate.

4. Results

Prior to this thesis, Wnt5a was identified in co-culture of marrow cells with stromal cells as a soluble factor, to be important for HSC maintenance *in vitro*.

In this study, the role of Wnt5a in hematopoiesis will be further analysed *in vitro* and *in vivo* under steady-state conditions as well as in leukemia.

4.1. *Wnt5a* expression in hematopoietic tissues and cell fractions

Published reports described *Wnt5a* was expressed in mesenchymal cells [98] and B lymphocytes [139]. Thus, at the beginning of the project, we explored the expression of *Wnt5a* in immature and mature hematopoietic cell populations. For this purpose, *Wnt5a* expression was analysed in sorted hematopoietic stem cells and their progenitor populations LSK, MP (myeloid progenitor) and CLP (common lymphoid progenitor) and in mature cell populations, granulocytes and B cells as well as the positive control stromal cell line UG26-1B6 by quantitative real-time PCR.

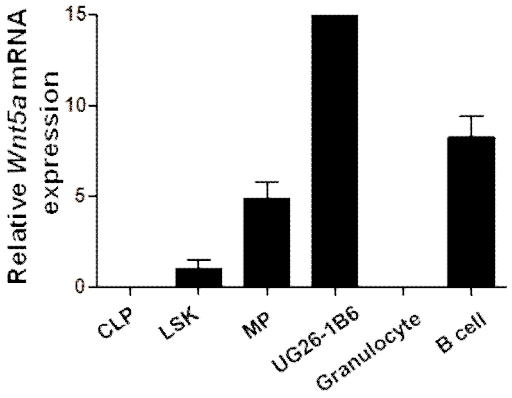

Figure 8. *Wnt5a* expression in hematopoietic cell populations. Relative expression of *Wnt5a* in hematopoietic cell populations and stroma cell line UG26-1B6. Expression of *Wnt5a* in CLPs, LSKs, MPs, $B220^+$ B cells, $Gr\text{-}1^+$ $Cd11b^+$ granulocytes and UG26-1B6 stroma cell line calculated using 2^delta CT x 100% and Rpl39 houskeeping gene; relative expression of *Wnt5a* compared to LSK population;

We detected *Wnt5a* expression in different subpopulations of hematopoietic cells: LSKs (Lin^- $SCA\text{-}1^+$ KIT^+) showed a low expression, whereas MPs (Lin^- $SCA\text{-}1^-$ KIT^+) and lymphoid mature B cells showed relatively high expression. However, *Wnt5a* expression was not detected in CLPs or mature granulocytes (Figure 8). The highest level of expression was found in the embryo-derived stromal cell line UG26-1B6 [136]. These analyses show that *Wnt5a* is expressed in subpopulations of hematopoietic cells and stromal cells. Thus, *Wnt5a* could have both intrinsic and extrinsic effects on hematopoiesis in both cell types.

4.2. Extrinsic effects of Wnt5a: progenitor frequency in co-cultures lacking Wnt5a

As described above, *Wnt5a* is highly expressed in the HSC-supportive stromal cells UG26-1B6. To test whether modulations in the level of Wnt5a affect HSCs by extrinsic mechanisms, we performed *ex vivo* experiments using stromal cells of *Wnt5a* knockout mice (B6;129S7-Wnt5atm1Amc/J mice backcrossed to B6;129S2). Since *Wnt5a*$^{-/-}$ mice die before birth, we isolated stromal cells from the E10.5 Aorta-Gonade-Mesonephros (AGM) region and performed co-culture experiments with HSCs.

Lineage negative (Lin$^-$) bone marrow (Ly5.1/*Wnt5a*$^{+/+}$) cells, which present a population of immature cells including HSCs and progenitor cells, but are depleted from mature cells, were co-cultured on primary AGM stroma, isolated from *Wnt5a*$^{-/-}$, *Wnt5a*$^{+/-}$ and their wild type (WT) littermate mice. AGM region was isolated on E10.5, the region and the time point hematopoiesis takes place in the embryo. Primary AGM stroma is a potent supporter of murine hematopoiesis [147] and is therefore a suitable cultivation system, to investigate maintenance and differentiation potential of HSCs. In this experiment, we wanted to find out the influence of stromal Wnt5a on the extrinsic maintenance and differentiation potential of HSCs.

In two independent experiments, one after one week of co-culture and one after two weeks of co-culture of AGM stroma with Lin$^-$ hematopoietic cells, the cultures were harvested. In the first experiment, we determined how lack of *Wnt5a* in stromal cells affects the production of progenitor cells, and the cultures were seeded in cytokine-containing methylcellulose, to allow hematopoietic progenitors to form detectable colonies after ten to twelve days in culture.

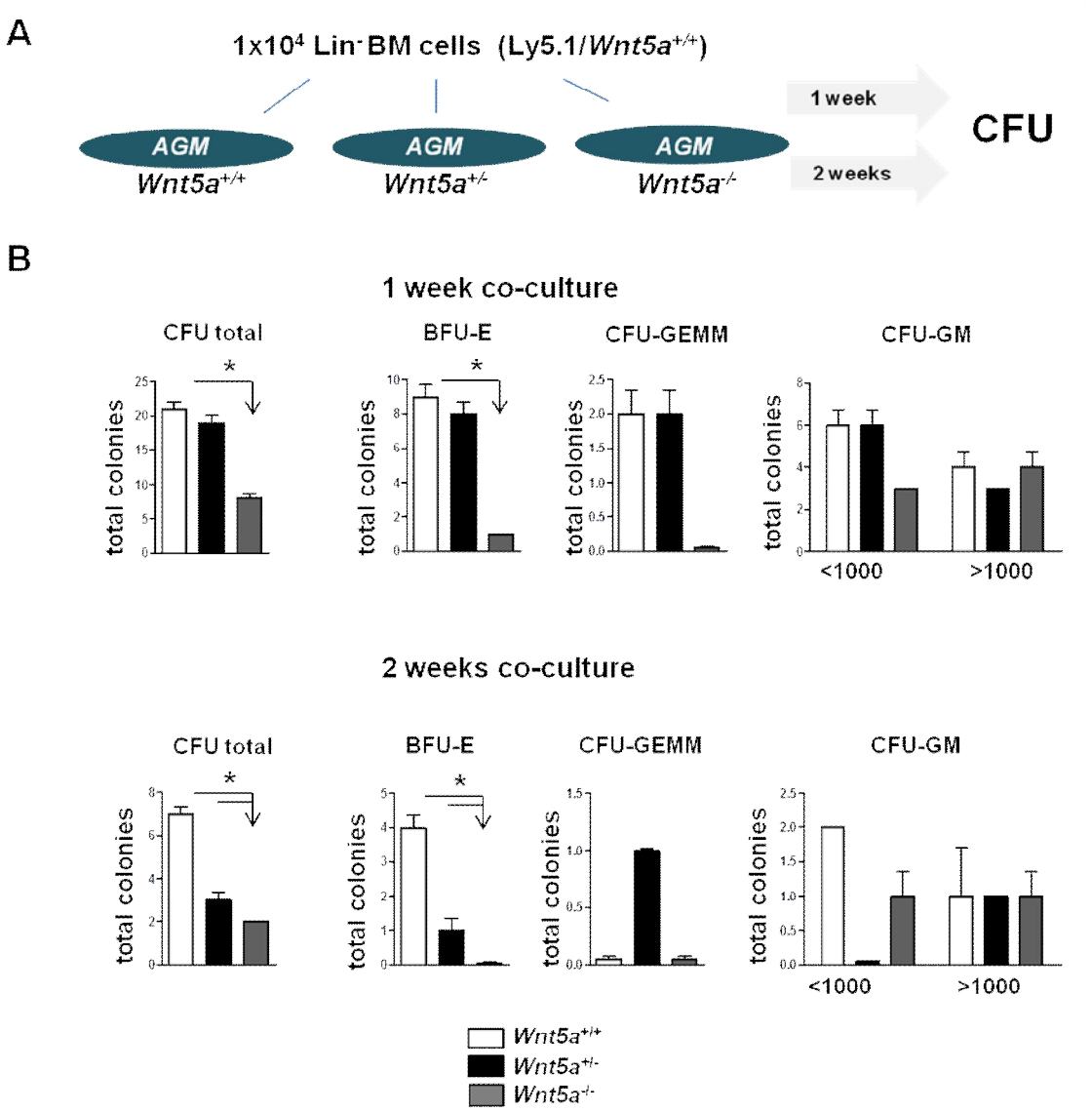

Figure 9. Progenitor frequency in co-cultures lacking *Wnt5a*. **(A)** Experimental design for co-culture experiments; 1x10^4 Lin$^-$ BM cells (Ly5.1/*Wnt5a*$^{+/+}$) were co-cultured on *Wnt5a*$^{+/+}$ (white bar), *Wnt5a*$^{+/-}$(black bar) and *Wnt5a*$^{-/-}$ (grey bar) primary AGM (aorta-gonade-mesonephros) stroma for one and two weeks; **(B)** CFU-assay was carried out with the co-cultured WT cells and total colonies were counted after 10 days. BFU-E = burst-forming unit erythroid; CFU-GEMM = CFU-granulocyte, erythroid, macrophage, megakaryocyte; CFU-GM = CFU-granulocyte (CFU-G), CFU-macrophage (CFU-M), and CFU-granulocyte macrophage (CFU-GM); Mean ± SEM, *p<0.05.

Analysing the one week co-cultures, we recovered a significant lower amount of colony-forming cells from co-cultures with Wnt5a deficient AGM stroma, which was reflected in all different colony types (CFU-GM, CFU-GEMM, and BFU-E), whereas at one week of co-culture on *Wnt5a*$^{+/-}$ AGM stroma showed similar results as co-cultures on control AGM stroma. One week later, in two weeks co-cultures, we not only saw a significant decrease in total colonies co-cultured on *Wnt5a*$^{-/-}$ AGM stroma, but also in those co-cultures on *Wnt5a*$^{+/-}$, which was reflected most strongly in the amount of

formed BFU-E. These results show that Wnt5a is required for proper maintenance of hematopoietic progenitors in co-cultures (Figure 9).

4.3. Characterization of hematopoietic cells in B6;129S2-Wnt5atm1Amc/J mice

The results of the experiment with loss of secreted Wnt5a in stromal cells show that stromal Wnt5a regulates early hematopoiesis in co-cultures *in vitro*. The question then arose, whether loss of Wnt5a affects hematopoiesis *in vivo*. *Wnt5a*$^{+/-}$ knockout mice were generated by Yamaguchi *et al*. [100]. *Wnt5a*$^{-/-}$ mice are perinatal lethal, the complete knockout of *Wnt5a* in the embryo results in severe embryonic development defects followed by asphyxia and embryo death just prior to birth at embryonic day 19 (E19). In Chapter 4.3.1 we demonstrate the importance of backcrossing of the mouse strain B6;129S7-Wnt5atm1Amc/J. In order to characterize *Wnt5a*$^{-/-}$ hematopoietic tissues, fetal liver was isolated on E14.5 (Ch 4.3.2.). In Chapter 4.3.3., adult hematopoiesis was characterized from *Wnt5a*$^{+/-}$ mice compared to their wild type (WT) littermates. All Wnt5a knockout experiments were carried out with B6;129S2 - Wnt5atm1Amc/J mice.

4.3.1. Backcrossing of the mouse strain B6; 129S2-Wnt5atm1Amc/J mice

In the initial characterization experiments, we detected no differences in the B cell compartment of *Wnt5a*$^{+/-}$ adult hematopoiesis (Figure 10). This was unexpected, as Liang *et al.* analysed in 2003 the same knockout mouse strain in terms of mature B cell hematopoiesis and showed that Wnt5a negatively regulates B220^{+} CD43^{-} IgM^{+} B cell proliferation in hematopoiesis [139]. As Liang *et al.* declared already the importance of the background of the mice, we backcrossed the mouse strain B6; 129S7 to B6; 129S2 for 3-6 generations (F3-F6) and analysed the littermates (F3-F6). The next figure is demonstrating the phenotypically changes in B220^{+} CD43^{-} IgM^{+} B cell populations in Spleen and PB after backcrossing.

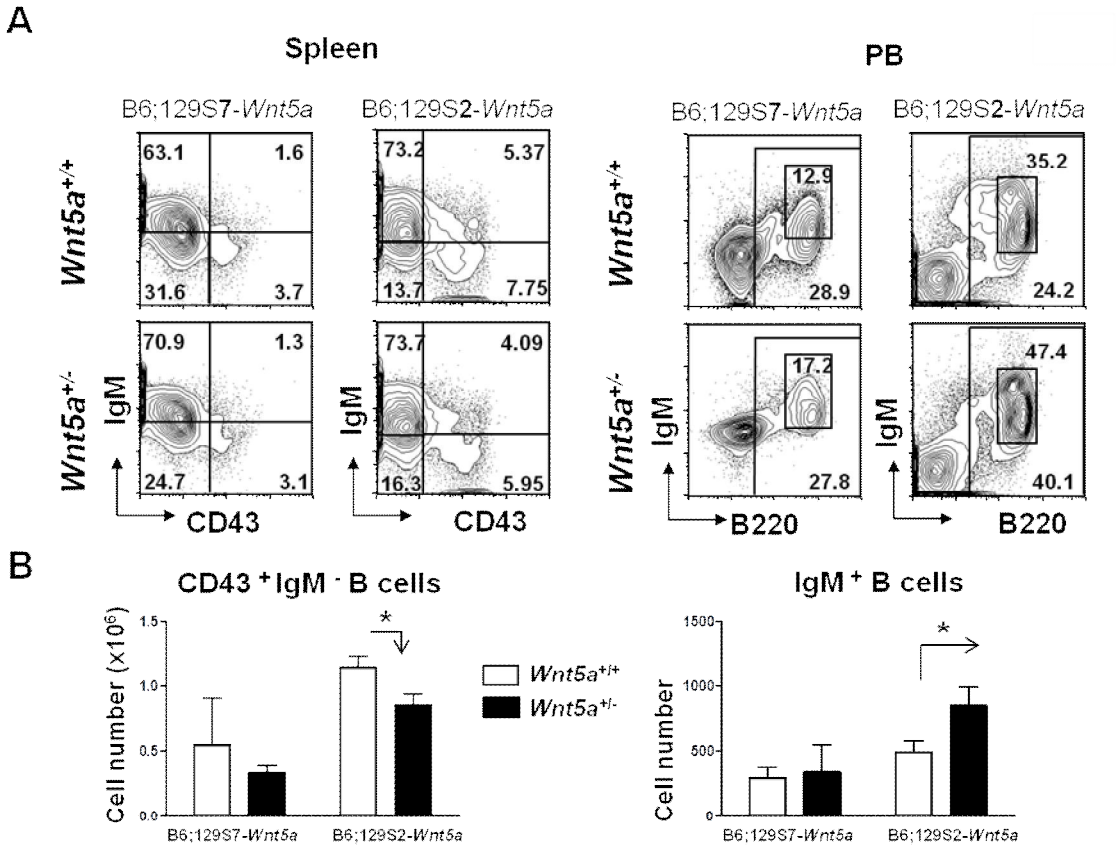

Figure 10. Comparison of mature hematopoiesis before (B6; 129S7) and after backcrossing (B6;129S2). **(A)** Representative FACS blots with gating strategy of Spleen and PB for B cell population; WT and *Wnt5a*$^{+/-}$ mice are compared before and after backcrossing (**B**) Absolute numbers of B cell populations of Spleen and PB of *Wnt5a*$^{+/-}$ mice (black bars) and the WT littermates (white bars); Mean ± SEM; *p<0.05.

In Spleen, the CD43^{+} IgM^{-} B cells are decreased (B6; 129S2-Wnt5a). This can be seen in Figure 10 after backcrossing (on the right), while in previous experiments, no change was detectable in this population (on the left). In PB, we could not detect any changes in B cell populations in the mouse strain B6; 129S7-Wnt5a (on the left) as published in 2003 [139]. After backcrossing to B6; 129S2 we could see more B220^{+} IgM^{+} cells in *Wnt5a*$^{+/-}$ mice (on the right), which is in accordance with previous publication. These phenotypical changes in Wnt5a-dependent hematopoiesis after backcrossing indicate the importance of backcrossing mouse strains, in order to minimize mutations gained through inbreeding. The results gained from the backcrossed mice were used for the thesis.

4.3.2. Characterization of fetal hematopoiesis

Wnt5a heterozygous mice were kept on a strict B6; 129S2 background and intercrosses of *Wnt5a* heterozygous mice were performed to generate *Wnt5a*$^{-/-}$ embryos. In all experiments the *Wnt5a*$^{+/+}$ (WT) littermates were used as control group. In the experiments with FL, we also included analyses of *Wnt5a*$^{+/-}$ embryos as an additional group.

Early hematopoiesis in fetal liver

Early stages of hematopoietic hierarchy were determined by flow cytometry. The gating strategy was as shown in Figure 11. Other than the anaylses of adult mice shown later, fetal HSCs may express low levels of the lineage marker CD11b [148], and this marker was therefore not included in the lineage cocktail, but analysed separately.

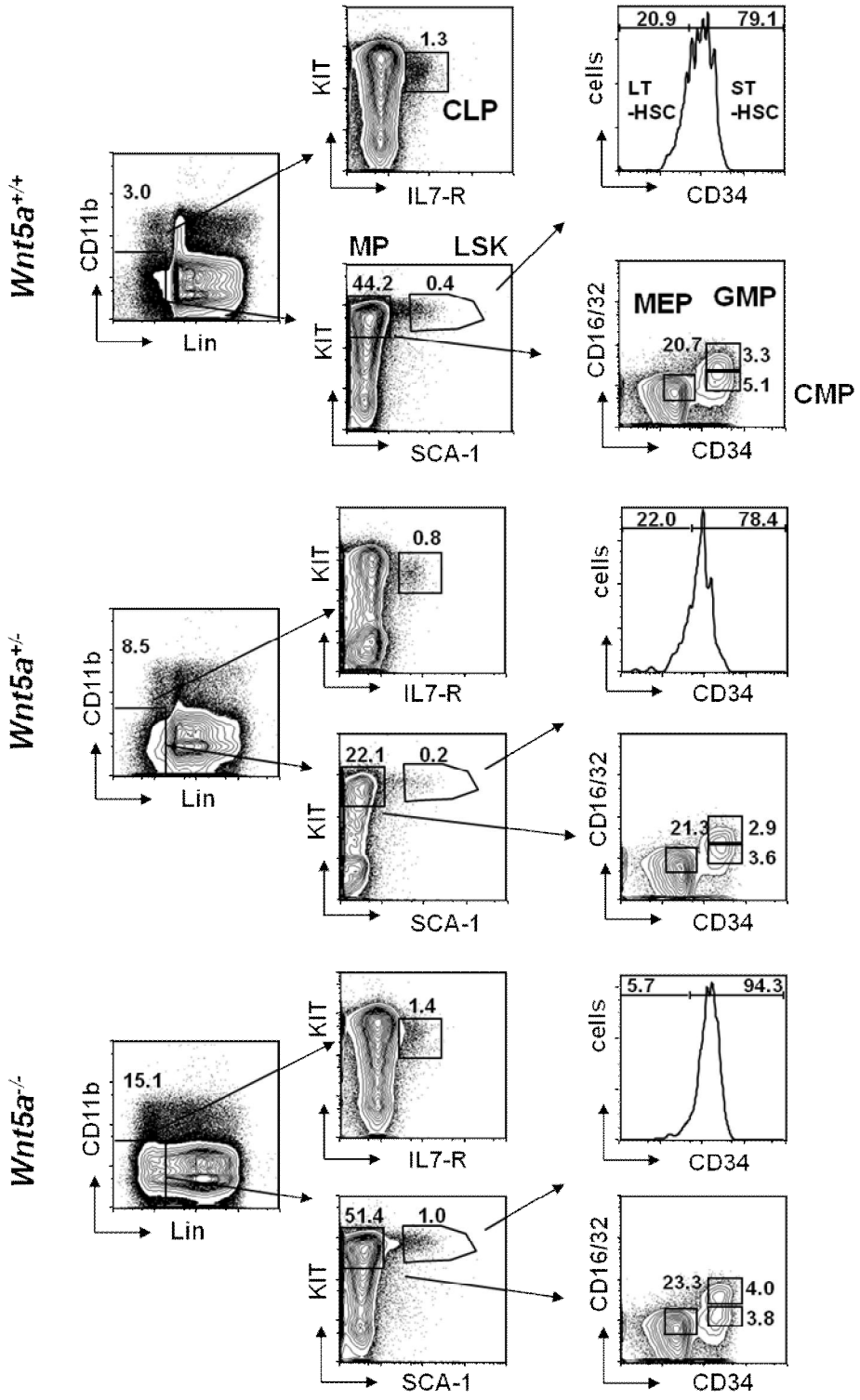

Figure 11. Gating strategy for flow cytometry staining of HSCs and progenitor populations in fetal liver (FL). Gating strategy for Lin$^-$ CD11b^{med} MP, CLP and LSK (LT-HSC and ST-HSC) populations of *Wnt5a*$^{+/+}$, *Wnt5a*$^{+/-}$ and *Wnt5a*$^{-/-}$ FL.

In FL of *Wnt5a*-deficient animals, we observed no change in the FL cellularity between *Wnt5a*$^{+/+}$, *Wnt5a*$^{+/-}$ and *Wnt5a*$^{-/-}$ organs (Figure 12A). Moreover, there was no impact of lower levels of Wnt5a detectable on common lymphoid progenitors (CLP, Lin$^-$ KIT^{med}

IL7-R$^+$) as well on myeloid progenitors (MP, Lin$^-$ SCA-1$^-$ KIT$^+$), but on more committed myeloid progenitors. The MEP (megakaryocyte-erythroid progenitor) fraction was significantly increased in *Wnt5a*$^{-/-}$ and *Wnt5a*$^{+/-}$ FL. In even earlier cell types, the percentage or absolute number of LSK (Lin$^-$ CD11b$^{-/low}$ SCA-1$^+$ KIT$^+$) cells of *Wnt5a*$^{-/-}$ and *Wnt5a*$^{+/-}$ when compared with WT littermate control embryos, was unchanged. However, more comprehensive analysis of the LSK fraction revealed in *Wnt5a*$^{-/-}$ embryos significant decreases in the percentage of CD34$^-$ LSKs, whereas the CD34$^+$ LSKs were significantly increased. In contrast, in *Wnt5a*$^{+/-}$ FL cells, the percentage of CD34$^-$ cells in the LSK fraction was increased, whereas the CD34$^+$ LSK cells were significantly decreased. Former repopulation studies showed that all long-term reconstituting stem cell activity resides in the CD34$^+$ KIT$^+$ SCA-1$^+$ fraction in FL [149]. This is in contrast to CD34 expression on HSCs during adult hematopoiesis [6]. Thus, CD34 is an activation marker and expressed on hematopoietic stem cells from perinatal to five weeks old mice. After this time point the CD34 surface marker is less expressed on HSCs and finally in ten - twelve weeks old mice the majority of the HSCs are CD34$^+$ [150]. Our results show that the level of Wnt5a only affects the earliest stages of hematopoiesis and erythroid progenitors in fetal liver tissue and probably their activation status.

Functional studies were done to closer examine whether the noted changes in immunophenotype of erythroid progenitors and LSKs by colony forming assay (CFU-Assay) and transplantation studies. Examination of colony-forming cells showed that, compared to WT cells, the number of colony-forming cells was decreased in *Wnt5a*$^{+/-}$ FL and further decreased in *Wnt5a*$^{-/-}$ FL, suggesting an intrinsic defect in colony-forming ability dependent on Wnt5a. Thus, loss of Wnt5a results in decreased progenitor cell activity (Figure 12B).

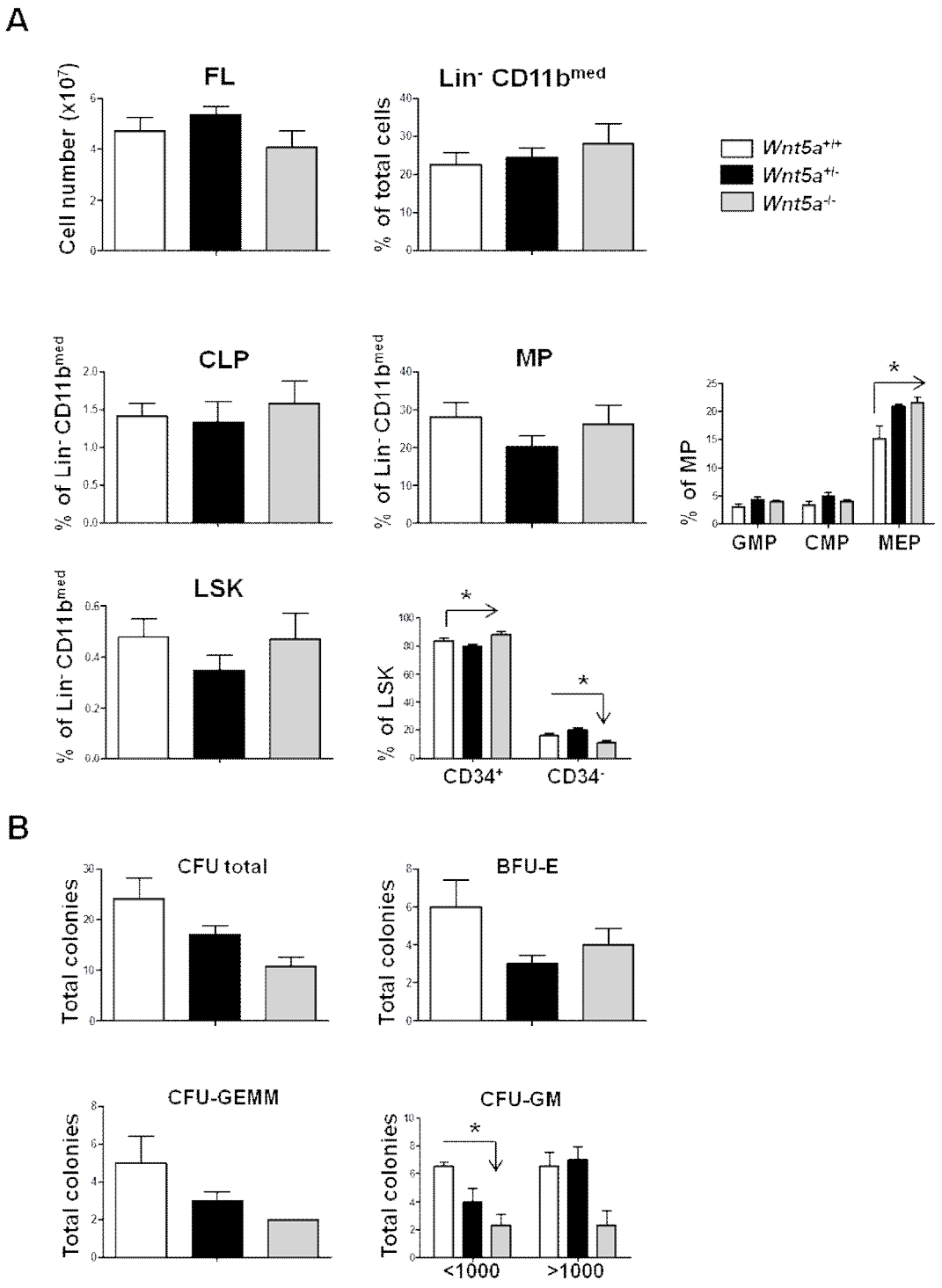

Figure 12. Alterations in early hematopoiesis Wnt5a$^{-/-}$ FL. **(A)** Total cell number of fetal liver (FL) number of cells per FL; controls are littermates; *Wnt5a*$^{+/+}$ n=17 (white bar), *Wnt5a*$^{+/-}$ n=20 (black bar), *Wnt5a*$^{-/-}$ n=9 (grey bar) and the progenitor populations in fetal liver from the three different genotypes shown in percentages; **(B)** Colony forming assay: Total number of colonies formed from FL, *Wnt5a*$^{+/+}$(white bar), *Wnt5a*$^{+/-}$(black bar), *Wnt5a*$^{-/-}$(grey bar); Mean ± SEM; *p<0.05.

Mature hematopoiesis in fetal liver

Since we found changes in the earliest stages of hematopoiesis, we wondered whether Wnt5a would affect mature hematopoietic cell populations.

The mature lymphoid cell compartments were determined by the surface markers CD3, the T cell co-receptor, and B220 (CD45RA) detecting B cells. Additionally, the surface markers CD43 and IgM were used in combination with B220 to delineate different B cell subpopulations. While B220 is expressed on all B-lineage cells, CD43 is only expressed on pre- and pro-B cells and IgM is only expressed on mature B cells. Further surface markers like CD5 and CD19 can help to distinguish further subpopulations, B-1a and B-1b B cells, but were out of the scope in this work [151].

The mature myeloid cell fraction was determined by the use of the combination of surface markers Gr-1 and CD11b (Mac-1) for detection of granulocytes and monocytes. The gating strategy can be seen in Figure 13A.

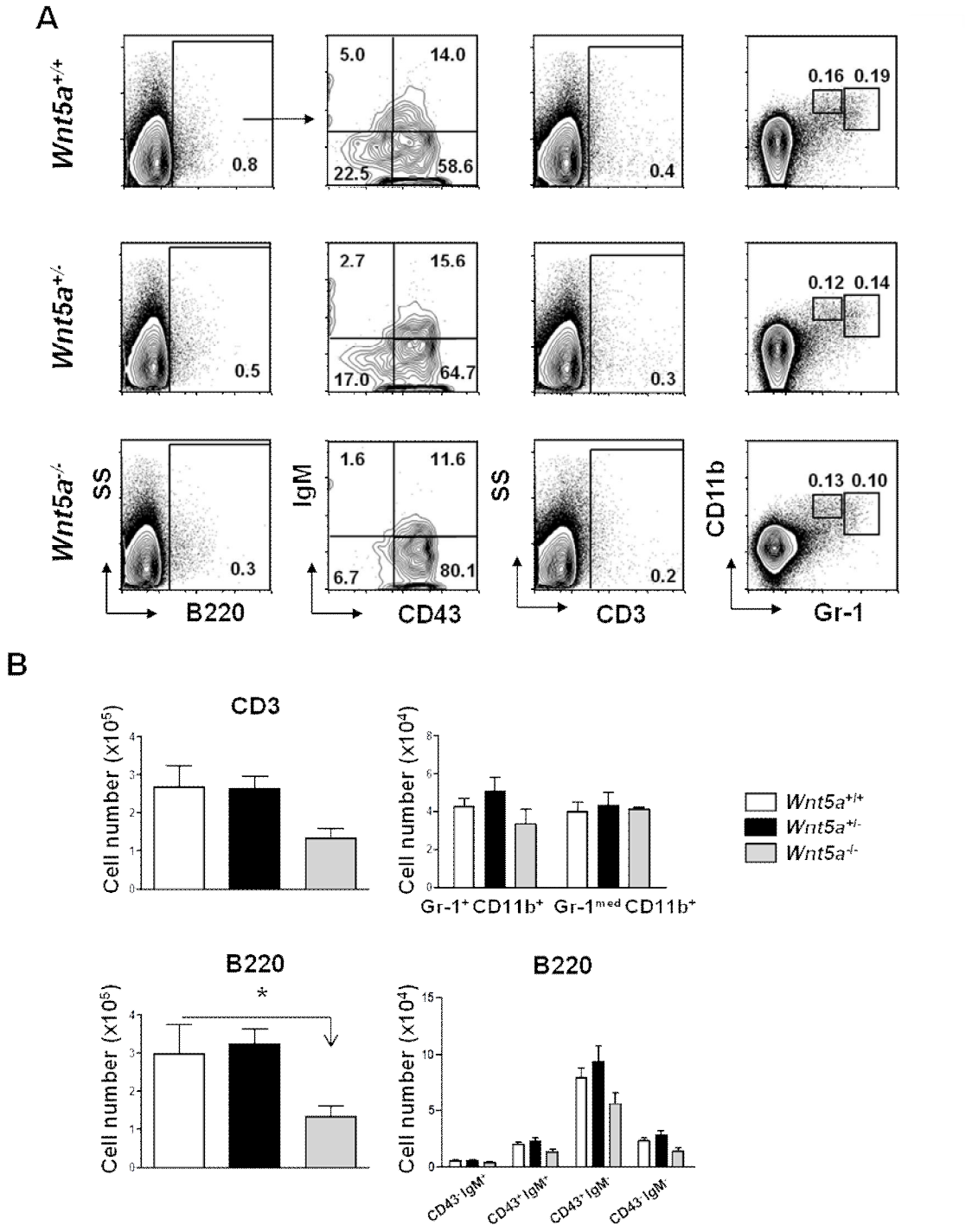

Figure 13. Alteration in mature hematopoiesis of *Wnt5a*$^{-/-}$ fetal liver (FL). **(A)** Gating strategy for mature cell staining of FL **(B)** Absolute numbers of lymphoid and myeloid mature cells are shown for FL (E14.5). Number of cells per FL; controls are littermates; *Wnt5a*$^{+/+}$ n=17 (white bars), *Wnt5a*$^{+/-}$ n=20 (black bars), *Wnt5a*$^{-/-}$ n=9 (grey bars) Mean ± SEM; *p<0.05.

In a previous study in *Wnt5a*$^{-/-}$ fetal livers, it was found that the population of B220^{+} CD43^{-} IgM^{+} cells was increased and proliferating [139]. In contrast to this report, we found that the absolute number of B220^{+} B cells is significantly decreased in *Wnt5a*$^{-/-}$ FL. The decrease in B cells could not be attributed to a specific subpopulation of

mature or immature B cells. In contrast to B cells, distribution of $CD3^+$ T cells, or granulo- and monocytes were not altered in *Wnt5a*$^{-/-}$, *Wnt5a*$^{+/-}$, compared to *Wnt5a*$^{+/+}$ (WT) cells (Figure 13B).

In summary, early hematopoiesis, and particularly the balance between $CD34^+$ LSKs and $CD34^-$ LSKs were altered in *Wnt5a*$^{-/-}$ FL. It is known that all long-term reconstituting stem cell activity resides in the $CD34^+$ KIT^+ $SCA\text{-}1^+$ fraction in FL [149] and that CD34 expression is lower in ST-HSCs when they are activated into active proliferating ST-HSCs. Therefore, our results favour the view that in *Wnt5a*$^{-/-}$ FL the number of LT-HSC may be increased, which suggests a role of Wnt5a in primitive hematopoiesis of fetal development.

Yet, our results revealed a reduced capacity of LT-HSCs to form colonies and we speculate, therefore, that *in vivo*, Wnt5a may also be important for maintaining functional capacity of HSCs, particularly the LT-HSC compartment.

Our results show that Wnt5a does not affect the number of mature T cell or myeloid populations. Like published previously [139], the most strongly affected mature cell population is the B cell compartment. However, what is puzzling is that the reported findings showed increased $B220^+$ $CD43^-$ IgM^+ compartment [139] whereas we found the opposite: a decreased $B220^+$ compartment in FL cells.

At this moment, we have no clear-cut explanation for this divergence. One of the possibilities might be related to the fact that the published *Wnt5a*$^{+/-}$ mice might have been backcrossed onto its B6; 129S7 background for many generations [139], which might have led to compensatory mechanisms. Thus, for all subsequent work, we backcrossed the *Wnt5a*$^{+/-}$ mice to B6; 129S2 animals. This backcrossing has the additional advantage that we can compare the results directly to those of the *Sfrp1*$^{-/-}$ (*Sfrp2*$^{+/-}$) mice we published previously [59].

4.3.3. Characterization of adult hematopoiesis

To find out whether the effects found in E14.5 FL persisted after birth, we also studied hematopoiesis in adult mice. One problem in this study is that *Wnt5a*$^{-/-}$ die prior to birth (E19) [100]. Thus, only adult mice were studied lacking one allele of Wnt5a (*Wnt5a*$^{+/-}$). We previously found that in co-cultures on *Wnt5a*$^{+/-}$ AGM stroma, colony-forming cell production is decreased (Figure 9).

Another issue we took into account is the result from other studies, in which it has been shown that female mice show fluctuations in hematopoiesis depending on their menstrual cycle [152], and that sFRP-1, a Wnt-inhibitor and binding partner of Wnt5a is estrogen-regulated during that cycle [152]. Therefore, to circumvent possible problems in data interpretation due to the menstrual cycle, we restricted our studies to male eight to ten weeks old mice. *Wnt5a*$^{+/-}$ mice and there *Wnt5a*$^{+/+}$ littermates were analysed.

Alterations in late steady-State hematopoiesis

Liang *et al.* [139] showed an important role of Wnt5a in the proliferation of B220^{+} CD43^{-} IgM^{+} B cells in unchallenged animals. Therefore, we first examined the role of Wnt5a in mature steady-state hematopoiesis in PB, BM and Spleen using flow cytometry. The gating strategy for mature cells was used is shown in Figure 15-17.

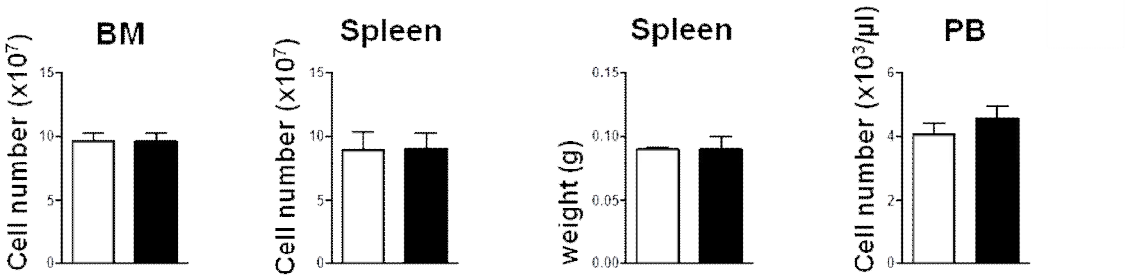

Figure 14. Cellularity analysis of adult *Wnt5a*$^{+/-}$ mice. (**A**) Cell counts from bone marrow (BM, four long bones: two femurs and two tibia per mouse), Spleen and peripheral blood, *Wnt5a*$^{+/+}$ n=15 (white bars), *Wnt5a*$^{+/-}$ n=15 (black bars); controls are littermates. Mean ± SEM.

The PB, BM and Spleen cellularity as well as the weight of the Spleen was unchanged in *Wnt5a*$^{+/-}$ mice compared to their *Wnt5a*$^{+/+}$ littermates (Figure 14).

The blood cell counts do, in general, not show major changes in *Wnt5a*$^{+/-}$ animals. We only found a slightly elevated percentage of hematocrit concentration in the peripheral blood (Table15).

Table 15: Blood cell counts in the PB. WBC, white blood cell; Lymph, lymphocyte; Mono, monocyte; Gran, granulocyte; Eos, eosinophile; RBC, red blood cell; HCT, hematocrit; PLT, platelet; NS, not significant; controls are littermates. Mean ± SEM.

	Wnt5a$^{+/+}$ (n=14)	**Wnt5a$^{+/-}$ (n=13)**	**P value**
WBC (10^3/µl)	4.08 ± 0.43	4.55 ± 0.47	ns
Lymph (10^3/µl)	2.73 ± 0.37	2.91 ± 0.29	ns
Mono (10^3/µl)	0.17 ± 0.03	0.27 ± 0.05	ns
Gran (10^3/µl)	1.05 ± 0.14	1.36 ± 0.23	ns
Eos (10^3/µl)	0.05 ± 0.01	0.05 ± 0.01	ns
RBC (10^6/µl)	10.20 ± 0.40	11.08 ± 0.27	ns
HCT (%)	53.68 ± 2.22	59.23 ± 1.6	0.05
PLT (10^3/µl)	1299 ± 106	1378 ± 181	ns

Phenotypical analysis was performed similarly to the fetal liver analysis. The gating strategy is shown on examples of samples from adult mice in Figure 15-17.

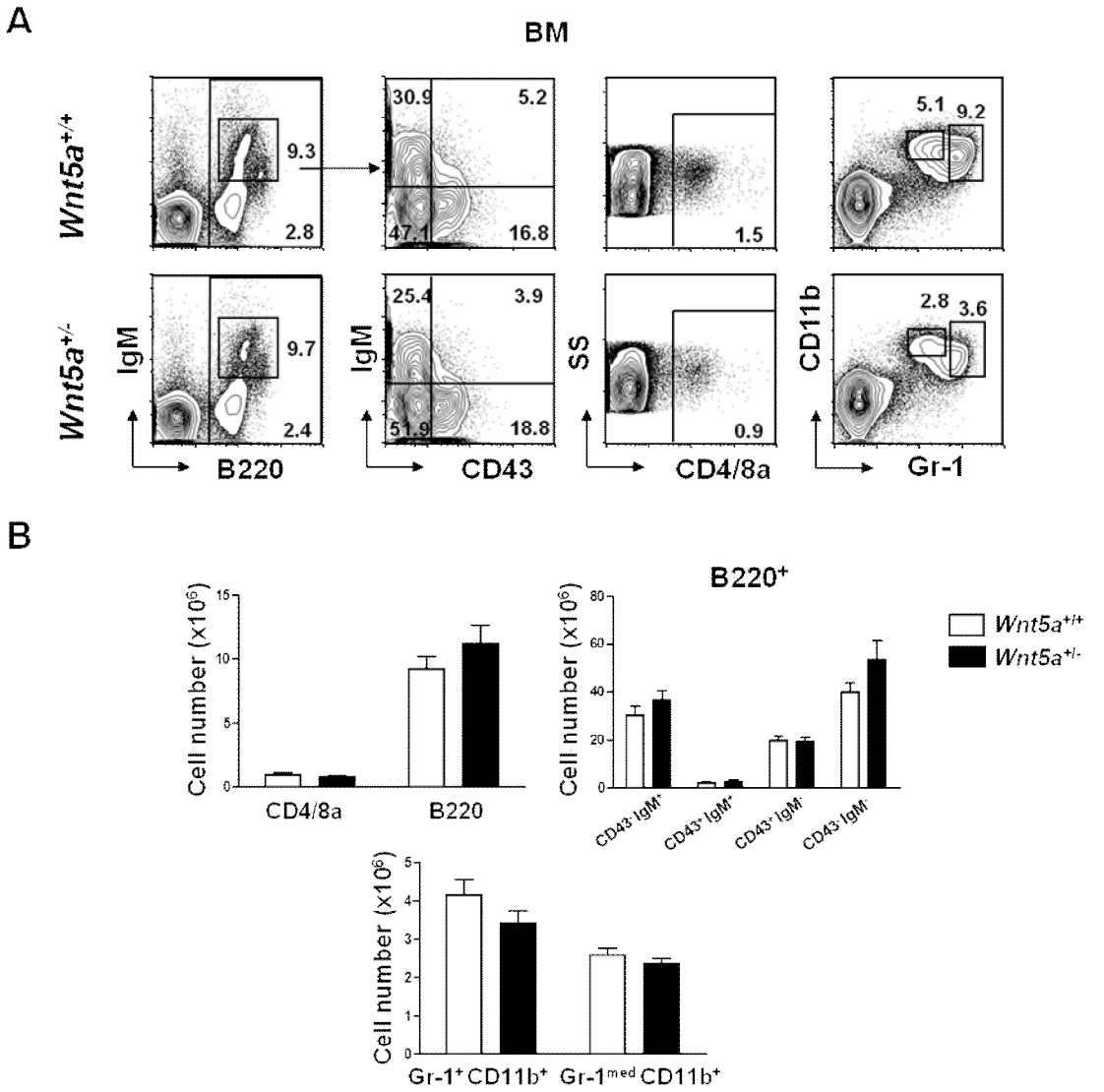

Figure 15. Gating strategy and analysis of mature cell populations in BM. **(A)** Gating strategy of BM for lymphoid and myeloid cell populations. **(B)** Absolute numbers of T cells, B cell populations, granulocytes and monocytes in BM of *Wnt5a*$^{+/-}$ mice n=15 (black bars) and the WT littermates n=15 (white bars); Mean ± SEM.

In the bone marrow (BM), we detected no changes in mature hematopoiesis concerning lymphoid or myeloid lineages (Figure 15).

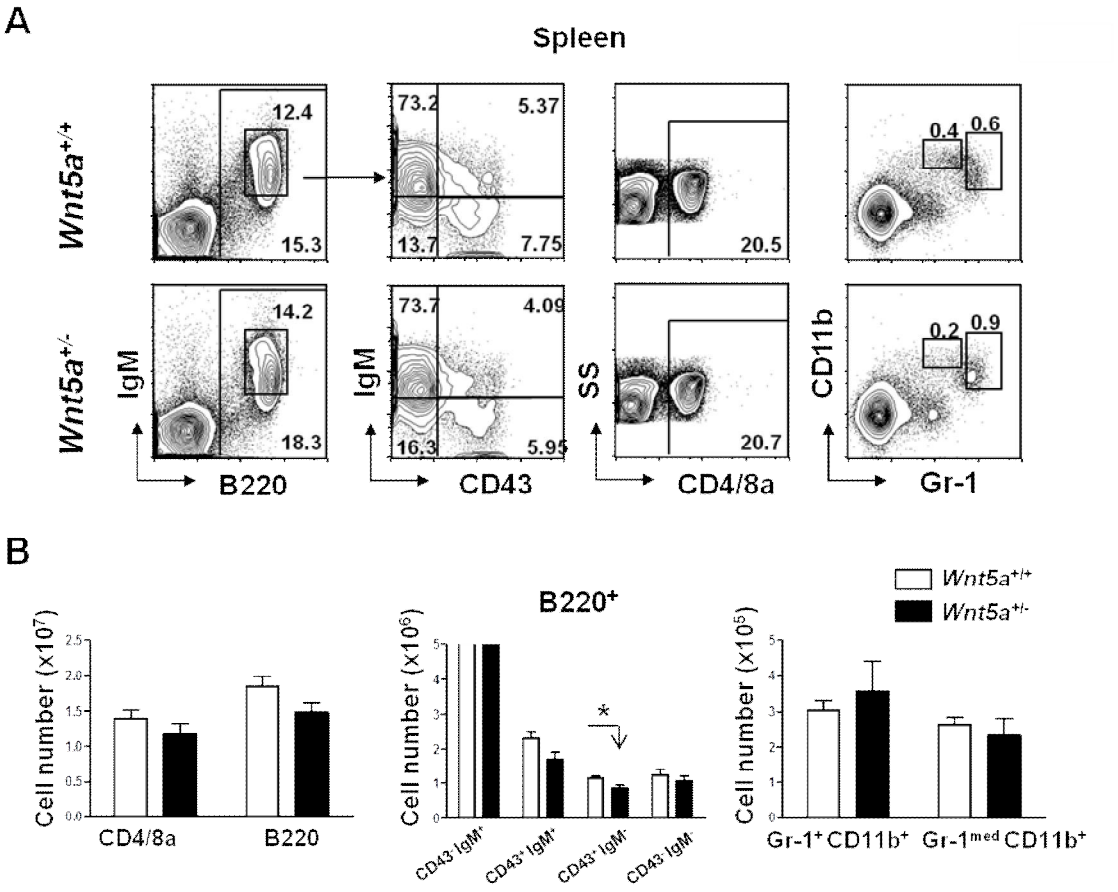

Figure 16. Gating strategy and analysis of mature cell populations in Spleen. **(A)** Gating strategy of Spleen for lymphoid and myeloid cell populations. **(B)** Absolute numbers of T cells, B cell populations, granulocytes and monocytes in Spleen of *Wnt5a*$^{+/-}$ mice n=15 (black bars) and the WT littermates n=15 (white bars); Mean ± SEM; *p<0.05.

In Figure 16A, representative FACS plots of Spleen, isolated from control and *Wnt5a*$^{+/-}$ mice with gates for mature cells, are shown. In the Spleen, we find, like in E14.5 FL (Figure 13), a significant decrease in the absolute number of B220^{+} CD43^{+} IgM^{+} pre-B cells, in the absence of a detectable change in mature B220^{+} CD43^{-} IgM^{+} cells (Figure 16B).

To find out whether these changes can also be seen in the circulation, the mature cell populations from the peripheral blood (PB) were analysed in the same manner as in BM and Spleen (Figure 17).

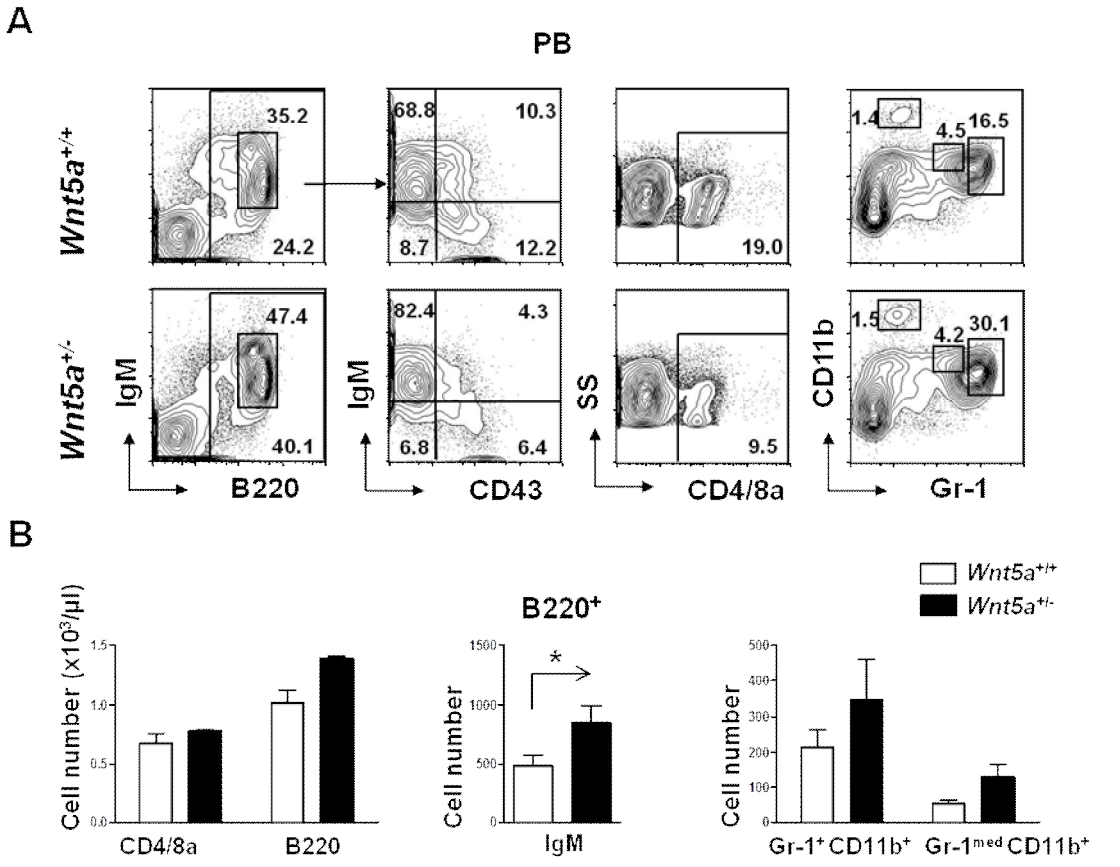

Figure 17. Gating strategy and analysis of mature cell populations in Peripheral Blood (PB). (**A**) Gating strategy of PB for lymphoid and myeloid cell populations; controls are littermates. (**B**) Absolute numbers of T cells, B cell populations and granulocytes and monocytes in PB of *Wnt5a*$^{+/-}$ mice n=15 (black bars) and the WT littermates n=15 (white bars); Mean ± SEM; *p<0.05.

Again, in PB of *Wnt5a*$^{+/-}$ mice, myeloid cells and T cells are unchanged in absolute number as compared to WT littermates. But, unlike in Spleen and E14.5 FL, in PB the B cell maturation appears to be skewed towards the more mature B cell population, ($B220^+$ IgM^+), which is significantly increased and is now similar to that reported [139].

To find out whether other changes detected, such as those found in early hematopoiesis in the fetal liver ($CD34^+$ LSKs) were also found in adult mice, the number of cells belonging to the early stages of the hematopoietic hierarchy was determined by flow cytometry. The gating strategy used, is shown in Figure 18+19.

Alterations in early Steady-State hematopoiesis

In these experiments, we analysed the BM and the Spleen. In Figure 18A, the gating strategy for HSC and progenitor populations in BM is shown.

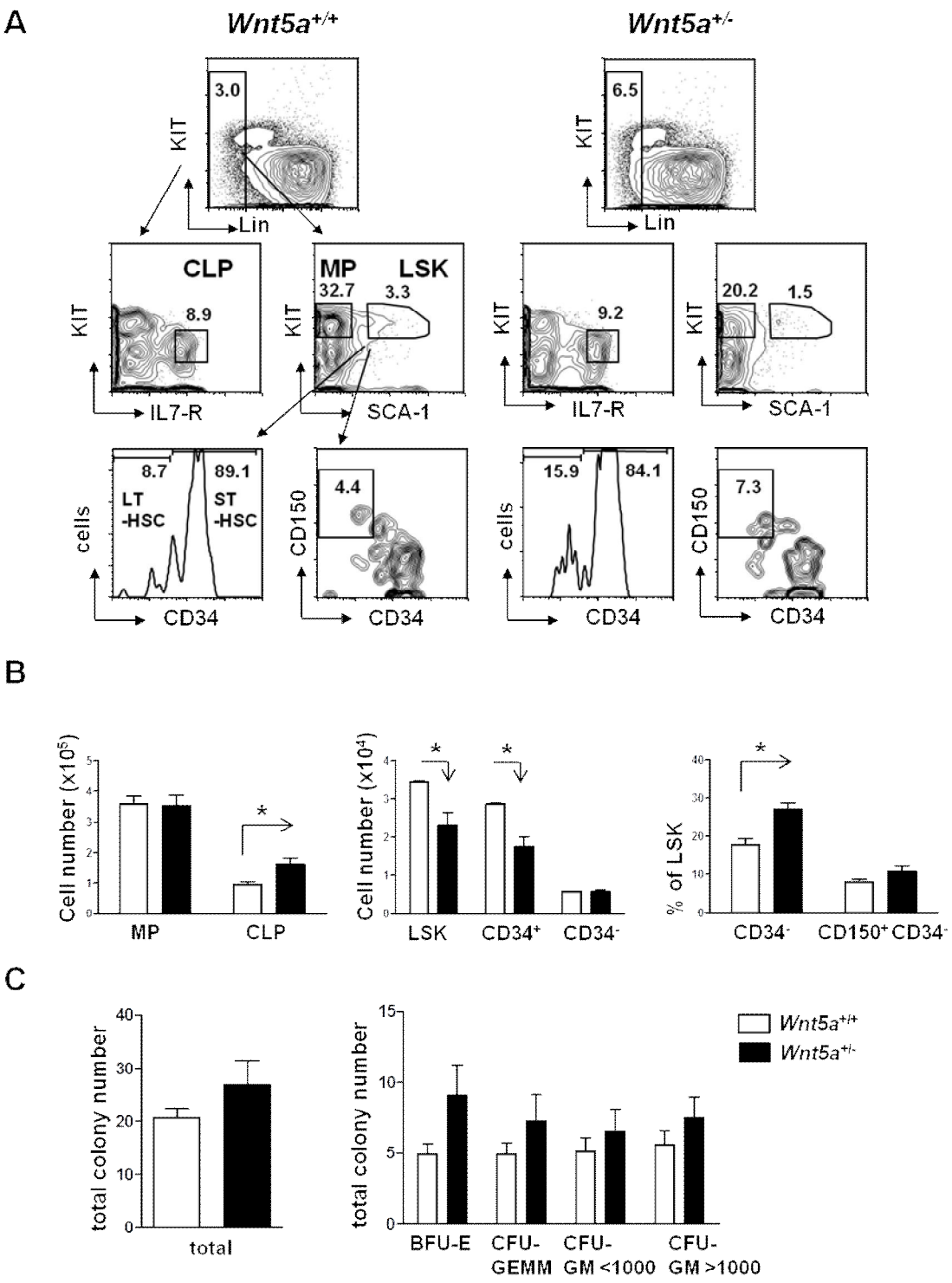

Figure 18. Alterations in early hematopoiesis in the BM of adult *Wnt5a*$^{+/-}$ mice. **(A)** Gating strategy of BM for MP, CLP and LSK (LT-HSC and ST-HSC); **(B)** Absolute numbers of HSC and progenitor populations in BM; The number of cells belonging to the early stages of hematopoietic hierarchy was determined by flow cytometry; **(C)** Total numbers of colonies formed from four long bones, BFU-E = burst-forming unit erythroid; CFU-GEMM = CFU-granulocyte, erythroid, macrophage, megakaryocyte; CFU-GM = CFU-granulocyte (CFU-G), CFU-macrophage (CFU-M), and CFU-granulocyte macrophage (CFU-GM); WT littermates n=15 (white bars), *Wnt5a*$^{+/-}$ mice n=15 (black bars); Mean ± SEM *p<0.05.

Like we found earlier in E14.5 FL, the analysis of early hematopoietic cells in the BM of Wnt5a$^{+/-}$ mice revealed no detectable alterations of the myeloid progenitors (MP, Lin$^-$ SCA-1$^-$ KIT$^+$). However, in contrast to the results with FL (Figure 11+12), the cell number of common lymphoid progenitors (CLP, Lin$^-$ Kit^{med} IL7-R$^+$) was significantly increased in *Wnt5a*$^{+/-}$ BM. In addition, we also found a significant decrease in the percentage and absolute number of LSK (Lin$^-$ SCA-1$^+$ KIT$^+$) cells of *Wnt5a*$^{+/-}$ BM when compared with *Wnt5a*$^{+/+}$ littermate control mice. This decline of cell number was also reflected in the absolute number of short-term HSCs. Interestingly, however, in contrast to the earlier results with FL, the percentages of long-term HSCs (LT-HSC, CD34$^-$ CD150$^+$ -HSCs) [11] within the LSK cell fraction was significantly increased, suggesting an increased maintenance of the earliest population of HSCs (Figure 18B).

The analysis of the primitive hematopoietic cell compartment in Spleen of *Wnt5a*$^{+/-}$ mice showed no changes in cell number of Lin$^-$cells, CLPs, MPs or LSKs compared to their WT littermate controls (Figure 19A+B).

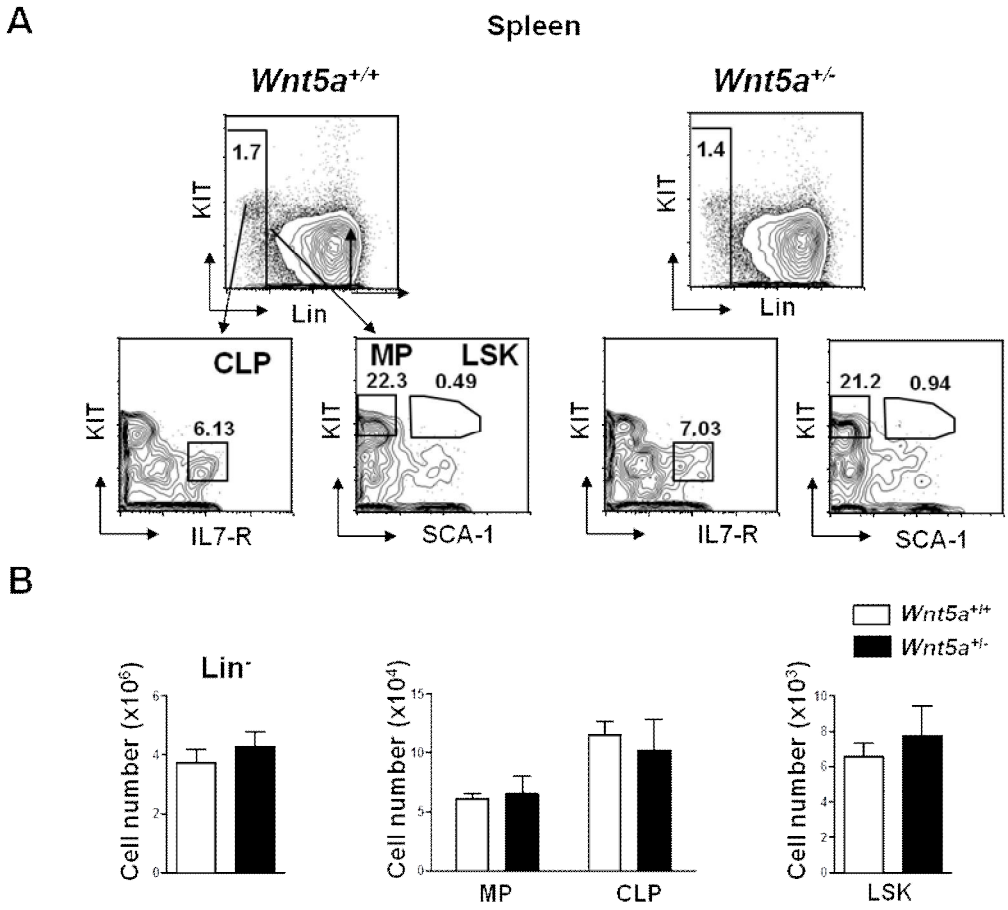

Figure 19. Analysis of early hematopoiesis in the Spleen of adult Wnt5a$^{+/-}$ mice. **(A)** Gating strategy of Spleen for MP, CLP and LSK (LT-HSC and ST-HSC); **(B)** Absolute numbers of HSC and progenitor populations in Spleen; The number of cells belonging to the early stages of hematopoietic hierarchy was determined by flow cytometry; WT littermates n=15 (white bars), *Wnt5a*$^{+/-}$ mice n=15 (black bars); Mean ± SEM *p<0.05.

Thus, we observed significant alterations in the relative and absolute numbers of immunophenotypically defined early (ST- and LT-HSC) and mature subpopulations ($CD43^+$ IgM^- B cells) of cells in BM. In Spleen, the primitive hematopoiesis was unchanged. However, pre-B cells were found to be reduced in number. Changes in B cell number are also detectable in PB. Interestingly, where in FL and Spleen the number of mature $CD43^-$ IgM^+ B cells is decreased, the opposite was found in the PB.

To find out whether not only the immunophenotypical subpopulations are distributed differently in *Wnt5a* mutant mice, but also the functionally defined subpopulations of hematopoietic progenitors and HSCs, we performed functional cellular assays. First, we performed, colony forming assay to quantify multi-potential progenitors and lineage-restricted progenitors of the erythroid (BFU-E), granulocytic, monocyte-macrophage, and megakaryocyte-myelopoietic pathways (CFU-GM and CFU-GEMM). This assay showed that on a clonal level, the number of colony-forming cells, such as BFU-E, CFU-GM and the mixed colonies CFU-GEMM was unchanged in *Wnt5a*$^{+/-}$ mice. Thus, less Wnt5a does not result in changed progenitor cell activity behaviour in adult mice (Figure 18C).

4.4. Stem cell assay: Transplantation of *Wnt5a*$^{+/-}$ HSCs (Intrinsic)

The increase of $CD150^+$ $CD34^-$ LSKs (which closely correspond to LT-HSCs) of *Wnt5a*$^{+/-}$ adult mice suggests that a decrease of Wnt5a in HSCs may influence the number, and/or proliferative activity of these cells. Since cell cycle regulation is required for proper self-renewal and regenerative proliferation, these results suggest that Wnt5a may affect the functional activity of HSCs. To address the functional HSC activity of $CD150^+CD34^-$ LSKs, *in vivo* reconstitution experiments need to be performed, which reveal not only their regenerative potential, but also their quality in terms of self-renewal capacity in serial transplantations.

4.4.1. Transplantation of whole BM

Since we found that *Wnt5a* transcripts are present in LSK cells, it is possible that Wnt5a has **intrinsic effects** on HSC. To test this hypothesis, *Wnt5a*$^{+/-}$ BM cells were transplanted into lethally irradiated WT mice and analysed for the reconstitution ability of the *Wnt5a*-deficient HSC.

In this experiment, $2.5x10^5$ bone marrow cells of *Wnt5a*$^{+/-}$ mice and their WT littermates (both CD45.2) were transplanted into lethally irradiated WT (129S2/C57BL/6.SJL)F1 (CD45.1xCD45.2; Ly5.1xLy5.2) mice. To assess regeneration by donor cells, regeneration was followed in the peripheral blood of recipient mice after five and ten weeks and mice were sacrificed after 16 weeks, followed by analysis of BM and PB (1°). In these transplantation experiments, donor and recipient cells could be distinguished, by staining for CD45.1 (Ly5.1) and CD45.2 (Ly5.2) surface antibodies, and analysed using flow cytometry.

To study self-renewal of the regenerated HSCs, we took into account the possibility that *Wnt5a*$^{+/+}$ and *Wnt5a*$^{+/-}$ HSCs could have been regenerated to different levels. Thus, we sorted donor-type Ly5.2$^+$ Lin$^-$ Kit$^+$ cells from recipient bone marrow and a calculated amount of 1000 LSKs for each donor genotype were transplanted into 2° recipient mice [58] (Figure 20A).

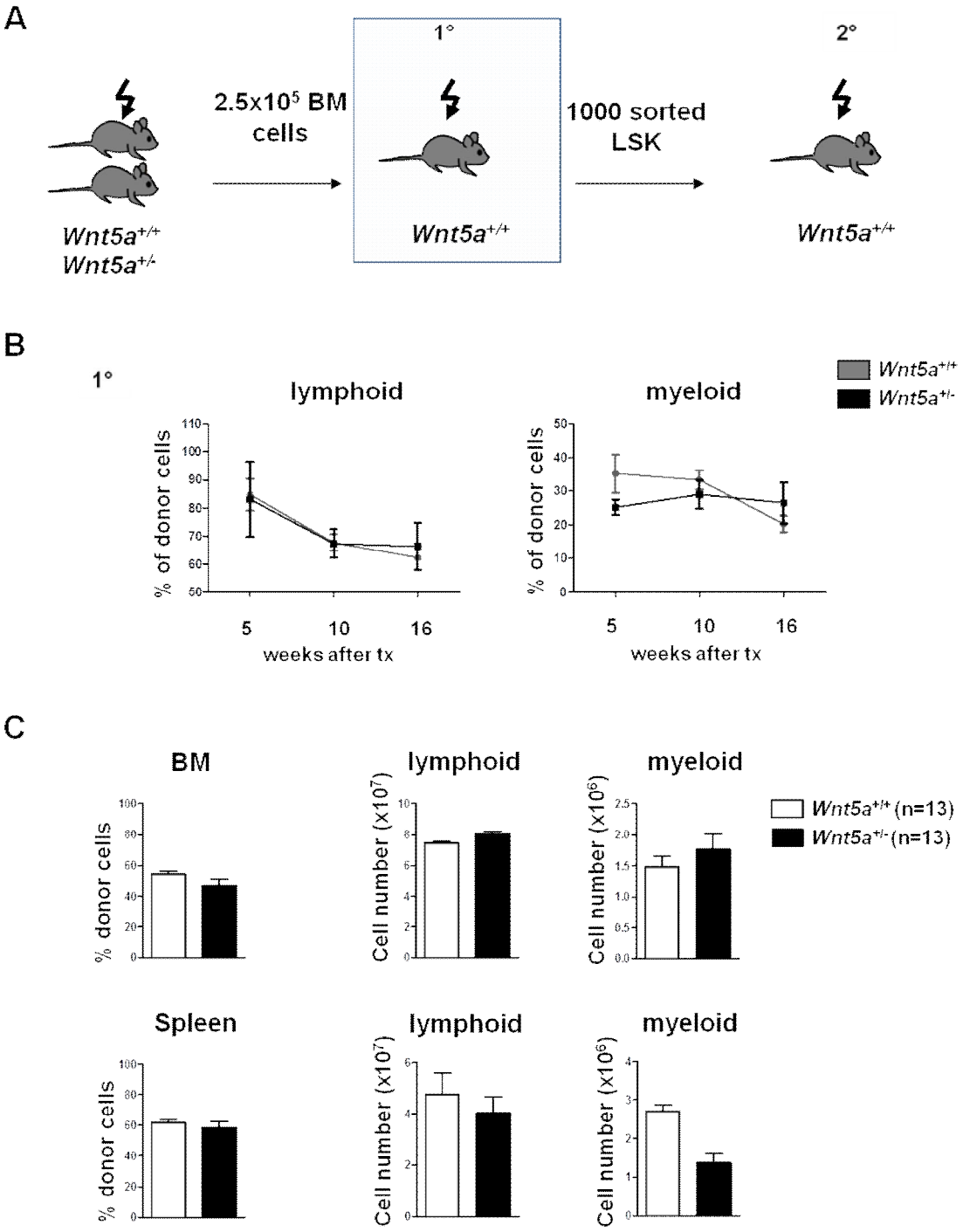

Figure 20. Intrinsic transplantation of *Wnt5a*$^{+/-}$ BM in WT microenvironment. 1° transplantation. **(A)** Serial transplantation flow chart. 250 000 whole bone marrow (BM) cells (Ly5.2) of WT and *Wnt5a*$^{+/-}$ mice were injected into lethally irradiated WT mice (Ly5.1) (1° transplants). Sixteen weeks post transplantation, BM, Spleen and PB was isolated and analysed by FACS analysis for hematopoietic stem cells, their progenitor cells and mature cells. **(B)** The pattern of lymphoid and the myeloid engraftment in the PB of WT and *Wnt5a*$^{+/-}$ in process after five, ten and 16 weeks. **(C)** The engraftment levels in BM and Spleen of 1° after 16 weeks. WT BM cells n=13 (white bars and grey lines), *Wnt5a*$^{+/-}$ BM cells n=13 (black bars and black lines); Mean ± SEM; *p<0.05.

1° Transplantation

Transplantation of whole BM from WT or *Wnt5a*$^{+/-}$ mice showed similar lymphoid and myeloid engraftment in PB after five, ten and 16 weeks post transplantation (Figure 20B). In BM after 16 weeks, the donor engraftment of both genotypes is about 50% of total cells. We found no detectable differences either in lymphoid or myeloid engraftment in BM. In Spleen, we observed donor engraftment of about 60% of total cells, again with similar number of engrafted lymphoid and myeloid cells (Figure 20C).

Our analysis of the recipient BM after 16 weeks showed that both the percentage and absolute number of MP and LSK cells regenerated from *Wnt5a*$^{+/-}$ donor BM was unchanged when compared with WT-donor-derived BM cells. Though in BM, the number of mature cells appears similar for WT and *Wnt5a*$^{+/-}$ donor BM, the donor-derived common lymphoid progenitor population CLP, demonstrated a significantly lower absolute cell number in BM of recipient mice (Figure 21A).

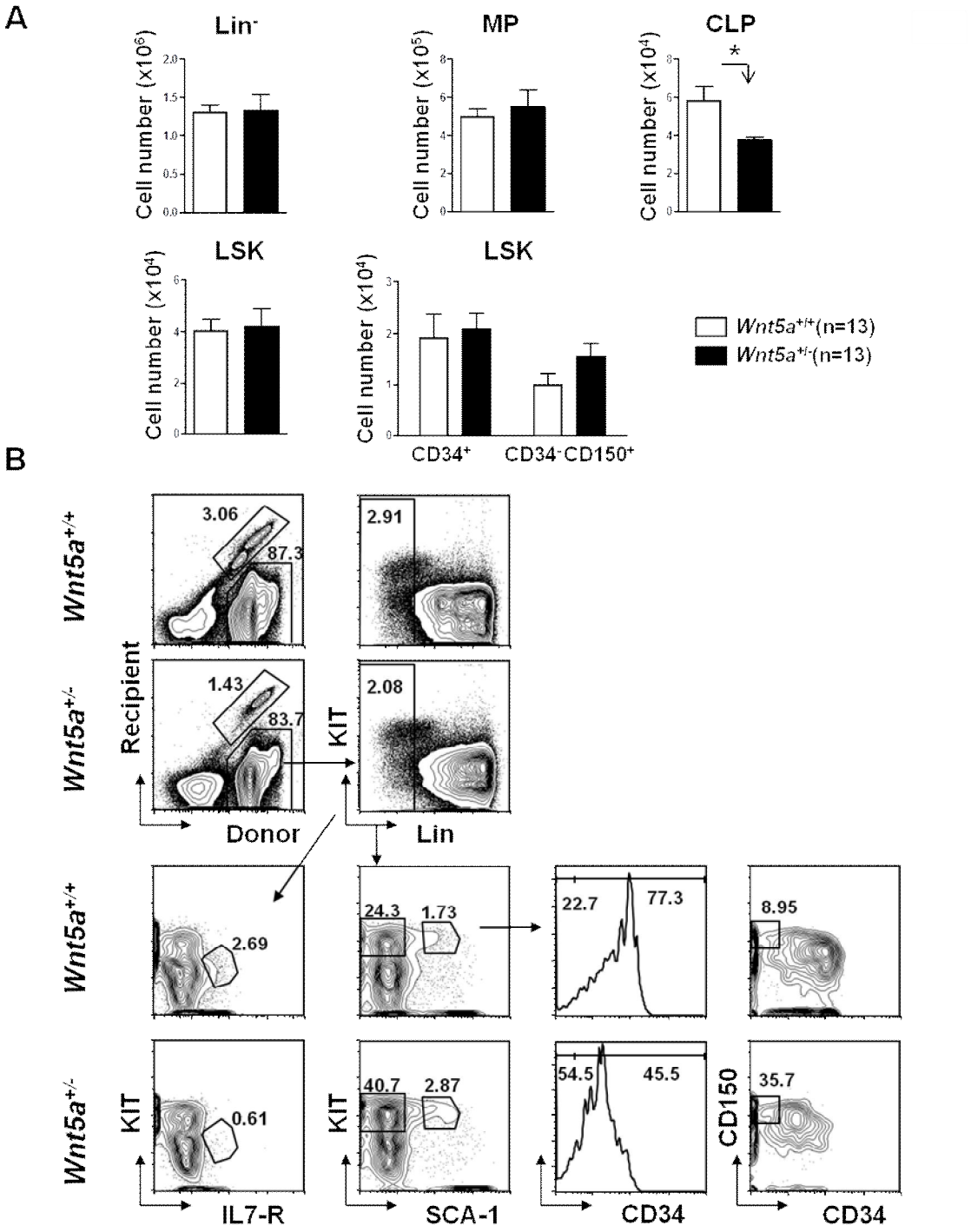

Figure 21. Intrinsic transplantation of *Wnt5a*$^{+/-}$ BM into WT microenvironment. 1° transplantation. **(A)** Sixteen weeks post transplantation, the engraftment levels of HSC and progenitor populations in BM is shown. WT BM cells n=13 (white bars), *Wnt5a*$^{+/-}$ BM cells n=13 (black bars); Mean ± SEM; *p<0.05 **(B)** Representative FACS plots of HSC and progenitor staining.

More comprehensive analysis of the LSK fraction revealed a slight, but not significant increase in absolute number of donor CD150^{+} CD34^{-} LSKs (LT-HSCs) of Wnt5a$^{+/-}$ BM (Figure 21A+B). These results show that *Wnt5a*-deficiency does not in general affect hematopoiesis, but appears to affect regeneration of CLPs.

2° Transplantation

Although engraftment from both Wnt5a donor genotypes was similar in 1° recipients, this does not enable predictions about regeneration of self-renewing HSCs. To find out self-renewing HSCs were regenerated from *Wnt5a*$^{+/-}$ and *Wnt5a*$^{+/+}$ donor HSCs *in vivo*, secondary transplantation of these HSCs was carried out. For this purpose, HSCs were sorted from 1° recipients and were transplanted in equal numbers into lethally irradiated 2° WT (129S2xLy5.1)F1 (Ly5.1xLy5.2 heterozygote) recipient mice (Figure 22A). Figure 22B is representing the sorting strategy for 2° transplantation.

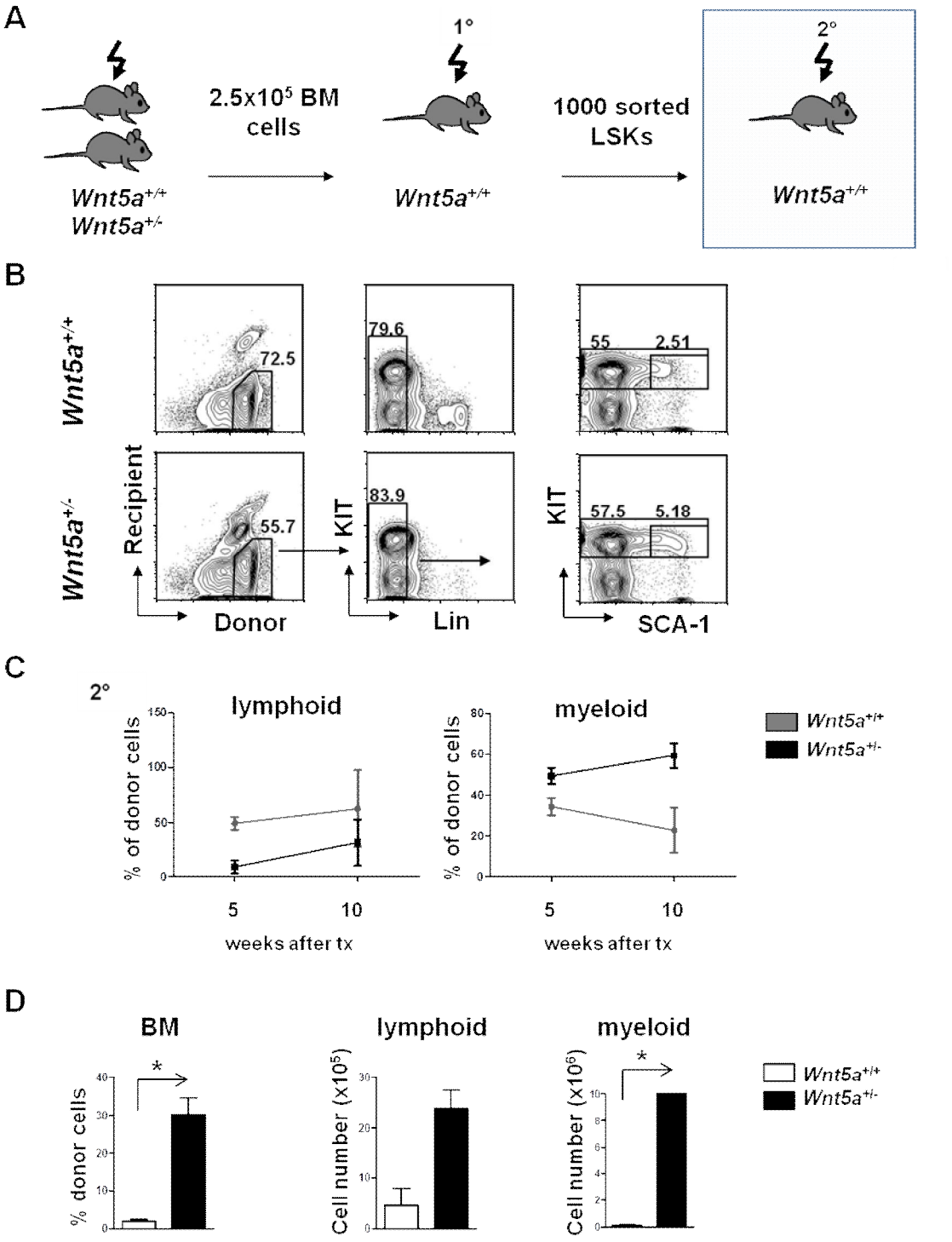

Figure 22. Intrinsic transplantation of Wnt5a$^{+/-}$ BM in WT microenvironment. 2° transplantation. (A) Serial transplantation flow chart. 1000 sorted LSKs (Ly5.2^{+} Lin^{-} KIT^{+} SCA-1^{+}) were transplanted into lethally irradiated WT recipients (2° transplants). 16 weeks post transplantation, BM and PB was isolated and analysed by FACS for hematopoietic stem cells, their progenitor cells and mature cells. **(B)** Sort scheme for 2° transplantation. **(C)** The pattern of lymphoid and the myeloid engraftment in the PB in process after five and ten weeks. **(D)** The engraftment levels in BM of 2° after 16 weeks. WT BM cells n=4 (white bars and grey lines), *Wnt5a*$^{+/-}$ BM cells n=2 (black bars and black lines)

By tracking engraftment in PB after five and ten weeks post transplantation, we found no obvious differences between lymphoid and myeloid engraftment from HSCs regenerated from *Wnt5a*$^{+/+}$ or *Wnt5a*$^{+/-}$ cells in 2° recipients (Figure 22C) In contrast to PB, the analysis of the BM after 16 weeks in 2° transplantation surprisingly revealed a significant higher donor engraftment level of HSCs regenerated from *Wnt5a*$^{+/-}$ HSCs as compared to *Wnt5a*$^{+/+}$ control cells (Figure 22D+23).

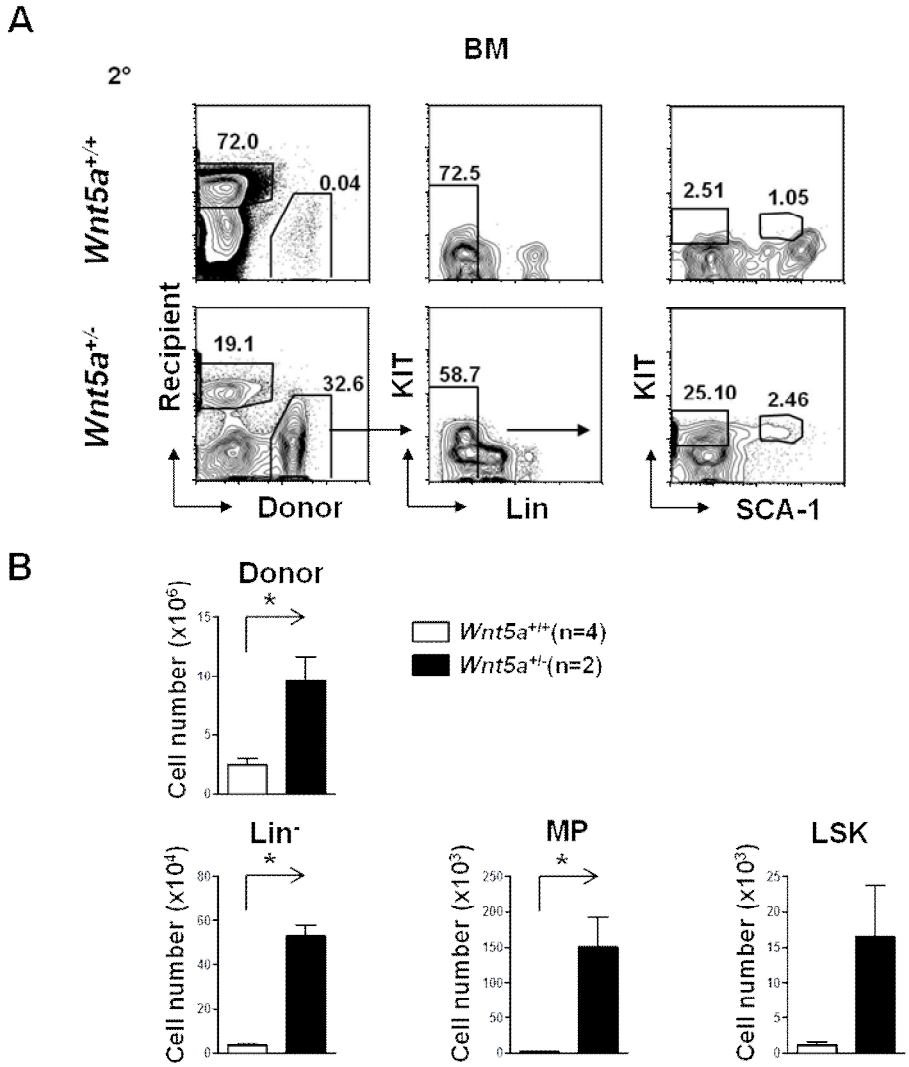

Figure 23. Intrinsic transplantation of *Wnt5a*$^{+/-}$ BM in WT microenvironment. 2° transplantation. (**A**) Representative FACS plots of HSC and progenitor staining **(C)** Sixteen weeks post transplantation, the engraftment levels of HSCs and progenitor populations in BM is shown. Mean ± SEM; *p<0.05.

This increase was also reflected in the absolute cell number of both Lin$^-$ cells and MPs. In addition, the *Wnt5a*$^{+/-}$ derived LSK cells tended to be higher in cell number, but this did not reach significance in our experiments. We performed an additional intrinsic transplantation approach (Chapter 4.4.2), as the 2° engraftment level of the control

group as well as the number of experimental animals was not sufficiently achieved (WT n=4; *Wnt5a*$^{+/-}$ n=2).

4.4.2. Transplantation of sorted LT-HSC

In order to confirm these results and to correct for possible transfer effects of differences in initial donor HSCs (Figure 18B), a second, slightly different approach of intrinsic transplantation was carried out. Notably here, all mice received an equal number (300 cells) of highly purified CD150^{+} CD34^{-} LSK cells from *Wnt5a*$^{+/+}$ and *Wnt5a*$^{+/-}$ donor mice. Cells with this phenotype were highly enriched in HSC activity [11]. Sixteen weeks after regeneration, they were serially transplanted, again using 300 highly purified regenerated donor CD150^{+} CD34^{-} LSK cells per mouse until tertiary transplantation (3°, Figure 24). At each transplantation, mice were analysed for engraftment in PB (five, ten and 16 weeks post transplantation), sacrificed after 16 weeks, and analysed for repopulation of rare populations in the BM (Figure 25A+B).

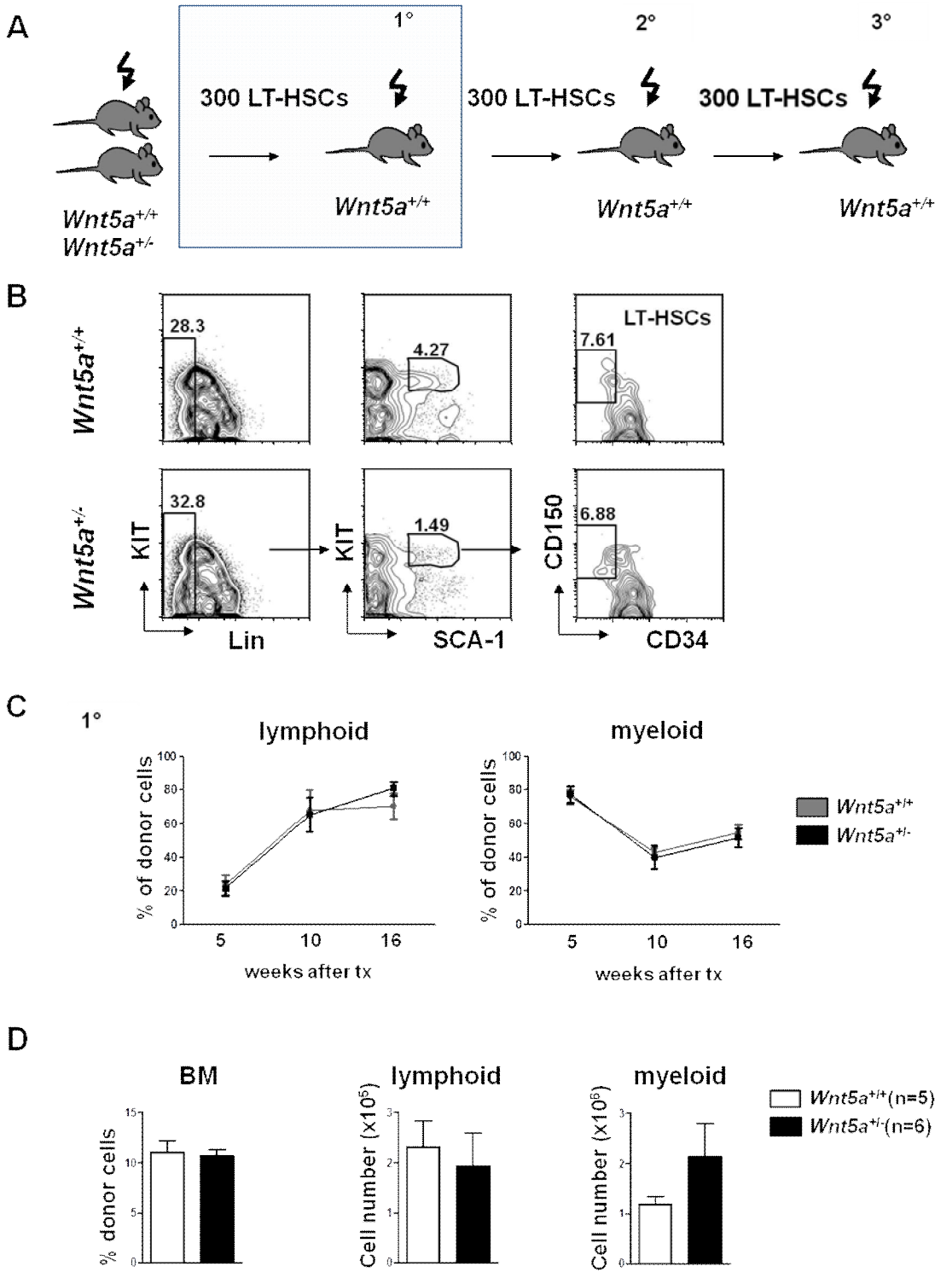

Figure 24. Intrinsic transplantation of *Wnt5a*$^{+/-}$ LT-HSC in WT microenvironment. 1° transplantation. **(A)** Serial transplantation flow chart. 300 sorted LT-HSC (Lin^{-} KIT^{+} SCA-1^{+} CD34^{-} CD150^{+}) cells (Ly5.2) of WT and *Wnt5a*$^{+/-}$ mice were injected into lethally irradiated WT mice (Ly5.1) (1° transplants). 16 weeks post-transplantation, BM and PB was isolated and analysed by FACS for hematopoietic stem cells, progenitor cells and mature cells. **(B)** Sort scheme for 1° transplant. **(C)** The pattern of lymphoid and the myeloid engraftment in the PB of WT and *Wnt5a*$^{+/-}$ cells in process after five, ten and 16 weeks. **(D)** The engraftment levels in BM of 1° after 16 weeks. WT BM cells n=5 engrafted mice out of 8 (white bars and grey lines); *Wnt5a*$^{+/-}$ BM cells n=6 engrafted mice out of 8 (black bars and black lines); Mean ± SEM; *p<0.05;

1° Transplantation

Tracking lymphoid and myeloid engraftment level in PB after five, ten and 16 weeks post transplantation showed no difference in engraftment of *Wnt5a*$^{+/+}$ and *Wnt5a*$^{+/-}$ cells (Figure 24C), which is comparable with the results for PB engraftment in Chapter 4.4.1.

In BM after 16 weeks, the donor engraftment of both genotypes is about 12% of total cells. There is no detectable difference in lymphoid or myeloid engraftment in BM (Figure 24D).

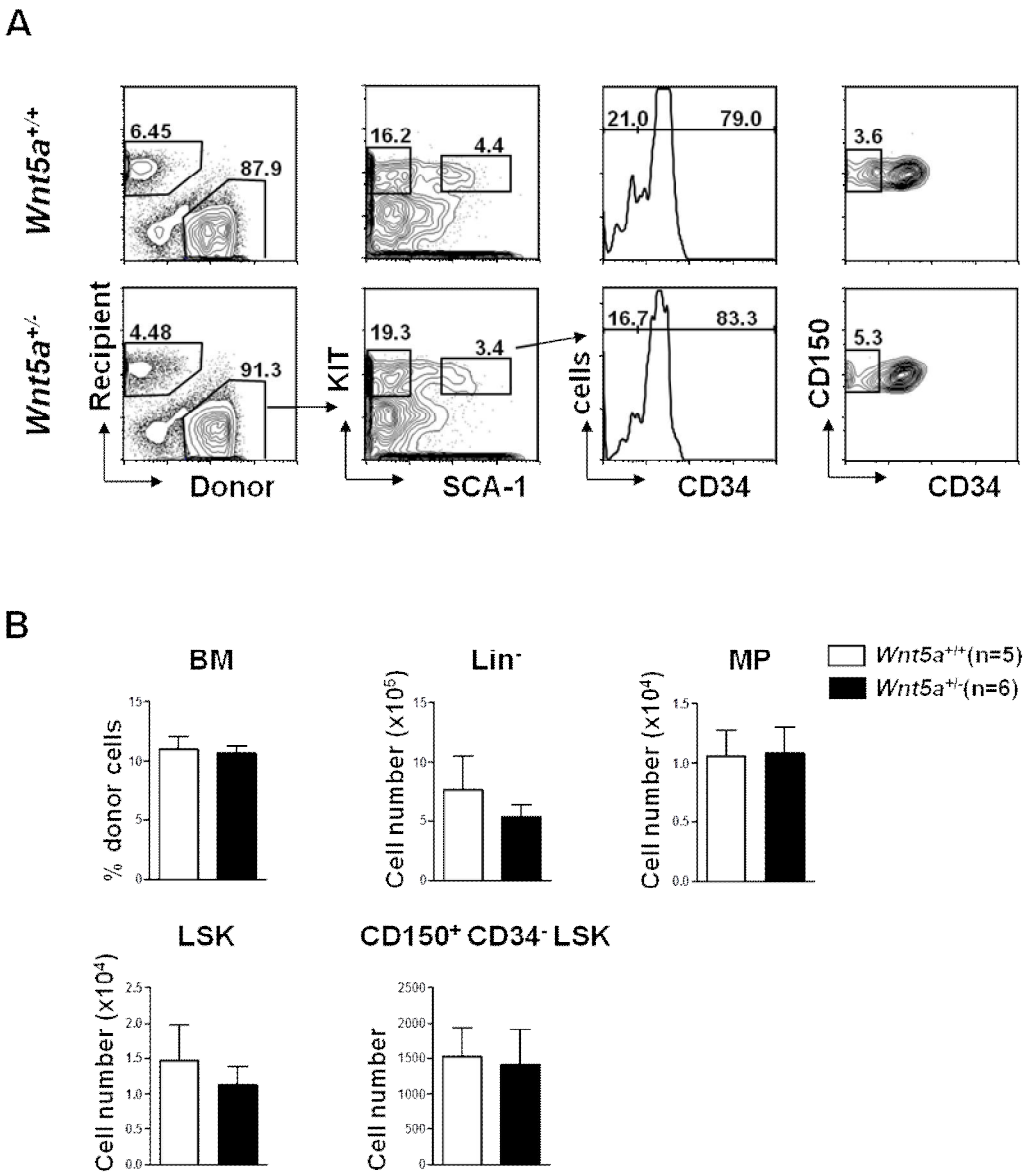

Figure 25. Intrinsic transplantation of *Wnt5a*$^{+/-}$ LT-HSC in WT microenvironment. 1° transplantation. **(A)** Representative FACS plots of HSC and progenitor staining 16 weeks post transplantation, **(B)** The engraftment levels of HSC and progenitor populations in BM is shown. WT BM cells n=5 engrafted mice out of 8 (white bars); *Wnt5a*$^{+/-}$ BM cells n=6 engrafted mice out of 8 (black bars); Mean ± SEM; *p<0.05;

Thus, as in the transplantations with whole BM, in primary recipients there is no detectable difference in the ability of $CD150^+$ LSKs from either WT or *Wnt5a*$^{+/-}$ mice to engraft HSC and progenitor cell populations (Figure 25).

2° Transplantation

In order to find out whether *Wnt5a*$^{+/+}$ and *Wnt5a*$^{+/-}$ HSCs have regenerated different numbers of self-renewing cells *in vivo*, secondary transplantation was carried out. For this purpose, again, highly purified $CD150^+$ $CD34^-$ LSKs (300 cells) of *Wnt5a*$^{+/-}$ and *Wnt5a*$^{+/+}$ BM from 1° transplanted mice were sorted and retransplanted in B6 Ly5.1 mice (Figure 26A). The sort scheme can be seen in Figure 26B.

In the 2° recipients, we observed a lower level of lymphoid engraftment of *Wnt5a*$^{+/-}$ donor cells compared to the control. (Figure 26C), whereas myeloid engraftment level was not affected, compared to WT donor cell engraftment.

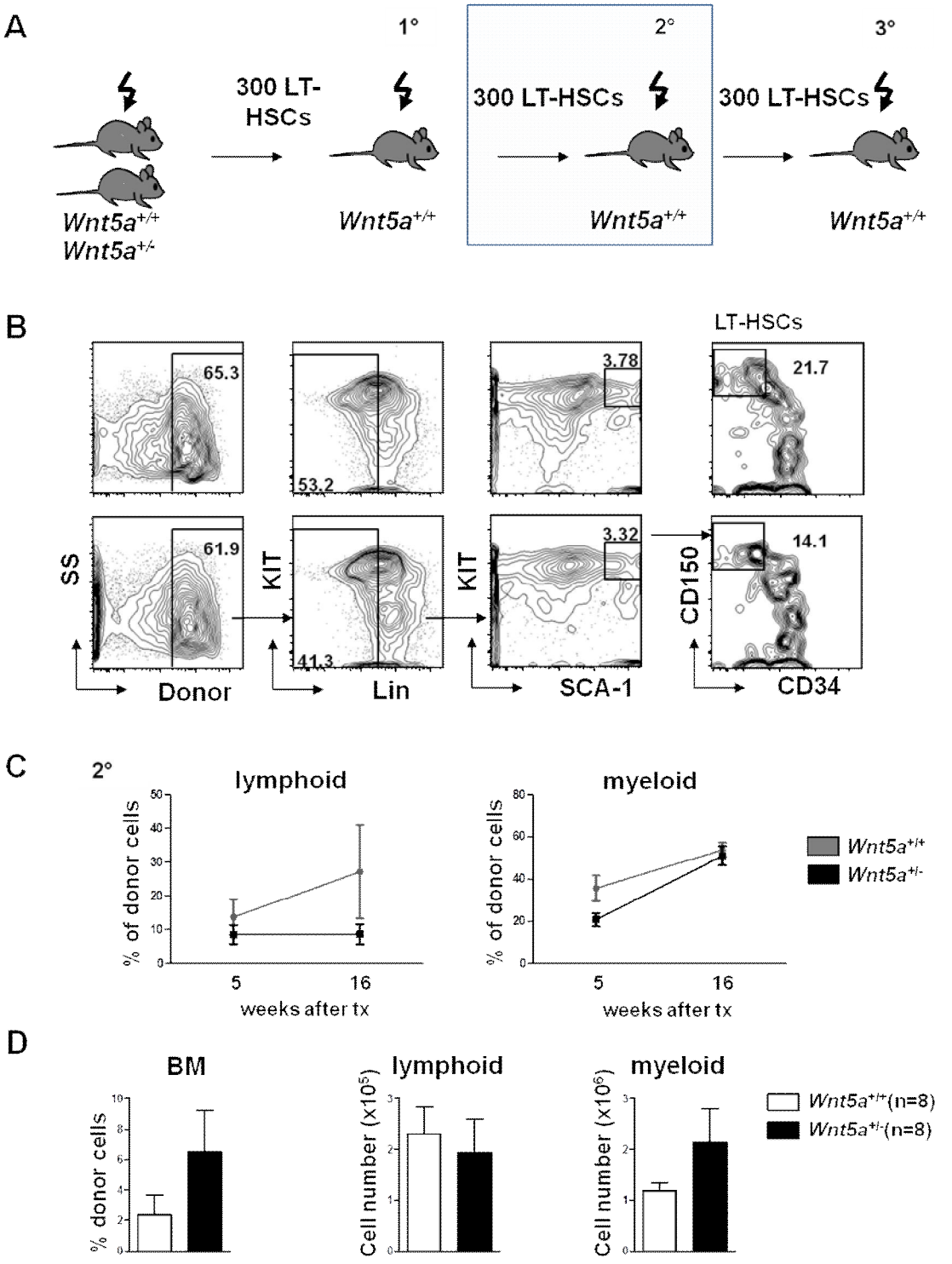

Figure 26. Intrinsic transplantation of *Wnt5a*$^{+/-}$ LT-HSCs in WT microenvironment. 2° transplantation. **(A)** Serial transplantation flow chart. 300 sorted LT-HSC (Lin^{-} KIT^{+} SCA-1^{+} CD34^{-} CD150^{+}) cells (Ly5.2) of WT and *Wnt5a*$^{+/-}$ mice were injected into irradiated WT mice (Ly5.1) (2° transplants). Sixteen weeks post transplantation, BM and PB was isolated and analysed by FACS for hematopoietic stem cells, progenitor cells and mature cells. **(B)** Sort scheme for 2° transplantation. **(C)** The pattern of lymphoid and the myeloid engraftment in the PB of WT and *Wnt5a*$^{+/-}$ cells in process after five and 16 weeks. **(D)** The engraftment levels in BM of 2° after 16 weeks. WT BM cells n=8 engrafted mice out of 8 (white bars); *Wnt5a*$^{+/-}$ BM cells n=8 engrafted mice out of 8 (black bars); Mean ± SEM; *p<0.05;

Interestingly, while in the whole BM transplantation (4.4.1), the engraftment of *Wnt5a*$^{+/-}$ donor HSCs in BM is significantly higher in 2° transplantation after 16 weeks (Figure 22B) compared to WT donor cell engraftment, the engraftment of highly purified *Wnt5a*$^{+/-}$ donor HSC in BM is increased, but doesn't show significant relevance. In addition, while the lymphoid lineage is slightly underrepresented in the BM, myeloid engraftment level is almost 2-fold higher compared with the *Wnt5a*$^{+/+}$ cell engraftment (Figure 26D).

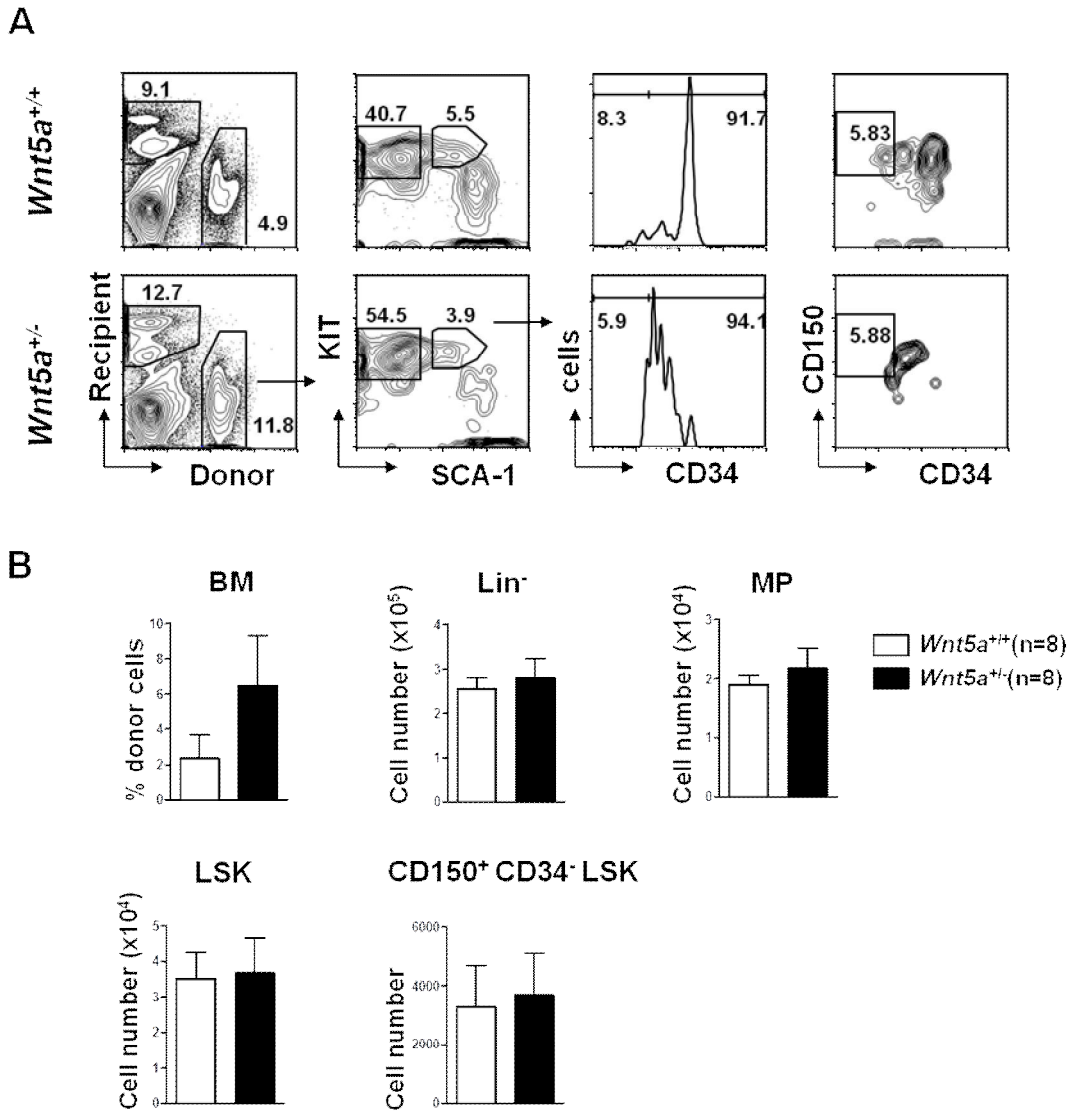

Figure 27. Intrinsic transplantation of *Wnt5a*$^{+/-}$ LT-HSCs in WT microenvironment. 2° transplantation.

(A) Representative FACS plots of HSC and progenitor staining 16 weeks post transplantation, **(B)** The engraftment level of donor cells is shown in percentage. The total cell number of HSC and progenitor populations in BM is shown. WT BM cells n=8 (white bars), *Wnt5a*$^{+/-}$ BM cells n=8 (black bars); Mean ± SEM.

Thus, the result from 2° transplantation of highly purified cells is similar to the 2° transplantation with whole BM: the donor engraftment is higher, especially in the myeloid compartment. Yet, the lymphoid compartment seems unaffected. In absolute cell numbers, however, HSCs and progenitor cells (MP and CLP) appear similar to WT donor HSCs (Figure 27).

Tertiary transplantation (3°)

In order to magnify these mild changes in secondary recipients and verify irreversible changes in HSC behaviour and number later on, the LT-HSC has to get activated again by sort and tertiary transplantation (3°). For this purpose, again, highly purified $CD150^+$ $CD34^-$ LSKs (300 cells) of *Wnt5a*$^{+/-}$ and *Wnt5a*$^{+/+}$ BM from 2° transplanted mice were sorted out and retransplanted in B6 Ly5.1 mice (Figure 28A). The sort scheme can be seen in Figure 28B.

In the 3° recipients, we observed a lower level of lymphoid engraftment of *Wnt5a*$^{+/-}$ donor cells compared to the control (Figure 28C), whereas myeloid engraftment level was unchanged, compared to WT donor cell engraftment.

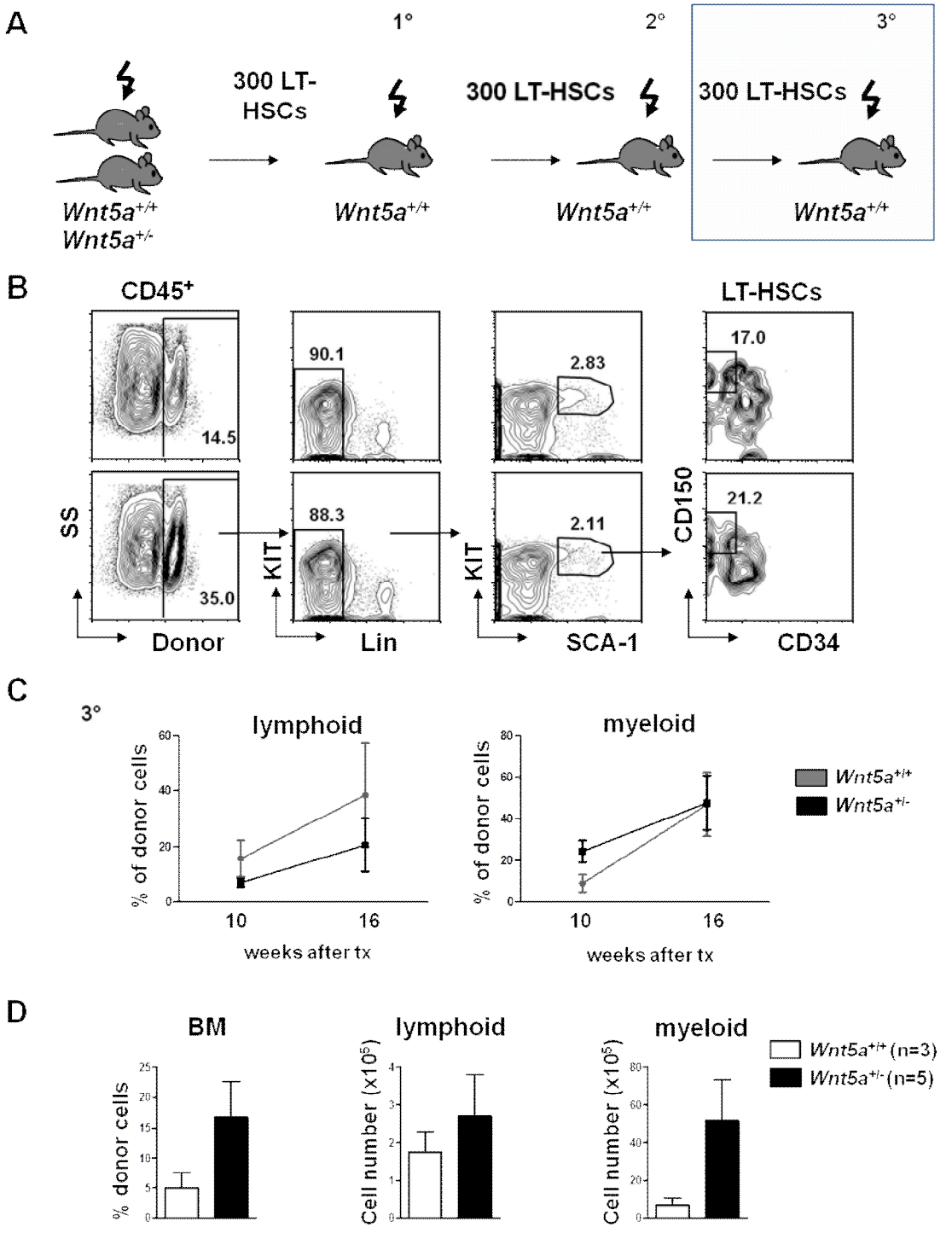

Figure 28. Intrinsic transplantation of *Wnt5a*$^{+/-}$ LT-HSC in WT microenvironment. 3° transplantation. (**A**) Serial transplantation flow chart. 300 sorted LT-HSC (Lin^{-} KIT^{+} SCA-1^{+} CD34^{-} CD150^{+}) cells (Ly5.2) of WT and *Wnt5a*$^{+/-}$ mice were injected into irradiated WT mice (Ly5.1*Ly5.2/F1) (3° transplantation). 16 weeks post transplantation, BM and PB was isolated and analysed by FACS for hematopoietic stem cells, their progenitor cells and mature cells. **(B)** Sort scheme for 3° transplant. **(C)** The pattern of lymphoid and the myeloid engraftment in the PB of WT and *Wnt5a*$^{+/-}$ cells in process after 10 and 16 weeks. **(D)** The engraftment levels in BM of 3° after 16 weeks. *Wnt5a*$^{+/+}$ n=3/5, *Wnt5a*$^{+/-}$ n=5/6.Mean ± SEM; *p<0.05;

In BM of the 3° recipients, the engraftment of *Wnt5a*$^{+/-}$ donor CD150+ CD34- LSKs is not significantly increased. While the lymphoid lineage is unchanged, the myeloid lineage again tends to be slightly, but not significantly higher compared to the *Wnt5a*$^{+/+}$ cell engraftment (Figure 28D).

Analysis of HSCs and progenitor populations in BM of 3° transplantation after 16 weeks, revealed the fact, that despite a good detectable engraftment of both *Wnt5a*$^{+/-}$ and *Wnt5a*$^{+/+}$ donor cells of both lymphoid and myeloid lineages, we were unable to detect donor-type CD150^{+} CD34^{-} LSKs from *Wnt5a*$^{+/-}$ donors (Figure 29A+B, 30).

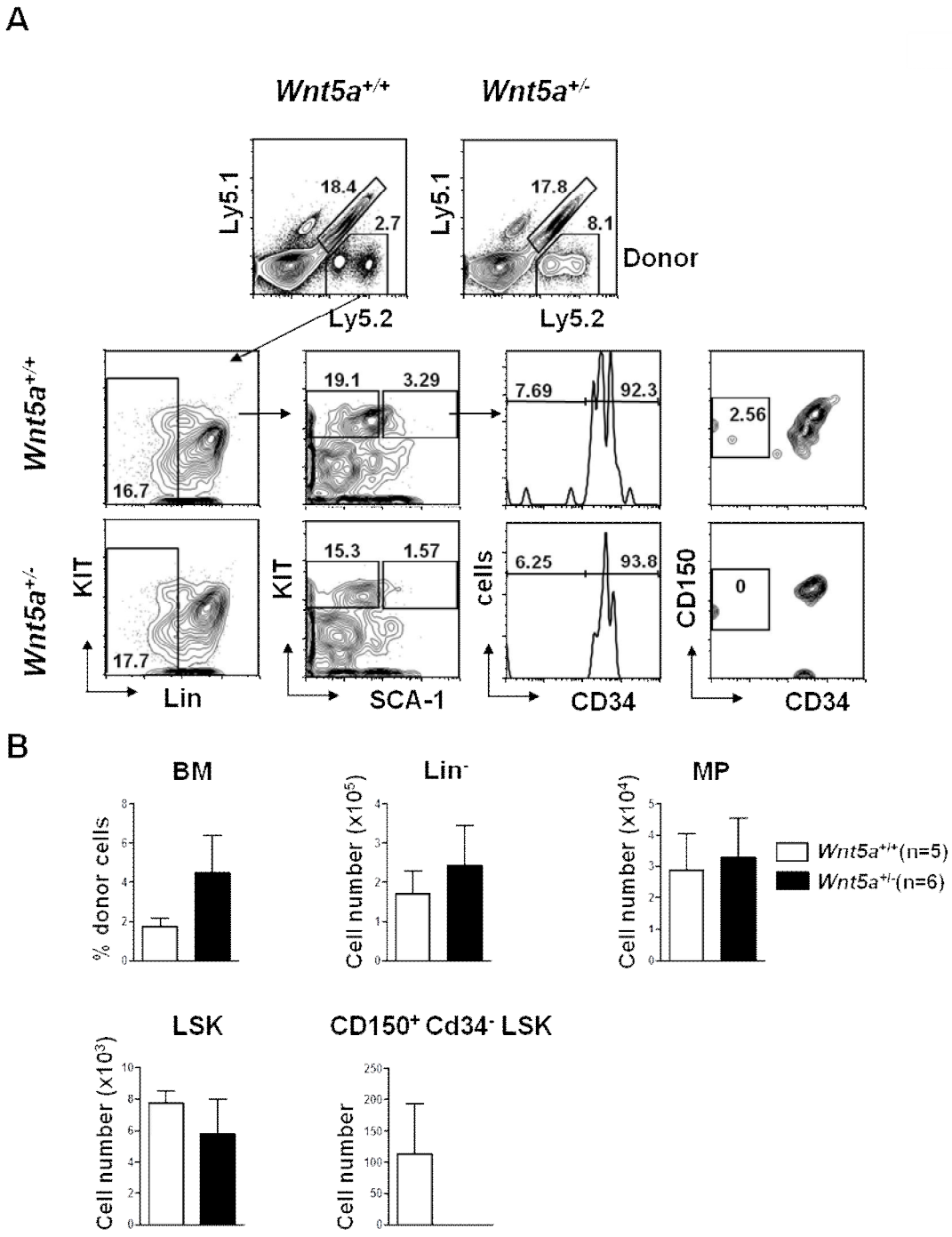

Figure 29. Intrinsic transplantation of *Wnt5a*$^{+/-}$ LT-HSC in WT microenvironment. 3° transplantation. (A) Representative FACS plots of HSC and progenitor staining 16 weeks post transplantation of BM **(B)** The engraftment level of donor cells is shown in percentage. The total cell number of HSCs and progenitor populations in BM is shown. WT BM cells n=5 (white bars); *Wnt5a*$^{+/-}$ BM cells n=6 (black bars); Mean ± SEM.

HSCs are functionally defined by their ability to reconstitute the whole blood system and their ability to self-renew. This task could be managed by asymmetric division [153]. In Figure 30, we demonstrate the self-renewal capacity of WT LT-HSCs compared to *Wnt5a*$^{+/-}$ LT-HSCs in serial transplantations. In every transplantation (1°-3°), *Wnt5a*$^{+/-}$ LT-HSCs show reduced self-renewal ability.

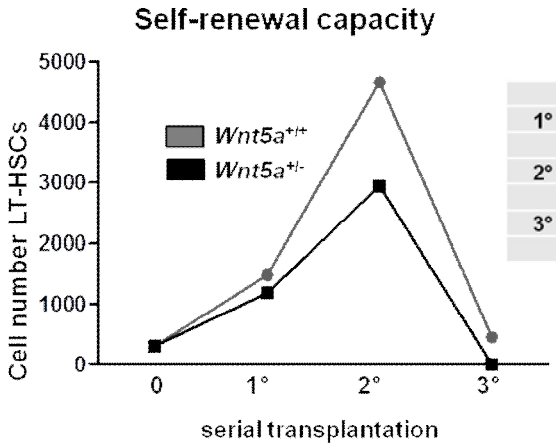

		in	out	fold change
1°	*Wnt5a*$^{+/+}$	300	1475	4,92
	Wnt5a$^{+/-}$	300	1180	3,93
2°	*Wnt5a*$^{+/+}$	300	4666	15,55
	Wnt5a$^{+/-}$	300	2941	9,80
3°	*Wnt5a*$^{+/+}$	300	453	1,51
	Wnt5a$^{+/-}$	300	0	0,00

Figure 30. Capacity for self-renewal of LT-HSCs. Graph showing the capacity for self-renewal of LT-HSCs in total cell number in serial transplantations; WT (grey line); *Wnt5a*$^{+/-}$ (black line); table: total LT-HSCs (in/out/fold change).

Although our inability to detect CD150^{+} CD34^{-} donor cells from *Wnt5a*$^{+/-}$ donors could correspond to HSC exhaustion, the lack of cells from both donor cell genotypes precluded a definitive conclusion on this issue. In conclusion, we found trends in a higher overall and myeloid engraftment, no significant differences were found in engraftment of *Wnt5a*$^{+/+}$ and *Wnt5a*$^{+/-}$ CD150+ CD34- LSKs (LT-HSCs) in 1°, 2°, or 3° transplantations. Based on our findings, we can conclude that there are no obvious intrinsic effects of Wnt5a-deficiency on engraftment of CD150^{+} CD34^{-} LSK cells.

4.5. Study of signalling in LSKs from *Wnt5a*$^{+/-}$ mutant mice

In *Wnt5a*$^{+/-}$ mice, expression of Wnt5a is diminished in all tissues, so both intrinsic and extrinsic effects occur. We here explored possible alterations in signalling pathways and their molecules, which could be involved in HSCs. Wnt5a is a member of the Wnt signalling pathways, which is roughly divided into canonical and non-canonical arms. Canonical Wnt ligands signal through beta- and to a lesser degree through gamma-catenin and are critically involved in cell fate determination and stem/progenitor self-renewal [67] [59], explained in detail in Chapter 1.4. Wnts also signal through beta-catenin-independent or non-canonical pathways that regulate crucial events during

embryonic development. The mechanisms of non-canonical receptor activation are more complex, since different “sub-arms” can be followed in parallel in this pathway. An additional level of complexity is that canonical and non-canonical pathways cross talk, and how Wnts trigger the one as opposed to the other pathway depends on the receptor context expressed by the cell of interest [154].

Wnt5a is mostly known as regulator of non-canonical Wnt signalling through Frizzled and ROR receptors and other molecules, triggering GTP-binding adaptors and a calcium release in the cells. Release of calcium is also one mechanism though which canonical and non-canonical Wnt signalling may cross-talk (Figure 31).

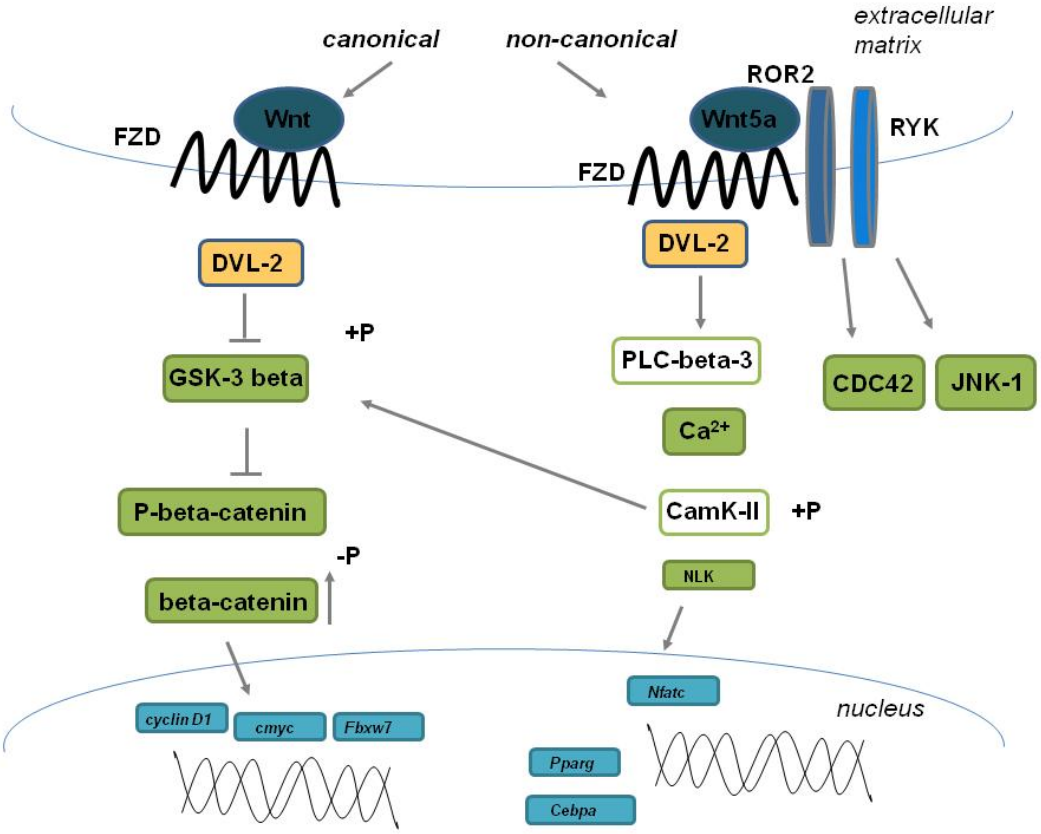

Figure 31. Overview of Wnt5a-dependent Wnt signalling.

In hematopoiesis, much work has been performed about the role of catenin-dependent signalling in normal and malignant development. Yet, not so much is known about the exact role of other members of the pathway and their activation mechanisms in HSCs. In order to chart out and identify possible molecular mechanisms underlying altered Wnt signalling in HSCs from *Wnt5a*$^{+/-}$ mice, we studied several molecules involved in Wnt signalling, downstream of Wnt5a activation [98]. Since it is not feasible to obtain sufficient numbers of early hematopoietic cells for Western blot analyses, we used a

different approach to study signalling in single cells, immunofluorescence staining [59, 99]. For these experiments, LSK, MP and CLP populations were sorted from bone marrow samples of WT (*Wnt5a*$^{+/+}$) and *Wnt5a*$^{+/-}$ adult littermates (Figure 32). After cell sorting, single-cells were stained for different proteins and protein modifications involved in either canonical or non-canonical (alternative) Wnt pathways using immunofluorescence staining.

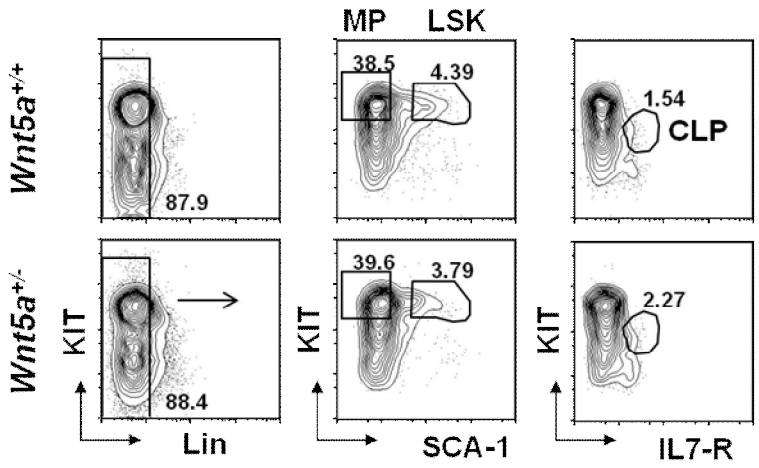

Figure 32. Sorting of MP, CLP and LSK populations out of BM of *Wnt5a*$^{+/+}$ and *Wnt5a*$^{+/-}$ mice. Sorting strategy of BM gated on PI negative cells for MP, CLP and LSK (LT-HSC and ST-HSC).

4.5.1. Canonical Wnt signalling

When canonical signalling is off, the scaffolding protein Axin together with the tumour suppressor APC form a Beta-catenin (beta-catenin) destruction complex that binds cytosolic beta-catenin and enables phosphorylation of beta-catenin by casein kinase 1 (CK1) and glycogen synthase kinase-3 beta (GSK-3 beta). The resulting Phospho-beta-catenin is degraded in the proteosom. Wnt/beta-catenin signalling is turned on through Wnt signals binding to canonical frizzled receptors (Fz) and its co-receptors low-density lipoprotein receptor-related protein 5 and 6 (LRP-5 and LRP-6) The Fz/LRP6 formation via Dishevelled (DVL2) promotes the phosphorylation of LRP-6 through membrane associated GSK-3 beta. The complex recruits Axin to the membrane and disrupts the Axin/APC/GSK-3 beta complex and inhibits the phosphorylation of beta-catenin. This ultimately allows stabilization/ accumulation of beta-catenin, which can then translocate into the nucleus. .Through its binding to TCF/LEF, several genes including *Myc, osteopontin (Spp1), suppressor of cytokine signalling 2 (Socs2), P2Y purinoceptor 14 (P2ry14) and Cyclin-D1 (Ccnd1)* [71]; [72] are transcriptional activated. Our experiments demonstrate that in Wnt5a$^{+/-}$ LSK cells

compared to Wnt5a$^{+/+}$ cells, DVL2 was expressed significantly higher. Additionally, GSK-3 beta protein was reduced, the beta-catenin destruction complex is less active, followed by overexpression of beta-catenin, which is transferred to the nucleus. Accumulated beta-catenin binds to TCF/LEF resulting in transcriptional activation of Cyclin-D1, which is overexpressed in *Wnt5a*$^{+/-}$ LSKs compared to *Wnt5a*$^{+/+}$ LSKs (Figure 33).

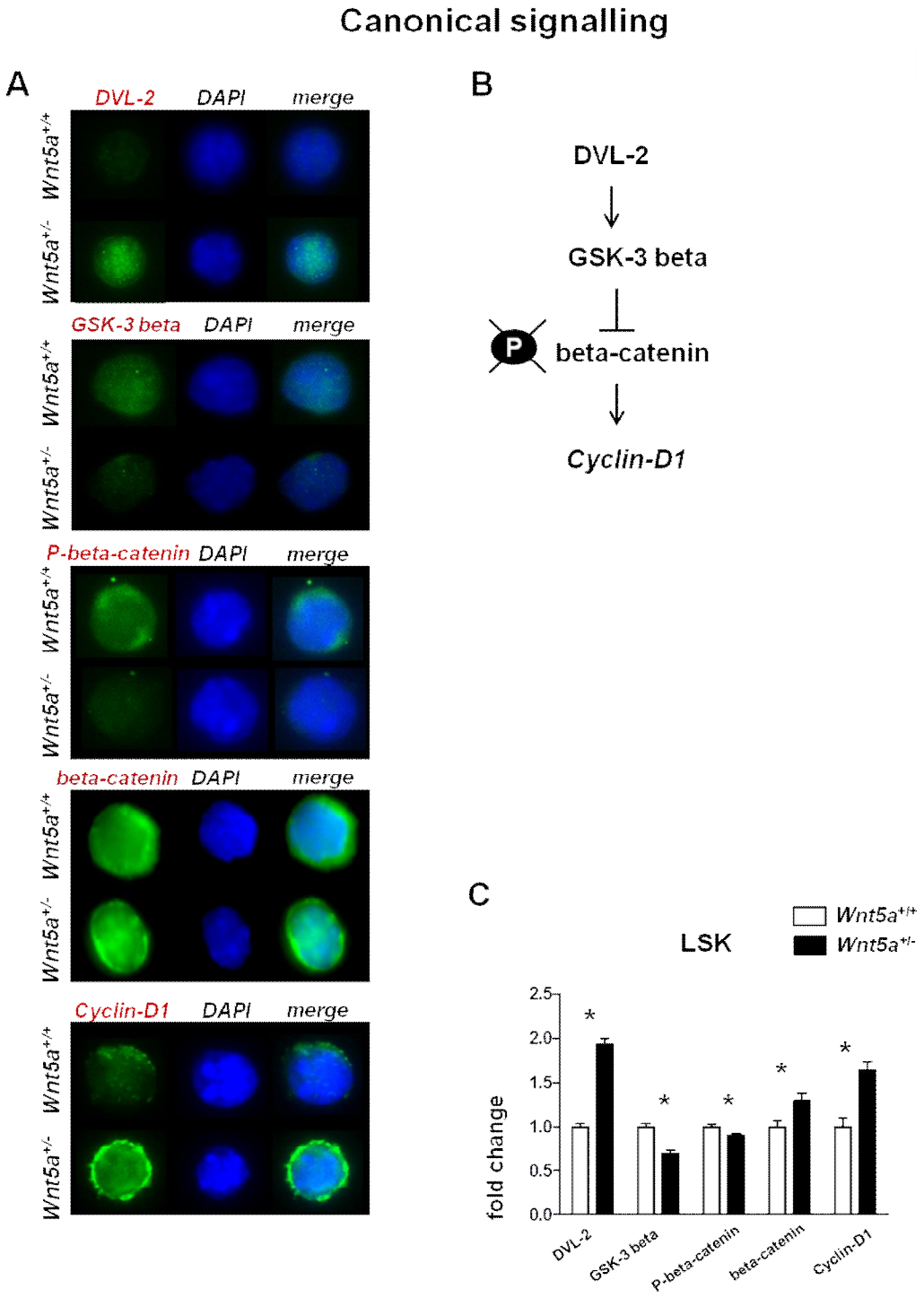

Figure 33. Activation of canonical Wnt signalling through Wnt5a in sorted LSKs. (A) Representative pictures of single-cell stains showing the expression of proteins involved in canonical Wnt signalling (left side), the nuclear counterstaining with DAPI (middle) and merge of both (right). **(B)** Schematic illustration of canonical Wnt signalling **(C)** For quantification of the proteins involved in Wnt/beta-catenin pathway in WT (white bars) and *Wnt5a*$^{+/-}$ (black bars) LSKs, 30 cells were snapped on Leica fluorescent microscope, 100-fold enlarged. Total pixel were quantified by ImageJ; Mean ± SEM; *p<0.05.

As shown in Figure 34, MP and LSK populations are both regulated in a similar manner in canonical signalling, both showing a clear activation (upregulation of DVL2, down regulation of phospho beta -catenin, resulting in upregulation of total beta-catenin. These experiments thus clearly demonstrate that reduction of non-canonical Wnt5a increases canonical signalling in HSCs as well as the progenitor populations, MP and CLP, indicating that Wnt5a is a negative regulator of canonical Wnt signalling in LSK cells.

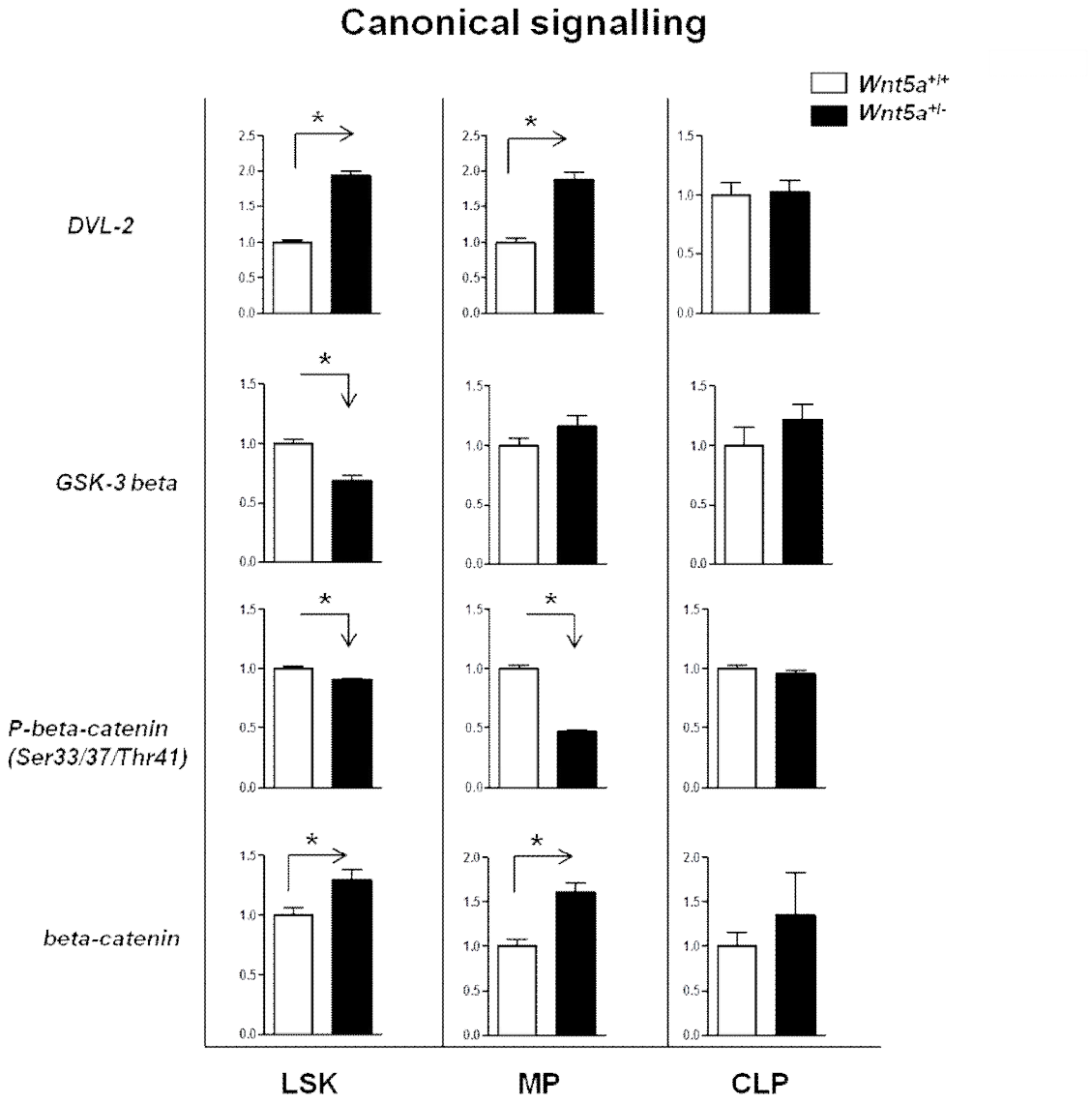

Figure 34. Activation of canonical Wnt signalling through Wnt5a in sorted LSKs, MPs and CLPs. For quantification of the proteins (DVL2, P-beta-catenin and beta-catenin) involved in canonical Wnt signalling in LSK, MP and CLP cell in WT (white bars) and *Wnt5a*$^{+/-}$ (black bars). Total pixel were quantified by ImageJ; Mean ± SEM; *p<0.05.

4.5.2. Non-canonical Wnt signalling

In non-canonical Wnt signalling, the signalling path chosen depends on a number of factors. Where canonical signalling is defined as being transmitted through catenin, non-canonical signalling paths are diverse, defined not only by frizzled and dishevelled receptors, but also using alternative receptors, like ROR1/2 tyrosine kinase receptors which also directly bind some Wnt factors and activate non-canonical signalling through release of Ca^{2+}. Calcium release activates calcium/calmodulin-dependent kinase-II (CaMK-II) and protein kinase C (PKC). The calcium-dependent pathway diverges and can activate the NF-AT-pathway, or the TAK1/NLK pathway which both lead to transcriptional activation. Interestingly, the NLK-mediated pathway inhibits canonical Wnt signalling through phosphorylation of Lef-1 and thereby mediating its subsequent degradation [155]. Thus, through this calcium-dependent pathway, non-canonical Wnt signals inhibit canonical signalling.

To find out whether this pathway is active in HSCs, we first stimulated sorted WT $CD34^-$ $Flk2^+$ LSK cells with Wnt5a and analysed for the Ca^{2+} Influx using flow cytometry. These experiments were performed within the scope of a Wnt5a collaboration. For previous studies of this group, they characterized LT-HSCs as CD34-$Flk2^+$ LSK cells. $Flk2^+$ is like CD150 a surface marker, expressed on LT-HSCs [156]. In reason of comparability, we isolated the cells by staining for Flk2 instead of CD150. As a positive control, Ca^{2+} release was activated by addition of ionomycin. After full stimulation, free Ca^{2+} was quenched by calcium chelator EGTA (Figure 35A). We added murine recombinant Wnt5a to a final concentration of 300 ng/ml after one minute. A Ca^{2+} influx is detectable in LSK cells. After seven minutes a higher concentration of Wnt5a was added (700 ng/ml), resulting in a constantly rising Ca^{2+} influx (Figure 35B). In Figure 35C one can see the measuring in $CD34^-$ and $CD34^+$ LSKs. This plot suggests a stronger response to Wnt5a in LT-HSC ($CD34^-$ LSK) as compared to ST-HSC ($CD34^+$ LSK).

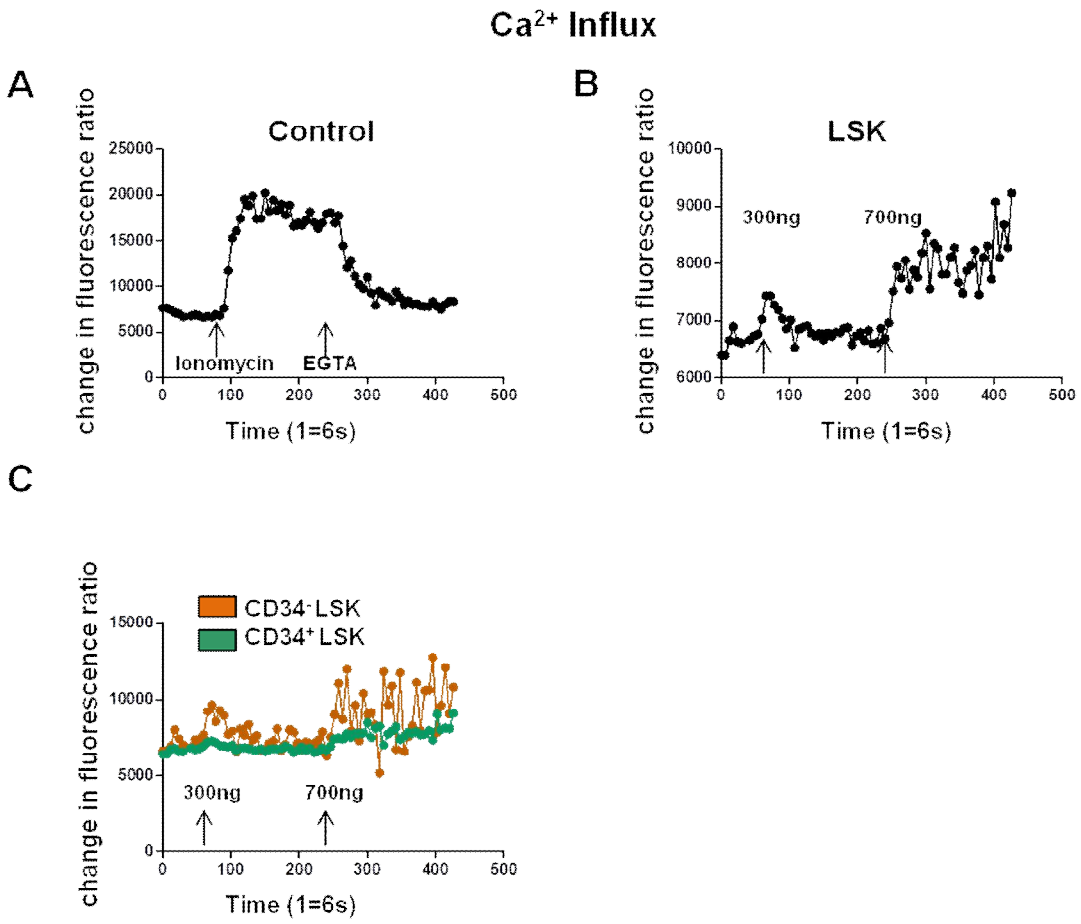

Figure 35. Ca^{2+} influx of LSKs released through Wnt5a The response to Wnt5a was measured by adding murine recombinant Wnt5a to a final concentration of 300 ng/ml 1 min after start of the measurement. After 7 min 700 ng/ml was added. **(A)** Control plot: ionomycin was used as positive control for Ca^{2+} release. EGTA (calcium chelator) served as negative control; **(B)** Ca^{2+} influx measured in sorted LSK; **(C)** Ca^{2+} influx measured in $CD34^-$ and $CD34^+$ LSK population.

This experiment demonstrated that Wnt5a stimulates a calcium response in LSK cells, which appears to be stronger in $CD34^-$ LSKs, which are highest enriched in LT-HSCs [99]. Therefore, we analysed several proteins in *Wnt5a*$^{+/-}$ LSKs, MPs and CLPs that are involved in beta-catenin independent non-canonical Wnt signalling pathways. Here, we investigated two categories of the non-canonical pathway:

The Wnt5a/Ca^{2+} signalling

Figure 35 show that Wnt5a stimulation releases Ca^{2+} in LSK cells, which are highly enriched for HSCs. The increase of Ca^{2+} level in the cell is thought to be regulated by DVL-mediated activation of phospholipase C (PLC). Released Ca^{2+} activates PKC alpha and δ, which in turn may activate the small G protein CDC42, which regulates cell adhesion and tissue separation in *Xenopus* [157], as well as CaMK-II, which

phosphorylates and thereby activates TAK1 (MAP3K7), which activates the NLK kinase and further downstream, the transcription factor NF-AT.

We found that in LSK cells isolated from *Wnt5a*$^{+/-}$ mice, the protein level of DVL2 is significantly higher. As mentioned above, we could show that Wnt5a is a regulator of Ca^{2+} release in HSC. Therefore, we evaluated the protein level of activated CaMK-II (P-CaMK-II). Interestingly, although we observed a significant decrease of whole CaMK-II levels, we found a significant increase in its activated form: P-CaMK-II. This suggests that despite lower CaMK-II levels, it was more activated. This was confirmed by our finding that transcription factors NF-AT and NLK were also expressed at higher levels in *Wnt5a*$^{+/-}$ LSKs (Figure 36).

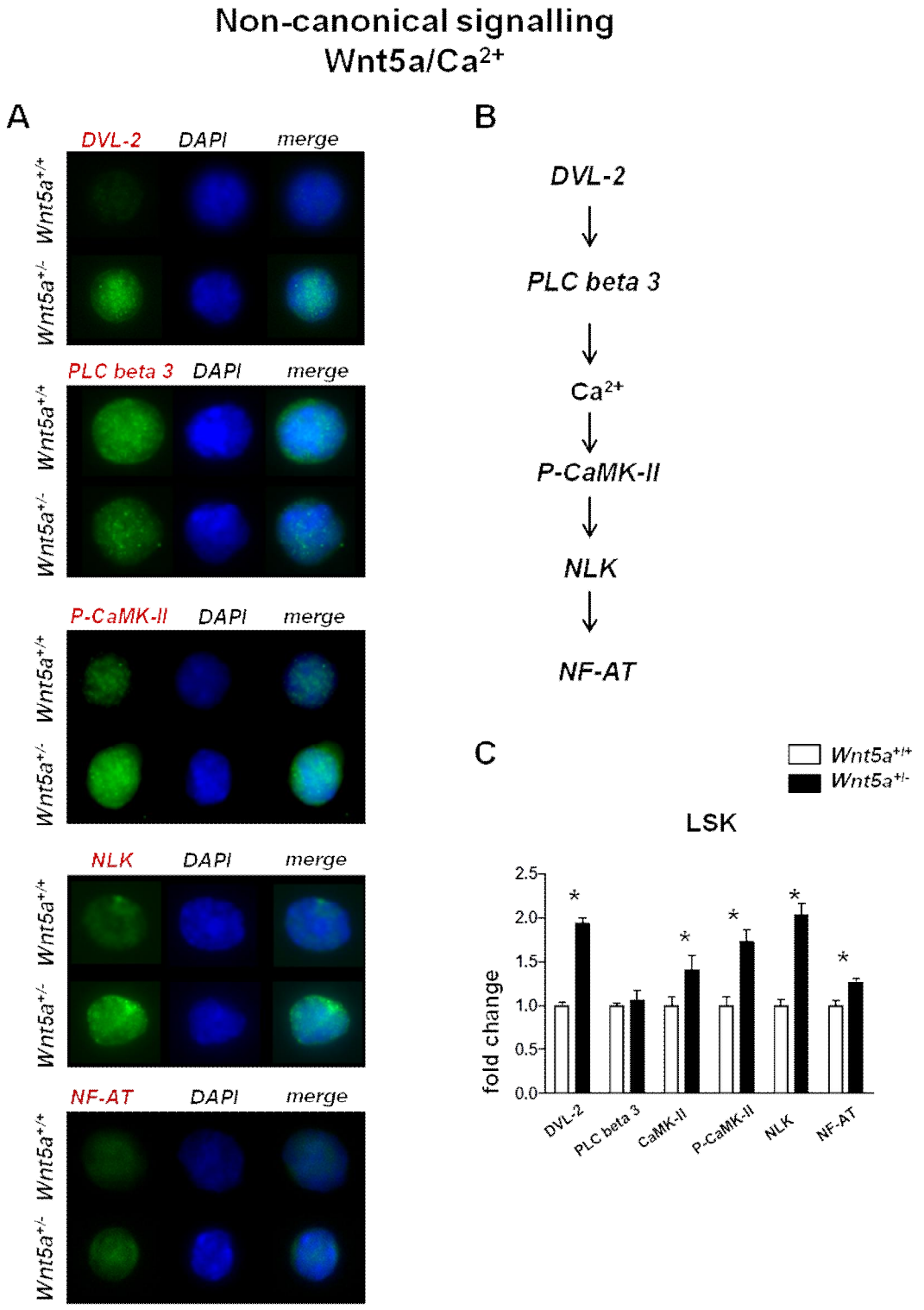

Figure 36. Activation of non-canonical Wnt signalling through Wnt5a in sorted LSK. (A) Single-cell stains showing the expression of proteins (DVL2, P-CaMK-II, NLK, NF-AT) involved in non-canonical Wnt/Ca^{2+} signalling; **(B)** Schematic illustration of non-canonical Wnt5a/Ca^{2+} signalling **(C)** Quantification of the proteins using ImageJ; Mean ± SEM; *p<0.05. **(A)** Representative pictures of single-cell stains showing the expression of proteins (DVL2, P-CaMK-II, NLK, NF-AT) involved in non-canonical Wnt signalling (left side), the nuclear counterstaining with DAPI (middle) and merge of both (right). **(B)** Schematic illustration of non-canonical Wnt/Ca^{2+} signalling **(C)** For quantification of the proteins involved in Wnt/Ca^{2+} pathway in WT (white bars) and *Wnt5a*$^{+/-}$ (black bars) LSKs, 30 cells were snaped on Leica fluorescent microscope, 100-fold enlarged. Total pixel were quantified by ImageJ; Mean ± SEM; *p<0.05.

Non-canonical Wnt signalling was also investigated in progenitor cells. Interestingly, we found that the results not always corresponded to those observed in LSK cells. For instance, although in MPs, DVL2 and P-CaMK-II are significantly higher expressed in Wnt5a$^{+/-}$ cells, there is no impact on the protein levels of NF-AT and NLK in MP detectable. In CLP from Wnt5a$^{+/-}$ mice show a lower level of active P-CaMK-II level and like in LSK cells, but despite this observation, a higher level of the kinase NLK was found (Figure 37).

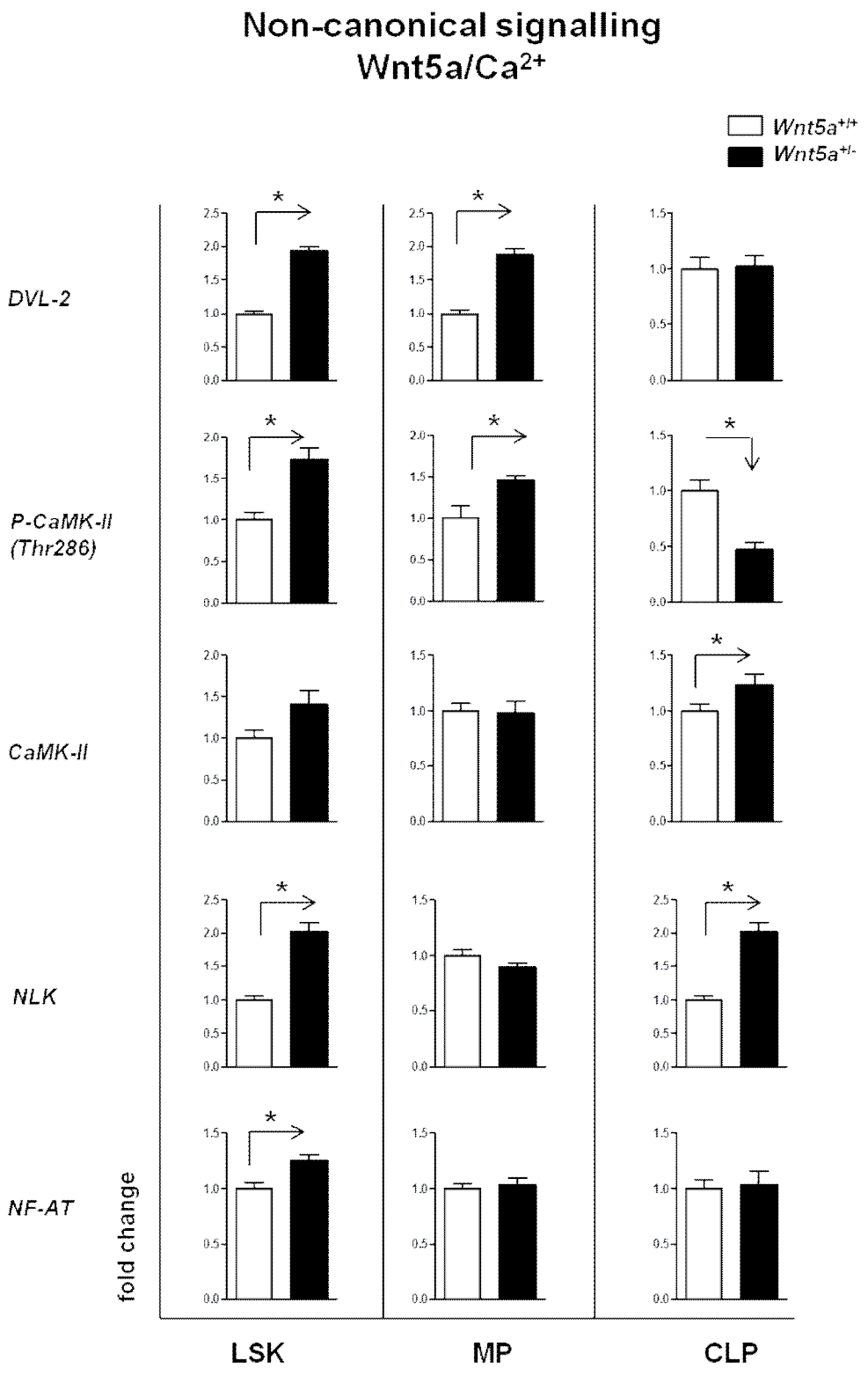

Figure 37. Activation of non-canonical Wnt signalling through Wnt5a in sorted LSKs, MPs and CLPs. For quantification of the proteins (DVL2, CaMK-II, P-CaMK-II, NLK, NF-AT) involved in non-canonical Wnt5a/Ca^{2+} signalling in LSK, MP and CLP cell populations in WT (white bars) and *Wnt5a*$^{+/-}$ (black bars). Total pixel were quantified by ImageJ; Mean ± SEM; *p<0.05.

The Wnt5a/PCP (planar cell polarity) signalling arm

This non-canonical pathway is stimulated through Frizzled, Dishevelled or ROR2 and primarily modulates cell cytoskeletal changes required for cell movement and cell division. This pathway is first detectable during embryogenesis and may involve the Wnt5a-binding ROR2 receptor tyrosine kinase and Frizzled 2. Downstream of CDC42, this arm of non-canonical signalling involves the Jun-N-terminal kinase (JNK), the activated P-JNK and CDC42. In our experiments, we demonstrated that ROR2 and P-JNK1 expression is unchanged in LSKs, even though JNK1 total protein is significantly decreased in LSKs (Figure 38).

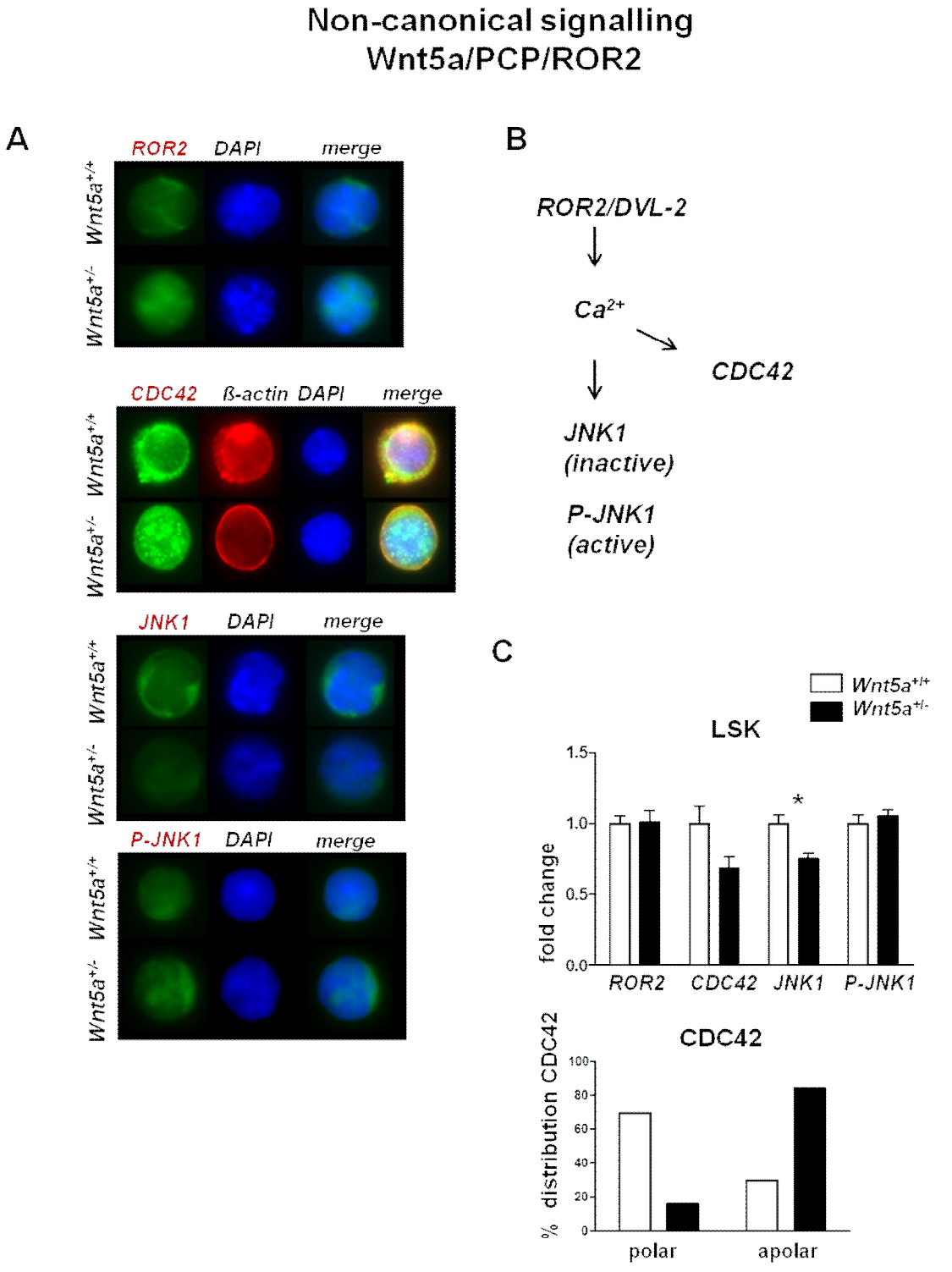

Figure 38. Activation of non-canonical Wnt/PCP/ROR2 signalling through Wnt5a in sorted LSK. (A) Representative pictures of single-cell stains showing the expression of proteins (ROR2, CDC42, JNK1, P-Jnk1) involved in non-canonical Wnt/PCP/ROR2 signalling (left side), the nuclear counterstaining with DAPI (middle) and merge of both (right). Double staining was carried out for CDC42 and beta-actin **(B)** Schematic illustration of non-canonical Wnt/PCP/ROR2 signalling **(C)** For quantification of the proteins involved in Wnt/PCP/ROR2 pathway in WT (white bars) and *Wnt5a*$^{+/-}$ (black bars) LSKs, 30 cells were snaped on Leica fluorescent microscope, 100-fold enlarged. Total pixel were quantified by ImageJ; polar and apolar distribution of CDC42 was measured; Mean ± SEM; *p<0.05.

Notably, the level of CDC42 was not significantly changed in *Wnt5a*$^{+/-}$ LSKs, but the frequency of polarity, which is important for proper cell movement [158-159], was noticeably reduced. Beta-actin was stained additionally, also known as cytoskeletal actin in order to detect cytoskeletal structures. In *Wnt5a*$^{+/-}$ LSKs, CDC42 is contributed apolar. Florian *et al.* demonstrated an increased CDC42 activity in aged HSCs, which is associated with a high percentage of apolarity for tubulin and CDC42 [99].

In summary, we showed that Wnt5a stimulates calcium release in LSK cells. In addition, LSK cells isolated from *Wnt5a*$^{+/-}$ mice a higher level of both beta-catenin-dependent canonical and NF-AT-dependent non-canonical signalling over CaMK-II and JNK1, but a reduced level of CDC42 and cellular polarization. This finding suggests that Wnt5a negatively regulates both canonical and non-canonical CAMK-II --> NLK --> NF-AT signalling, but stimulates the CDC42 Rho-GTPase-dependent pathway in LSK cells.

4.5.3. Cell cycle analysis by immunofluorescence

The upregulation of canonical Wnt targets such as Cyclin-D1 suggests that a decrease of Wnt5a in HSCs may increase the proliferative activity of these cells. In Chapter 4.5.1 the upregulation of the major mediator beta-catenin could be already shown in *Wnt5a*$^{+/-}$ LSKs and MPs. Cyclin-D1 is a downstream transcriptional target of the beta-catenin/TCF/LEF pathway and is known to regulate G1-S transition of the cell cycle. Since the CD34^{-} LSKs are increased in *Wnt5a*$^{+/-}$ mice, we studied molecules involved in cell cycle regulation in these cells: Cyclin-D1, PPAR gamma (PPARγ), C/EBP alpha (C/EBPα) and the F-box protein Fbxw7. Cyclin-D1 and C/EBP alpha are both involved in regulation of HSC self-renewal [160-161]. PPAR gamma, as a transcription factor, is responsible for the expression of C/EBP alpha [162-163]. *Cebpa* knockout mice showed impaired adipogenesis and reduced size and number of mitochondria per cell, suggesting a role in mitochondrial biogenesis. The F-box protein Fbxw7 is known to regulate leukemic stem cell quiescence by reducing the level of *c-myc* [164], a further direct transcriptional target of beta-catenin.

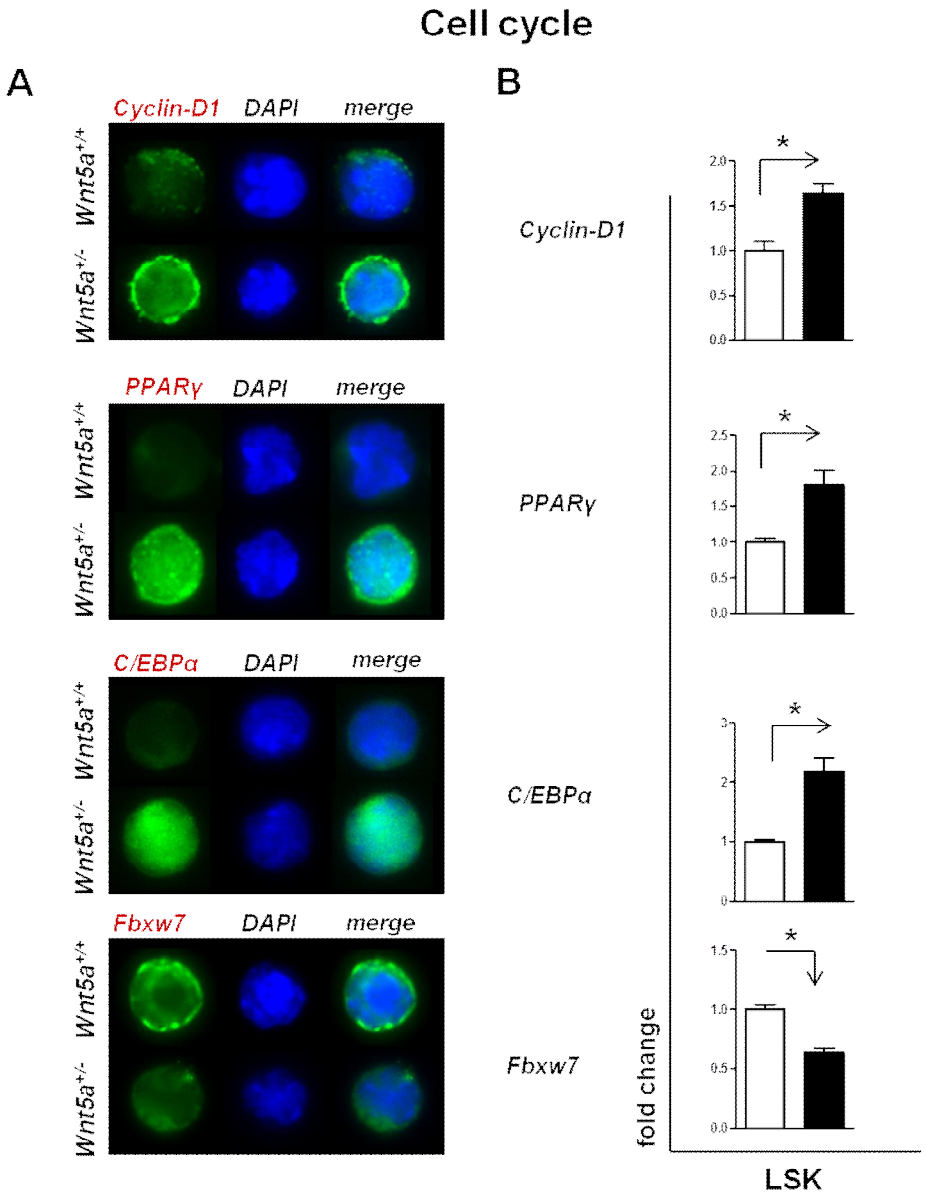

Figure 39. Expression of proteins that are involved in cell cycle regulation in sorted *Wnt5a*$^{+/+}$ and *Wnt5a*$^{+/-}$ LSKs. (A) Single-cell stains showing the expression of proteins (Cyclin-D1, PPARγ, C/EBPα , Fbxw7) involved in cell cycle regulation in LSKs during steady-state conditions; **(B)** Quantification of the protein levels using ImageJ; Mean ± SEM; *p<0.05. **(A)** Representative pictures of single-cell stains showing the expression of proteins (Cyclin-D1, PPARγ, C/EBPα, Fbxw7) involved in cell-cycle regulation (left side), the nuclear counterstaining with DAPI (middle) and merge of both (right). **(B)** For quantification of the proteins involved in cell-cycle regulation in WT (white bars) and *Wnt5a*$^{+/-}$ (black bars) LSKs, 30 cells were snaped on Leica fluorescent microscope, 100-fold enlarged. Total pixel were quantified by ImageJ; Mean ± SEM; *p<0.05.

In sorted LSK cells from eight to ten weeks old *Wnt5a*$^{+/+}$ and *Wnt5a*$^{+/-}$ mice, it could be shown that the increased beta-catenin levels are associated with a significant increased expression of catenin targets: Cyclin-D1, as well as the transcription factors PPARγ and C/EBPα are significantly upregulated. At the same time, the Fbxw7 protein, a component of the SCF^{Fbxw7} ubiquitin ligase which promotes quiescence, is

downregulated in LSKs of *Wnt5a*$^{+/-}$ mice [165]. All together, these results strongly suggest that Wnt5a dampens cell cycle progression in LSK cells (Figure 39), MPs and CLPs (Figure 40).

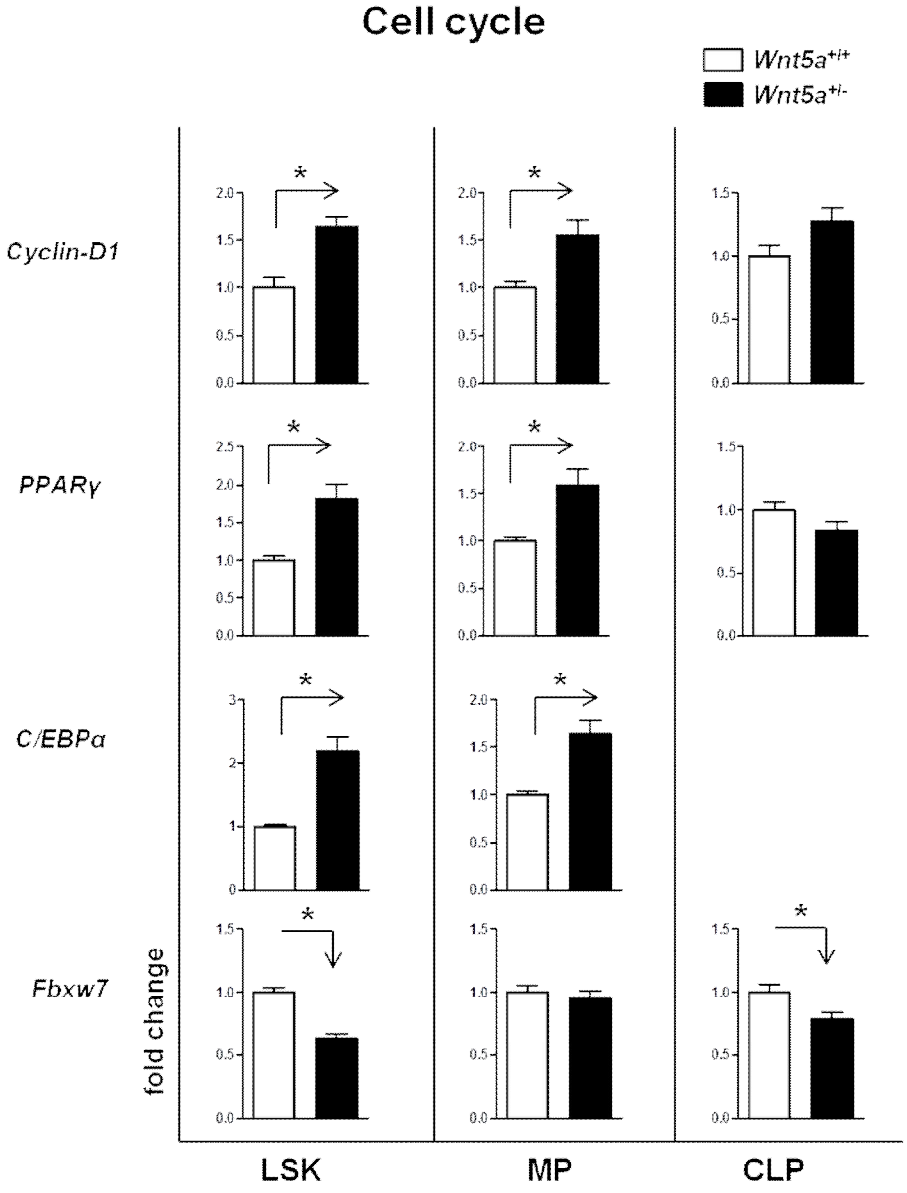

Figure 40. Expression of proteins that are involved in cell cycle regulation in sorted *Wnt5a*$^{+/+}$ and *Wnt5a*$^{+/-}$ LSKs, MPs and CLPs. For quantification of the protein level of molecules (Cyclin-D1, PPARγ, C/EBPα and Fbxw7) involved in cell cycle regulation in LSK, MP and CLP cell populations in WT (white bars) and *Wnt5a*$^{+/-}$ (black bars). Total pixel were quantified by ImageJ; Mean ± SEM; *p<0.05.

Wnt5a is highly expressed in stromal cells surrounding the HSCs in steady state conditions. The isolated HSCs resided for eight to ten weeks in a *Wnt5a* deficient microenvironment before the cells got isolated for immunofluorescence analysis and intrinsic transplantation assay. We assume that this time in the *Wnt5a*-deficient

microenvironment can condition the HSCs. Also, apparently, all of these changes in signalling do not result in lasting effects on the repopulating ability of *Wnt5a*$^{+/-}$ HSCs transplanted in a WT environment, suggesting that most of the signalling changes are, in fact, caused by extrinsic mechanisms. The extrinsic effect on the HSCs will be further examined in the next chapter.

4.6. Characterization of the niche compartment in B6;129S2-Wnt5atm1Amc/J mice

During homeostasis, the BM niche is known to support HSC by maintaining the balance between quiescence, self-renewal and differentiation [23, 25]. After bone marrow transplantation, the donor HSCs have to home and engraft to the niche and interact with the niche in order to restore homeostatic milieu [21]. Till now, although signalling between niche and the engrafting HSCs is not yet discovered many recent studies tried to identify the cellular components of the niche and their signalling pathways [166-167]. Osteoblasts have been shown be part of the endosteal niche and are known to support hematopoiesis in vitro [168-169]. As we detected in Chapter 4.2., Wnt5a as soluble signal from the niche is important for HSC maintenance *in vitro*. Co-cultures with HSCs on *Wnt5a*$^{-/-}$ AGM primary stroma, showed reduced colony forming ability. Thus, in the following paragraph, we transplanted WT BM cells into Wnt5a deficient microenvironment and studied Wnt5a-dependent microenvironmental effect on the WT cells by analyzing their self-renewal and differentiation ability by serial transplantation. Since we have shown in Chapter 4.4.1 and 4.4.2 that there is no intrinsic effect of *Wnt5a*-deficiency, the extrinsic role of Wnt5a might be more important. Additionally, we tested the homing efficiency and signalling pathways of the WT cells (1° Wnt5a$^{+/-}$). Furthermore, we characterized the components of the BM niche in Wnt5a$^{+/-}$ mice, as it was shown before that Wnt5a/Ror2 signalling plays a role in the biology of mesenchymal stem cells [170] [171].

4.6.1. Transplantation of BM into *Wnt5a*-deficient microenvironment (Extrinsic)

Loss of Wnt5a in stromal cells had severe effects on the production of hematopoietic progenitors in *in vitro* co-culture experiments (Figure 9, Chapter 4.2.). In order to assess the extent of a possible extrinsic effect *in vivo*, we analysed engraftment of WT Ly5.1 HSC in *Wnt5a*$^{+/-}$ and littermate WT control mice (primary transplants, 1°). For this

purpose, WT HSCs were transplanted into irradiated, *Wnt5a*-deficient mice and followed for their development into all lineages. During secondary transplantation of the 1° WT cells into WT microenvironment, one can analyse the quality of the HSC concerning their self-renewal capacity.

Primary transplantation (1°)

In this experiment, we transplanted bone marrow cells of B6.SJL (Ly5.1, CD45.1) mice intra-hepatically into lethally irradiated new born pups of B6;129S2-Wnt5atm1Amc/J. This experiment was not planned with adult mice, because of sensitivity of this knockout mouse strain to opportunistic infections (by bacterial strains (Streptococcus) not monitored by FELASA procedures) and consequent lethality after irradiation within 2 weeks, despite co-injection of helper cells. Transplanted newborns, were analysed for engraftment in PB of juvenile and adult animals (five, ten and 16 weeks post transplantation), sacrificed at 16 weeks and analysed for repopulation of rare populations in the BM and Spleen (Figure 41). Like in the previous experiments, the donor cells could be distinguished from the recipient cells, by expression of different CD45 (Ly-5) isoforms (CD45.1/CD45.2) and analysis by flow cytometry.

In PB, the engraftment in *Wnt5a*$^{+/+}$ and *Wnt5a*$^{+/-}$ recipients was very similar in both myeloid and lymphoid engraftment after five, ten and 16 weeks (Figure 41B). Sixteen weeks after transplantation in 1° recipients, we observed in BM a tendentially lower engraftment of WT cells in *Wnt5a*$^{+/-}$ microenvironment. The engraftment level in the Spleen is unchanged. The maintenance of donor LSKs and MPs of 1° *Wnt5a*$^{+/-}$ was unchanged, however the ratio on LT-HSC (CD34^{-} CD150^{+} LSK) was slightly, but not statistically significantly decreased (Figure 41C).

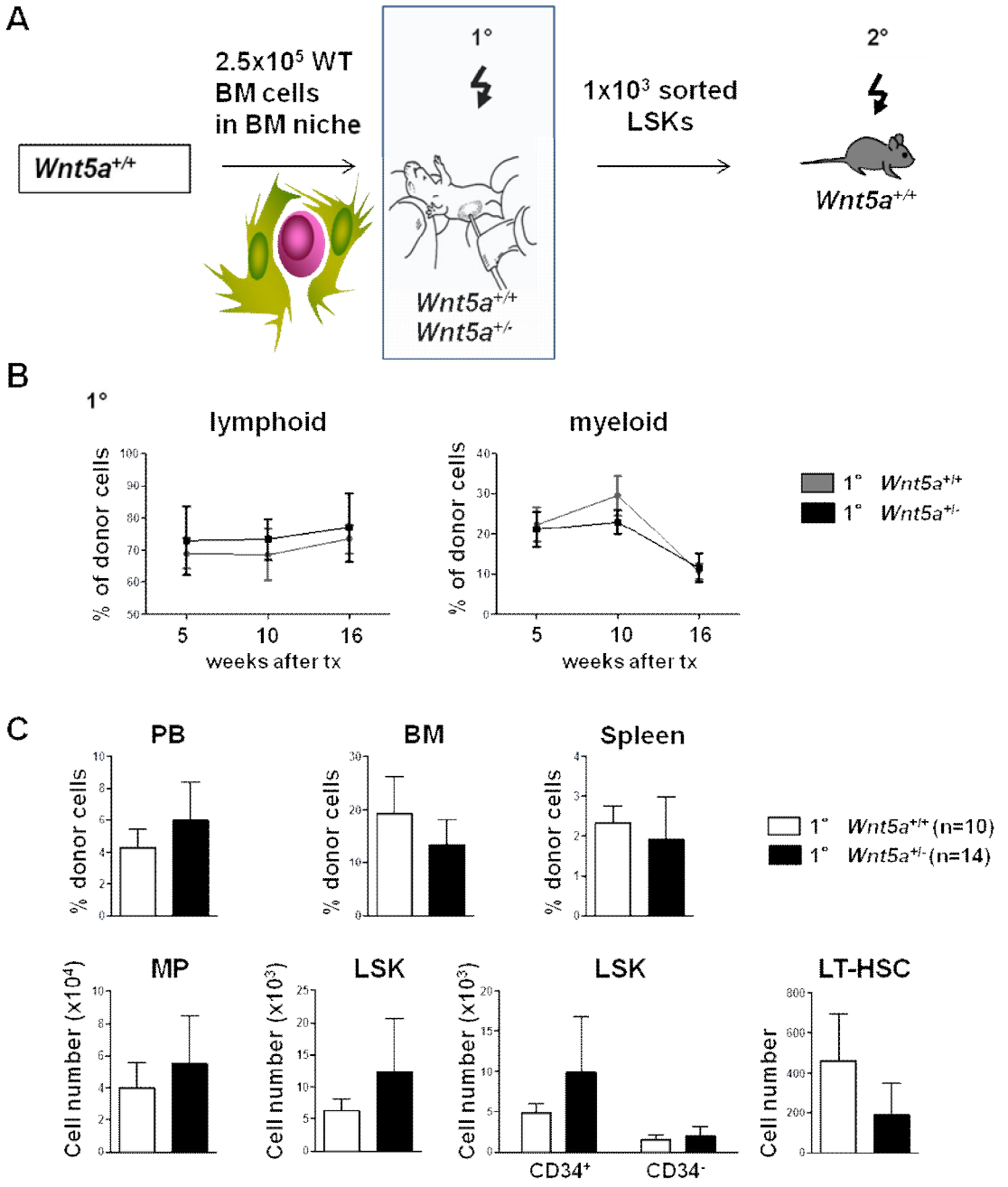

Figure 41. Extrinsic regulation of WT HSC engraftment in the *Wnt5a*$^{+/-}$ microenvironment. 1° transplantation. **(A)** Serial transplantation flow chart. 250 000 whole bone marrow (BM) cells (Ly5.1) were intra-hepatically injected into lethally irradiated newborn pubs of *Wnt5a*$^{+/-}$ mice and their WT littermates (1° transplants). Sixteen weeks post transplantation, BM, Spleen and PB were isolated and analysed by FACS analysis for hematopoietic stem cells, their progenitor cells and mature cells. **(B)** The pattern of lymphoid and the myeloid engraftment in the PB of WT cells in different microenvironments in process after five, ten and 16 weeks. **(C)** The engraftment levels in PB, BM and Spleen of 1° after 16 weeks. **(D)** Absolute numbers of engrafted MP, LSK and LT-HSC in the BM of primary recipients. 1° WT n=10 (white bars and grey lines), 1° *Wnt5a*$^{+/-}$ n=14 (black bars and black lines). Mean ± SEM.

Secondary transplantation (2°)

As we have demonstrated in other experiments using *Sfrp1*$^{-/-}$ or *Ptn*$^{-/-}$ recipients, the observation of mild effects in primary recipients do not predict sometimes major and irreversible changes in HSC behaviour and number only observed at later time points after secondary (2°) transplantation [57, 172].

In these experiments, we used WT 2° recipients (129xB6), so that any phenotypical changes would depend only on the microenvironment of the 1° recipient. To correct for possible “carry-over” or “transfer” effects, we sorted the WT donor (CD45.1) LSK cells from 1° recipients and transplanted 1000 LSK from either the 1° *Wnt5a*$^{+/+}$ or the 1° *Wnt5a*$^{+/-}$ recipients into lethally irradiated 2° WT (adult) B6 mice. (CD45.2) (Figure 42A).

Interestingly and unexpectedly, we found a total failure of engraftment of donor cells from 1° *Wnt5a*$^{+/-}$ mice in 2° recipients in PB (five, ten and 16 weeks) and in the BM after 16 weeks (Figure 42B). In Figure 42C, the representative FACS plots show the donor LSK and MP population reconstituted from 1° WT mice and the failure of engraftment of the cells from 1° *Wnt5a*$^{+/-}$ mice. These results clearly indicate that in the primary *Wnt5a*$^{+/-}$ recipients, the ability of the microenvironment to maintain LT-HSC is lost and therefore the experiment point out the importance of the extrinsic niche signal Wnt5a for HSC maintenance *in vivo*.

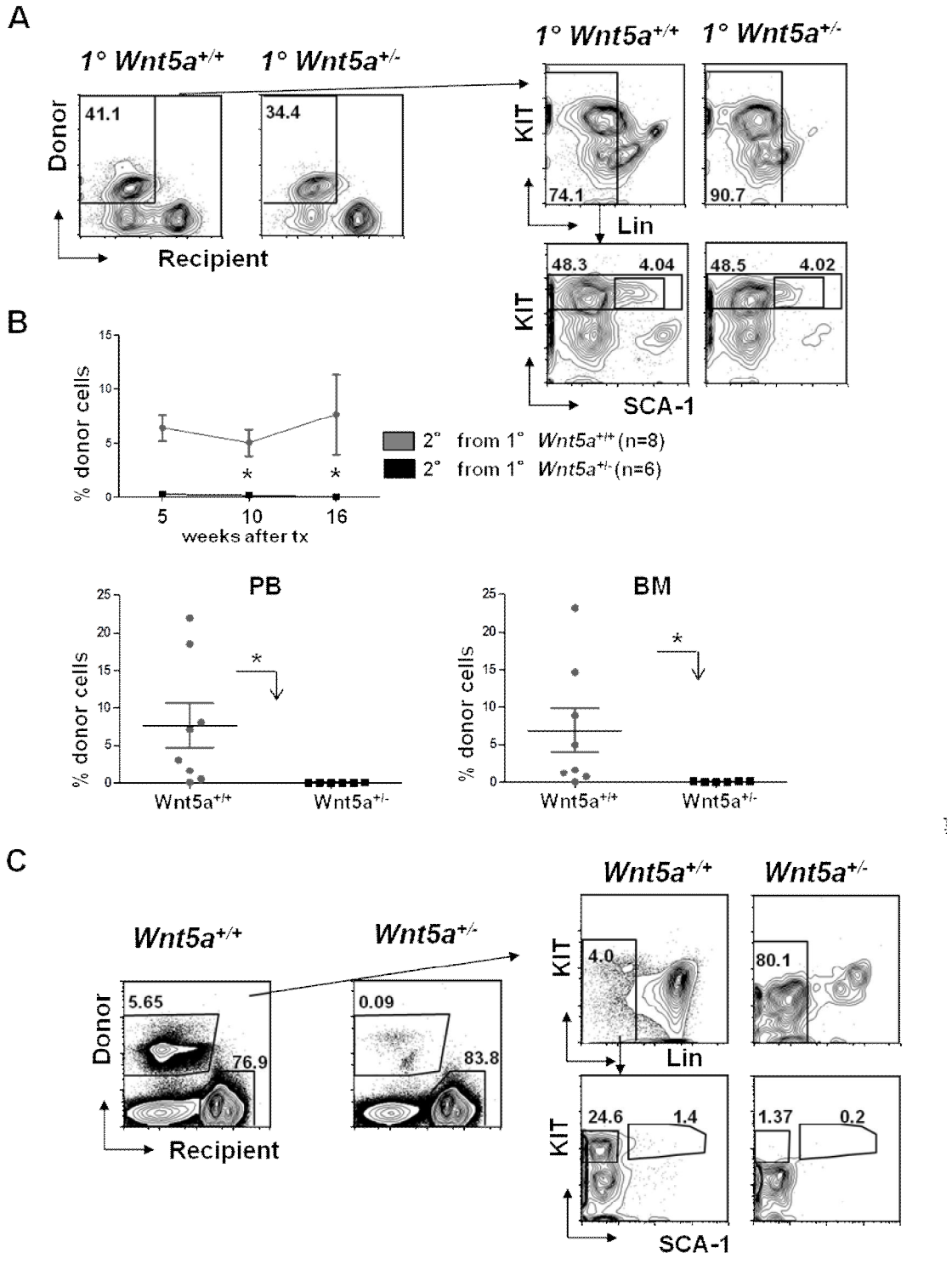

Figure 42. Extrinsic regulation of WT HSCs engraftment in *Wnt5a*$^{+/-}$ microenvironment. 2° transplantation. **(A)** Sorting scheme: The isolated BM from 1° transplantation was sorted for Ly5.1^{+} Lin^{-} KIT^{+} cells. 1000 LSKs per mouse were transplanted into WT recipients (Ly5.2) 2°. **(B)** The pattern of engrafted donor cells from 1° in process after five, ten and 16 weeks. **(C)** The engraftment levels in PB and BM of 2° after 16 weeks. **(D)** Representative FACS plots showing the total engraftment and the donor HSC; ° WT n=8 (grey lines and circles), 2° *Wnt5a*$^{+/-}$ n=6 (black lines and squares). Two individual experiments; Mean ± SEM; *p<0.05.

The severity of the loss of HSC activity was unexpected, but reproducible. Since we found no major effects in number or long-term activity of *Wnt5a*$^{+/-}$ CD150^{+} CD34^{-} LSKs (LT-HSC) (Figure 28), we wondered what the underlying mechanism of the failed self-renewal could be. During aging, Wnt5a is upregulated in HSCs [77] and 3° transplanted HSC are 56 weeks of age. One could, therefore expect that intrinsic effects might have occurred. The fact that we do not observe such effects indicates that extrinsic effects of Wnt5a are more important for the behaviour of HSCs. Considering the downregulation of CDC42 and JNK1 in *Wnt5a*$^{+/-}$ LSK cells (Figure 38), and these molecules are important for cell movement, we hypothesized that deficiency of *Wnt5a* in the microenvironment might impair the homing of HSCs in the 2° recipients.

4.6.2. Transplantation of BM into Wnt5a deficient microenvironment (Extrinsic)-Homing assay

The total failure of donor cells from 1° *Wnt5a*$^{+/-}$ HSCs to engraft in secondary transplantation might be the consequence of deficient HSC localization in the BM [23, 173-174]. To test this hypothesis, a homing assay was performed. In this assay, engrafted WT (Ly5.1x129S2)F1 BM cells from 1° *Wnt5a*$^{+/-}$ and 1° *Wnt5a*$^{+/+}$ recipients, were sorted out and 4000 LSK cells together with 30000 MPs were transplanted into lethally irradiated WT (B6x129S2)F1 2° recipient mice. The number of donor HSCs homed in the recipient's marrow 16-hours after the transplant was examined by flow cytometry (Figure 43A). The congenic system (Ly5.1/Ly5.2) was used to distinguish donor cells from recipient cells.

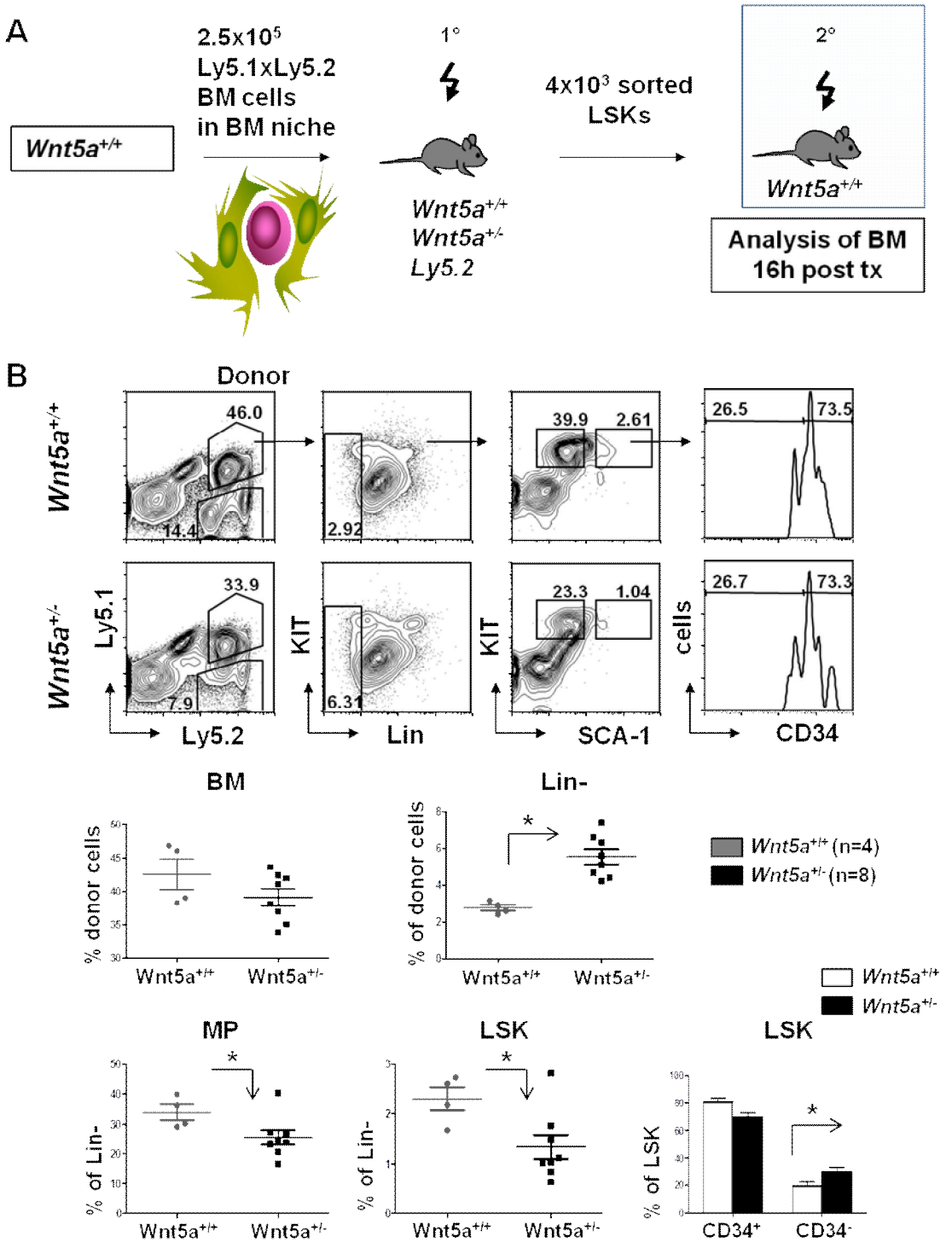

Figure 43. Wnt5a extrinsically alters homing efficiency of HSCs in 2° transplantation. (A) Homing assay: 250 000 whole bone marrow (BM) cells (Ly5.1xLy5.2) were intra-hepatically injected into irradiated newborn pubs of 1° Wnt5a$^{+/-}$ mice and their 1° WT littermates. Sixteen weeks post transplantation, BM was isolated and sorted for LSKs, MPs and CLPs, positive for Ly5.1/Ly5.2 expression. 4000 LSK together with 30 000 MP were transplanted into 2° WT recipients (Ly5.2). After 16h the mice were analysed **(B)** Engraftment levels of donor cells and different hematopoietic cell departments. 1° WT n=4 (white bars and grey circles), 1° *Wnt5a*$^{+/-}$ n=8 (black bars and squares). Mean ± SEM; *p<0.05.

Strikingly, whereas significantly more WT Lin^- cells (out of 1° *Wnt5a*$^{+/-}$ mice) engrafted into the BM after transplantation, the more primitive cell populations MP and LSK cells (1° *Wnt5a*$^{+/-}$) show a significantly decreased homing potential. The percentage of LT-HSCs ($CD34^-$ LSK) within the LSK population is significantly increased (Figure 43B).

As a conclusion, we found that HSCs regenerated in a *Wnt5a*$^{+/-}$ microenvironment show defective homing. Thus, Wnt5a is important for localization of the primitive hematopoietic cell population in the BM. As a result of the defective homing, HSC self-renewal is severely reduced.

Steady-state extrinsic homing

In order to find out, if *Wnt5a*-deficiency of the BM niche can directly influence the homing of HSCs to the BM after transplantation, we transplanted WT cells into *Wnt5a*$^{+/-}$ mice and the WT littermate controls, and analysed the engrafted cells 16 hours post transplantation (Figure 44).

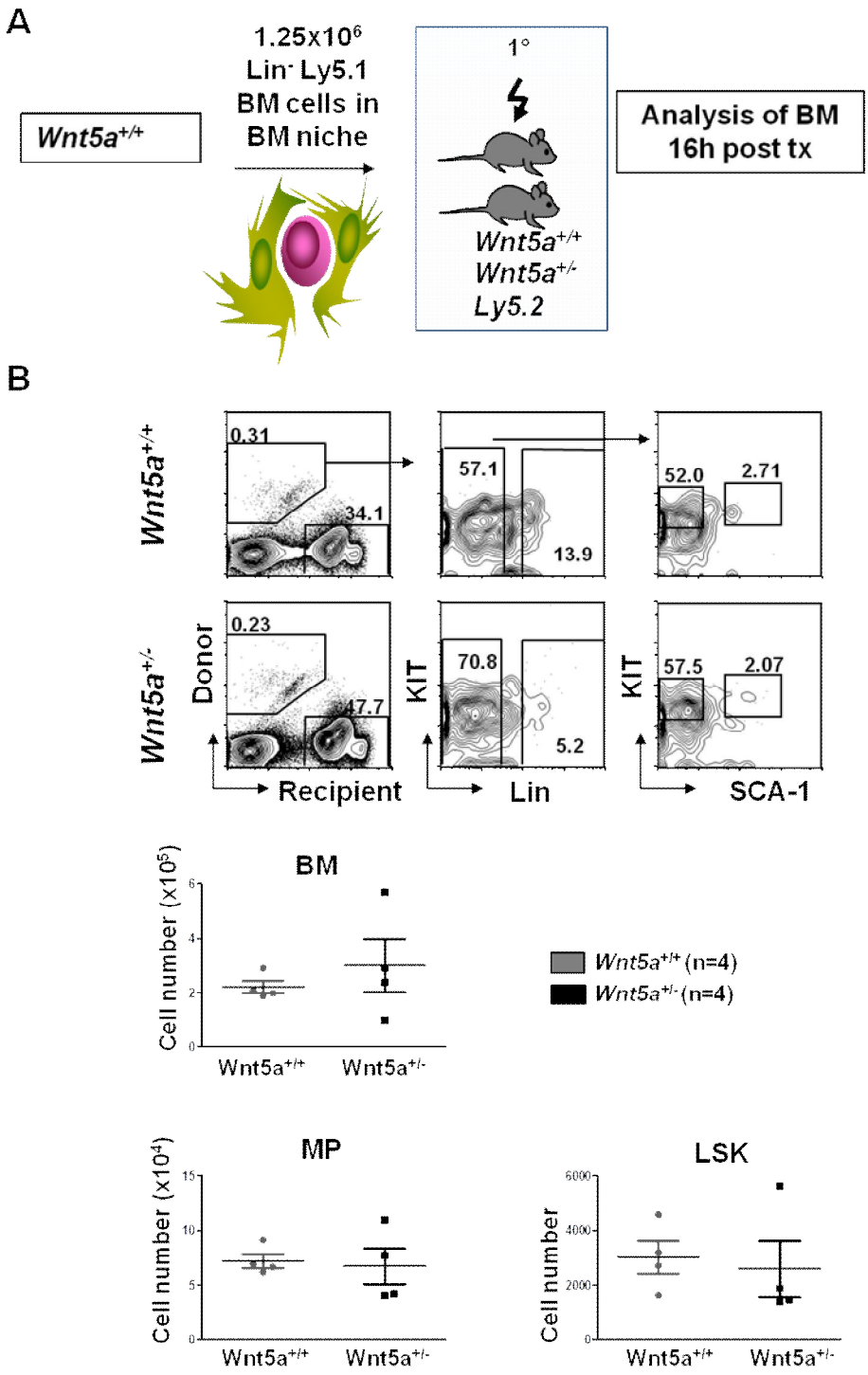

Figure 44. Homing efficiency of HSC in *Wnt5a*$^{+/-}$ microenvironment. (A) Homing assay: 1.25x10^6 Lin$^-$ BM cells (Ly5.1) were injected into lethally irradiated *Wnt5a*$^{+/-}$ mice and their WT littermates. 16 hours post transplantation, BM was isolated and analysed by FACS **(B)** Engraftment levels of donor cells and different hematopoietic cell departments. Donor cells in WT niche n=4 (grey circles), donor cells in *Wnt5a*$^{+/-}$ niche n=4 (black squares). Mean ± SEM; *p<0.05.

Although we detected a slight decrease in LSKs that localized in the BM, we could not see significant changes. The conclusion of this experiment is that regulation of the HSC

homing does not occur directly after transplantation, but is imposed on HSCs over a period of time during HSC regeneration (Figure 44).

4.6.3. Study of Wnt signalling of *Wnt5a*$^{+/+}$ LSKs, engrafted to *Wnt5a*$^{+/-}$ microenvironment

The previous results show that Wnt5a extrinsically conditions regenerated HSCs and regulates their ability to home to the BM. As a possible consequence, Wnt5a positively regulates the quality and maintenance of the cells, in a long-term manner. We here wanted to identify the underlying changes in molecular signalling in the HSCs regenerated in either a WT or a *Wnt5a*-deficient environment.

As already outlined in the study of signalling in LSK cells from steady-state *Wnt5a*$^{+/+}$ and *Wnt5a*$^{+/-}$ mice in Chapter 4.4., we here focused on the study of the balance between canonical and non-canonical Wnt signalling. For this purpose, engrafted 1° WT LSK cells were sorted out of the bone marrow of 1° *Wnt5a*$^{+/+}$ and 1° *Wnt5a*$^{+/-}$ recipients (Figure 45A). Subsequently, single-cells were stained for different proteins involved in either canonical or non-canonical pathways using immunocytofluorescence staining (Figure 45B).

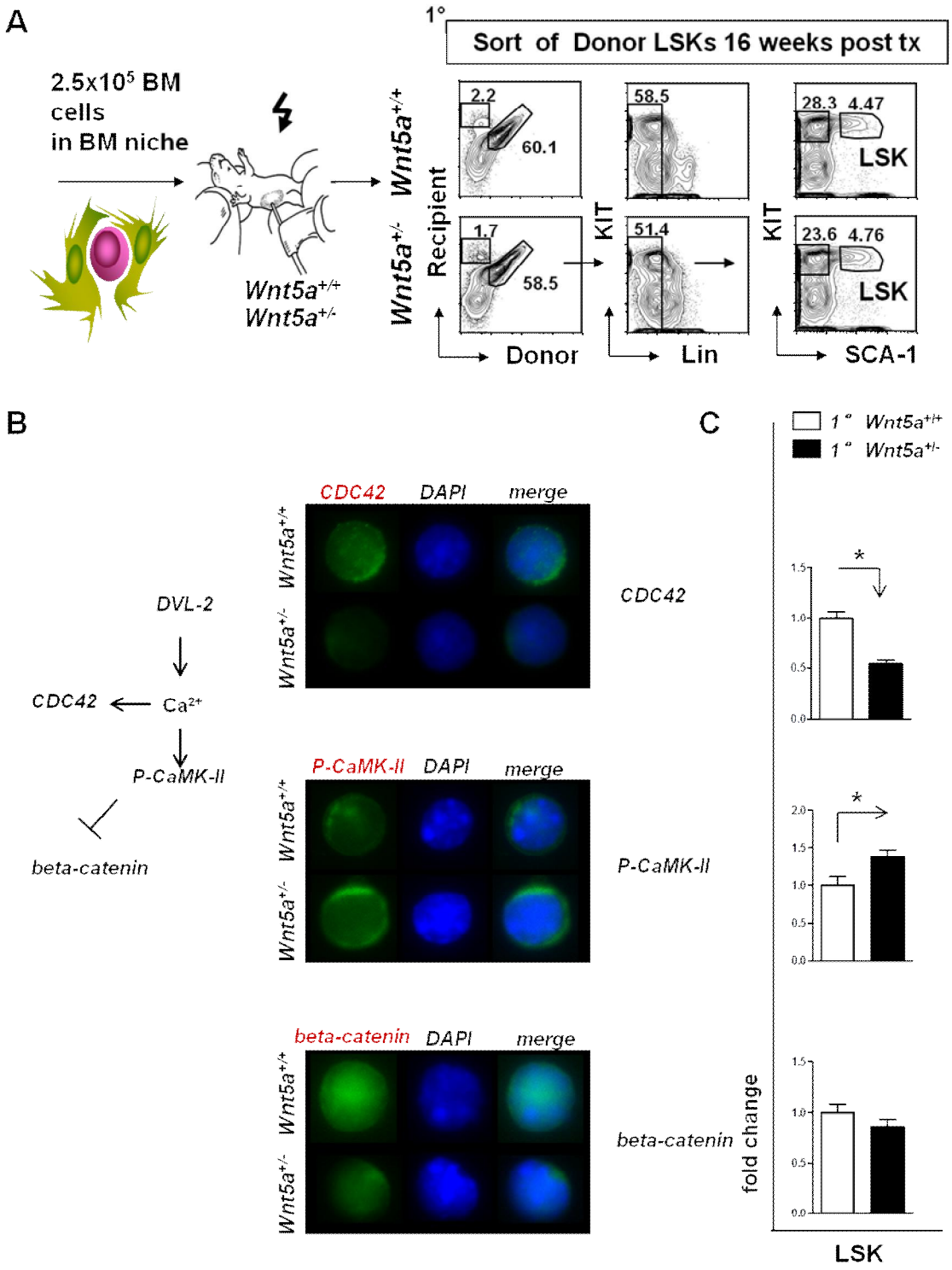

Figure 45. Analysis of molecular mechanisms of LSK cells from 1° extrinsic transplantation. **(A)** Serial transplantation flow chart. 250 000 whole bone marrow (BM) cells (Ly5.1x129) were intra-hepatically injected into lethally irradiated newborn pubs of Wnt5a$^{+/-}$ mice and their WT littermates (1° transplants). Sixteen weeks post transplantation, BM was isolated and sorted for donor derived LSK cells (Ly5.1xLy5.2^{+} Lin^{-} KIT^{+} SCA-1^{+}). The molecular regulation of this population was further analysed **(B)** Representative pictures of single cell stains of sorted donor LSKs from proteins involved in canonical and non-canonical signalling (left side), the nuclear counterstaining with DAPI (middle) and merge of both (right) **(C)** For quantification of the proteins in donor LSKs, 1° WT (white bars), 1° *Wnt5a*$^{+/-}$ (black bars), 30 cells were snaped on Leica fluorescent microscope, 100-fold enlarged. Total pixel were quantified by ImageJ; Mean ± SEM; *p<0.05.

Canonical signalling

In LSK cells, the phosphorylated beta-catenin (inactive) was significantly reduced, but, surprisingly, since total catenin is regulated through its phosphorylation, no changes in total beta-catenin level could be detected (Figure 45C). These results indicate that despite decreased level of phosphorylated beta-catenin in 1° *Wnt5a*$^{+/-}$ LSKs canonical Wnt signalling may not be affected.

Non-canonical signalling

As we have clearly shown in Chapter 4.5.2, Wnt5a is a regulator of Ca^{2+} release. Therefore, we evaluated the calcium-dependent Wnt signalling protein level of activated CaMK-II (P-CaMK-II). Interestingly, we found a significant increase in P-CaMK-II and a significant decrease of whole CaMK-II protein in sorted LSKs from 1° *Wnt5a*$^{+/-}$ compared to 1° *Wnt5a*$^{+/+}$ recipients (Figure 46). Thus, it appears that CaMK-II is hyperphosphorylated.

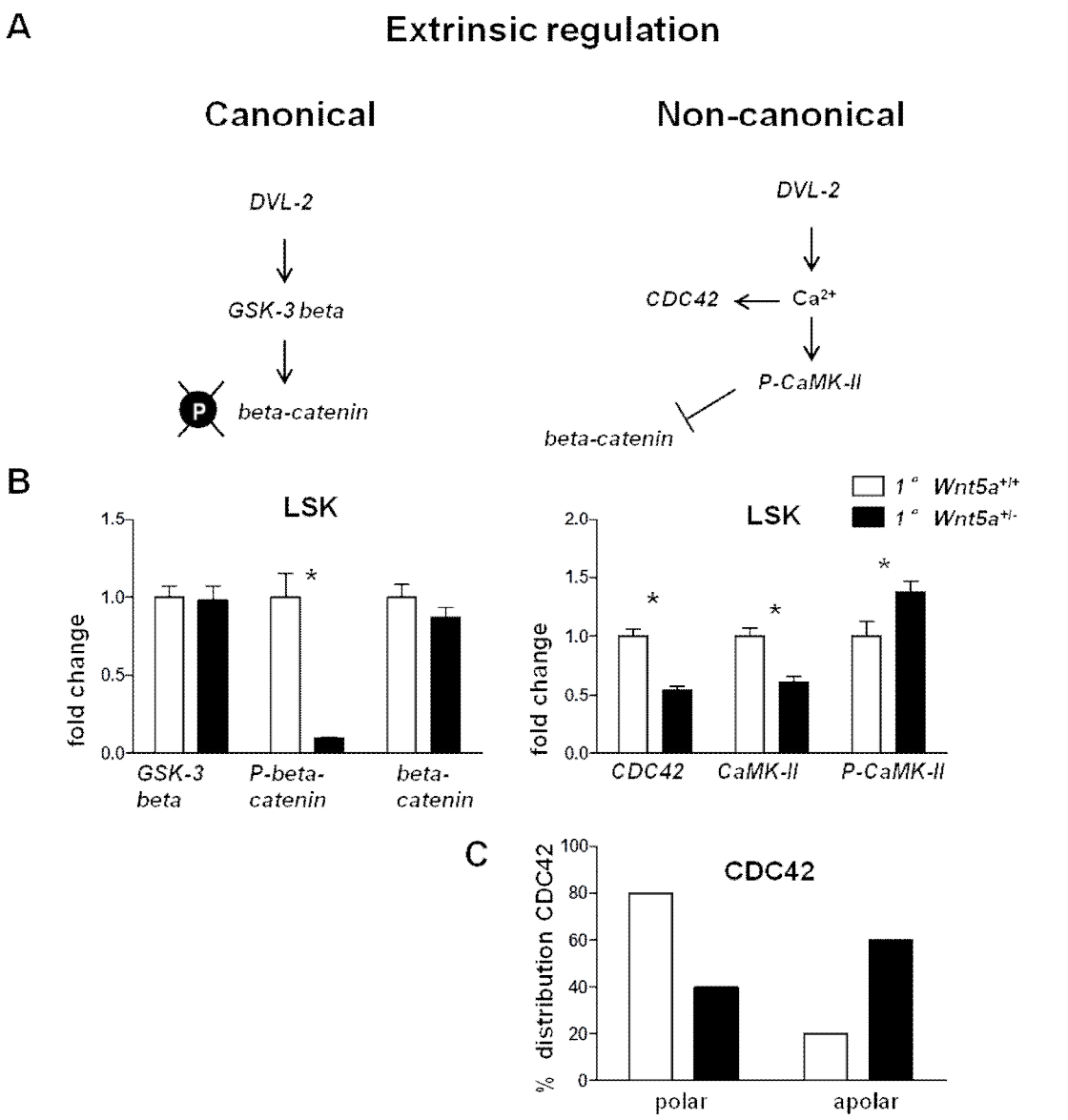

Figure 46. Analysis of molecular mechanisms of LSK cells from 1° extrinsic transplantation. (A) Schematic summary of canonical and non-canonical pathway **(B)** For quantification of the proteins GSK-3 beta, P-beta-catenin, beta-catenin, CDC42, CaMK-II, P-CaMK-II in donor LSKs, 1° WT (white bars) and 1° *Wnt5a*$^{+/-}$ (black bars **(C)** graph showing the percentage of polar and apolar distribution of CDC42 expression of 1° Wnt5a$^{+/+}$ LSKs (white bars) and 1° *Wnt5a*$^{+/-}$ 1° LSKs (black bars); 30 cells were snaped on Leica fluorescent microscope, 100-fold enlarged. Total pixel were quantified by ImageJ; Mean ± SEM; *p<0.05.

Moreover, we show that Wnt5a treatment of young HSCs activates the small Rho GTPase CDC42 [99]. In the experiments here, we find that the level of CDC42 is significantly downregulated in sorted LSKs from 1° *Wnt5a*$^{+/-}$ compared to 1° *Wnt5a*$^{+/+}$ recipients. In addition, since CDC42 activity correlates with apolarized phenotype of HSCs [107], we find more cells with apolar CDC42 distribution, thus suggesting a higher activity of CDC42 in LSKs from 1° *Wnt5a*$^{+/-}$ recipients.

Taken together, the study of LSK cells isolated from 1° *Wnt5a*$^{+/+}$ and 1° *Wnt5a*$^{+/-}$ recipients show a change in molecular regulation of WT LSKs through upregulation of calcium-dependent non-canonical signalling via CDC42 and P-CaMK-II. This effect is mediated through signals from the *Wnt5a*-deficient niche.

4.6.4. Characterization of the niche compartment by FACS and differentiation potential

Multipotent stromal cells (MSCs), osteoblastic lineage cell (OBC) derivatives as well as endothelial cells, adipocytes and chondrocytes are part of the bone marrow (BM) niche and contribute to hematopoietic stem cell (HSC) maintenance (Figure 3). *In vivo,* MSCs have the potential to differentiate into adipogenic, chondrogenic and osteogenic lineage cells. Takada *et al.* [175] reported that Wnt5a regulates cell fate from adipogenesis to osteoblastogenesis of bone marrow multipotent mesenchymal stem cells in the presence of PPAR-γ [175]. Since we discovered changes concerning self-renewal and homing in the behaviour of WT HSCs engrafted in the *Wnt5a*$^{+/-}$ niche, we wished to find out whether the niche itself and its different cell compartments show an abnormal distribution in *Wnt5a*$^{+/-}$ mice. Therefore, we started to study the bone marrow stromal cells from *Wnt5a*$^{+/-}$ mutant mice. For this purpose, the bone marrow was isolated and the remaining bones were crushed. After collagenase treatment of the bone fragments, the cells were combined and analysed using flow cytometry [36, 176] (Figure 47A).

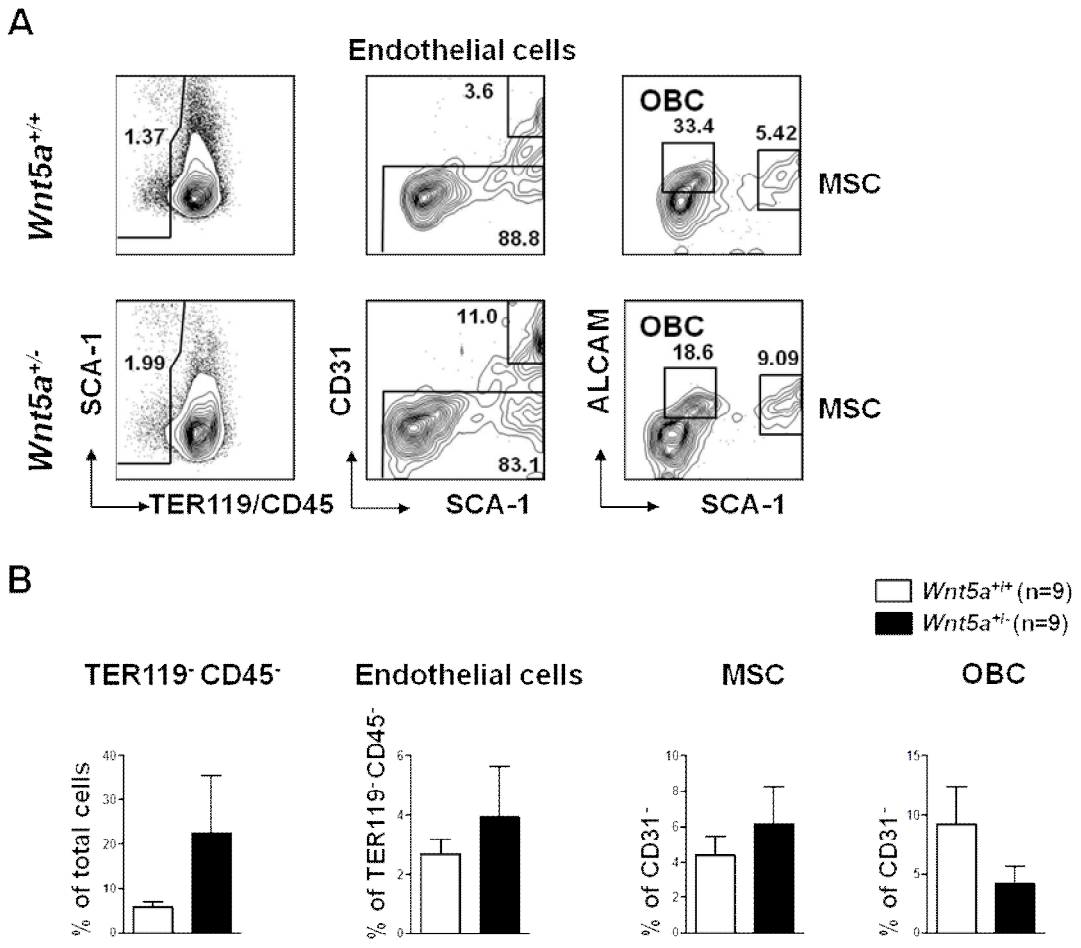

Figure 47. BM niche compartment of *Wnt5a*$^{+/-}$ mice. (A) Representative FACS profile of ALCAM and SCA-1 expression in CD45^{-} CD31^{-} TER119^{-} cells to distinguish endothelial cells, MSCs and OBCs **(B)** Percentages of the BM stromal cell populations TER119^{-} CD45^{-}, EC, MSC and OBC; *Wnt5a*$^{+/+}$ n=9 (white bars), *Wnt5a*$^{+/-}$ n=9 (black bars); Mean ± SEM.

We analysed the BM niche as previously described by others [36]. We were able to discern the following subpopulations of niche cells:

Endothelial cells (ECs): TER119/CD45/CD31^{+}/SCA-1^{+},

Multipotent stromal cells (MSCs): TER119/CD45/CD31^{-}/SCA-1^{+}, and

Osteoblastic cells (OBCs): TER119/CD45/CD31^{-}/ALCAM^{+}/SCA-1^{-}

These experiments showed that BM from collagenase-treated crushed bones of *Wnt5a*$^{+/-}$ mice and their WT littermates, comprise a tendentially higher percentages of hematopoietic-depleted SCA-1^{+} cells (MSCs), and an increase in CD31^{+} expressing ECs. Moreover, regarding MSCs (SCA-1^{+} ALCAM^{-} cells), which are known to regulate LT-status of HSCs are slightly increased in percentage. In contrast, OBCs (CD45^{-}/TER119^{-}/CD31^{-}) which are important for regulation of HSCs over cell adhesion, are tendentially underrepresented (Figure 47).

Thus, our experiments show that in *Wnt5a*$^{+/-}$ BM, there is increased angiogenesis (CD31^{+} ECs), but a similar number of OBCs and MSCs. To study the hypothesis that diverging cell composition in niche of *Wnt5a*$^{+/-}$ has an effect on the cellular function of the cells in more detail, we performed functional analyses of OBCs and MSCs from *Wnt5a*$^{+/-}$ and their WT littermates *in vitro* by differentiation assays and proliferation curves.

MSCs are known to have the ability to differentiate into three lineages (adipogenic, osteogenic, chondrogenic). In this study, the ability of MSCs was validated to differentiate into adipocytes and osteocytes. Adipocytes are recognizable by detecting fatty vesicles via Oil Red O staining. Osteogenic induced cells will form a mineralized matrix, which can be visualized by von Kossa staining.

Firstly, MSCs were sorted as described above out of *Wnt5a*$^{+/+}$ and *Wnt5a*$^{+/-}$ endosteum BM, mixed up with BM from collagenase treated bones. The sorted cells (Figure 48) were then cultured and differentiation was induced (passage 2).

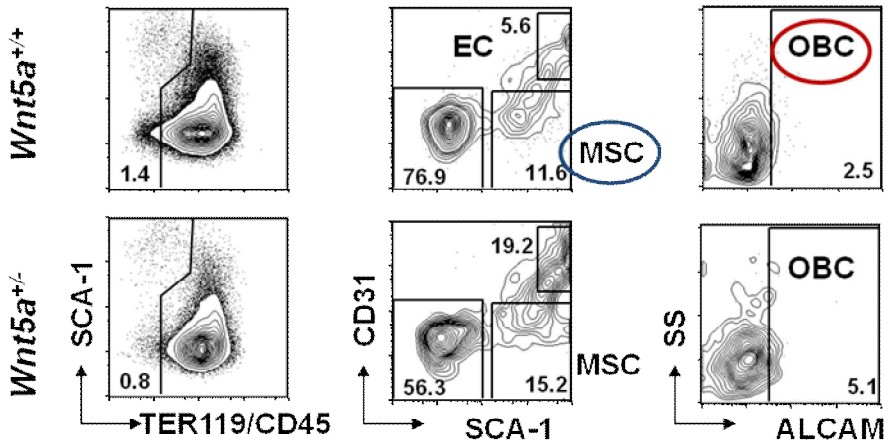

Figure 48. BM niche compartment of *Wnt5a*$^{+/-}$ mice. Sorting scheme of MSCs and OBCs; CD45^{-} CD31^{-} TER119^{-} cells were gated. Out of this cell population SCA-1^{+} cells were sorted as MSCs; SCA-1^{-} population was gated for ALCAM expression and sorted as OBCs.

Adipogenic and osteogenic differentiation was induced in confluent cultures grown from sorted MSCs of WT and *Wnt5a*$^{+/-}$ mice. Notably, whereas adipogenic differentiation was detectable in cells of both genotypes at a similar level, the quantification of osteogenesis by exercising the von Kossa stain revealed a higher level of calcium deposition in cultures derived from *Wnt5a*$^{+/-}$ MSCs. Thus, less Wnt5a in mesenchymal stromal cells enhances calcium deposition by cells cultured under osteogenic conditions (Figure 49).

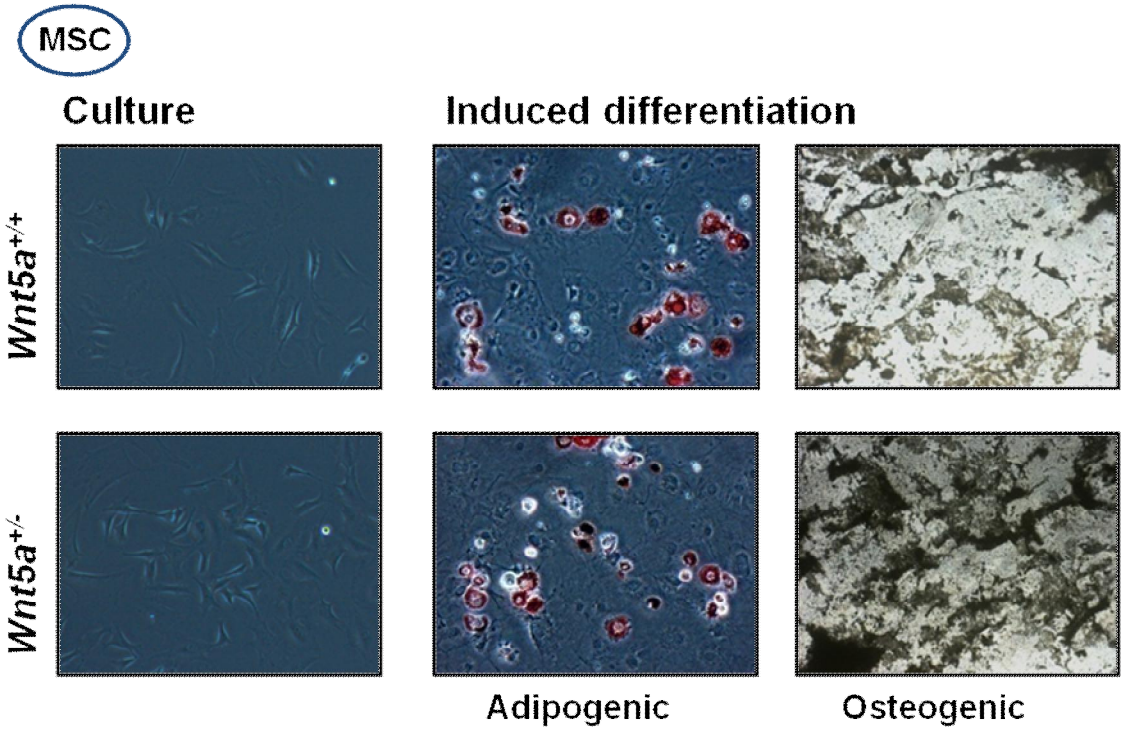

Figure 49. MSC culture: Induced adipogenic and osteogenic differentiation. Microscopy of cultured MSCs of *Wnt5a*$^{+/+}$ and *Wnt5a*$^{+/-}$ mice; Induced differentiation into adipogenic and osteogenic lineage (10x).

Additionally, we also isolated OBCs (TER119/CD45/CD31^{-}/ALCAM^{+}/SCA-1^{-}) from *Wnt5a*$^{+/+}$ and *Wnt5a*$^{+/-}$ endosteum BM mixed up with BM from collagenase treated bones and we cultured these for three weeks (Figure 50).

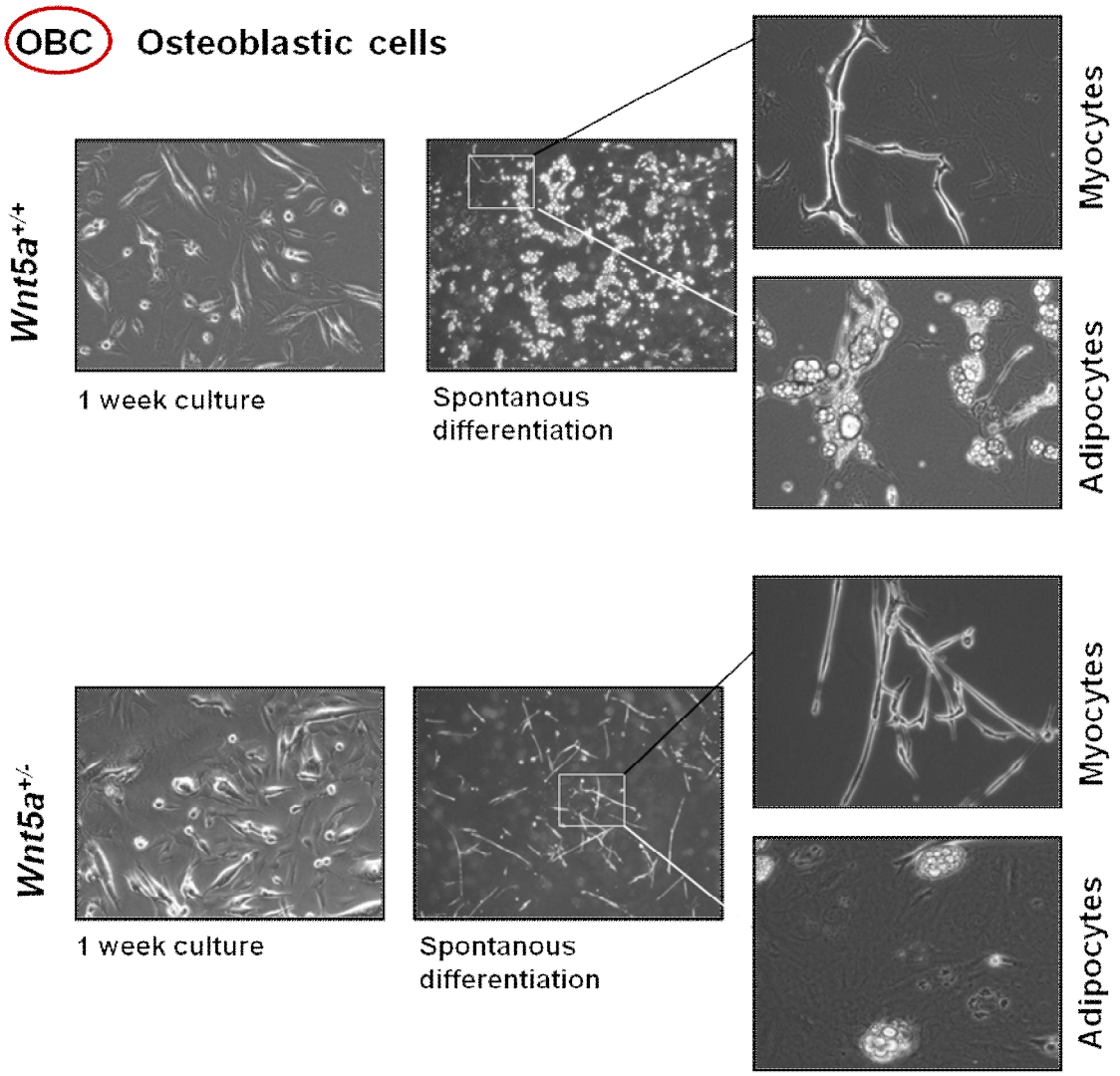

Figure 50. OBC culture: spontaneous differentiation. Microscopy of cultured OBCs after one and three weeks (2x). Spontaneous differentiation was detected after three weeks into adipogenic and muscular lineage (10x).

Although differentiation was not specifically induced, OBCs spontaneously differentiated into clones of various cell types, particularly into adipogenic lineage and what appeared to be the myocyte lineage. Whereas *Wnt5a*$^{+/+}$ OBCs cells showed mainly adipogenic differentiation and less myocytic cells, sorted *Wnt5a*$^{+/-}$ OBCs basically differentiated into myocytes by default (Figure 50). Thus, we show that OBCs are mature mesenchymal cells, but not necessarily belong to the osteogenic lineage.

The sorted MSCs and OBCs were cultured and colony-forming unit-fibroblasts (CFU-F) determined and growing curves of CFU-F-derived cultures were calculated (Figure 51A+B).

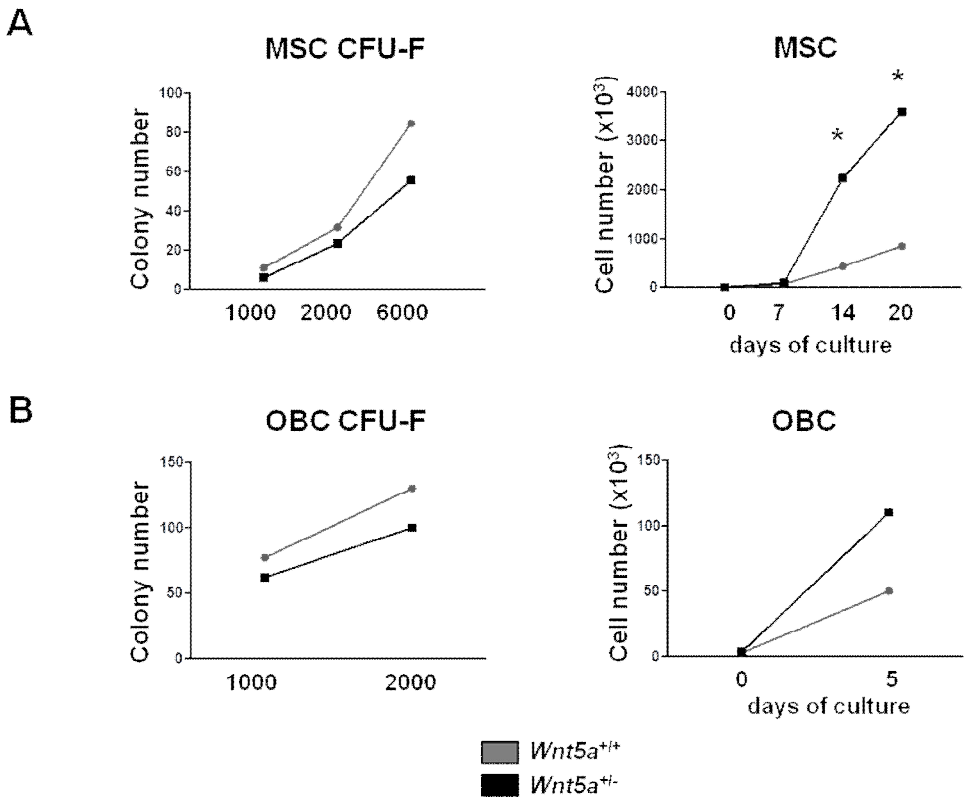

Figure 51. CFU-F and growing curves of sorted and cultured MSC and OBC populations. **(A)** MSCs of *Wnt5a*$^{+/+}$ and *Wnt5a*$^{+/-}$ mice were sorted and cultured. On the left: CFU-F were counted; different cell numbers were seeded: 2000, 3000, 6000 cells and counted after seven days; on the right: MSCs were further cultivated and cell number counted after seven, 14, 20 days of culture **(B)** OBCs of *Wnt5a*$^{+/+}$ and *Wnt5a*$^{+/-}$ mice were sorted and cultured. On the left: CFU-F was counted; different cell numbers were seeded: 1000 and 2000 cells and counted after seven days; on the right: OBCs were further cultivated and cell number counted after five days of culture. *Wnt5a*$^{+/+}$ (grey lines), *Wnt5a*$^{+/-}$ (black lines); Mean ± SEM.

The number of formed colonies of *Wnt5a*$^{+/-}$ MSCs after one week was slightly decreased compared to *Wnt5a*$^{+/+}$ MSCs. But growing curves show that if MSCs are cultured further, up to three weeks, the number of cells grown from *Wnt5a*$^{+/-}$ MSCs is significantly higher in number than those cultured from *Wnt5a*$^{+/+}$ MSCs. The same growth effect could be seen in OBCs, in a much shorter five day-culture.

In conclusion, the niche in *Wnt5a*$^{+/-}$ mice shows a different balance of cells with more ECs than in WT mice. In addition, although the number of OBCs and MSCs is similar between *Wnt5a*$^{+/-}$ und *Wnt5a*$^{+/+}$ WT marrow cells, *Wnt5a*$^{+/-}$ MSCs show stronger calcification and OBCs comprise a relatively large myogenic compartment.

4.7. Wnt5a in leukemia

Since many years, it has been known that aberrant intracellular signalling, mediated by the Wnt family of secreted glycoproteins promotes tumour progression [177]. Most of the studies concerning this signalling pathway have focused on beta-catenin-dependent signalling in tumour formation. However, recent studies suggest also a role of non-canonical wnt signalling candidates in leukemia. Wnt4 is known to inhibit cell growth in leukemia-derived cell lines [178] and Wnt11 plays a role in the progression of CML [179]. The role of the typical non-canonical signalling ligand, Wnt5a is controversial, and both tumour-promoting and tumour-suppressive roles in cancer have been reported. For example, breast cancer patients have an increased risk of death and aggressive disease, when Wnt5a is downregulated [180-181]. In melanoma, the opposite is true and patients with high expression of Wnt5a show a poor prognosis [182]. Since Wnt5a can be expressed by tissue-specific cells as well as cells of their niche, the question raised, whether Wnt5a in the microenvironment of the cancer cell or in the cancer cell itself is a determinative factor for cancer development. It has been demonstrated that the Wnt5a promoter is methylated in leukemic cells patients and demethylated in complete remission cases [183], suggesting the clinical relevance of Wnt5a expression in leukemia. As we could show before in this thesis that Wnt5a can extrinsically influence the maintenance of the hematopoietic stem cell, the tumour suppressor or tumour-promoting role of Wnt5a in leukemia has to be further elucidated.

4.7.1. Transplantation of oncogene-expressing BM into Wnt5a deficient microenvironment (Extrinsic)

Severe osteoblastic defects have been reported to occur in blast-crisis CML [124, 184]. In order to study the influence of *Wnt5a*$^{+/-}$ BM niche on leukemogenesis, leukemia was induced by injecting BCR/ABL expressing WT HSCs into lethally irradiated *Wnt5a*$^{+/-}$ and WT mice. CML is a myeloproliferative disorder and occurs in humans amongst others as a result of a t (9; 22) translocation that results in a fusion between the genes encoding the ABL tyrosine kinase and BCR. The resulting fusion oncogenic protein BCR/ABL has constitutive tyrosine kinase activity [185].

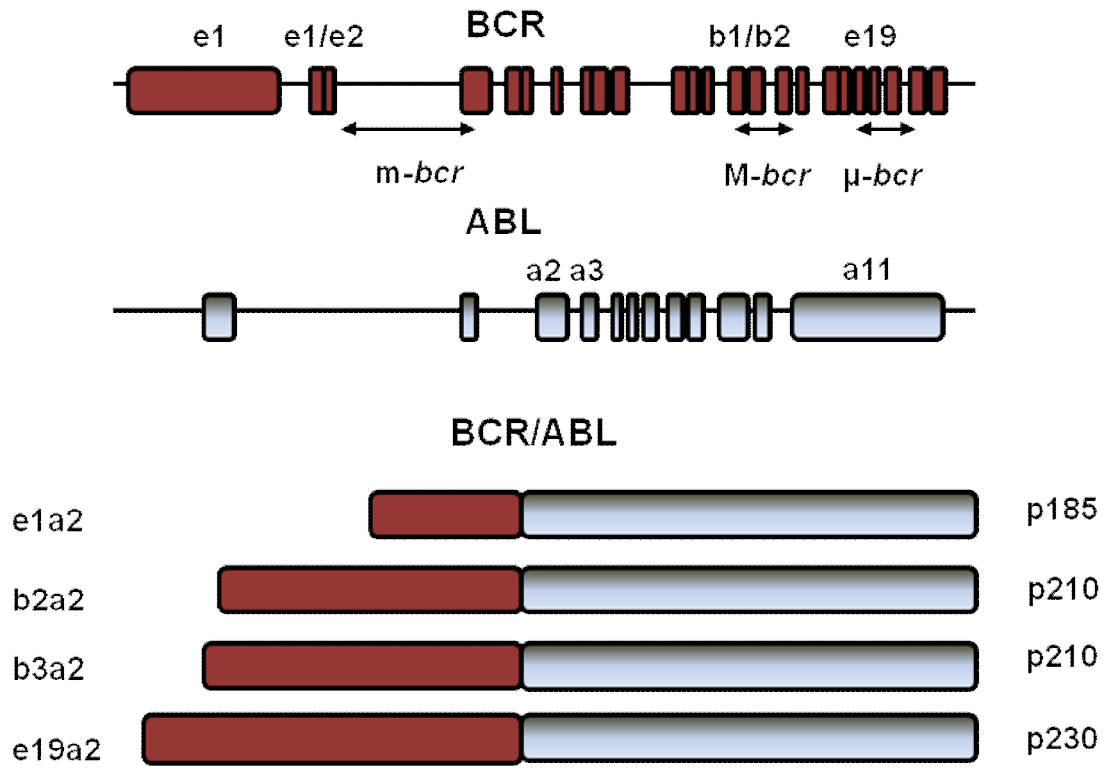

Figure 52. Gene map of BCR and ABL and fusion transcripts. The translocation of the chromosomes 9q and 22q leads to the arrangement of the Philadelphia-Chromosome that includes BCR/ABL fusion gene. Different breakpoints occur, leading to four known fusion genes: e1a2=p185; b2a2/b3a2=p210; e19a2=p230); the boxes illustrate the exons;

In many patients with CML and in about 20% of patients with ALL, the breakpoint in the BCR gene occurs in the M-bcr region, resulting in BCR/ABL transcript containing a b3a2 and/or b2a2 junction encoding a 210 kD fusion protein (p210 $^{BCR/ABL}$) [186] [187] [188]. In most patients with Philadelphia-positive ALL and CML and AML, the breakpoint in BCR is upstream, in the m-bcr region, resulting in BCR/ABL mRNA molecules with a e1a2 junction translated into smaller 185 kD BCR/ABL fusion protein (p185$^{BCR/ABL}$) [189] [190] [191] [192] (Figure 52).

In order to study the influence of *Wnt5a*$^{+/-}$ BM niche on BCR/ABL-induced leukemogenesis, leukemia was induced by injecting BCR/ABL expressing WT HSCs into lethally irradiated *Wnt5a*$^{+/-}$ and WT mice.

In brief, 5-FU treated B6 mice were sacrificed after 4 days and the BM was infected by retrovirus carrying the oncogene p185 e1-a2 BCR/ABL and GFP. 1x10^5 GFP expressing Lin$^-$ cells were intra-hepatically transplanted into lethally irradiated pubs of the mouse strain B6;129S7-Wnt5atm1Amc/J mice, backcrossed to 129S2xB6 for three to six generations (F3-F6), containing *Wnt5a*$^{+/+}$ and *Wnt5a*$^{+/-}$ newborn mice (Figure 53A). The mice were sacrificed, when following criteria for disease were apparent. Healthy mice were sacrificed after 120 days.

Criteria for lympho-myeloproliferative disease (LMPD) in mice (adapted from Bethesda proposals for classification of nonlymphoid hematopoietic neoplasms in mice [193]):

Monitoring

- General condition:
    - Drastically reduced: dehydrated, apathic, horrent coat, heavy breathing, edema, cachectic;
- Ingestion:
    - Reduced > 24h, body weight reduced;
- Motion activity:
    - Retired, sleepy;
- Behaviour:
    - Apathic, isolated;
- Development of LMPD:
    - Leukocytes in PB: >30.000/µl;
    - Splenomegaly

A

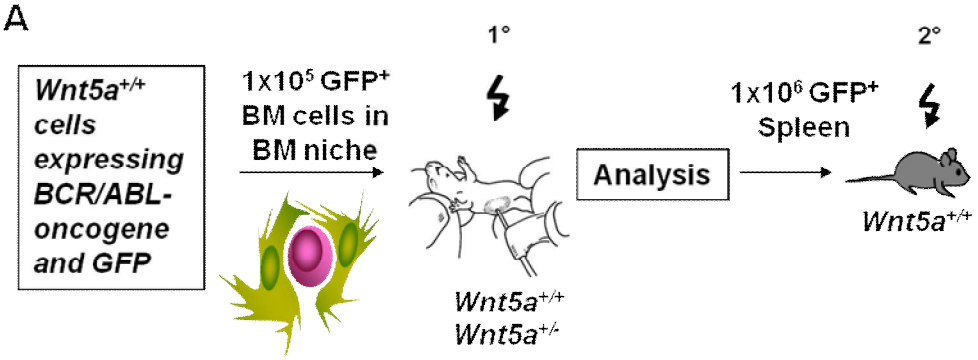

B

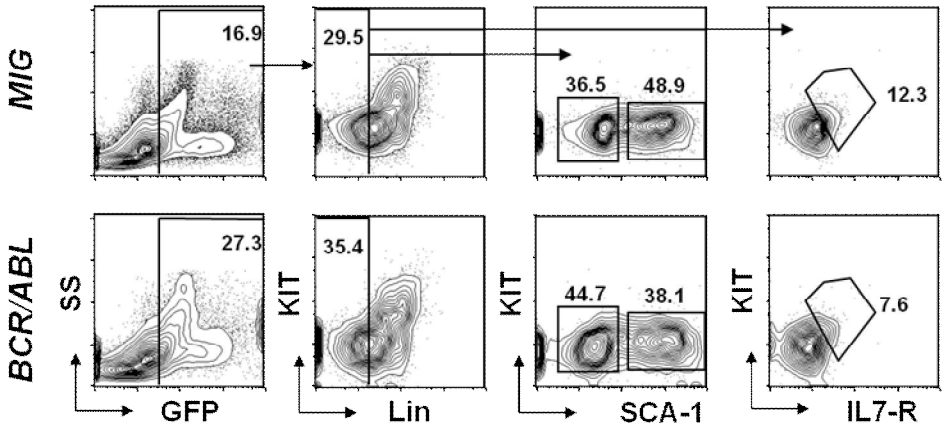

C

	MIG	*Wnt5a*$^{+/+}$ BCR/ABL	*Wnt5a*$^{+/-}$ BCR/ABL	*Wnt5a*$^{+/-}$ BCR/ABL healthy
Mice (n)	0/12	15/15	16/25	9/25

D

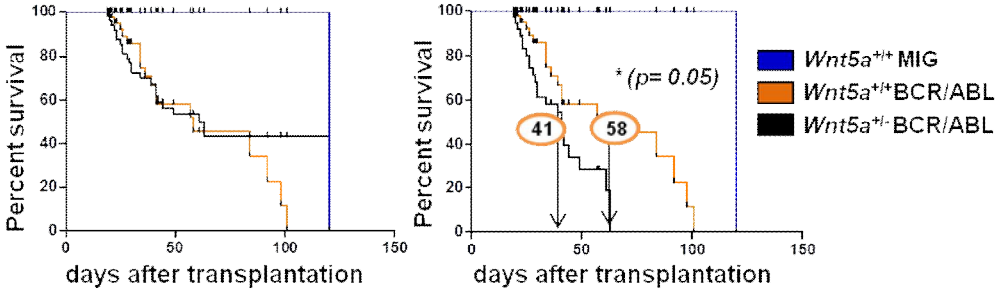

Figure 53. WT BCR/ABL expressing cells in *Wnt5a*$^{+/-}$ microenvironment. **(A)** Serial transplantation flow chart. *Wnt5a*$^{+/+}$ Lin^{-} cells were injected intra-hepatically into lethally irradiated newborn pubs containing *Wnt5a*$^{+/-}$ and WT mice (1°). After severe disease symptoms, mice were sacrificed and analysed by FACS for hematopoietic stem cells, their progenitor cells and mature cells. A set of BCR/ABL expressing Spleen cells was retransplanted into WT mice. **(B)** Representative FACS plots of BM cells from 5-FU treated mice after infection, gated on PI^{-} GFP^{+} Lin^{-}cells; 1x10^{5} GFP^{+} cells were transplanted. **(C)** Table of not diseased vs. diseased mice **(D)** Kaplan-Meier survival plots visualizing the percentage of survival over time (days after transplantation), in three groups: MIG (control vector) in *Wnt5a*$^{+/+}$ MIG and *Wnt5a*$^{+/-}$ MIG mice n=12 (blue curve), *Wnt5a*$^{+/+}$ BCR/ABL n=15 (orange curve) and *Wnt5a*$^{+/-}$ BCR/ABL n=25 (black curve). On the left side, the survival plot is constituted with mice within group *Wnt5a*$^{+/-}$ BCR/ABL that did not get diseased. On the right side, the mice are out taken the experiment. As estimated by Kaplan-Meier method, *Wnt5a*$^{+/-}$ mice BCR/ABL die significantly earlier (median survival: 41days) compared to *Wnt5a*$^{+/+}$ BCR/ABL mice (median survival: 58 days); *p=0.05.

The diseased mice developed different types of LMPD within a time range of 19 (*Wnt5a*$^{+/-}$) and 101 days (*Wnt5a*$^{+/+}$) (Figure 53+55). The experiment was stopped on day 120 post transplantation.

When analyzing the Kaplan-Meier survival plot, it could be assessed that *Wnt5a*$^{+/-}$ mice developed LMPD within a significantly shortened latency time compared to their WT littermates. The median survival for *Wnt5a*$^{+/+}$ mice is 58 days, whereas the median survival for *Wnt5a*$^{+/-}$ mice is significantly shortened to 41 days.

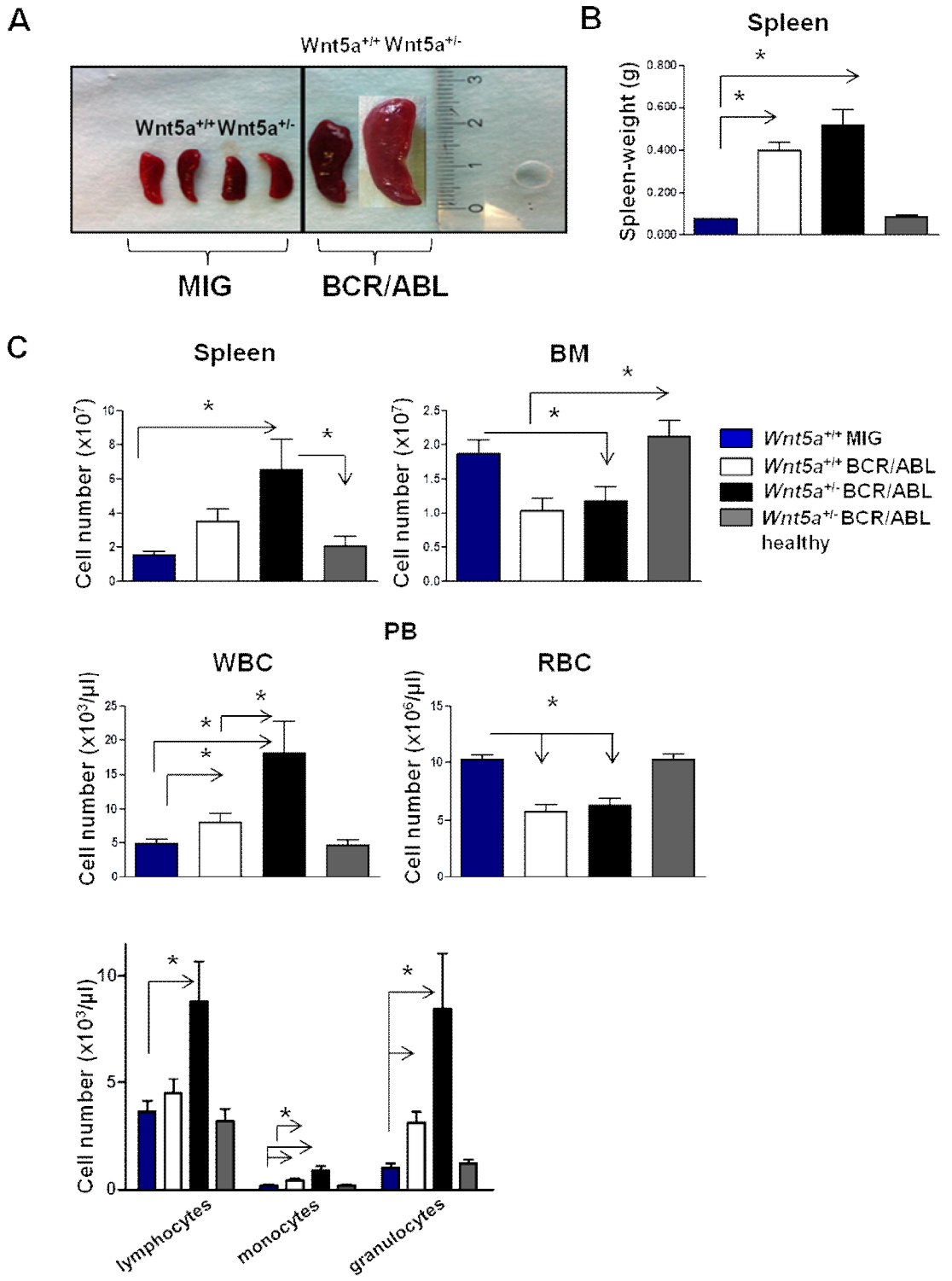

Figure 54. Induced LMPD in *Wnt5a*$^{+/-}$ mice. (A) Figure of Spleen from representative animals of the experiment **(B)** Average of Spleen weights from four mentioned groups: MIG, *Wnt5a*$^{+/+}$ BCR/ABL, *Wnt5a*$^{+/-}$ BCR/ABL and *Wnt5a*$^{+/-}$ BCR/ABL healthy (injected mice that remained free form disease) **(C)** Total cell number of Spleen, PB and BM; PB was further analysed for WBC (white blood cells), RBC (red blood cells), lymphocytes, monocytes and granulocytes.*Wnt5a*$^{+/+}$ MIG and *Wnt5a*$^{+/-}$ MIG mice n=12 (blue bars), *Wnt5a*$^{+/+}$ BCR/ABL n=15 (white bars), and *Wnt5a*$^{+/-}$ BCR/ABL n=16 (black bars), *Wnt5a*$^{+/-}$ BCR/ABL healthy n=9 (grey bars). Mean ± SEM; *p<0.05.

Wnt5a$^{+/-}$ recipients of BCR/ABL^{+} WT donor cells not only developed disease in a shortened latency time, but also showed a more severe form of leukemia.

In diseased recipients transplanted with BCR/ABL^{+} (GFP^{+}) WT donor cells, the Spleen size was increased compared to the healthy control MIG mice or the healthy BCR/ABL-treated *Wnt5a*$^{+/-}$. Importantly, the splenomegaly of diseased *Wnt5a*$^{+/-}$ recipient mice was more outspoken than that in *Wnt5a*$^{+/+}$ recipients (Figure 54A). The splenomegaly was also reflected in the Spleen-weight of the different groups: the Spleen-weight of the mice with LMPD was significantly increased in both recipient genotypes compared to the MIG control mice (Figure 54B).

In Figure 54C the total cell number of the hematopoietic organs is demonstrated. Only the Spleens of *Wnt5a*$^{+/-}$ recipients were significantly increased in cell number compared to the MIG control and *Wnt5a*$^{+/-}$ healthy recipient mice, injected with BCR/ABL expressing cells. The BM cellularity was significantly decreased in both groups of diseased recipients (*Wnt5a*$^{+/+}$ and *Wnt5a*$^{+/-}$) compared to the MIG control recipients.

As mentioned above, in nine out of 25 (36%) cases, the WT cells expressing BCR/ABL did not develop LMPD in *Wnt5a*$^{+/-}$ recipient mice. These mice remained healthy during the 120 day observation period. When analyzing Spleen-size, Spleen-weight and the cellularity of hematopoietic organs of these mice, the outcomes were comparable with the WT (*Wnt5a*$^{+/+}$) recipients, which were transplanted with MIG control cells.

The more aggressive form of LMPD triggered in *Wnt5a*$^{+/-}$ recipient mice, is also illustrated by the WBC in peripheral blood. In diseased *Wnt5a*$^{+/-}$ mice, the WBC number showed a significant increase compared to *Wnt5a*$^{+/+}$ recipients. Whereas in PB, myeloid cells are significantly increased in both genotypes compared to the MIG control, we found that the lymphoid lineage is significantly increased only in *Wnt5a*$^{+/-}$ recipient mice compared to *Wnt5a*$^{+/+}$ recipients. Moreover, the LMPD mice were analysed in terms of type of leukemia (Figure 55).

In Figure 55, examples for different types of hematologic diseases in BM are illustrated.

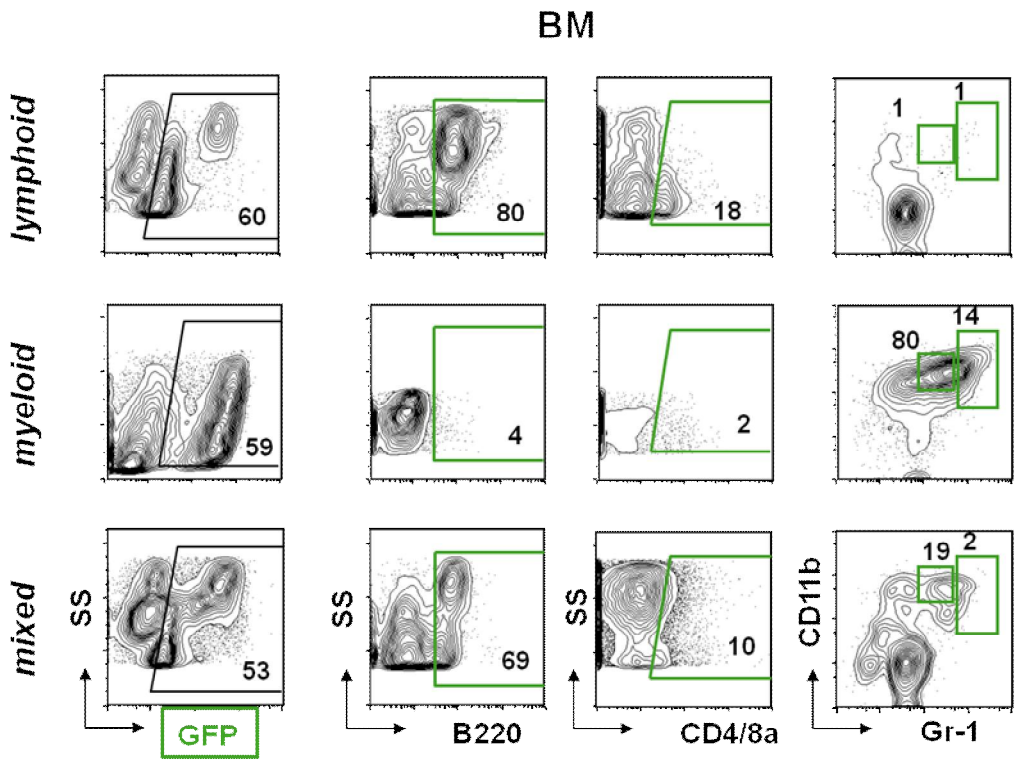

Figure 55. Different types of hematologic diseases. FACS plots showing examples for lymphoid, myeloid and mixed type of disease in BM of WT mice. BM gated on PI^-GFP^+ cells; B220-, CD4/8a- Gr-1- and CD11b-expression is illustrated within GFP^+ cells.

The BM was gated for B cells, T cells granulocytes and monocytes on PI^- and GFP^+ cells. We classified the diseases upon following criteria into three groups:

- lymphoid: GFP expressing B cells and T cells (lymphoid cells) make up upon 80% of all GFP^+ cells
- myeloid: GFP expressing granulocytes and monocytes (myeloid cells) make up upon 80% of all GFP^+ cells
- mixed: GFP expressing lymphoid and myeloid cells make up each more than 20% of all GFP^+ cells

In line with the increase in lymphoid cells in the PB of LMPD mice, in *Wnt5a*$^{+/-}$ recipients there is a higher incidence of lymphoid disease compared to the *Wnt5a*$^{+/+}$ recipients (Table 16).

Recipient Genotype	healthy	lymphoid	myeloid	mixed	Total studied
Wnt5a$^{+/+}$	0	5	3	7	15
Wnt5a$^{+/-}$	9	8	3	5	25

Table 16: Development of different types of hematologic disease. Number of mice that developed lymphoid, myeloid and mixed disease of *Wnt5a*$^{+/+}$ and *Wnt5a*$^{+/-}$ mice as well as healthy *Wnt5a*$^{+/-}$ representatives. Different types of disease are combined and designated as LMPD.

In the LMPD mice, we also analysed the mature and more primitive hematopoietic cells by flow cytometry. As the expression of BCR/ABL is located before the GFP cassette in the MIG vector, we assumed that all GFP$^+$ cells also express BCR/ABL. The following analysis concentrates on the comparison of two groups: The development of WT BCR/ABL-infected BM cells transplanted either into lethally irradiated *Wnt5a*$^{+/+}$ or in *Wnt5a*$^{+/-}$ mice.

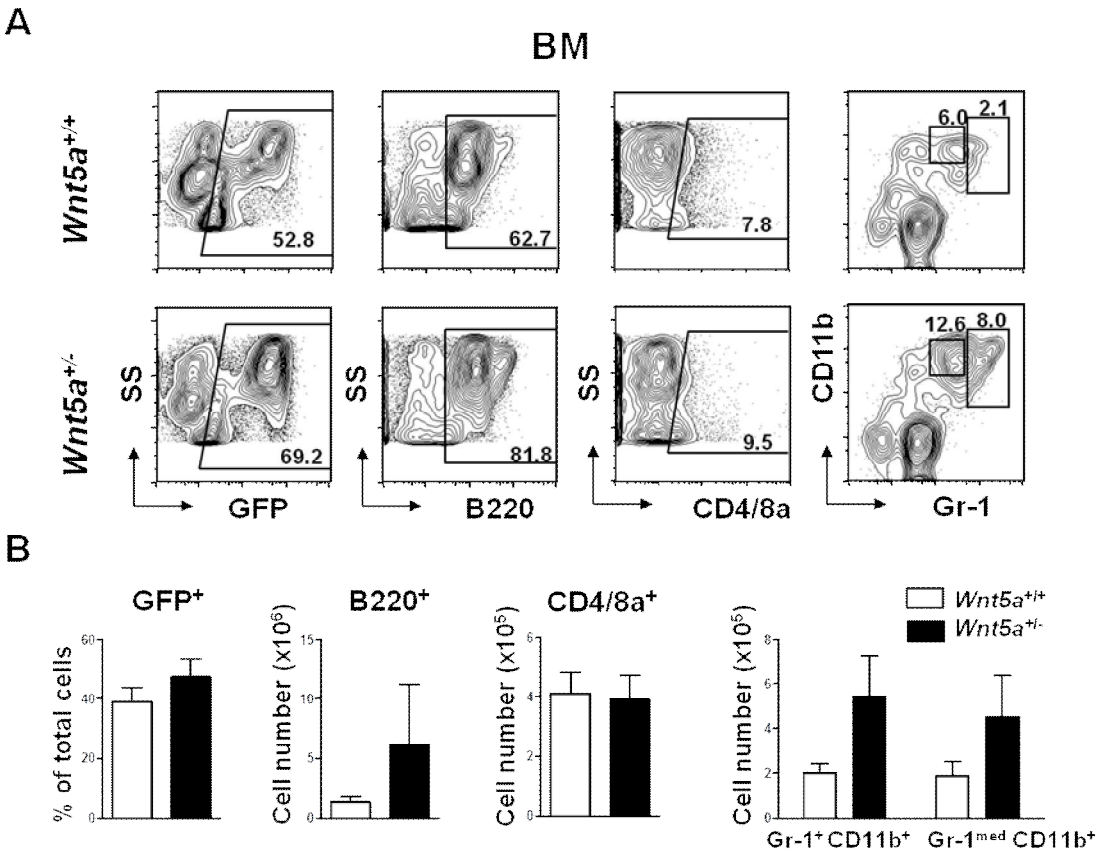

Figure 56. Mature, BCR/ABL expressing cells in BM of diseased mice. (A) Representative FACS plots of mature cell staining of lymphoid and myeloid populations, gated on PI negative GFP positive cells of BCR/ABL expressing cells in both Wnt5a$^{+/+}$ and *Wnt5a*$^{+/-}$ mixed LMPD mice **(B)** The engraftment level of GFP$^+$ BCR/ABL expressing cells in BM. The total cell number of B220$^+$, CD4/8a, granulocytes and monocytes that express GFP are shown of *Wnt5a*$^{+/+}$ diseased mice n=15 (white bars) compared to *Wnt5a*$^{+/-}$ diseased mice n=16 (black bars); Mean ± SEM.

In *Wnt5a*$^{+/-}$ recipient mice, the percentage of GFP$^+$ cells is unchanged. The GFP$^+$ cells are represented in both lineages, lymphoid and myeloid. The amount of GFP expressing B220$^+$ cells, CD4/8a cells as well as Gr-1$^+$ Cd11b$^+$ and Gr-1$^+$ Cd11b^{med} populations in BM is not different (Figure 56).

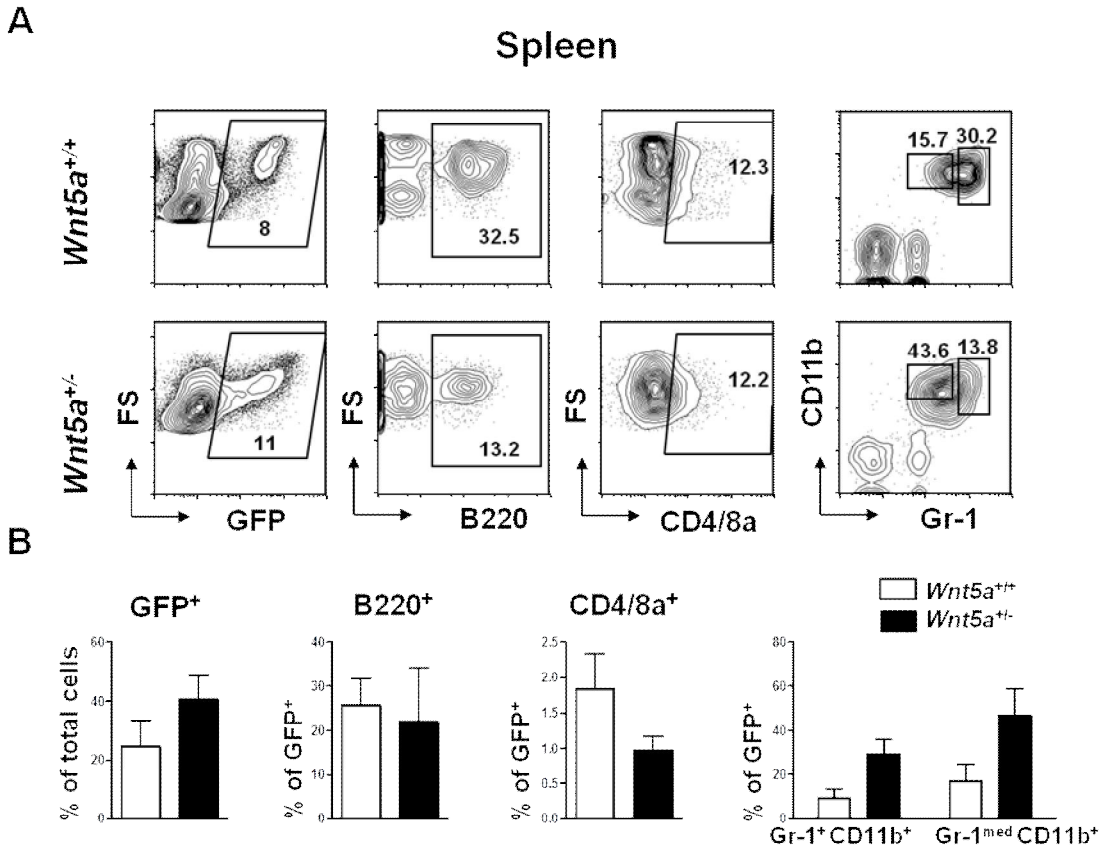

Figure 57. Mature, BCR/ABL expressing cells in Spleen of diseased mice. (**A**) Representative FACS plots of mature cell staining of lymphoid and myeloid populations, gated on PI^- GFP^+ cells of BCR/ABL expressing cells in either *Wnt5a*$^{+/+}$ or *Wnt5a*$^{+/-}$ mixed LMPD mice **(B)** The engraftment level of GFP^+ BCR/ABL expressing cells in Spleen. The total cell number of $B220^+$ cells, $CD4/8a^+$ cells, granulocytes and monocytes that express GFP are shown of *Wnt5a*$^{+/+}$ diseased mice n=15 (white bars) compared to *Wnt5a*$^{+/-}$ diseased mice n=16 (black bars); Mean ± SEM.

Similarly, in the Spleen of *Wnt5a*$^{+/-}$ recipient mice, the percentage of GFP^+ cells is unchanged. In addition, the GFP^+ cells are represented in both lineages, lymphoid and myeloid. Comparable with the BM analysis (Figure 56), there is no change in GFP^+ mature cell populations in Spleen (Figure 57).

In order to obtain more information about the engraftment and maintenance of BCR/ABL-expressing HSCs in the *Wnt5a*-deficient microenvironment, the number of early stages of hematopoietic hierarchy was determined by flow cytometry of BM and Spleen cells. The gating strategy can be seen in Figure 58A.

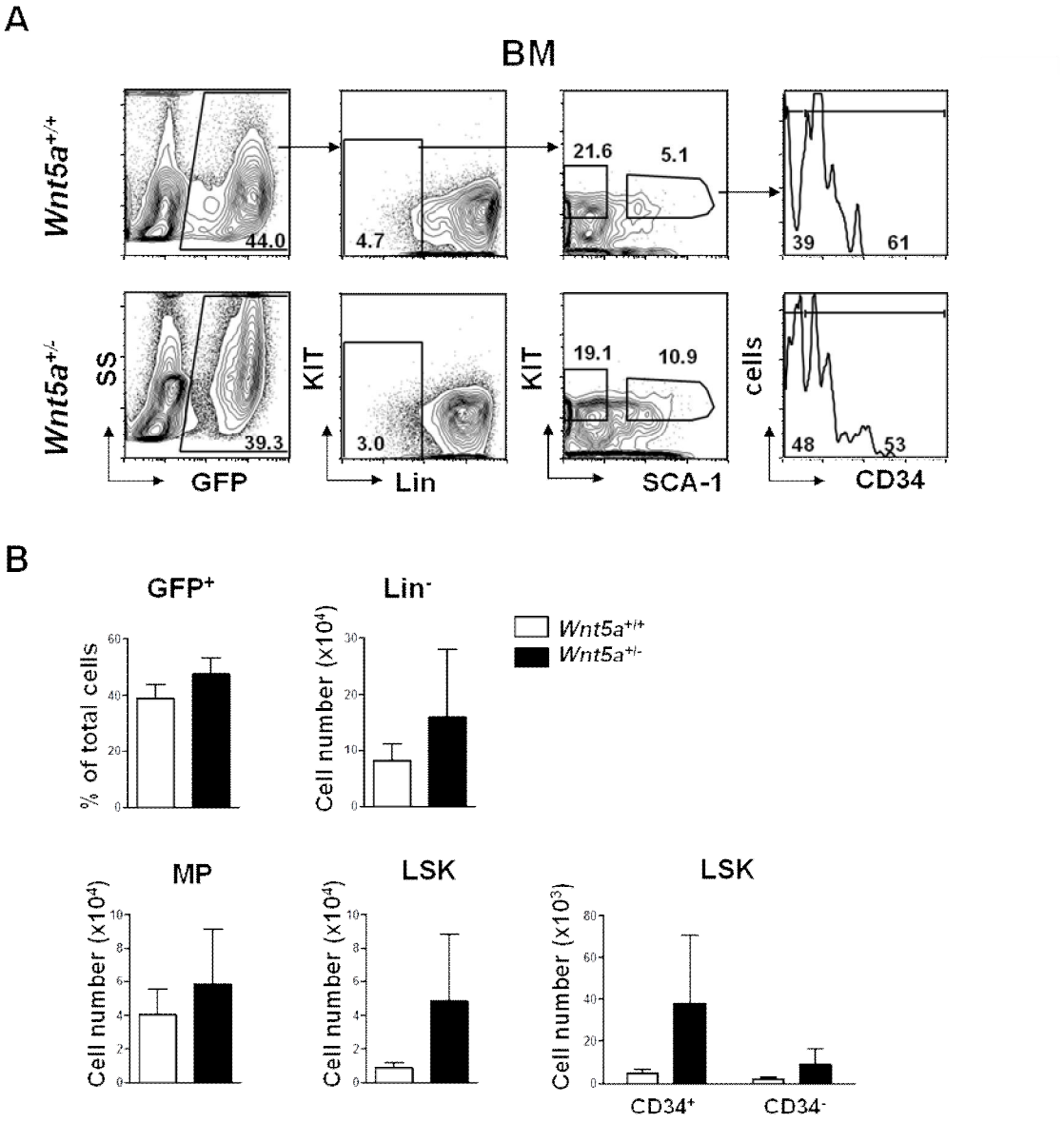

Figure 58. Early hematopoiesis of BCR/ABL expressing cells in BM of diseased mice. (A) Representative FACS plots of BM for MPs, CLPs and LSKs (LT-HSCs and ST-HSCs) gated on PI^- GFP^+ cells of BCR/ABL expressing cells in both *Wnt5a*$^{+/+}$ and *Wnt5a*$^{+/-}$ diseased mice **(B)** The engraftment level of GFP^+ BCR/ABL expressing cells in BM. The total cell number of MPs, CLPs and LSKs (LT-HSC and ST-HSC) that express GFP are shown of *Wnt5a*$^{+/+}$ diseased mice n=15 (white bars) compared to *Wnt5a*$^{+/-}$ diseased mice n=16 (black bars); Mean ± SEM.

The analysis of GFP-expressing cells in BM (GFP^+) of *Wnt5a*$^{+/-}$ recipient mice in terms of primitive hematopoiesis revealed no detectable impact on the myeloid progenitors (MP, GFP^+ Lin^- $SCA\text{-}1^-$ KIT^+). However, a slight increase was noted in the percentage (Figure 58A) as well as the absolute number of LSK (GFP^+ Lin^- $SCA\text{-}1^+$ KIT^+) cells and both, short-term HSCs and long-term HSCs (LT-HSC, $CD34^-CD150^+$ -HSCs) within the GFP+ LSK cell fraction (Figure 58B) of *Wnt5a*$^{+/-}$ recipient BM when compared with the BM of *Wnt5a*$^{+/+}$ recipients.

In clinical LMPD, extramedullary hematopoiesis and splenomegaly is frequently observed [194]. In Spleens of LMPD mice, the GFP$^+$ Lin- population in *Wnt5a*$^{+/-}$ recipient Spleens revealed a detectable decrease compared to *Wnt5a*$^{+/+}$ recipients. Moreover, a significant decrease in the percentage of CLP (GFP$^+$ Lin$^-$ KIT^{med} IL7-R$^+$) cells was observed in *Wnt5a*$^{+/-}$ recipients. In addition, we also found a decrease in the LSKs (GFP$^+$ Lin$^-$ SCA-1$^+$ KIT$^+$) of *Wnt5a*$^{+/-}$ recipient Spleen when compared with *Wnt5a*$^{+/+}$ recipient littermates. A closer look at the LSK fraction revealed an increase in the absolute number of short-term CD34$^+$ HSCs and a significantly decrease of long-term HSCs (LT-HSC, GFP$^+$ CD34$^-$ CD150$^+$-HSCs) in *Wnt5a*$^{+/-}$ recipient mice (Figure 59).

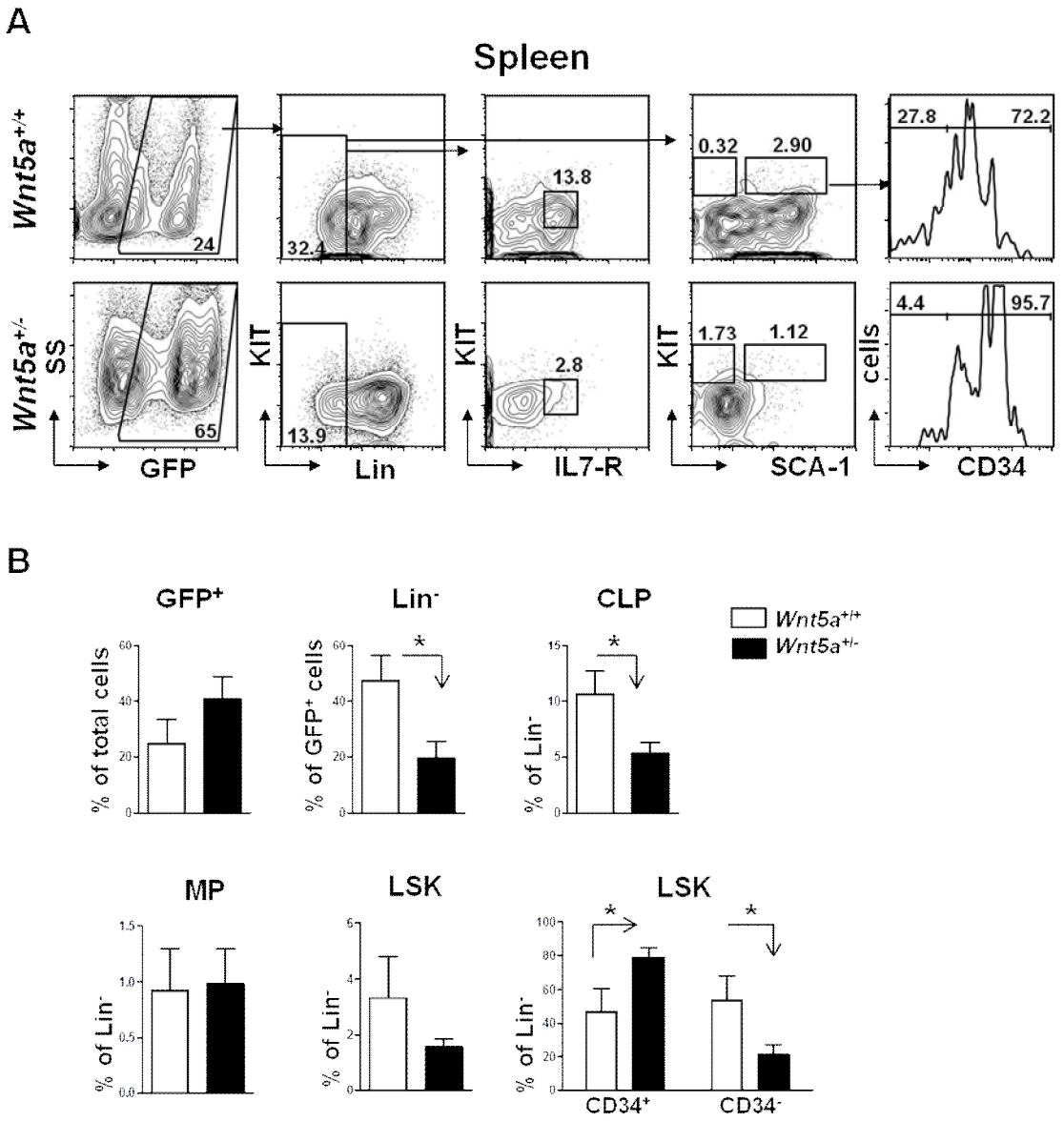

Figure 59. Early hematopoiesis of BCR/ABL expressing cells in Spleen of diseased mice. **(A)** Representative FACS plots of Spleen for MPs, CLPs and LSKs (LT-HSC and ST-HSC) gated on PI$^-$ GFP$^+$ cells of BCR/ABL expressing cells in both *Wnt5a*$^{+/+}$ and *Wnt5a*$^{+/-}$ diseased mice **(B)** The engraftment level of GFP$^+$ BCR/ABL expressing cells in Spleen. The total cell number of MPs, CLPs and LSKs (LT-

HSC and ST-HSC) that express GFP are shown of *Wnt5a*$^{+/+}$ diseased mice n=15 (white bars) compared to *Wnt5a*$^{+/-}$ diseased mice n=16 (black bars); Mean ± SEM.

Concluding, the outcome of LMPD, induced by BCR/ABL expressing cells, is dependent on Wnt5a signalling from the niche. In order to test the functionality of the putative leukemic stem cells (LICs), we performed retransplantation experiments.

4.7.2. Retransplantation of primary induced LMPD

In primary mice, one can only show development of an LMPD. In order to find out whether the LMPD is leukemically transformed, serial transplantations are required. For this purpose, freshly isolated Spleen cells (1x10^6 GFP$^+$) of *Wnt5a*$^{+/-}$ and WT recipients with LMPD were transplanted into sublethally irradiated WT B6 mice. Surprisingly, and perhaps in line with the failure to self-renew of normal HSCs (Figure 41), only the GFP$^-$ expressing cells that engrafted in the 1° *Wnt5a*$^{+/+}$ microenvironment developed leukemia in 2° recipients, within 45 days. In contrast, the GFP expressing cells that engrafted in the 1° *Wnt5a*$^{+/-}$ microenvironment and developed LMPD, were unable to re-establish leukemia in secondary mice (Figure 60).

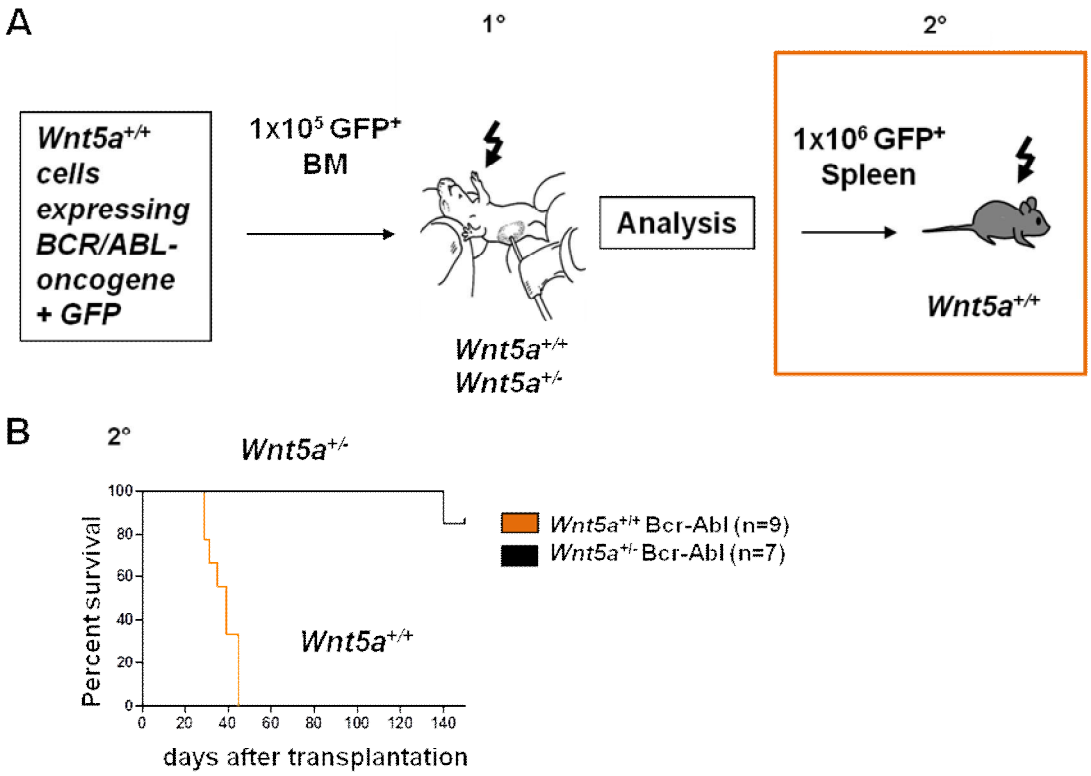

Figure 60. Secondary transplantation of Spleen cells of diseased mice. (A) Serial transplantation flow chart. 2°: 1x10^6 of BCR/ABL expressing Spleen cells were retransplanted in sublethally irradiated WT mice. **(B)** Kaplan-Meier survival plot visualizing the percentage of survival over

time (days after transplantation), in two groups *Wnt5a*$^{+/+}$ BCR/ABL n=9 (orange curve) and *Wnt5a*$^{+/-}$ BCR/ABL n=7 (black curve).

These results highly suggest that leukemia-development, even with expression of a so-called “strong” oncogene like BCR/ABL, is dependent on Wnt5a signalling of the niche. The *Wnt5a*$^{+/-}$ mice developed a more severe LMPD with a shorter latency time and developed a more aggressive form of LMPD in aspect of enhanced white blood formation in PB and colonalization of Spleen. Unexpectedly though, despite the presence of an increased pool of GFP expressing cells in Spleen, none of the 2° recipients receiving GFP$^+$ cells from primary *Wnt5a*$^{+/-}$ recipients with BCR/ABL$^+$ LMPD, induced leukemia in secondary transplanted WT mice.

4.7.3. Transplantation of BCR/ABL expressing BM cells into Wnt5a deficient microenvironment-Homing assay

The diminished self-renewal of normal HSCs was at least in part due to severely decreased homing (Figure 43) and decreased CDC42 activity (Figure 45). In order to test whether a similar mechanism might underlie the failure of GFP$^+$ cells generated in mice developing LMPD in the *Wnt5a*-deficient microenvironment, a homing assay was performed [23, 174]. In this assay, 1.25×10^6 GFP$^+$ cells from the BM of WT donor mice were transplanted into lethally irradiated eight to ten weeks old *Wnt5a*$^{+/+}$ and *Wnt5a*$^{+/-}$ recipients and the number of HSCs engrafted in the recipient’s marrow 16-hours after the transplantation was examined by flow cytometry (Figure 61A).

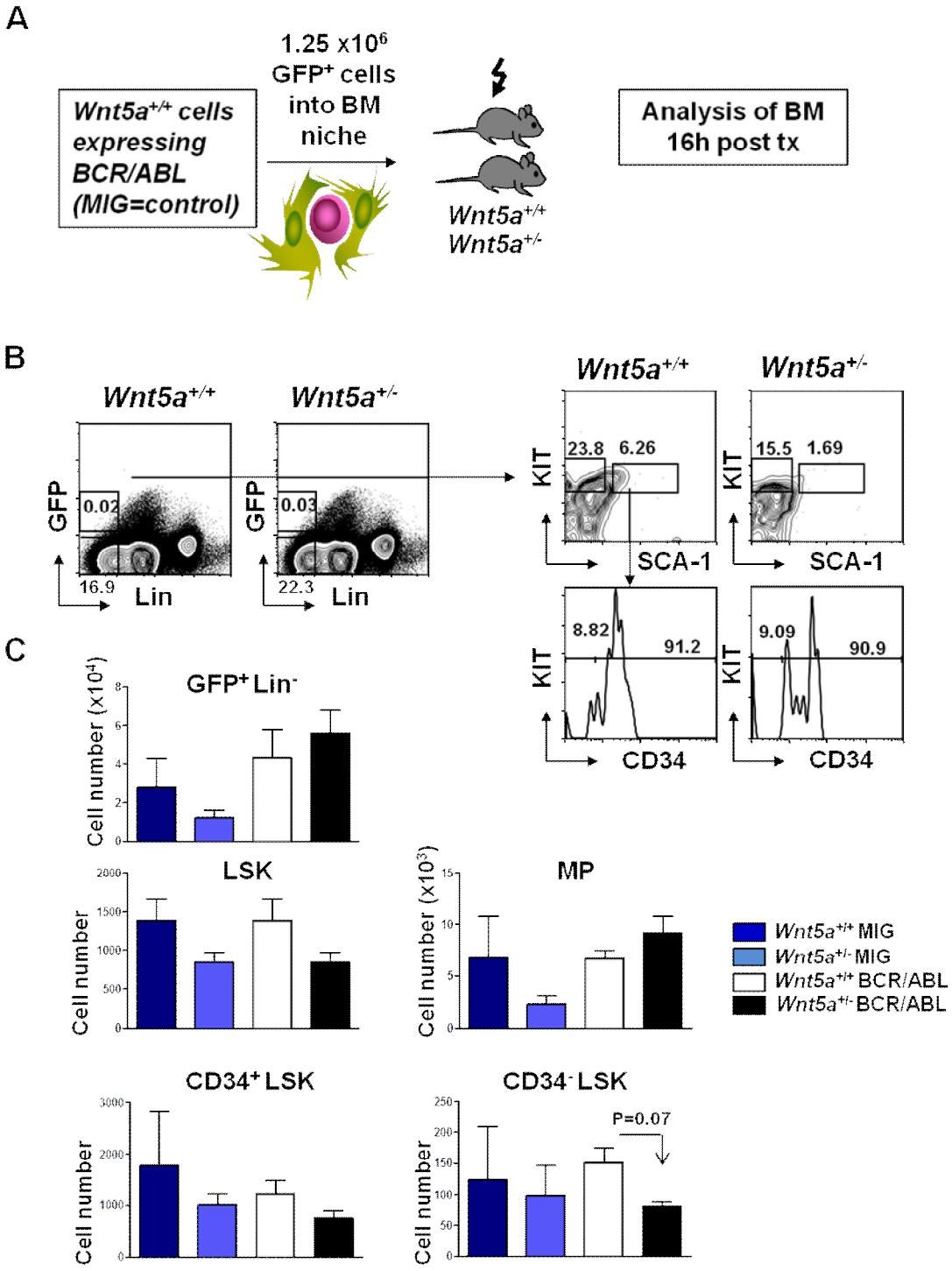

Figure 61. Homing of WT BCR/ABL expressing cells in *Wnt5a*$^{+/-}$ microenvironment. (A) Serial transplantation flow chart. *Wnt5a*$^{+/+}$ Lin^{-} cells, expressing BCR/ABL, were injected into lethally irradiated *Wnt5a*$^{+/-}$ and WT mice (1°). As a control MIG (control vector) expressing *Wnt5a*$^{+/+}$ Lin^{-} cells were transplanted the same way. After 16 h, homing of HSC and progenitor populations were analysed by FACS **(B)** Representative FACS plots gated on PI^{-} GFP^{+} Lin^{-} cells and the subpopulations MPs and LSKs (LT-HSC and ST-HSC) of *Wnt5a*$^{+/+}$ BCR/ABL and *Wnt5a*$^{+/-}$ BCR/ABL mice; **(C)** Graphs, presenting the homing efficiency of four groups: *Wnt5a*$^{+/+}$ MIG n=3 (dark blue bars), *Wnt5a*$^{+/-}$ MIG n=3 (light blue bars); *Wnt5a*$^{+/+}$ BCR/ABL n=3 (white bars); *Wnt5a*$^{+/-}$ BCR/ABL n=3 (black bars).

The experiment revealed that the progenitor populations, Lin^- cells and MPs that express GFP (BCR/ABL) show a higher homing efficiency to the BM of both in WT and *Wnt5a*$^{+/-}$ than the MIG controls. In the LSK population; the cell number of homed cells is decreased in *Wnt5a*$^{+/-}$ *BCR/ABL* recipient mice compared to WT BCR/ABL recipients. Especially, the LT-HSC population ($CD34^-$ LSK) of *Wnt5a*$^{+/-}$ recipients shows a nearly significant (p=0.07) decrease compared to the cell number of LT-HSC of WT recipient littermate controls (Figure 61B+C).

These results indicate an impact in homing of BCR/ABL expressing HSCs. Less Wnt5a in the BM microenvironment causes impaired engraftment of BCR/ABL-expressing progenitor cells: where Lin^- and myeloid progenitors appear to home equally well in *Wnt5a*$^{+/+}$ and *Wnt5a*$^{+/-}$ recipients, more primitive LSK and LT-HSC show a specific homing impairment in the *Wnt5a*$^{+/-}$ environment

In Chapter 4.6.2 we found a comparable effect on hematopoietic stem and progenitor cells, which engrafted for 16 weeks in *Wnt5a*$^{+/-}$ niche. In leukemic experiments, this could also explain the ´make or break´ principle of arising LMPD in *Wnt5a*$^{+/-}$ mice, since *Wnt5a*$^{+/-}$ recipient mice either develop a severe LMPD, which is not transplantable into 2° recipients, or do not even develop LMPD. In both cases, the failure to develop leukemia is reminiscent of the failure of normal HSC to self-renew once they have been regenerated in a *Wnt5a*-deficient environment.

4.7.4. Study of the Wnt signalling of BCR/ABL expressing cells from *Wnt5a*$^{+/+}$ and *Wnt5a*$^{+/-}$ diseased mice

Since there are relevant and persistent differences in the development and outcome of leukemia dependent on Wnt5a in the microenvironment, the molecular regulation of hematopoietic cells of diseased mice, was analysed. In Figure 62A, the sorting scheme of LSKs and MPs is shown. Unfortunately, it was not possible, to sort a sufficiently high number of BCR/ABL^+ GFP^+ expressing LSKs out of the BM of LMPD mice for immunofluorescence staining. Since all of the LMPD mice showed a sizeable GFP^+ $B220^+$ population, the $B220^+$ B cells were taken as a “pseudo” indicator for changes in signalling, on the assumption that expression of BCR/ABL would lead to similar changes in signalling in different cell types (Figure 62B).

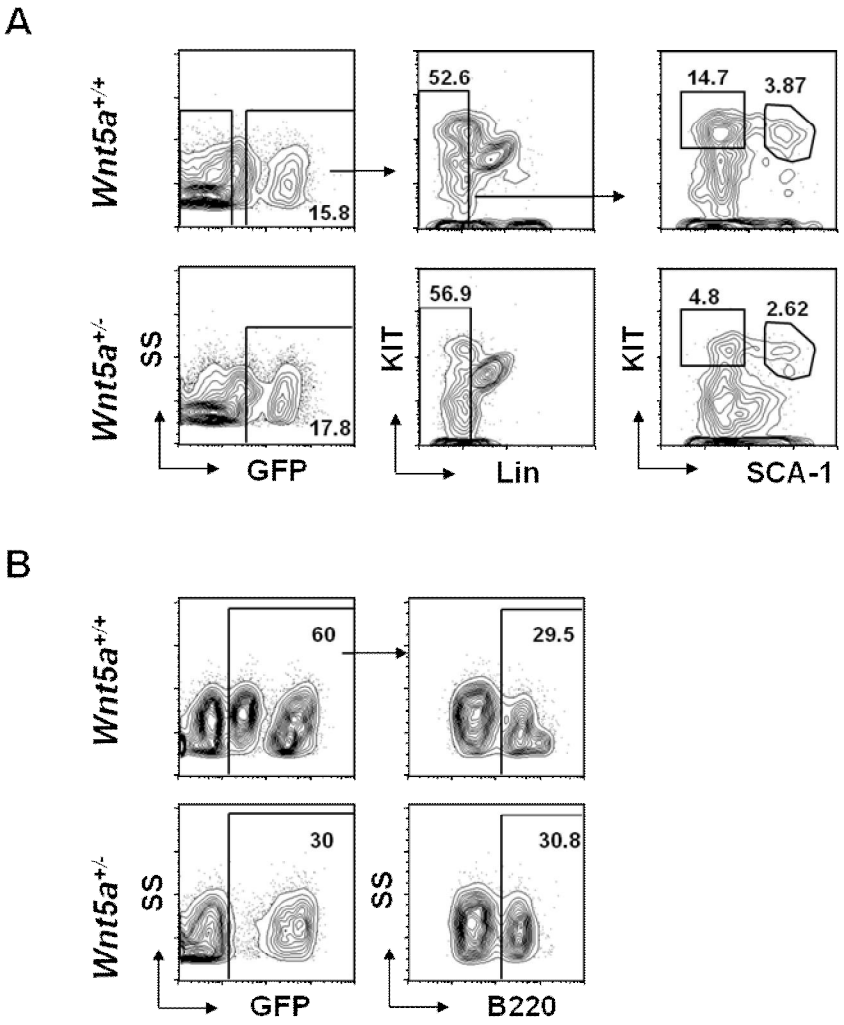

Figure 62. Sorting of BCR/ABL expressing hematopoietic BM populations. (A) Sorting scheme: The isolated BCR/ABL expressing BM from 1° *Wnt5a*$^{+/+}$and 1° *Wnt5a*$^{+/-}$transplantation was sorted for donor derived GFP^{+} LSKs and MPs **(B)** Sorting scheme: The isolated BCR/ABL expressing BM from 1° *Wnt5a*$^{+/+}$ and 1° *Wnt5a*$^{+/-}$transplantation was sorted for donor derived GFP^{+} B220^{+} cells.

Canonical Wnt signalling

Activated canonical signalling is reported in various types of cancer. In Chapter 4.4., we demonstrated the activation of canonical signalling in steady-state LSK cells and LSK cells isolated from *Wnt5a*$^{+/-}$ recipient mice. Here, we demonstrate an important role of canonical Wnt signalling in BCR/ABL induced *Wnt5a*$^{+/-}$ diseased mice.

In *Wnt5a*$^{+/-}$ recipient mice, less Wnt5a ligand is available. As a consequence beta-catenin signalling we find enhanced activation through DVL2 and phosphorylation of the kinase GSK-3 beta and consequently dephosphorylation of beta-catenin. The transcription of several genes, involved in tumourgenesis, is activated (Figure 63). These results might be one of the explanations for the GFP^{+} cells showing a shorter

latency time for development of LMPD and the more severe form of LMPD in *Wnt5a*$^{+/-}$ recipient mice.

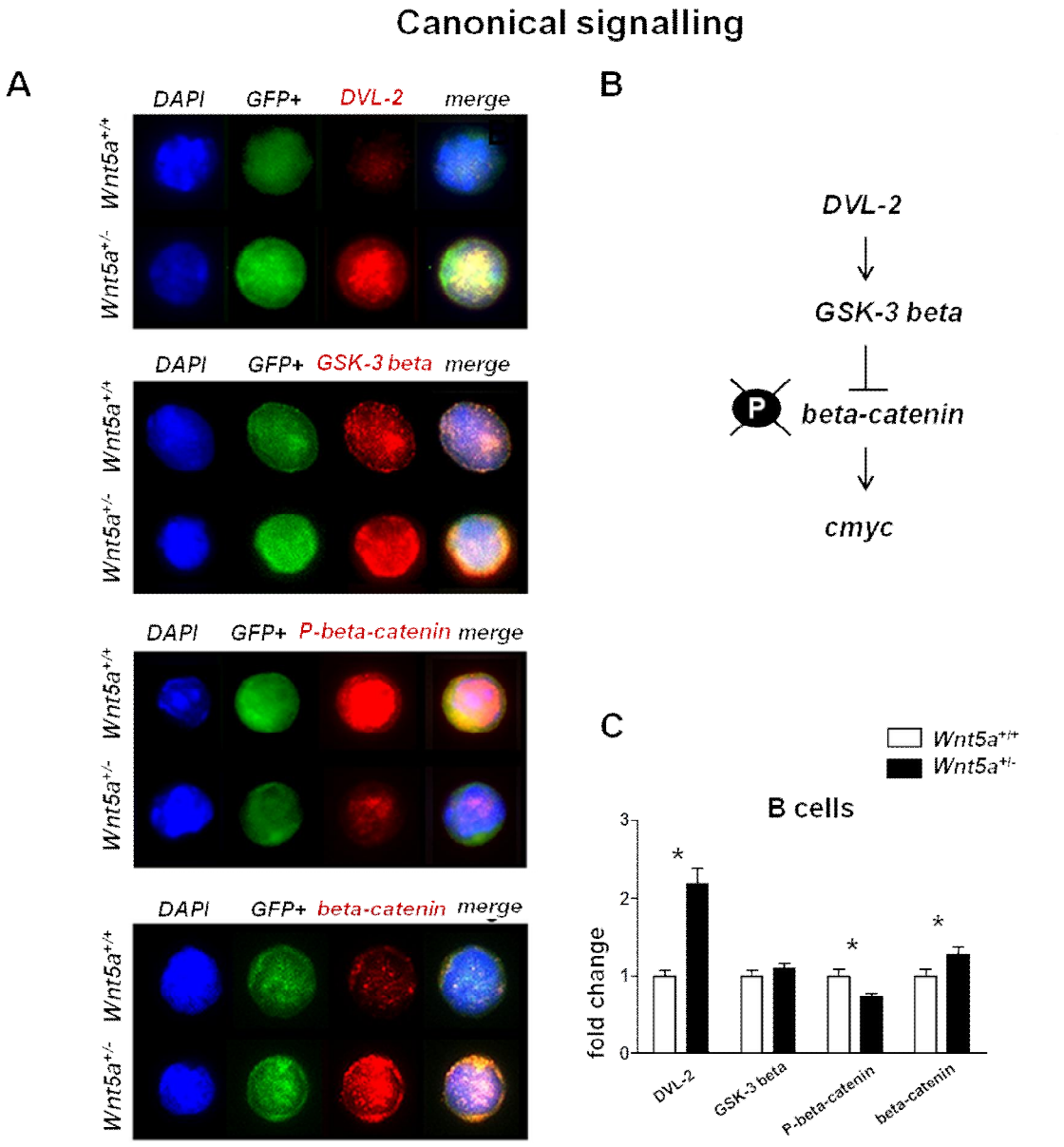

Figure 63. Activation of canonical Wnt signalling in *Wnt5a*$^{+/-}$ diseased mice. (A) Representative pictures of single-cell stains showing the expression of proteins involved in canonical Wnt signalling (red) in BCR/ABL expressing B cells (GFP/green) of *Wnt5a*$^{+/+}$ and *Wnt5a*$^{+/-}$ diseased mice, the nuclear counterstaining with DAPI (blue) and merge of both (coloured/right). **(B)** Schematic illustration of canonical Wnt signalling **(C)** For quantification of the proteins involved in Wnt/beta-catenin pathway in WT (white bars) and *Wnt5a*$^{+/-}$ (black bars) B cells , 30 cells were snaped on Leica fluorescent microscope, 100-fold enlarged. Total pixel were quantified by ImageJ; Mean ± SEM; *p<0.05.

Non-canonical Wnt signalling

In addition, like under steady-state conditions, the BCR/ABL^{+} (GFP^{+}) cells were also analysed for changes in the components of non-canonical signalling. The sorted GFP^{+}

B220^{+} B cells were analysed for the expression of proteins involved in calcium-dependent non-canonical Wnt signalling.

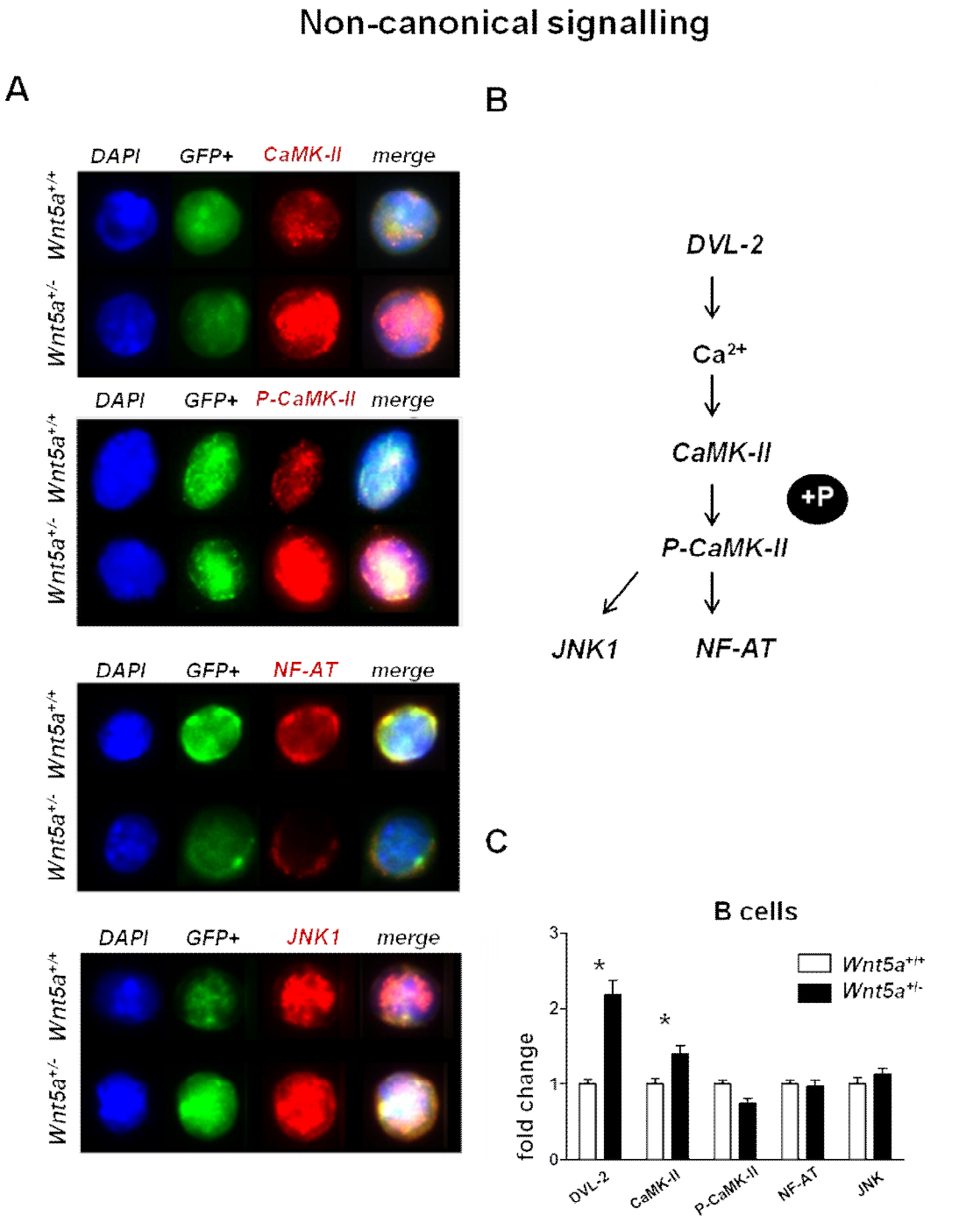

Figure 64. Downregulation of non-canonical Wnt signalling in *Wnt5a*$^{+/-}$ diseased mice. (A) Representative pictures of single-cell stains showing the expression of proteins involved in non-canonical Wnt signalling (red) in BCR/ABL expressing B cells (GFP/green) of *Wnt5a*$^{+/+}$ and *Wnt5a*$^{+/-}$ diseased mice, the nuclear counterstaining with DAPI (blue) and merge of both (coloured/right). **(B)** Schematic illustration of non-canonical Wnt signalling **(C)** For quantification of the proteins involved in non-canonical Wnt pathway in WT (white bars) and *Wnt5a*$^{+/-}$ (black bars) B cells , 30 cells were snaped on Leica fluorescent microscope, 100-fold enlarged. Total pixel were quantified by ImageJ; Mean ± SEM; *p<0.05.

Interestingly, in contrast to our findings with untreated HSCs (Figure 36), downregulation of the activated form of CaMK-II (P-CaMK-II) could be detected. Moreover, we detected no changes in NF-AT and JNK1 expression between GFP^+ $B220^+$ cells from *Wnt5a*$^{+/-}$ and *Wnt5a*$^{+/+}$ recipients (Figure 64).

In summary, these results indicate that in BCR/ABL-induced LMPD, there is a Wnt5a-dependent regulation of canonical signalling over beta-catenin. The *Wnt5a*-deficient microenvironment supports the activation of beta-catenin, while calcium-dependent non-canonical Wnt dependent signalling is unchanged.

4.7.5. Characterization of the niche compartment of BCR/ABL induced diseased mice by FACS

Several papers have shown that the composition of the niche and the reaction of niche cells to malignancies contribute to leukemia formation and survival. Indeed, recent studies showed that LMPD progressively remodels the endosteal BM niche into a self-reinforcing leukemic niche which impairs normal hematopoiesis, favours leukemic stem cell (LSC) function, and contributes to BM fibrosis [124]. The differences in the development of LMPD by BCR/ABL oncogene-expressing cells in the *Wnt5a*$^{+/-}$ microenvironment compared to WT microenvironment, as well as the enhanced canonical and apparently unaffected non-canonical Wnt signalling in the hematopoietic compartment of *Wnt5a*$^{+/-}$ recipient mice with LMPD (Chapter 4.7.1) led us to the hypothesis that the cellular composition of the niche is changed in *Wnt5a*$^{+/-}$ recipients with LMPD compared to WT recipients with LMPD.

In previous experiments described in Chapter 4.6.4., the microenvironmental compartment was analysed in terms of normal steady-state in *Wnt5a*$^{+/-}$ mice compared to their *Wnt5a*$^{+/+}$ WT littermates. Here, we examined the BM niche in the presence of BCR/ABL^+ LMPD cells in *Wnt5a*$^{+/-}$ and *Wnt5a*$^{+/+}$ recipient mice by FACS analysis, in detail for OBCs and MSCs (Figure 65).

In our experiments, the recipient mice with LMPD were sacrificed when severe symptoms appeared. For the purpose of analyzing the niche, we gated BM cells in a similar manner as shown in Figure 47. Here, we detected a significant higher percentage of the $TER119^-$ $CD45^-$ non-hematopoietic fraction of cells in Wnt5a$^{+/-}$ recipient mice with LMPD (Figure 61). The endothelial cells and the MSCs are unchanged in percentages of the $TER119^-$ $CD45^-$ $CD31^+$ fraction in both *Wnt5a*$^{+/+}$ and

Wnt5a$^{+/-}$ recipient genotypes of mice with LMPD compared to the MIG controls. Interestingly, we found a significant decrease in the fraction of OBCs (TER119$^-$ CD45$^-$ CD31$^-$ SCA-1$^-$ ALCAM$^+$) in *Wnt5a*$^{+/+}$ (WT) recipient mice with LMPD, which agrees well with recent findings [124].

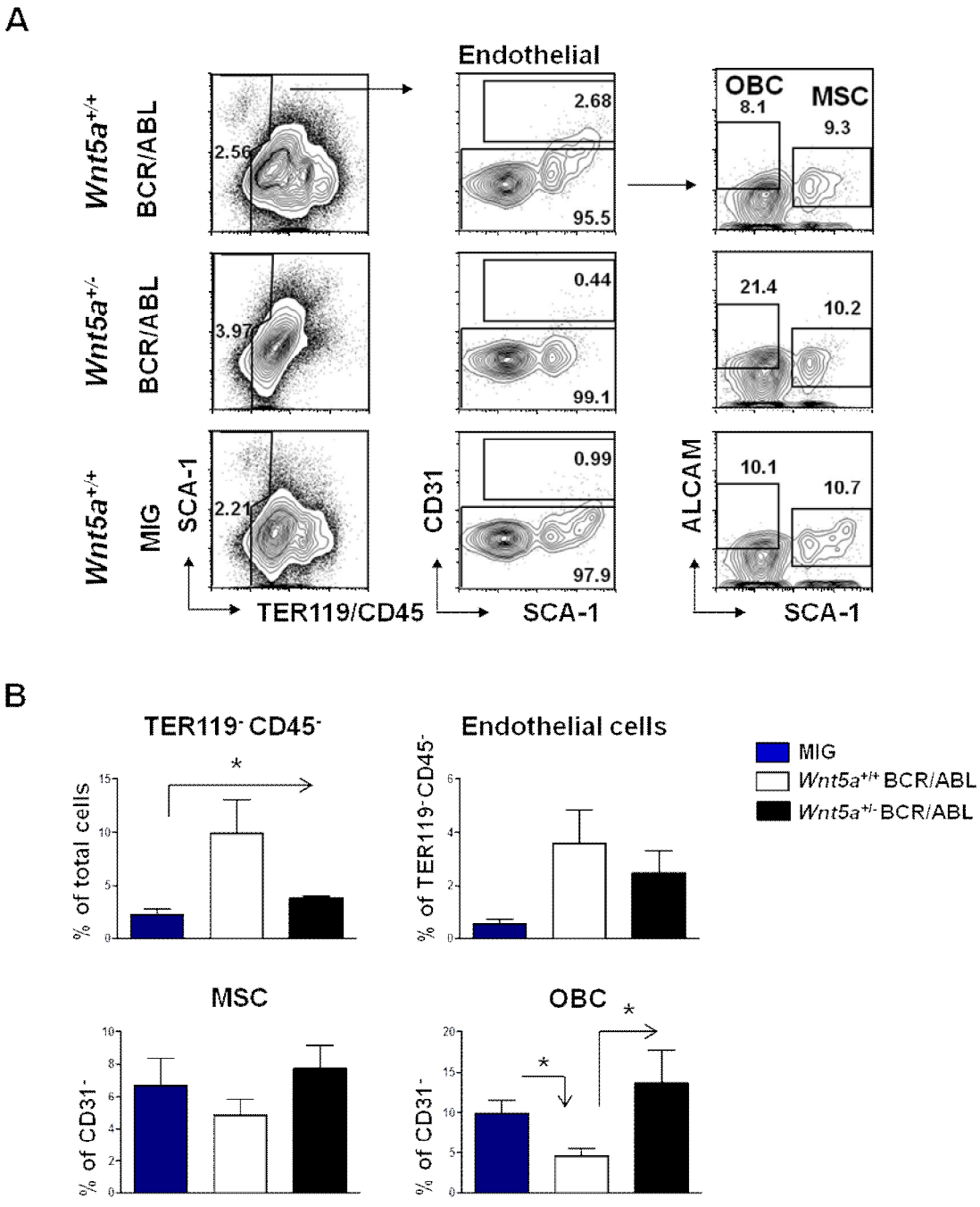

Figure 65. BM niche compartment of *Wnt5a*$^{+/-}$ diseased mice. (A) Representative FACS profile of ALCAM and SCA-1 expression in CD45$^-$ CD31$^-$ TER119$^-$ cells to distinguish endothelial cells, MSCs and OBCs in the diseased mice (1°) **(B)** Percentages of the BM stromal cell populations TER119$^-$ CD45$^-$, EC, MSC and OBC; *Wnt5a*$^{+/+}$ n=9 (white bars), *Wnt5a*$^{+/-}$ n=9 (black bars); Mean ± SEM; *p<0.05.

Additionally, in *Wnt5a*$^{+/-}$ recipient mice with LMPD, the fraction of OBCs is comparable to MIG controls. Since it has been argued that the loss of OBCs induced by the presence of GFP^{+} BCR/ABL^{+} cells would correspond to a leukemia-promoting niche [124], the failure to form such an OBC-depleted niche in *Wnt5a*$^{+/-}$ recipients could contribute to the fact that these mice do not develop transplantable leukemia, or remain disease-free.

In summary, in all of the recipient mice, the primary BCR/ABL expressing cell population transplanted was the same, only the microenvironment was different. Thus, our results strongly indicate that Wnt5a is required for remodelling of the OBC compartment in the niche and for the emergence of a self-renewing population of LSCs. By analyzing the outcome of LMPD, we can say that the development of LMPD in *Wnt5a*$^{+/-}$ recipient mice either shows a shorter latency time and a more aggressive outcome of disease or does not lead to disease at all in 36% of the mice, which may suggest an important role for *Wnt5a* in homing of the cells to the niche. Surprisingly, and in line with the failure to self-renew of normal HSCs, only the GFP-expressing cells that engrafted in the 1° *Wnt5a*$^{+/+}$ microenvironment developed leukemia in 2° recipients. By analyzing Wnt signalling we could detect a shift from non-canonical signalling to canonical signalling by increased beta-catenin expression. This project could not finally identify *Wnt5a* as a tumour suppressor as *Wnt5a*$^{+/-}$ mice developed LMPD in first transplantation, but failed to develop leukemia in secondary recipients. This fact indicates leukemic stem cell exhaustion due to less *Wnt5a* expression in the BM

5. Discussion

Hematopoietic stem cells (HSCs) are highly proliferative during fetal development. This fetal program is lasting until three to four weeks after birth [195-196]. In the adult hematopoietic system, the HSCs are quiescent, and these dormant cells can then be found within the endosteal BM niche, close to Osteopontin$^+$ and N-cadherin$^+$ osteoblasts. It is generally assumed that the interaction between HSCs and niche cells induces quiescence and keeps HSCs mainly in G0/G1 of the cell cycle. Since the number of HSCs, which are able to reconstitute the whole blood system, is probably limited, the activation and proliferation of HSCs is tightly regulated. So far, many investigators have shown that soluble signals from the niche are responsible for driving the HSCs into cell cycle. However, in none of these studies, HSC quality is preserved.

Recently, we have shown that Pleiotrophin, a signal expressed from the BM niche, regulates repopulation-behaviour of HSCs [58] and sFRP-1, which is highly expressed by niche cells, extrinsically regulates cycling activity and maintenance of hematopoietic stem cells [59]. SFRP-1 is known as Wnt inhibitor and also as binding partner of the principal non-canonical stimulator Wnt5a.

The role of non-canonical Wnt signalling in hematopoiesis is not entirely clear due to the complexity of the many different downstream signalling events [84].Cadherin EGF LAG seven-pass G-type receptor 2 (Celsr2/Flamingo) is a newly investigated cadherin, which is involved in the Wnt/planar cell polarity pathway. In *Celsr2*-deficient mice, hematopoiesis has never been investigated, but it was shown that the development and planar organization of ependymal cilia are impaired, leading to defective brain development [197]. The Rho GTPase, CDC42 is also involved in Wnt/planar cell polarity pathway and it was shown by conditional mouse models that *Cdc42*-deficiency in hematopoietic cells led to defects in quiescence, homing and retention in the bone marrow [198].

It was shown before, that non-canonical signalling is essential in the microenvironment, as stroma cells deficient in NLK are defective in maintaining hematopoietic progenitors [199]. NF-ATc1 is a calcium-activated transcription factor. NF-ATc1 knockout mice show perinatal lethality. By a conditional knockout of NF-ATc1 in 10 days old pubs, researchers could detect the outcome of osteopetrosis and inhibition of osteoclastogenesis [200].

In previous *in vitro* studies, Wnt5a was detected as a soluble stroma-derived factor, required for maintenance of HSC in cultures without direct cell-cell contact between HSC and stromal cells [98]. In addition, Wnt5a maintains HSC quiescence through stimulation of CDC42 and repression of canonical signalling [94]. Wnt5a transcripts could be detected throughout the embryo and fetal development. In adults, Wnt5a is

mainly expressed in stromal cells [69, 102], in osteoblasts [103], at a very low level in HSCs of young adult mice and is upregulated during HSC aging [99]. Thus, Wnt5a might be important for the interactions between HSC and their niche with regard to maintenance and proliferation. Nevertheless, the role of Wnt5a in the regulation of early embryo and primitive adult hematopoiesis has never been explored.

The aim of this thesis was to examine the role of Wnt5a in the regulation of hematopoiesis as well as in the regulation of HSC function and in leukemia. We found that Wnt5a secreted by the microenvironment is required for HSC maintenance *in vivo*. Surprisingly, the signalling is regulated over both canonical and non-canonical Wnt signalling pathways. An important intermediate of Wnt5a-dependent non-canonical planar dell polarity signalling is CDC42. Signalling through the small GTPAse CDC42 and this pathway is regulating cytoskeletal remodelling, which impacts on the homing efficiency of HSCs into the BM microenvironment after HSC transplantation. Results in this thesis show that Wnt5a is also crucial for development of the BM niche compartment in steady state as well as for the development of a leukemic niche. Indeed, Wnt5a is also required for the development of leukemia-initiating cells.

5.1. Functions of Wnt5a in steady-state hematopoiesis

5.1.1. Fetal hematopoiesis

Wnt5a expression was detected in FL (E14, E16, and E18) and neonatal livers (P7 and P14) and showed a gradual increase during liver development [201]. Wnt5a is expressed in cell populations enriched for fetal liver HSCs ($AA4.1^+$ $SCA\text{-}1^+$) and progenitor cells as well as in FL stromal cells [139].

Our results demonstrate a role of Wnt5a in mature and primitive fetal hematopoiesis. $Wnt5a^{-/-}$ embryos could be bred but only be analysed in fetal tissues because of perinatal lethality. In E14.5 *Wnt5a*$^{-/-}$ fetal liver, we detected a decreased amount of $B220^+$ B cells. But, more interestingly, the long-term repopulating $CD34^+$ LSK cells were significantly increased whereas the supposedly quiescent $CD34^-$ LSKs were decreased. As *Wnt5a*$^{-/-}$ knockout mice show severe outgrowth defects in several tissues and show a reduced number of proliferating cells in the progressive zone and the primitive streak mesoderm [100], we were surprised to find an increase of phenotypical HSCs in *Wnt5a*$^{-/-}$ fetal livers. In line with the decreased proliferative defect in *Wnt5a*$^{-/-}$ embryos, we also found decreased progenitor cell activity in fetal liver cells, suggesting differences in the regulation of proliferation in stem cells and progenitors.

In this study, we demonstrated a decreased number of $B220^+$ cells in *Wnt5a*$^{-/-}$ FL. A previous study showed opposite effects and reported a 35% increase in the proportion of B lineage cells ($B220^+$) in Wnt5a null fetal livers [139]. One possible explanation for this discordance could be that in ours and the reported study, the *Wnt5a*$^{-/-}$ mice were bred on different backgrounds ((129S2xC57BL/6.J) F1 in our study and 129S2 in the reported study [138]). Liang *et al.* showed in the paper that *Wnt5a* knockout mice with different backgrounds may give different results [139]. Another possible difference in the two studies is that we analysed E14.5 FL whereas the previous study reported on E19 tissues. As mentioned above, Wnt5a expression in FL was shown in FL E14, E16, and E19 and in postnatal liver and interestingly the expression increased gradually [201]. The different amounts of Wnt5a mRNA in the cells of E14 liver and E19 liver might explain the unequal finding. Thus, in the former study and here, a Wnt5a dependent B cell proliferation can be shown.

Nevertheless, our results show for the first time, aberrations in the distribution of phenotypical primitive hematopoietic cells ($CD34^+$ LSKs) in *Wnt5a*$^{-/-}$ fetal liver. As there is an intrinsic defect in colony-forming ability in $Wnt5a^{-/-}$ FL, the question raise if there are changes in repopulation activity and stem cell quality. One has to carry out

transplantation assays in order to answer this issue. FL transplantations with WT cells are well established in our laboratory. For transplantation, $1x10^6$ freshly isolated FL cells per mouse are required. As the FL liver cells of $Wnt5a^{-/-}$ embryo are limited in number, we would need many preceded breedings to gain adequate number of cells for transplantation. Due to these practical reasons, we decided to leave out this experiment.

5.1.2. Adult hematopoiesis

As noted above, *Wnt5a* is transcribed in $AA4.1^+$ $SCA\text{-}1^+$ fetal liver cells and $AA4.1^-$ progenitor cells as well as in FL stromal cells [139]. In adult tissues, *Wnt5a* is strongly expressed by BM stromal cells and the stromal cell line UG26-1B6 (Figure 8, [98]). In hematopoietic cells *Wnt5a* is not detectable in CLPs and granulocytes, but can be amplified from LSKs (low level), MPs and B cells (chapter 4.1). These results demonstrate that Wnt5a is widely expressed both in selected hematopoietic lineages throughout hematopoietic hierarchy as well as niche cells. Thus, it is unclear whether Wnt5a regulates hematopoiesis through intrinsic or extrinsic mechanisms.

Intrinsic Extrinsic

The balance between HSC proliferation, self-renewal and quiescence is carefully regulated, to ensure blood homeostasis for the lifetime of an individual. HSCs are carefully regulated by an intricate interplay between **cell-intrinsic** mechanisms (inside the HSC and their progeny) and **cell-extrinsic** factors (from outside of the HSCs) produced by the microenvironment. Alterations in this fine-tuned regulatory network leads to aberrant HSC cell cycle regulation, diminished HSC function, and may promote development of hematological malignancy.

In experimental settings, intrinsic and extrinsic regulation and its impact on HSC quality are investigated *in vivo* by long-term repopulation assays.

In the experiments reported here, we detected no changes in mature hematopoiesis concerning lymphoid or myeloid lineages in the BM. Interestingly, in Spleen, the absolute number of pre-B cells, expressing CD43 surface marker but no IgM surface marker, is significantly lower, whereas the mature IgM^+ $B220^+$ cells are unchanged in numbers. In contrast in PB, the circulating mature IgM^+ $B220^+$ cell number is increased. As we found that Wnt5a is strongly expressed in B cells of fetal liver and adult

hematopoietic tissues, one could speculate about a Wnt5a dependency in B-lymphoid regulation development. Former publications demonstrated that Wnt5a overexpressing stromal cells stimulate HSCs to overproduce B lineage lymphocytes. Wnt5a did not influence myeloid or dendritic cell development [202].

Our phenotypical analysis of early hematopoietic cells in the BM of haploinsufficient *Wnt5a*$^{+/-}$ mice revealed that in adult BM, the number of CLPs was significantly increased in *Wnt5a*$^{+/-}$ mice. In addition, we also found a significant increase in the percentage and absolute number of the population of long-term HSCs-containing CD34^{-} CD150^{+} LSKs [11]. Previous studies showed that adult human BM CD34^{+} Lin^{-} primitive progenitor cells express Wnt5a [70]. Cell culture experiments, in which Wnt5a was added to study the effects of Wnt5a, demonstrated that Wnt5a enhances repopulation activity of progenitor cells [203] and that ST- and LT-HSC repopulation was increased by maintaining the HSCs in a quiescent G0 state [104]. The latter results might provide an explanation of the increase in CLPs and CD34^{-} CD150^{+} LSKs, as one could speculate that when added Wnt5a decreases cell cycle activity, decrease of Wnt5a might enhance that. We propose to examine the proliferation status of CLPs and CD34^{-} CD150^{+} LSKs in future experiments. Standard methods are applicable like BrdU staining and Ki-67. BrdU can be incorporated into the newly synthesized DNA of dividing cells. By staining for BrdU, one can reveal if *Wnt5a*-deficient CLPs and CD34^{-} CD150^{+} LSKs show more proliferation. Ki-67 protein is present during all active phases of the cell cycle (G1, S, G2/M), but is absent from resting cells (G0). The Ki-67 staining should reveal the cell cycle status of *Wnt5a*-deficient CLPs and CD34^{-} CD150^{+} LSKs. The cell cycle kinetics for these rare populations were challenging for us because of the limiting numbers of cells available per mouse. Recent studies suggest therefore a carrier cell technique to isolate small cell populations for cell cycle kinetics. This technique is described in Challen *et al.* and might successfully help to identify proliferation and cell cylce status of *Wnt5a*-deficient CLPs and CD34^{-} CD150^{+} LSKs [204].

In order to study and identify possible molecular mechanisms which show alterations in *Wnt5a*$^{+/-}$ mice, several molecules involved in Wnt signalling, downstream of Wnt5a, were analyzed in *Wnt5a*$^{+/-}$ LSK cells. Our experiments demonstrate that in *Wnt5a*$^{+/-}$ LSKs the canonical Wnt signalling is upregulated. The Frizzled-binding intermediate DVL2 was expressed significantly higher, indicating a higher propensity of cells to respond to Wnt factors. Additionally, GSK-3 beta protein was reduced, which would make the beta-catenin destruction complex less active. Indeed, beta-catenin is present

in *Wnt5a*$^{+/-}$ cells at higher levels, as well as localized more in the nucleus in steady state LSK cells. Nuclear beta-catenin is known to bind to TCF/LEF resulting in transcriptional activation of cyclin-D1, which is indeed also overexpressed in *Wnt5a*$^{+/-}$ LSKs compared to *Wnt5a*$^{+/+}$ LSKs. Consistent with the reported finding that Wnt5a directly inhibits canonical Wnt signalling in LSK cells [104].

Our findings support the view that *Wnt5a*$^{+/-}$ HSCs are more **proliferative** by enhanced canonical signalling. Under steady state conditions this is particularly notable in increased committed CLPs in BM and more mature B cells in the circulation. We found that the cell cycle is more activated in *Wnt5a*$^{+/-}$ LSKs and that these cells display more cyclin-D1 expression. Cyclin-D1 is a molecule, which primarily regulates G1 and its expression marks transition from G0 to G1 and promotes subsequent cell cycle progression. Additionally, we show that Fbxw7 is downregulated in *Wnt5a*$^{+/-}$ LSKs. Fbxw7 is an ubiquitin ligase that control hematopoietic stem cell quiescence over destabilisation of another canonical Wnt target: c-Myc. Thompson et al. reported that loss of Fbxw7 function leads to a severe depletion of the HSC pool and HSC self-renewal capacity due to the loss of quiescence [205], suggesting that the loss of Fbxw7 we observe, may result in increased cell cycle activity in *Wnt5a*$^{+/-}$ HSCs. The hypothesis that *Wnt5a*$^{+/-}$ HSCs are more proliferative is additionally supported by higher expression of PPARγ and C/EBPα. Recent studies have shown that by blocking the canonical Wnt signalling with the co-receptor antagonist Dickkopf-1 (DKK1) the expression of PPARγ is enforced, resulting in HSC differentiation [206]. In *Wnt5a*$^{+/-}$ LSKs canonical Wnt signalling and PPARγ expression is enhanced, thus we propose a canonical independent activation of PPARγ expression in LSKs.

C/EBPα and Cyclin D1 are both involved in regulation of HSC self-renewal [160] [161]. In addition, C/EBPα is known as a master regulator of myeloid differentiation [58, 207] and is overexpressed in LSKs and MPs in *Wnt5a*$^{+/-}$ BM, but despite of less LSK cells in the BM of *Wnt5a*$^{+/-}$ mice, we did not see any changes in cell number of myeloid progenitors and mature cells.

Wnt5a is known as the key regulator of non-canonical Wnt signalling [99], and we could show that Wnt5a stimulates the Ca^{2+} release in HSCs (Chapter 4.5) and activate phosphorylation of CaMK-II in *Wnt5a*$^{+/-}$ LSKs. Thus it is surprising that in *Wnt5a*$^{+/-}$ LSK, we detected a significant increase in P-CaMK-II, a significant decrease of the whole CaMK-II protein and a significant overexpression of the transcription factors NF-AT and NLK in *Wnt5a*$^{+/-}$ LSKs. These results suggest that under steady state conditions, Wnt5a plays a dual role in non-canonical signalling and may also inhibit this pathway.

One explanation for the unexpected result that decreased Wnt5a may actually result in increased non-canonical signalling, might be the availability of other non-canonical Wnts or different Wnt receptors and the consequent down-or upregulation of Wnt signalling in hematopoietic cells. Wnt5a binds to various Fzd receptors (Fz2, Fz3, Fz4, Fz5, Fz6, Fz7, Fz8, Fmi) [88], as well as ROR2 and RYK [95], Signalling through these receptors antagonizes canonical Wnt/beta-catenin signalling [96], probably through stimulation of the calcium-dependent signalling. RYK is expressed by HSCs, and inhibition of RYK, blocked the ability of Wnt5a to induce HSC quiescence. As a consequence, proliferation is induced and repopulating ability diminished [97]. Thus, in order to understand the regulation of non-canonical signalling, the expression of other non-canonical Wnt mediators, frizzled receptors and the pseudokinase RYK in both *Wnt5a*$^{+/+}$ and *Wnt5a*$^{+/-}$ LSKs, should be established.

The enhanced proliferation of the *Wnt5a*$^{+/-}$ HSCs by activated canonical signalling and activated NF-ATc1-dependent non-canonical signalling suggested a reduced stem cell quality. However, transplantation of purified *Wnt5a*$^{+/-}$ CD34^{-} CD150^{+} LSKs into a lethally irradiated WT mouse did not reveal **any obvious intrinsic defects** in engraftment upon serial transplantations (until 3° transplantation). Therefore, the phenotypically differences we find in *Wnt5a*$^{+/-}$ hematopoietic cells under steady state conditions, most likely arise by extrinsical Wnt5a-deficiency in the microenvironment.

5.2. Extrinsic regulation

As described in Chapter 4.2, one week co-cultures with WT HSCs on both *Wnt5a*$^{-/-}$ and *Wnt5a*$^{+/-}$ AGM primary stroma, show dramatically reduced number of cells with colony forming ability. These results show that Wnt5a is required for proper maintenance of hematopoietic progenitors in co-cultures *in vitro* and supports the hypothesis of a role of Wnt5a in extrinsic regulation of progenitor production. Although experiments designed to show extrinsic regulation initially showed no major effects of microenvironmental Wnt5a-deficiency, the ability of the HSCs, regenerated in the *Wnt5a*$^{+/-}$ microenvironment, to maintain engraftment is lost in secondary recipients.

We found in WT donor LSK from *Wnt5a*$^{+/-}$ recipients cells, that canonical signalling was unchanged. But, an increase in activate CaMK-II (P-CaMK-II) protein level could be detected, with a decreased level of CDC42. However, we also observe that CDC42 expression is less polarized in engrafted LSK cells, suggesting that despite lower levels, the remaining CDC42 is, in fact, more active. The Rho GTPase, CDC42 is involved in Wnt/planar cell polarity pathway and it was shown by conditional mouse models that *Cdc42*-deficiency in hematopoietic cells led to defects in quiescence, homing and retention in the bone marrow [198]. An important intermediate of non-canonical Wnt/Ca^{2+} pathway is CaMK-II. CaMK-II was shown to interact with Osterix during osteoblast differentiation [208]. CaMK-II-deficiency in hematopoietic cells has not been investigated yet.

In Figure 66, a possible model is shown, which includes the effects observed in WT cells after their regeneration in a *Wnt5a*-deficient microenvironment. The first feature included, suggests that Wnt5a regulates **proliferation**. Our co-culture experiments indicate that stem and progenitor cells are recruited quickly into cell cycle on *Wnt5a*$^{-/-}$ primary stromal cells and, an important consequence of this might be loss of repopulation quality. *In vivo*, during the regenerative response after myeloablation, it has been reported that Wnt10b is upregulated in both stromal and HSCs in the BM followed by increased beta-catenin expression [209]. As enhanced beta-catenin signalling is detectable in *Wnt5a*$^{+/-}$ mice under steady state conditions in general, we suggest comparing the WT HSCs (1° Wnt5a$^{+/-}$) stem cell behaviour with the steady state situation in Wnt5a$^{+/-}$ knockout mice, discussed in Chapter 5.1. These results go along with those of Scheller *et al.* [210] and Kirstetter *et al.*[211], showing that activation of beta-catenin enforced cell cycle entry of hematopoietic stem cells, thus leading to exhaustion of the LT-stem cell pool. In this thesis, the exhaustion of the LT-HSC pool can be detected after secondary transplantation, triggered by Wnt5a-

deficient microenvironment. The WT cells, which engrafted into *Wnt5a*$^{+/-}$ microenvironment lost their quality and failed to engraft into secondary recipients.

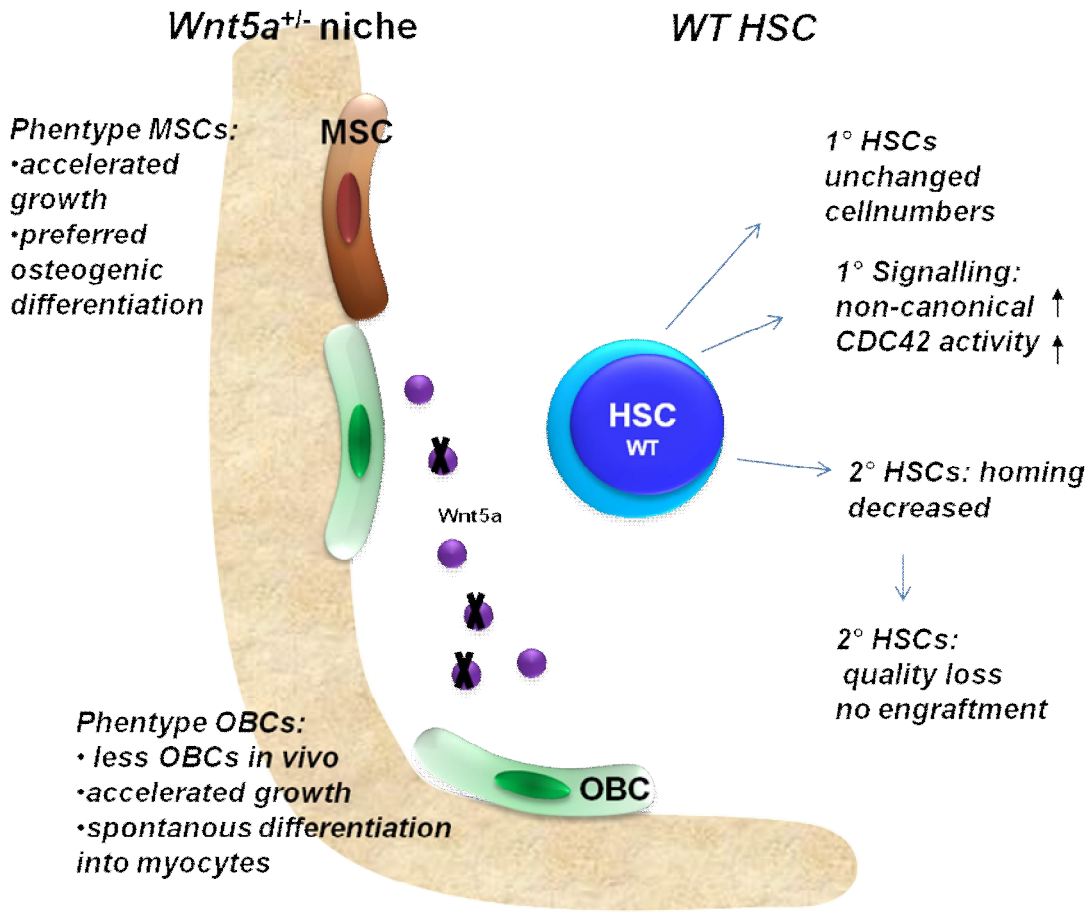

Figure 66. Extrinsic regulation. Possible model of the interaction between the *Wnt5a*$^{+/-}$ endosteal BM niche and the engrafted WT HSCs after transplantation.

Another feature for the effect of Wnt5a-deficiency is that we found no engraftment in secondary recipients. This observation indicates that extrinsic Wnt5a is required for engraftment. What is not entirely clear is how Wnt5a acts. Engraftment depends on migration of stem cells to the marrow, their transmigration, lodgement and subsequent controlled proliferation and differentiation. So, the first possibility is that Wnt5a drives **cell migration and adhesion.** Indeed, former studies indicate a requirement of Wnt5a signalling in cell adhesion and the control of cell polarity and directional migration in melanoma cells and T cells through the Fz3 receptor [212]. Of relevance for stem cells, although not specifically addressed, is that in T cells, the chemokine CXCL12 upregulates non-canonical Wnt intermediates, such as Wnt5a, Wnt7a, Rho GTPAse (unfortunately not specified which one), Fzd2 and Fzd3, and that Wnt5a upregulates

expression of CXCR4 and potentiates migration towards CXCL12 through activation of the calcium-dependent PKC activation [105]. In addition, we found apolar expression of CDC42, indicative of activation of this Rho GTPase, which is a critical regulator of the cytoskeletal rearrangements required for cell adhesion and migration [198, 213]. Our experiments detected a decreased homing efficiency of LSKs and MPs regenerated in *Wnt5a*$^{+/-}$ mice, indicating that environmental Wnt5a regulates the ability of regenerated cells to home into the BM niche, which regulates HSCs and their maintenance.

The observed increased relative CDC42 activity leads to a third possible feature in our observations: lack of engraftment could also be the result of increased **cell senescence**. In this thesis, WT HSCs regenerated in 1° *Wnt5a*$^{+/-}$ BM niche, display apolar expression of CDC42, as well as reduced self-renewal capacity [214] and have a 2-fold reduced ability to home to the BM endosteum [215]. Thus, the regenerated HSCs in 1° *Wnt5a*$^{+/-}$ recipients appear to show features of aging. Florian et al. [107] demonstrated that increased activity of CDC42 in aged HSCs is causally linked to HSC aging and leads to a loss of polarity in aged HSCs.

A fourth aspect of possible mechanisms involved in the loss of engraftment of HSCs regenerated in *Wnt5a*$^{+/-}$ environment, is that in this particular environment, MSCs are tendentially overrepresented and show a highly proliferative phenotype. In contrast, the number of osteoblasts in *Wnt5a*$^{+/-}$ mice is reduced. This finding is in line with the observation that IL-1 beta induces MSC differentiation into osteoblasts through the non-canonical Wnt5a/ROR2 pathway [216]. As MSCs are mainly responsible for HSC maintenance and OBC precursors for bone formation, this finding might influence the ability of the niche to sustain HSC quality. It is known that although skeletal development is not grossly affected [100, 103], the bone volume of distal femurs is lower in *Wnt5a*$^{+/-}$ mice, so is the osteoclast number and osteoblast number. Since the effects on HSC regeneration occur after transplantation in irradiated *Wnt5a*$^{+/-}$ mice, Wnt5a might not only play a direct role in HSC behaviour, but also in the regeneration of BM niche populations MSC and OBC after irradiation. This aspect was not further explored in this thesis. However, in a future experiment, one could propose to study sublethal irradiation of *Wnt5a*$^{+/-}$ and *Wnt5a*$^{+/+}$ newborn pups and analyse the HSCs and niche cells after 16 weeks of regeneration. This experiment should show whether regeneration of niche populations occurs in a different manner in Wnt5a-deficient animals.

In addition, since the number of LT-HSC is regulated by increases or decreases in the OBC population in BM [23, 25, 217], it is important to study both alterations in niche regeneration and concomitant regeneration of HSCs. OBCs have been shown to affect

HSCs through secretion of various matrix proteins, like for instance osteopontin, which negatively regulates HSC numbers in the BM. Osteopontin knockout results in increase number of HSCs [218-219].

To address this aspect in more detail, we generated osteoblast-lineage cell-specific Wnt5a-deficient mice by crossing $Wnt5a^{fl/fl}$ with Osterix-Cre mice. The analysis is not part of this thesis, but will be important for future studies of the role of Wnt5a, secreted from osteoblast-lineage cells on hematopoiesis.

5.3. Wnt5a in Leukemia

Several investigators have shown that Wnt5a and its downstream effectors act as tumoursuppressors. In patients with AML, CML and CLL, Wnt5a promoter was found to be methylated at diagnosis, and demethylated in complete remission, suggesting a possible clinical relevance of Wnt5a in leukemia [183]. Our experiments specifically addressed the question if stroma cells deficient for Wnt5a influence the development of leukemia in an extrinsic manner and whether the Wnt5a-deficient environment regulates the maintenance and differentiation of BCR/ABL$^+$ leukemic stem cells.

Our results described in Chapter 4.7, show that the leukemia development *in vivo* is dependent on Wnt5a signals from the niche. Upon transplantation of e1a2 p185-BCR/ABL transduced cells in newborn recipients, lympho-myeloproliferative disease (LMPD) developed. But three features distinguished LMPD in WT and the *Wnt5a*$^{+/-}$ recipients:

A) Remarkably, 36% (9/25) of the *Wnt5a*$^{+/-}$ recipients remained healthy, with the expression of GFP$^+$ cells throughout life at levels comparable to MIG controls.

B) Those *Wnt5a*$^{+/-}$ that developed LMPD, developed a more aggressive form of the disease, with larger contribution of lymphoid cells, a shorter latency time, higher levels of GFP$^+$ cells in the circulation and larger Spleen sizes and an expanded GFP$^+$ LSK pool.

C) Despite an expanded GFP$^+$ LSK pool, the LMPD developed in *Wnt5a*$^{+/-}$ recipients was not transplantable into 2° WT recipients.

Additional differences were found in the molecular activity of Wnt signalling mediators in GFP$^+$ B lymphoid cells from WT and *Wnt5a*$^{+/-}$ recipients with increased beta-catenin expression and unchanged Wnt5a-dependent CaMK-II signalling in the BCR/ABL expressing hematopoietic cells exposed to *Wnt5a*$^{+/-}$ microenvironment.

Perhaps in line with our earlier finding that normal HSCs fail to self-renew and repopulate 2° recipients, only the GFP-expressing cells that engrafted in the 1° *Wnt5a*$^{+/+}$ microenvironment developed leukemia in 2° recipients.

There are several mechanisms which could be involved in the behaviour of GFP$^+$ cells in the *Wnt5a*$^{+/-}$ environment. The first cellular behaviour affected could be enhanced proliferation. Since increased canonical signalling is well established as a signal for enhanced proliferation, our findings that several components in this pathway (DVL2, beta-catenin) show increased expression, would support this notion. In this scenario, beta-catenin should translocate into the nucleus, bind transcription factor TCF/LEF and

induce transcription of many genes associated with proliferation including cyclin-D1 and c-Myc, Yes-associated protein and vascular endothelial growth factor [154] [220]. Other evidence supporting our view is that in ovarian cancer and thyroid carcinoma, Wnt5a inhibits proliferation through antagonism of beta-catenin-dependent transcription [221-222]. Thus, the notion of enhanced proliferation in Wnt5a-deficiency supports the role of Wnt5a as a tumoursuppressor. Whether downstream transcriptional targets of the catenin/TCF/LEF complex (Cyclin-D1, c-Myc, others) indeed show increased expression in GFP^+ BCR/ABL^+ cells from mice with LMPD remains to be established.

A second mechanism that could contribute to our finding that a significant proportion of *Wnt5a*$^{+/-}$ recipients remain healthy, and the failure of GFP^+ cells from *Wnt5a*$^{+/-}$ recipients to transplant LMPD in 2° recipients is activation of the planar cell polarity pathway, in particular the CDC42-dependent pathway. This is in analogy to our finding described in Chapter 5.4, where we saw increased apolar expression (and thus activation) of CDC42 in normal LSK cells regenerated in *Wnt5a*$^{+/-}$ recipients.

In previous work we demonstrated a Wnt5a-induced CDC42 signalling in aged HSC [99], which caused decreased homing and self-renewal ability. We here show that BCR/ABL expressing WT cells are transplanted into *Wnt5a*-deficient microenvironment and analyzed after 16 hours. The GFP^+ cells show decreased **homing** efficiency. This was unexpected, since normal LSK cells home normally in *Wnt5a*$^{+/-}$ recipients. It is only that after a 16 week regenerative period that LSK show decreased polarization and associated defects in homing. What we haven't studied is whether BCR/ABL expression might directly, and not over a time period of 16 weeks, change their behaviour through CDC42/Wnt5a signalling. Indeed, it has been reported a sustained activation of CDC42 GTPase through p210 (BCR/ABL) tyrosine kinase signalling in CML cells leading to homing defects [223]. Although we have used p185 (BCR/ABL) fusion protein in our studies, we do not expect gross differences in how p185 (BCR/ABL) and p210 (BCR/ABL) affect signalling, since both exhibit constitutively activated ABL kinase activity [224]. For this reason we propose that p185 (BCR/ABL) fusion protein expression might also result in CDC42 activation and -dependent homing defects. If this is the case, CDC42 activation by p185 BCR/ABL might also explain why BCR/ABL Spleen cells isolated from Wnt5a$^{+/-}$ recipients with LMPD did not develop 2° leukemia.

Our comprehensive analysis of the BM niche in recipient mice with LMPD showed that the fraction of **OBCs** in *Wnt5a*$^{+/-}$ recipients is significantly increased compared to WT recipients. This finding suggests a possible third mechanism by which BCR/ABL^+ cells may be affected in the *Wnt5a*$^{+/-}$ environment. Recent findings demonstrated that the

presence of leukemic BCR/ABL$^+$ cells in the marrow, remodels the niche through altering the balance between different cell populations [124]. Additionally severe osteoblastic defects are found in blast-crisis CML [124]. Thus, it is possible that Wnt5a contributes to the formation of the leukemic niche and that the BCR/ABL expressing cells are not capable of remodelling the niche in *Wnt5a*$^{+/-}$ recipients. Our results suggest that BCR/ABL expression stimulates MSCs to overproduce OBCs, which may be defective. As a consequence, the faulty remodelled niche might not support the development of self-renewing LCS.

Our finding that in *Wnt5a*$^{+/-}$ recipients with BCR/ABL$^+$ LMPD the population of OBCs is expanded could mean that the endosteal region might be present in a more pronounced manner. Since the prevailing view is that this region preferably houses dormant hematopoietic stem cells, this could mean that BCR/ABL$^+$ cells are more quiescent in *Wnt5a*$^{+/-}$ recipients.

In conclusion, we found that environmental Wnt5a is critical for regulating the outcome of BCR/ABL induced LMPD. We propose that BCR/ABL expressing cells with high tyrosine kinase activity are remodelling the BM niche via activation of beta-catenin-dependent Wnt signalling in BCR/ABL$^+$ cells. The niche responds to and interacts with the HSCs and putative LSCs via Wnt5a/CDC42 signalling, resulting in a reduced self-renewal capacity of LT-HSCs and putative LSCs. In Wnt5a$^{+/-}$ recipients with LMPD, we hypothesize that the BCR/ABL expressing cells fail to develop quiescence, resulting in complete differentiation exhaustion. A defining feature of BCR/ABL$^+$ LMPD is splenomegaly. We found that LMPD developed in *Wnt5a*$^{+/-}$ recipients resulted in larger Spleens in primary recipients. In secondary WT recipients, the BCR/ABL expressing Spleen cells could not transplant the initial LMPD indicating a loss of self-renewal of BCR/ABL$^+$ stem cells in Spleen.

Due to time constraints, several mechanisms that could contribute to the failure of HSCs and LSCs to engraft or transplant LMPD in secondary recipients could not be studied. For instance, it is known that E-Selectin-deficiency promotes HSC quiescence [44]. Since only endothelial cells in the vascular niche express this adhesion molecule, endothelial cells in *Wnt5a*$^{+/-}$ recipients might show increased staining with E-selectin. Also, it remains unexplored, BCR/ABL-expressing LSK cells in the BM are perhaps more persistent, which could be studied by transplanting **BM** cells from mice with LMPD into secondary WT recipients. A possible third contribution could be that despite that BCR/ABL is considered a “strong” oncogene, additional mutations are required for full transformation to blast crisis, and that such mutations occur at a lower frequency in *Wnt5a*$^{+/-}$ recipients. In human CML, progression from chronic phase to blast crisis has

been associated with mutations in genes such as GATA-2 and MAX, or deletions of the glycolytic enolase ENO1 [225-226]. We propose to analyze the BCR/ABL-expressing cells before transplantation and the cells isolated from mice with LMPD using exome sequencing. Another factor contributing to loss of self-renewal is that expression of the BCR/ABL oncogene is silenced and/or its kinase activity inhibited in *Wnt5a*$^{+/-}$ recipients. We propose to analyze BCR/ABL (ABL) activity by Western blot of GFP-expressing mature cells of the 1° *Wnt5a*$^{+/-}$ recipients with LMPD. As this could also be a possible cause why in 36% of the 1° *Wnt5a*$^{+/-}$ recipients no LMPD develops, BCR/ABL activity should also be studied in the GFP-expressing cells in the *Wnt5a*$^{+/-}$ recipient mice that remained free from disease.

5.4. Conclusion

In this project, the functions of the secreted Wnt protein Wnt5a in hematopoiesis and in lympho-myeloproliferative disease were investigated. Wnt5a was found to be important in steady-state early hematopoiesis, since *Wnt5a*$^{+/-}$ mice have less LSK cells in the BM. We demonstrate that reduced microenvironmental Wnt5a leads to loss of maintenance and self-renewal of HSCs *in vitro* and *in vivo*. Figure 67 is showing a proposed mechanism of Wnt5a-dependent cell-cell communication between HSCs and their niche. In Figure 67A, the WT situation in the endosteal niche is represented. HSCs reside close to the osteoblast (OBC)-lined endosteum and endosteum-associated Wnt5a is mainly secreted by OBCs. Figure 67B shows the imbalanced situation, where WT HSCs migrate and possibly engraft further away from the *Wnt5a*-deficient OBCs. The imbalance manifests itself as HSCs which show more activation, with less self-renewal, leading to an exhaustion of the LT-HSC pool.

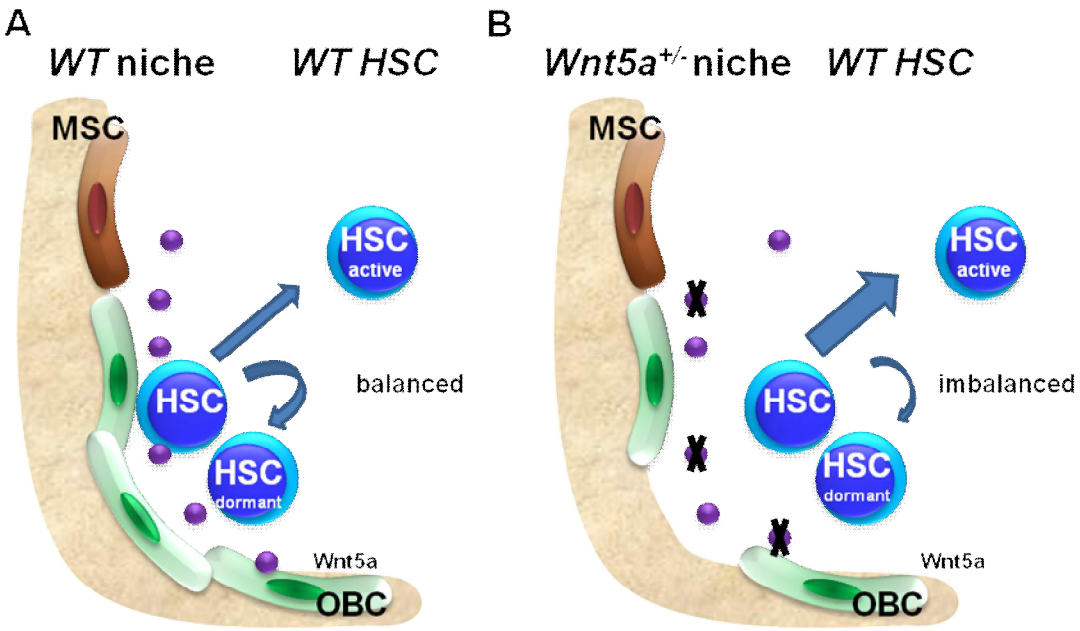

Figure 67. Endosteum: HSC cell division model. (A) Scheme showing the endosteal BM niche under steady state conditions; HSCs is residing close to the endosteal niche; cell division is balanced as the HSC is dividing into actively dividing HSC and dormant HSC **(B)** Scheme showing the endosteal BM niche in extrinsic transplantation assay; the WT HSC migrated to and engrafted in the Wnt5a$^{+/-}$ BM niche.; Arrows indicating an enhanced activation and less self-renewal of the HSCs during cell division.

Under leukemic conditions, as shown in Figure 67C, cells expressing the oncogene BCR/ABL migrate to the BM and show enhanced cell cycle and cell division activity, because of the activated cytoplasmic BCR/ABL, which activates canonical Wnt signalling. The BCR/ABL$^+$ stem cells show self-renewal and exist in a dormant state, as was demonstrated for CD34$^+$ cells, isolated from BCR/ABL$^+$ CML patients in which quiescent cells are also resistant to therapy [227]. In Figure 67D, the influence of microenvironmental Wnt5a during migration of BCR/ABL$^+$ cells is illustrated. We propose that like normal WT HSCs after 16 weeks in Wnt5a$^{+/-}$ niche, the BCR/ABL expressing WT HSCs may not engraft in close proximity of the Wnt5a-deficient endosteum. In addition BCR/ABL$^+$ cells are remodelling the niche and show dramatically enhanced activation and proliferation of MSCs. The niche remodelled in *Wnt5a*$^{+/-}$ recipients is a disadvantageous tumour microenvironment for the maintenance of putative LSCs. The leukostasis is imbalanced and cells with self-renewal capacity might not develop anymore. This hypothesis is supported by findings that BM-MSCs that overexpress Wnt5a and TGF-beta-induced proteins (Tgfbi) are induced in cancer cells by the stem cell mircroenvironment [228].

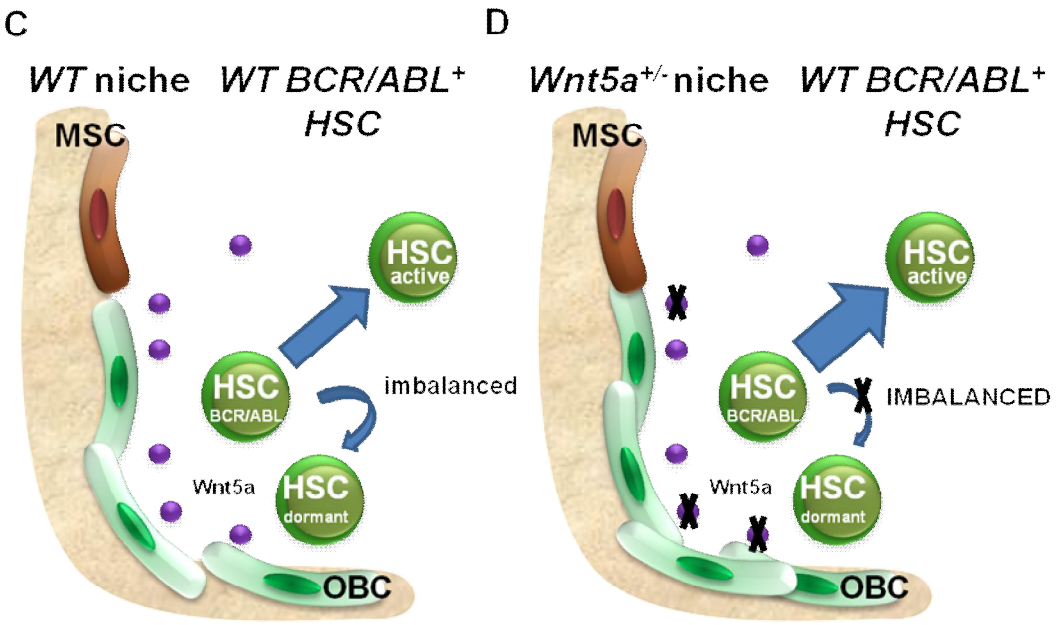

Figure 67. Endosteum: HSC cell division model under leukemic conditions.(C) Scheme showing the endosteal WT BM niche under leukemic conditions; **(D)** BCR/ABL expressing WT HSC is located in the Wnt5a$^{+/-}$ micrenvironment.

Briefly, this thesis demonstrates that the micrenvironment which regulates HSC requires Wnt5a. Thus, besides sFRP-1 [59] and PTN [58] another secreted factor originally identified in stromal cell line models: Wnt5a is part of a secretosome required for niche regulation of HSCs and putative LSCs.

There is supposed to be a Wnt5a-dependent intrinsic defect only in aged HSCs as it was shown in recent publication that LT-HSCs express only higher levels of Wnt5a during aging [99].

6. Summary

Hematopoietic stem cells (HSCs) reside in the bone marrow niche that regulates their self-renewal, proliferation activity and trafficking. These processes are regulated through interaction of several signalling molecules produced by the niche and HSCs themselves.

In this study, we investigated the role of the secreted molecule *Wnt5a* in terms of hematopoiesis and leukemia.

For the first time, we could show that the loss of one allele of the *Wnt5a* gene has an enormous effect on the primitive hematopoiesis *in vivo*. The numbers of LSK cells from the bone marrow of *Wnt5a*$^{+/-}$ mice were reduced; moreover the LT-HSCs proportion within the LSK fraction was increased. Strikingly, *Wnt5a*$^{+/-}$ LSKs showed enhanced Wnt signalling and more cell cycle activity. However, the reduced cell-intrinsic *Wnt5a* expression in HSCs showed no obvious effect on their stem cell quality.

Wnt5a is a soluble molecule that is mainly expressed by BM stromal cells. Notably, we identified that loss of Wnt5a in primary stromal cells decreased progenitor activity of co-cultured HSCs. In order to assess the extent of a possible effect of extrinsic Wnt5a loss on self-renewal capacity of HSCs *in vivo*, we performed serial transplantation experiments. Interestingly, we observed total failure of engraftment of WT HSCs in 2° recipients, after exposure to Wnt5a-deficient microenvironment in 1° recipients. These results revealed inability of *Wnt5a*-deficient microenvironment to maintain LT-HSCs indicating importance of the extrinsic Wnt5a for HSC maintenance. By analyzing the underlying molecular mechanisms, we indentified alterations in several non-canonical Wnt pathways. We report a shift from the *Wnt5a*/Ca^{2+} to the *Wnt5a*/CDC42 signalling pathway in HSCs after exposure to Wnt5a-deficient microenvironment. This resulted in homing defects of HSCs.

Since abnormalities in the niche may contribute to leukemogenesis, we studied the influence of the secreted protein Wnt5a on the development of BCR/ABL induced leukemia. In WT animals, BCR/ABL-transduced hematopoietic cells induced lympho-myeloproliferative disorder (LMPD) with a significant longer latency time than in *Wnt5a*$^{+/-}$ mice. These results demonstrate that extrinsic Wnt5a level affect the onset of hematologic disease. In addition, the *Wnt5a*$^{+/-}$ mice transplanted with WT BCR/ABL expressing cells developed a more aggressive form of LMPD in aspect of enhanced white blood cells in PB and Spleen compared to their controls. Furthermore, the BCR/ABL expressing HSC pool, consistent of the putative LSCs (leukemic stem cells), was significantly decreased in the Spleens of *Wnt5a*-deficient mice suggesting a role of

the extrinsic *Wnt5a* in self-renewal and maintenance of LSCs that is comparable with Wnt5a importance for maintenance of HSCs. Moreover, 36% of positively engrafted *Wnt5a*$^{+/-}$ transplanted with BCR/ABL-transduced cells survived and did not display any obvious abnormalities. This suggested an important role for *Wnt5a* in homing of the cells to the niche. Surprisingly, and in line with the failure to self-renew of HSCs, the BCR/ABL-expressing cells being exposed to Wnt5a-deficient microenvironment did not develop leukemia in 2° recipients compared to their controls. These results revealed inability of *Wnt5a*-deficient microenvironment to maintain LSCs. By analysing Wnt signalling in these animals we observed enhanced canonical signalling due to increased beta-catenin expression and unchanged non-canonical signalling.

We could show that extrinsic Wnt5a level affect the onset of hematologic disease and regulate leukemic stem cell quality. In summary, our results demonstrate that Wnt5a signalling in the BM niche is essential for the maintenance of HSCs and LSCs. We propose an involvement of a Wnt5a-dependent mechanism in homing/migration of HSCs in their BM niche.

7. Zusammenfassung

Während dieser Dissertation wurde die Rolle des löslichen Nischensignals Wnt5a bei der Regulation der Hämatopoese und der Entstehung von Leukämie untersucht.

Hämatopoetische Stammzellen (HSZ) befinden sich im Knochenmark umgeben von ihrer Nische, welche lösliche Signale produziert, die Prozesse wie Selbsterneuerung, Proliferation und Migration der HSZ steuern können.

Zum ersten Mal konnte *in vivo* bewiesen werden, dass der Verlust eines Allels des Wnt5a Gens eine erhebliche Wirkung auf die primitive Hämatopoese hat. In *Wnt5a*$^{+/-}$ Mäusen ist die Zahl der LSK Zellen reduziert, wobei der Anteil der langzeitrepopulierenden Stammzellen innerhalb der LSK Population erhöht ist. *Wnt5a*$^{+/-}$ LSKs weisen einen aktivierten Wnt Signalweg und einen erhöhten Zellzyklus auf. Wir konnten mit Hilfe von *in vivo* Repopulationsversuchen ausschließen, dass ein intrinsischer Effekt (Verlust von *Wnt5a*-Expression in hämatopoetischen Zellen) auf die Stammzellfunktion vorliegt.

Wnt5a ist ein lösliches Signalmolekül, das hauptsächlich vom Stroma exprimiert wird. Es konnte bei *ex vivo* HSZ Kokulturen auf Primärstroma gezeigt werden, dass *Wnt5a* die Repopulationsfähigkeit der Zellen extrinsisch stark beeinflusst. Um das Ausmaß des Verlustes von Wnt5a auf die Selbsterneuerungskapazität von HSZ *in vivo* zu bewerten, haben wir Stammzell-Transplantationsversuche durchgeführt. Interessanterweise verlieren HSZ, die *Wnt5a*$^{+/-}$ Mikroumgebung ausgesetzt waren, in sekundären Empfängern ihren Stammzellcharakter. Diese Ergebnisse zeigen, dass *Wnt5a* aus der Mikroumgebung des Knochenmarks für den Erhalt der hämatopoietischen Stammzelle essentiell ist und unterstreichen zudem erneut die wichtige Rolle der Mikroumgebung für die HSZ. Die molekulare Analyse der HSZ zeigt deutlich eine Überaktivierung des CDC42/*Wnt5a* Signalweges und ein daraus resultierendes verschlechtertes Homingverhalten.

Veränderungen in der Mikroumgebung, können auch zur Entstehung von Leukämie beitragen. In dieser Arbeit wurde im Mausmodell untersucht, ob *Wnt5a* in der Nische (extrinsisch) die Entwicklung einer BCR/ABL^{+} Leukämie beeinflusst. Es konnte gezeigt werden, dass die Latenzzeit der Erkrankung bereits von *Wnt5a* extrinsisch beeinflusst wird. Die leukämischen Zellen lösen die Erkrankung in der *Wnt5a*$^{+/-}$ Mikroumgebung schneller und deutlich aggressiver aus. Die hämatopoetischen Zellen in den erkrankten *Wnt5a*$^{+/-}$ Mäusen zeigten zudem einen aktivierten Beta-catenin-abhängigen Wnt Signalweg auf. Im Vergleich zur Kontrollgruppe, ist die Zahl der leukämischen Stammzellen (LSZ) in der Milz deutlich verringert. Zudem haben sie die Fähigkeit

verloren, die Erkrankung durch Retransplantation erneut auszulösen. Eine weitere Entdeckung ist, dass 36% der primär transplantierten *Wnt5a*$^{+/-}$ Mäuse nicht erkrankt sind. Dieses Phänomen muss noch eindeutiger untersucht werden, deutet aber erneut auf einen Wnt5a-abhängigen ´Homing´-/Migrations-Defekt hin.

Zusammenfassend konnten wir in dieser Arbeit zeigen, dass Wnt5a als extrinsisches Nischensignal das Homingverhalten der Zellen ins Knochenmark steuert und dort den Erhalt von HSZ aber auch LSZ sicherstellt.

8. Appendices

8.1. List of Figures

8.2. List of Tables

8.3. List of Abbreviations

5-FU	5-Fluorouracile
ALCAM	activated leukocyte cell adhesion molecule
APC	Allophycocyanin
BSA	Bovine serum albumine
CaMK-II	Calcium/calmodulin-dependent protein kinase type II
CDC42	Cell division control protein 42 homolog
C/EBP alpha	CCAAT/enhancer-binding protein alpha
CFA	Colony forming assay
CLP	Common lymphoid progenitor
c-Myc	Proto-oncogene c-Myc
Cyclin-D1	G1/S-specific cyclin-D1
CXCR4	C-X-C chemokine receptor type 4
CXCL12	C-X-C motif chemokine 12 (Stromal cell-derived factor 1/SDF-1)
DAPI	4,6-diamino-2-phenylindole dihydrochloride
DMEM	Dulbecco´s modified Eagle´s medium
DMSO	Dimetylsulfoxide
DNA	Desoxyribonucleic acid
DVL2	Segment polarity protein dishevelled homolog DVL2
BCP	1-bromo-3-chloropropane
BHA	Butylated hydroxyanisole
EGTA	Ethyleneglycoltetraacetic acid
FACS	Fluorescence activated cell sorting
Fbxw7	F-box/WD repeat-containing protein 7
FCS	Fetal Calf Serum
FITC	Fluoresceinisothiocyanat
GMP	Granulocyte-monocyte-progenitor
GSK-3 beta	Glycogen synthase kinase-3 beta
HBSS	Hank´s buffered salt solution
HEPES	2-(4-(2-Hydroxyethyl)- 1-piperazinyl)-ethansulfonsäure
Ig	Immunoglobulin
IL	Interleukin
JNK1	Stress-activated protein kinase JNK1
KO	Knockout
LSK	$Lin^- SCA\text{-}1^+ KIT^+$
LT-HSC	Long-term repopulating hematopoietic stem cell
MEP	Megakaryocyte-erythrocyte progenitor
MP	Multipotent progenitor

NF-ATc1	Nuclear factor of activated T-cells, cytoplasmic 1
NLK	Serine/threonine-protein kinase NLK (Nemo-like kinase)
PBS	phosphate buffered saline
PCR	Polymerase chain reaction
PE	R-Phycoerythrin
PI	Propidium iodide
PLC-beta-3	1-phosphatidylinositol 4,5-bisphosphate phosphodiesterase beta-3
PPAR-gamma	Peroxisome proliferator-activated receptor gamma
PTN	Pleiotrophin
qRT-PCR	quantitative real time PCR
ROR2	Tyrosine-protein kinase transmembrane receptor ROR2
RYK	Tyrosine-protein kinase RYK
sFRP-1	Secreted frizzled-related protein 1
ST-HSC	Short-term repopulating hematopoietic stem cell
Wnt5a	Wingless-type MMTV integration site family member Wnt5a
WT	Wild type

9. Publications

Parts of this dissertation have already been published.

- Istvanffy,R., Kröger M., **Eckl C.**, Gitzelmann S., Vilne B., Bock F., Graf S., Schiemann M., Keller U.B., Peschel C. & Oostendorp R.A.J. *Stromal pleiotrophin regulates repopulation-behavior of hematopoetic stem cells*. Blood, 2011.

- Florian, M. C., Nattamai, K. J., Dorr, K., Marka, G., Uberle, B., Vas, V., **Eckl, C**., Andra, I., Schiemann, M., Oostendorp, R. A., Scharffetter-Kochanek, K., Kestler, H. A., Zheng, Y., Geiger, H. *A canonical to non-canonical Wnt signalling switch in haematopoietic stem-cell ageing.* Nature, 2013.

- **Schreck, C**., Bock, F., Grziwok, S., Oostendorp, R. A., Istvanffy, R. *Regulation of hematopoiesis by activators and inhibitors of Wnt signalling from the niche.* Ann N Y Acad Sci, 2014.

10. Acknowledgments

Ich möchte mich an dieser Stelle bei allen bedanken, die zum Gelingen dieser Dissertation beigetragen haben.

Mein besonderer Dank gilt:

Herrn Prof. Dr. Christian Peschel und Herrn Prof. dr. Robert Oostendorp für die Möglichkeit dieses interessante und anspruchsvolle Thema im Rahmen meiner Dissertation im Labor für Stammzellphysiologie der III. Medizinischen Klinik für Hämatologie und Onkologie am Klinikum rechts der Isar zu bearbeiten. Vielen Dank für die umfangreiche Unterstützung und wertvollen Diskussionen.

Lynette Henkel und Matthias Schiemann vom Institut für medizinische Mikrobiologie für die zahlreiche Unterstützung am MoFlo.

Meinen liebgewonnenen Arbeitskollegen für die Einarbeitung, Unterstützung und die schöne Zeit, besonders Dr. Rouzanna Istvánffy und Franziska Bock, Charlotta Pagel, Sylke Gitzelmann, Sandra Grziwok, Baiba Vilne sowie allen Leuten der Trogerstrasse 32, Raum 1.11.

Meinen Freunden, die mir immer den nötigen Rückhalt und Ausgleich gegeben haben.

Und besonders meiner Familie - meinem Ehemann Eric, meiner Tochter Lilly, meinen Eltern und Schwiegereltern, die mich rundum unterstützt und gestützt haben. Ohne diese herzliche Unterstützung, wäre diese Arbeit nicht möglich gewesen.

Diese Arbeit wurde durch die Deutsche Forschungsgemeinschaft DFG OO8/5-1 (8833110) finanziert.

11. References

1. Palis, J. and M.C. Yoder, *Yolk-sac hematopoiesis: the first blood cells of mouse and man.* Exp Hematol, 2001. **29**(8): p. 927-36.

2. Medvinsky, A. and E. Dzierzak, *Definitive hematopoiesis is autonomously initiated by the AGM region.* Cell, 1996. **86**(6): p. 897-906.

3. Mikkola, H.K. and S.H. Orkin, *The journey of developing hematopoietic stem cells.* Development, 2006. **133**(19): p. 3733-44.

4. Wilson, A., et al., *Hematopoietic stem cells reversibly switch from dormancy to self-renewal during homeostasis and repair.* Cell, 2008. **135**(6): p. 1118-29.

5. Ikuta, K. and I.L. Weissman, *Evidence that hematopoietic stem cells express mouse c-kit but do not depend on steel factor for their generation.* Proc Natl Acad Sci U S A, 1992. **89**(4): p. 1502-6.

6. Osawa, M., et al., *Long-term lymphohematopoietic reconstitution by a single CD34-low/negative hematopoietic stem cell.* Science, 1996. **273**(5272): p. 242-5.

7. Christensen, J.L. and I.L. Weissman, *Flk-2 is a marker in hematopoietic stem cell differentiation: a simple method to isolate long-term stem cells.* Proc Natl Acad Sci U S A, 2001. **98**(25): p. 14541-6.

8. Kiel, M.J., et al., *SLAM family receptors distinguish hematopoietic stem and progenitor cells and reveal endothelial niches for stem cells.* Cell, 2005. **121**(7): p. 1109-21.

9. Balazs, A.B., et al., *Endothelial protein C receptor (CD201) explicitly identifies hematopoietic stem cells in murine bone marrow.* Blood, 2006. **107**(6): p. 2317-21.

10. Kent, D.G., et al., *Prospective isolation and molecular characterization of hematopoietic stem cells with durable self-renewal potential.* Blood, 2009. **113**(25): p. 6342-50.

11. Morita, Y., H. Ema, and H. Nakauchi, *Heterogeneity and hierarchy within the most primitive hematopoietic stem cell compartment.* J Exp Med, 2010. **207**(6): p. 1173-82.

12. Dykstra, B., et al., *Long-term propagation of distinct hematopoietic differentiation programs in vivo.* Cell Stem Cell, 2007. **1**(2): p. 218-29.

13. Benz, C., et al., *Hematopoietic stem cell subtypes expand differentially during development and display distinct lymphopoietic programs.* Cell Stem Cell, 2012. **10**(3): p. 273-83.

14. Seita, J. and I.L. Weissman, *Hematopoietic stem cell: self-renewal versus differentiation.* Wiley Interdiscip Rev Syst Biol Med, 2010. **2**(6): p. 640-53.

15. Yamamoto, R., et al., *Clonal analysis unveils self-renewing lineage-restricted progenitors generated directly from hematopoietic stem cells.* Cell, 2013. **154**(5): p. 1112-26.

16. Kondo, T., et al., *Identification and characterization of nucleophosmin/B23/numatrin which binds the anti-oncogenic transcription factor IRF-1 and manifests oncogenic activity.* Oncogene, 1997. **15**(11): p. 1275-81.

17. Morrison, S.J. and A.C. Spradling, *Stem cells and niches: mechanisms that promote stem cell maintenance throughout life.* Cell, 2008. **132**(4): p. 598-611.

18. Schreck, C., et al., *Regulation of hematopoiesis by activators and inhibitors of Wnt signalling from the niche.* Ann N Y Acad Sci, 2014. **1310**(1): p. 32-43.

19. Schofield, R., *The relationship between the Spleen colony-forming cell and the haemopoietic stem cell.* Blood Cells, 1978. **4**(1-2): p. 7-25.

20. Fuchs, E., T. Tumbar, and G. Guasch, *Socializing with the neighbors: stem cells and their niche.* Cell, 2004. **116**(6): p. 769-78.

21. Garrett, R.W. and S.G. Emerson, *Bone and blood vessels: the hard and the soft of hematopoietic stem cell niches.* Cell Stem Cell, 2009. **4**(6): p. 503-6.

22. Nagasawa, T., Y. Omatsu, and T. Sugiyama, *Control of hematopoietic stem cells by the bone marrow stromal niche: the role of reticular cells.* Trends Immunol, 2011. **32**(7): p. 315-20.

23. Calvi, L.M., et al., *Osteoblastic cells regulate the haematopoietic stem cell niche.* Nature, 2003. **425**(6960): p. 841-6.

24. Frassoni, F., N.G. Testa, and B.I. Lord, *The relative spatial distribution of erythroid progenitor cells (BFUe and CFUe) in the normal mouse femur.* Cell Tissue Kinet, 1982. **15**(4): p. 447-55.

25. Zhang, J., et al., *Identification of the haematopoietic stem cell niche and control of the niche size.* Nature, 2003. **425**(6960): p. 836-41.

26. Lo Celso, C., et al., *Live-animal tracking of individual haematopoietic stem/progenitor cells in their niche.* Nature, 2009. **457**(7225): p. 92-6.

27. Xie, Y., et al., *Detection of functional haematopoietic stem cell niche using real-time imaging.* Nature, 2009. **457**(7225): p. 97-101.

28. Sugiyama, T., et al., *Maintenance of the hematopoietic stem cell pool by CXCL12-CXCR4 chemokine signaling in bone marrow stromal cell niches.* Immunity, 2006. **25**(6): p. 977-88.

29. Kieslinger, M., et al., *Early B cell factor 2 regulates hematopoietic stem cell homeostasis in a cell-nonautonomous manner.* Cell Stem Cell, 2010. **7**(4): p. 496-507.

30. Ding, L., et al., *Endothelial and perivascular cells maintain haematopoietic stem cells.* Nature, 2012. **481**(7382): p. 457-62.

31. Mendez-Ferrer, S., et al., *Mesenchymal and haematopoietic stem cells form a unique bone marrow niche.* Nature, 2010. **466**(7308): p. 829-34.

32. Yamazaki, S., et al., *Nonmyelinating Schwann cells maintain hematopoietic stem cell hibernation in the bone marrow niche.* Cell, 2011. **147**(5): p. 1146-58.

33. Short, B., et al., *Prospective isolation of stromal progenitor cells from mouse BM.* Cytotherapy, 2001. **3**(5): p. 407-8.

34. Morikawa, S., et al., *Prospective identification, isolation, and systemic transplantation of multipotent mesenchymal stem cells in murine bone marrow.* J Exp Med, 2009. **206**(11): p. 2483-96.

35. Chan, C.K., et al., *Clonal precursor of bone, cartilage, and hematopoietic niche stromal cells.* Proc Natl Acad Sci U S A, 2013. **110**(31): p. 12643-8.

36. Nakamura, Y., et al., *Isolation and characterization of endosteal niche cell populations that regulate hematopoietic stem cells.* Blood, 2010. **116**(9): p. 1422-32.

37. Pinho, S., et al., *PDGFRalpha and CD51 mark human nestin+ sphere-forming mesenchymal stem cells capable of hematopoietic progenitor cell expansion.* J Exp Med, 2013. **210**(7): p. 1351-67.

38. Kiel, M.J. and S.J. Morrison, *Uncertainty in the niches that maintain haematopoietic stem cells.* Nat Rev Immunol, 2008. **8**(4): p. 290-301.

39. Ma, Y.D., et al., *Defects in osteoblast function but no changes in long-term repopulating potential of hematopoietic stem cells in a mouse chronic inflammatory arthritis model.* Blood, 2009. **114**(20): p. 4402-10.

40. Kiel, M.J., G.L. Radice, and S.J. Morrison, *Lack of evidence that hematopoietic stem cells depend on N-cadherin-mediated adhesion to osteoblasts for their maintenance.* Cell Stem Cell, 2007. **1**(2): p. 204-17.

41. Li, B., et al., *Endothelial cells mediate the regeneration of hematopoietic stem cells.* Stem Cell Res, 2010. **4**(1): p. 17-24.

42. Salter, A.B., et al., *Endothelial progenitor cell infusion induces hematopoietic stem cell reconstitution in vivo.* Blood, 2009. **113**(9): p. 2104-7.

43. Kiel, M.J., et al., *Hematopoietic stem cells do not depend on N-cadherin to regulate their maintenance.* Cell Stem Cell, 2009. **4**(2): p. 170-9.

44. Winkler, I.G., et al., *Vascular niche E-selectin regulates hematopoietic stem cell dormancy, self renewal and chemoresistance.* Nat Med, 2012. **18**(11): p. 1651-7.

45. Essers, M.A., et al., *IFNalpha activates dormant haematopoietic stem cells in vivo.* Nature, 2009. **458**(7240): p. 904-8.

46. Essers, M.A. and A. Trumpp, *Targeting leukemic stem cells by breaking their dormancy.* Mol Oncol, 2010. **4**(5): p. 443-50.

47. Barker, J.E., *Early transplantation to a normal microenvironment prevents the development of Steel hematopoietic stem cell defects.* Exp Hematol, 1997. **25**(6): p. 542-7.

48. Waskow, C., et al., *Viable c-Kit(W/W) mutants reveal pivotal role for c-kit in the maintenance of lymphopoiesis.* Immunity, 2002. **17**(3): p. 277-88.

49. Waskow, C., et al., *Hematopoietic stem cell transplantation without irradiation.* Nat Methods, 2009. **6**(4): p. 267-9.

50. Tzeng, Y.S., et al., *Loss of Cxcl12/Sdf-1 in adult mice decreases the quiescent state of hematopoietic stem/progenitor cells and alters the pattern of hematopoietic regeneration after myelosuppression.* Blood, 2011. **117**(2): p. 429-39.

51. Ma, Q., et al., *Impaired B-lymphopoiesis, myelopoiesis, and derailed cerebellar neuron migration in CXCR4- and SDF-1-deficient mice.* Proc Natl Acad Sci U S A, 1998. **95**(16): p. 9448-53.

52. Ma, Q., D. Jones, and T.A. Springer, *The chemokine receptor CXCR4 is required for the retention of B lineage and granulocytic precursors within the bone marrow microenvironment.* Immunity, 1999. **10**(4): p. 463-71.

53. Zou, Y.R., et al., *Function of the chemokine receptor CXCR4 in haematopoiesis and in cerebellar development.* Nature, 1998. **393**(6685): p. 595-9.

54. Tsai, J.J., et al., *Nrf2 regulates haematopoietic stem cell function.* Nat Cell Biol, 2013. **15**(3): p. 309-16.

55. Grundler, R., et al., *Dissection of PIM serine/threonine kinases in FLT3-ITD-induced leukemogenesis reveals PIM1 as regulator of CXCL12-CXCR4-mediated homing and migration.* J Exp Med, 2009. **206**(9): p. 1957-70.

56. Goldman, D.C., et al., *BMP4 **regulates** the hematopoietic stem cell niche.* Blood, 2009. **114**(20): p. 4393-401.

57. Fleming, H.E., et al., *Wnt signaling in the niche enforces hematopoietic stem cell quiescence and is necessary to preserve self-renewal in vivo.* Cell Stem Cell, 2008. **2**(3): p. 274-83.

58. Istvanffy, R., et al., *Stromal pleiotrophin regulates repopulation behavior of hematopoietic stem cells.* Blood, 2011. **118**(10): p. 2712-22.

59. Renstrom, J., et al., *Secreted frizzled-related protein 1 extrinsically regulates cycling activity and maintenance of hematopoietic stem cells.* Cell Stem Cell, 2009. **5**(2): p. 157-67.

60. Qian, H., et al., *Critical role of thrombopoietin in maintaining adult quiescent hematopoietic stem cells.* Cell Stem Cell, 2007. **1**(6): p. 671-84.

61. Hazen, A.L., et al., *SHIP is required for a functional hematopoietic stem cell niche.* Blood, 2009. **113**(13): p. 2924-33.

62. Walkley, C.R., et al., *Rb regulates interactions between hematopoietic stem cells and their bone marrow microenvironment.* Cell, 2007. **129**(6): p. 1081-95.

63. Raaijmakers, M.H., et al., *Bone progenitor dysfunction induces myelodysplasia and secondary leukaemia.* Nature, 2010. **464**(7290): p. 852-7.

64. Sesler, C.L. and M. Zayzafoon, *NFAT signaling in osteoblasts regulates the hematopoietic niche in the bone microenvironment.* Clin Dev Immunol, 2013. **2013**: p. 107321.

65. Baksh, D., G.M. Boland, and R.S. Tuan, *Cross-talk between Wnt signaling pathways in human mesenchymal stem cells leads to functional antagonism during osteogenic differentiation.* J Cell Biochem, 2007. **101**(5): p. 1109-24.

66. Ehninger, A. and A. Trumpp, *The bone marrow stem cell niche grows up: mesenchymal stem cells and macrophages move in.* J Exp Med, 2011. **208**(3): p. 421-8.

67. Yamane, T., et al., *Wnt signaling regulates hemopoiesis through stromal cells.* J Immunol, 2001. **167**(2): p. 765-72.

68. Wodarz, A. and R. Nusse, *Mechanisms of Wnt signaling in development.* Annu Rev Cell Dev Biol, 1998. **14**: p. 59-88.

69. Austin, T.W., et al., *A role for the Wnt gene family in hematopoiesis: expansion of multilineage progenitor cells.* Blood, 1997. **89**(10): p. 3624-35.

70. Van Den Berg, D.J., et al., *Role of members of the Wnt gene family in human hematopoiesis.* Blood, 1998. **92**(9): p. 3189-202.

71. Nygren, M.K., et al., *Wnt3A activates canonical Wnt signalling in acute lymphoblastic leukaemia (ALL) cells and inhibits the proliferation of B-ALL cell lines.* Br J Haematol, 2007. **136**(3): p. 400-13.

72. Logan, C.Y. and R. Nusse, *The Wnt signaling pathway in development and disease.* Annu Rev Cell Dev Biol, 2004. **20**: p. 781-810.

73. Bhanot, P., et al., *A new member of the frizzled family from Drosophila functions as a Wingless receptor.* Nature, 1996. **382**(6588): p. 225-30.

74. Janda, C.Y., et al., *Structural basis of Wnt recognition by Frizzled.* Science, 2012. **337**(6090): p. 59-64.

75. Bryja, V., et al., *The extracellular domain of Lrp5/6 inhibits noncanonical Wnt signaling in vivo.* Mol Biol Cell, 2009. **20**(3): p. 924-36.

76. MacDonald, B.T., K. Tamai, and X. He, *Wnt/beta-catenin signaling: components, mechanisms, and diseases.* Dev Cell, 2009. **17**(1): p. 9-26.

77. Boudin, E., et al., *The role of extracellular modulators of canonical Wnt signaling in bone metabolism and diseases.* Semin Arthritis Rheum, 2013.

78. Reya, T., et al., *A role for Wnt signalling in self-renewal of haematopoietic stem cells.* Nature, 2003. **423**(6938): p. 409-14.

79. Cobas, M., et al., *Beta-catenin is dispensable for hematopoiesis and lymphopoiesis.* J Exp Med, 2004. **199**(2): p. 221-9.

80. Koch, U., et al., *Simultaneous loss of beta- and gamma-catenin does not perturb hematopoiesis or lymphopoiesis.* Blood, 2008. **111**(1): p. 160-4.

81. Jeannet, G., et al., *Long-term, multilineage hematopoiesis occurs in the combined absence of beta-catenin and gamma-catenin.* Blood, 2008. **111**(1): p. 142-9.

82. Takada, S., et al., *Wnt-3a regulates somite and tailbud formation in the mouse embryo.* Genes Dev, 1994. **8**(2): p. 174-89.

83. Luis, T.C., et al., *Wnt3a deficiency irreversibly impairs hematopoietic stem cell self-renewal and leads to defects in progenitor cell differentiation.* Blood, 2009. **113**(3): p. 546-54.

84. Veeman, M.T., J.D. Axelrod, and R.T. Moon, *A second canon. Functions and mechanisms of beta-catenin-independent Wnt signaling.* Dev Cell, 2003. **5**(3): p. 367-77.

85. Yamada, M., et al., *NARF, an nemo-like kinase (NLK)-associated ring finger protein regulates the ubiquitylation and degradation of T cell factor/lymphoid enhancer factor (TCF/LEF).* J Biol Chem, 2006. **281**(30): p. 20749-60.

86. Lv, L., et al., *Nemo-like kinase (NLK) inhibits the progression of NSCLC via negatively modulating WNT signaling pathway.* J Cell Biochem, 2014. **115**(1): p. 81-92.

87. Xu, D., et al., *Expression of Nemo-like kinase after spinal cord injury in rats.* J Mol Neurosci, 2014. **52**(3): p. 410-8.

88. Kikuchi, A., et al., *Wnt5a: its signalling, functions and implication in diseases.* Acta Physiol (Oxf), 2012. **204**(1): p. 17-33.

89. Gavin, B.J., J.A. McMahon, and A.P. McMahon, *Expression of multiple novel Wnt-1/int-1-related genes during fetal and adult mouse development.* Genes Dev, 1990. **4**(12B): p. 2319-32.

90. Willert, K.H., *Isolation and application of bioactive Wnt proteins.* Methods Mol Biol, 2008. **468**: p. 17-29.

91. Nusse, R., *Wnts and Hedgehogs: lipid-modified proteins and similarities in signaling mechanisms at the cell surface.* Development, 2003. **130**(22): p. 5297-305.

92. Burrus, L.W. and A.P. McMahon, *Biochemical analysis of murine Wnt proteins reveals both shared and distinct properties.* Exp Cell Res, 1995. **220**(2): p. 363-73.

93. Burrus, D.R., J.M. Ernest, and J.C. Veille, *Fetal fibronectin, interleukin-6, and C-reactive protein are useful in establishing prognostic subcategories of idiopathic preterm labor.* Am J Obstet Gynecol, 1995. **173**(4): p. 1258-62.

94. Sugimura, R., et al., *Noncanonical Wnt signaling maintains hematopoietic stem cells in the niche.* Cell, 2012. **150**(2): p. 351-65.

95. Halford, M.M., et al., *A Fully Human Inhibitory Monoclonal Antibody to the Wnt Receptor RYK.* PLoS One, 2013. **8**(9): p. e75447.

96. van Amerongen, R., A. Mikels, and R. Nusse, *Alternative wnt signaling is initiated by distinct receptors.* Sci Signal, 2008. **1**(35): p. re9.

97. Povinelli, B.J. and M.J. Nemeth, *Wnt5a Regulates Hematopoietic Stem Cell Proliferation and Repopulation Through the Ryk Receptor.* Stem Cells, 2013.

98. Buckley, S.M., et al., *Maintenance of HSC by Wnt5a secreting AGM-derived stromal cell line.* Exp Hematol, 2011. **39**(1): p. 114-123 e1-5.

99. Florian, M.C., et al., *A canonical to non-canonical Wnt signalling switch in haematopoietic stem-cell ageing.* Nature, 2013. **503**(7476): p. 392-6.

100. Yamaguchi, T.P., et al., *A Wnt5a pathway underlies outgrowth of multiple structures in the vertebrate embryo.* Development, 1999. **126**(6): p. 1211-23.

101. Miyoshi, H., et al., *Wnt5a potentiates TGF-beta signaling to promote colonic crypt regeneration after tissue injury.* Science, 2012. **338**(6103): p. 108-13.

102. Reya, T., et al., *Wnt signaling regulates B lymphocyte proliferation through a LEF-1 dependent mechanism.* Immunity, 2000. **13**(1): p. 15-24.

103. Maeda, K., et al., *Wnt5a-Ror2 signaling between osteoblast-lineage cells and osteoclast precursors enhances osteoclastogenesis.* Nat Med, 2012. **18**(3): p. 405-12.

104. Nemeth, M.J., et al., *Wnt5a inhibits canonical Wnt signaling in hematopoietic stem cells and enhances repopulation.* Proc Natl Acad Sci U S A, 2007. **104**(39): p. 15436-41.

105. Ghosh, M.C., et al., *Activation of Wnt5A signaling is required for CXC chemokine ligand 12-mediated T-cell migration.* Blood, 2009. **114**(7): p. 1366-73.

106. Kuhl, M., et al., *The Wnt/Ca2+ pathway: a new vertebrate Wnt signaling pathway takes shape.* Trends Genet, 2000. **16**(7): p. 279-83.

107. Florian, M.C., et al., *Cdc42 activity regulates hematopoietic stem cell aging and rejuvenation.* Cell Stem Cell, 2012. **10**(5): p. 520-30.

108. Kawano, Y. and R. Kypta, *Secreted antagonists of the Wnt signalling pathway.* J Cell Sci, 2003. **116**(Pt 13): p. 2627-34.

109. Suzuki, H., et al., *Epigenetic inactivation of SFRP genes allows constitutive WNT signaling in colorectal cancer.* Nat Genet, 2004. **36**(4): p. 417-22.

110. Kele, J., et al., *SFRP1 and SFRP2 dose-dependently regulate midbrain dopamine neuron development in vivo and in embryonic stem cells.* Stem Cells, 2012. **30**(5): p. 865-75.

111. Satoh, W., et al., *Sfrp1 and Sfrp2 regulate anteroposterior axis elongation and somite segmentation during mouse embryogenesis.* Development, 2006. **133**(6): p. 989-99.

112. Satoh, W., et al., *Sfrp1, Sfrp2, and Sfrp5 regulate the Wnt/beta-catenin and the planar cell polarity pathways during early trunk formation in mouse.* Genesis, 2008. **46**(2): p. 92-103.

113. Warr, N., et al., *Sfrp1 and Sfrp2 are required for normal male sexual development in mice.* Dev Biol, 2009. **326**(2): p. 273-84.

114. Roux, S., *New treatment targets in osteoporosis.* Joint Bone Spine, 2010. **77**(3): p. 222-8.

115. Oostendorp, R.A., et al., *Long-term maintenance of hematopoietic stem cells does not require contact with embryo-derived stromal cells in cocultures.* Stem Cells, 2005. **23**(6): p. 842-51.

116. Nakajima, H., et al., *Wnt modulators, SFRP-1, and SFRP-2 are expressed in osteoblasts and differentially regulate hematopoietic stem cells.* Biochem Biophys Res Commun, 2009. **390**(1): p. 65-70.

117. Mao, J., et al., *Low-density lipoprotein receptor-related protein-5 binds to Axin and regulates the canonical Wnt signaling pathway.* Mol Cell, 2001. **7**(4): p. 801-9.

118. Mao, B., et al., *Kremen proteins are Dickkopf receptors that regulate Wnt/beta-catenin signalling.* Nature, 2002. **417**(6889): p. 664-7.

119. Surmann-Schmitt, C., et al., *Wif-1 is expressed at cartilage-mesenchyme interfaces and impedes Wnt3a-mediated inhibition of chondrogenesis.* J Cell Sci, 2009. **122**(Pt 20): p. 3627-37.

120. Malinauskas, T., et al., *Modular mechanism of Wnt signaling inhibition by Wnt inhibitory factor 1.* Nat Struct Mol Biol, 2011. **18**(8): p. 886-93.

121. Schaniel, C., et al., *Wnt-inhibitory factor 1 dysregulation of the bone marrow niche exhausts hematopoietic stem cells.* Blood, 2011. **118**(9): p. 2420-9.

122. Reya, T., et al., *Stem cells, cancer, and cancer stem cells.* Nature, 2001. **414**(6859): p. 105-11.

123. Lutzny, G., et al., *Protein kinase c-beta-dependent activation of NF-kappaB in stromal cells is indispensable for the survival of chronic lymphocytic leukemia B cells in vivo.* Cancer Cell, 2013. **23**(1): p. 77-92.

124. Schepers, K., et al., *Myeloproliferative neoplasia remodels the endosteal bone marrow niche into a self-reinforcing leukemic niche.* Cell Stem Cell, 2013. **13**(3): p. 285-99.

125. Rupec, R.A., et al., *Stroma-mediated dysregulation of myelopoiesis in mice lacking I kappa B alpha.* Immunity, 2005. **22**(4): p. 479-91.

126. Renstrom, J., et al., *How the niche regulates hematopoietic stem cells.* Chem Biol Interact, 2010. **184**(1-2): p. 7-15.

127. Wang, Y., et al., *The Wnt/beta-catenin pathway is required for the development of leukemia stem cells in AML.* Science, 2010. **327**(5973): p. 1650-3.

128. Zhao, C., et al., *Loss of beta-catenin impairs the renewal of normal and CML stem cells in vivo.* Cancer Cell, 2007. **12**(6): p. 528-41.

129. Jamieson, C.H., et al., *Granulocyte-macrophage progenitors as candidate leukemic stem cells in blast-crisis CML.* N Engl J Med, 2004. **351**(7): p. 657-67.

130. Wang, Y., X.X. Zhu, and C.S. Zhu, *[Abnormal methylation patterns of SFRP1 gene in cells of leukemia and inhibitation of arsenie trioxide on the SFRP1 gene].* Zhonghua Xue Ye Xue Za Zhi, 2013. **34**(2): p. 157-9.

131. Filipovich, A., et al., *Evidence for non-functional Dickkopf-1 (DKK-1) signaling in chronic lymphocytic leukemia (CLL).* Eur J Haematol, 2010. **85**(4): p. 309-13.

132. Moskalev, E.A., et al., *Concurrent epigenetic silencing of wnt/beta-catenin pathway inhibitor genes in B cell chronic lymphocytic leukaemia.* BMC Cancer, 2012. **12**: p. 213.

133. Hou, H.A., et al., *Distinct association between aberrant methylation of Wnt inhibitors and genetic alterations in acute myeloid leukaemia.* Br J Cancer, 2011. **105**(12): p. 1927-33.

134. Cheng, C.K., et al., *Secreted-frizzled related protein 1 is a transcriptional repression target of the t(8;21) fusion protein in acute myeloid leukemia.* Blood, 2011. **118**(25): p. 6638-48.

135. Oh, I.H., *Microenvironmental targeting of Wnt/beta-catenin signals for hematopoietic stem cell regulation.* Expert Opin Biol Ther, 2010. **10**(9): p. 1315-29.

136. Oostendorp, R.A., et al., *Embryonal subregion-derived stromal cell lines from novel temperature-sensitive SV40 T antigen transgenic mice support hematopoiesis.* J Cell Sci, 2002. **115**(Pt 10): p. 2099-108.

137. Oostendorp, R.A., K. Harvey, and E.A. Dzierzak, *Generation of murine stromal cell lines: models for the microenvironment of the embryonic mouse aorta-gonads-mesonephros region.* Methods Mol Biol, 2005. **290**: p. 163-72.

138. Ledran, M.H., et al., *Efficient hematopoietic differentiation of human embryonic stem cells on stromal cells derived from hematopoietic niches.* Cell Stem Cell, 2008. **3**(1): p. 85-98.

139. Liang, H., et al., *Wnt5a inhibits B cell proliferation and functions as a tumor suppressor in hematopoietic tissue.* Cancer Cell, 2003. **4**(5): p. 349-60.

140. Miething, C., et al., *Phosphorylation of tyrosine 393 in the kinase domain of Bcr-Abl influences the sensitivity towards imatinib in vivo.* Leukemia, 2003. **17**(9): p. 1695-9.

141. Kiel, M.J., et al., *Spatial differences in hematopoiesis but not in stem cells indicate a lack of regional patterning in definitive hematopoietic stem cells.* Dev Biol, 2005. **283**(1): p. 29-39.

142. Curtis, K.M., et al., *EF1alpha and RPL13a represent normalization genes suitable for RT-qPCR analysis of bone marrow derived mesenchymal stem cells.* BMC Mol Biol, 2010. **11**: p. 61.

143. Friedenstein, A.J., R.K. Chailakhyan, and U.V. Gerasimov, *Bone marrow osteogenic stem cells: in vitro cultivation and transplantation in diffusion chambers.* Cell Tissue Kinet, 1987. **20**(3): p. 263-72.

144. Friedenstein, A.J., et al., *Precursors for fibroblasts in different populations of hematopoietic cells as detected by the in vitro colony assay method.* Exp Hematol, 1974. **2**(2): p. 83-92.

145. Pittenger, M.F., et al., *Multilineage potential of adult human mesenchymal stem cells.* Science, 1999. **284**(5411): p. 143-7.

146. Jaiswal, N., et al., *Osteogenic differentiation of purified, culture-expanded human mesenchymal stem cells in vitro.* J Cell Biochem, 1997. **64**(2): p. 295-312.

147. Weisel, K.C., et al., *Stromal cell lines from the aorta-gonado-mesonephros region are potent supporters of murine and human hematopoiesis.* Exp Hematol, 2006. **34**(11): p. 1505-16.

148. Rebel, V.I., et al., *A comparison of long-term repopulating hematopoietic stem cells in fetal liver and adult bone marrow from the mouse.* Exp Hematol, 1996. **24**(5): p. 638-48.

149. Zeigler, F.C., et al., *Cellular and molecular characterization of the role of the flk-2/flt-3 receptor tyrosine kinase in hematopoietic stem cells.* Blood, 1994. **84**(8): p. 2422-30.

150. Ito, T., F. Tajima, and M. Ogawa, *Developmental changes of CD34 expression by murine hematopoietic stem cells.* Exp Hematol, 2000. **28**(11): p. 1269-73.

151. Kantor, A.B., et al., *Differential development of progenitor activity for three B-cell lineages.* Proc Natl Acad Sci U S A, 1992. **89**(8): p. 3320-4.

152. Yokota, T., et al., *Soluble frizzled-related protein 1 is estrogen inducible in bone marrow stromal cells and suppresses the earliest events in lymphopoiesis.* J Immunol, 2008. **181**(9): p. 6061-72.

153. Clevers, H., *Stem cells, asymmetric division and cancer.* Nat Genet, 2005. **37**(10): p. 1027-8.

154. Clevers, H. and R. Nusse, *Wnt/beta-catenin signaling and disease.* Cell, 2012. **149**(6): p. 1192-205.

155. Ishitani, T. and S. Ishitani, *Nemo-like kinase, a multifaceted cell signaling regulator.* Cell Signal, 2013. **25**(1): p. 190-7.

156. Lo Celso, C. and D. Scadden, *Isolation and transplantation of hematopoietic stem cells (HSCs).* J Vis Exp, 2007(2): p. 157.

157. Choi, S.C. and J.K. Han, *Xenopus Cdc42 regulates convergent extension movements during gastrulation through Wnt/Ca2+ signaling pathway.* Dev Biol, 2002. **244**(2): p. 342-57.

158. Nayak, R.C., et al., *Rho GTPases control specific cytoskeleton-dependent functions of hematopoietic stem cells.* Immunol Rev, 2013. **256**(1): p. 255-68.

159. Yang, F.C., et al., *Rac and Cdc42 GTPases control hematopoietic stem cell shape, adhesion, migration, and mobilization.* Proc Natl Acad Sci U S A, 2001. **98**(10): p. 5614-8.

160. Kozar, K., et al., *Mouse development and cell proliferation in the absence of D-cyclins.* Cell, 2004. **118**(4): p. 477-91.

161. Bereshchenko, O., et al., *Hematopoietic stem cell expansion precedes the generation of committed myeloid leukemia-initiating cells in C/EBPalpha mutant AML.* Cancer Cell, 2009. **16**(5): p. 390-400.

162. Chiu, C.H., et al., *Effect of a C/EBP gene replacement on mitochondrial biogenesis in fat cells.* Genes Dev, 2004. **18**(16): p. 1970-5.

163. Carmona, M.C., et al., *Mitochondrial biogenesis and thyroid status maturation in brown fat require CCAAT/enhancer-binding protein alpha.* J Biol Chem, 2002. **277**(24): p. 21489-98.

164. Takeishi, S., et al., *Ablation of Fbxw7 eliminates leukemia-initiating cells by preventing quiescence.* Cancer Cell, 2013. **23**(3): p. 347-61.

165. Iriuchishima, H., et al., *Ex vivo maintenance of hematopoietic stem cells by quiescence induction through Fbxw7α overexpression.* Blood, 2011. **117**(8): p. 2373-7.

166. Slayton, W.B., et al., *The role of the donor in the repair of the marrow vascular niche following hematopoietic stem cell transplant.* Stem Cells, 2007. **25**(11): p. 2945-55.

167. Hooper, A.T., et al., *Engraftment and reconstitution of hematopoiesis is dependent on VEGFR2-mediated regeneration of sinusoidal endothelial cells.* Cell Stem Cell, 2009. **4**(3): p. 263-74.

168. Taichman, R.S., M.J. Reilly, and S.G. Emerson, *Human osteoblasts support human hematopoietic progenitor cells in vitro bone marrow cultures.* Blood, 1996. **87**(2): p. 518-24.

169. Askmyr, M., et al., *What is the true nature of the osteoblastic hematopoietic stem cell niche?* Trends Endocrinol Metab, 2009. **20**(6): p. 303-9.

170. Hsu, S.H. and G.S. Huang, *Substrate-dependent Wnt signaling in MSC differentiation within biomaterial-derived 3D spheroids.* Biomaterials, 2013. **34**(20): p. 4725-38.

171. Cai, S.X., et al., *Stable genetic alterations of beta-catenin and ROR2 regulate the Wnt pathway, affect the fate of MSCs.* J Cell Physiol, 2014. **229**(6): p. 791-800.

172. Miyamoto, K., et al., *Foxo3a is essential for maintenance of the hematopoietic stem cell pool.* Cell Stem Cell, 2007. **1**(1): p. 101-12.

173. Nilsson, S.K., H.M. Johnston, and J.A. Coverdale, *Spatial localization of transplanted hemopoietic stem cells: inferences for the localization of stem cell niches.* Blood, 2001. **97**(8): p. 2293-9.

174. Arai, F. and T. Suda, *Maintenance of quiescent hematopoietic stem cells in the osteoblastic niche.* Ann N Y Acad Sci, 2007. **1106**: p. 41-53.

175. Takada, I., et al., *A histone lysine methyltransferase activated by non-canonical Wnt signalling suppresses PPAR-gamma transactivation.* Nat Cell Biol, 2007. **9**(11): p. 1273-85.

176. Schepers, K., et al., *Activated Gs signaling in osteoblastic cells alters the hematopoietic stem cell niche in mice.* Blood, 2012. **120**(17): p. 3425-35.

177. Nusse, R. and H.E. Varmus, *Many tumors induced by the mouse mammary tumor virus contain a provirus integrated in the same region of the host genome.* Cell, 1982. **31**(1): p. 99-109.

178. Garcia-Castro, B., et al., *Restoration of WNT4 inhibits cell growth in leukemia-derived cell lines.* BMC Cancer, 2013. **13**: p. 557.

179. Pizzatti, L., et al., *SUZ12 is a candidate target of the non-canonical WNT pathway in the progression of chronic myeloid leukemia.* Genes Chromosomes Cancer, 2010. **49**(2): p. 107-18.

180. Leris, A.C., et al., *WNT5A expression in human breast cancer.* Anticancer Res, 2005. **25**(2A): p. 731-4.

181. Dejmek, J., et al., *Wnt-5a protein expression in primary dukes B colon cancers identifies a subgroup of patients with good prognosis.* Cancer Res, 2005. **65**(20): p. 9142-6.

182. Da Forno, P.D., et al., *WNT5A expression increases during melanoma progression and correlates with outcome.* Clin Cancer Res, 2008. **14**(18): p. 5825-32.

183. Deng, G., et al., *WNT5A expression is regulated by the status of its promoter methylation in leukaemia and can inhibit leukemic cell malignant proliferation.* Oncol Rep, 2011. **25**(2): p. 367-76.

184. Frisch, B.J., et al., *Functional inhibition of osteoblastic cells in an in vivo mouse model of myeloid leukemia.* Blood, 2012. **119**(2): p. 540-50.

185. Deininger, M.W., J.M. Goldman, and J.V. Melo, *The molecular biology of chronic myeloid leukemia.* Blood, 2000. **96**(10): p. 3343-56.

186. Goldman, J.M., et al., *Bone marrow transplantation for chronic myelogenous leukemia in chronic phase. Increased risk for relapse associated with T-cell depletion.* Ann Intern Med, 1988. **108**(6): p. 806-14.

187. de Klein, A., et al., *A cellular oncogene is translocated to the Philadelphia chromosome in chronic myelocytic leukaemia.* Nature, 1982. **300**(5894): p. 765-7.

188. Ravandi, F., et al., *Chronic myelogenous leukaemia with p185(BCR/ABL) expression: characteristics and clinical significance.* Br J Haematol, 1999. **107**(3): p. 581-6.

189. Chan, L.C., et al., *A novel abl protein expressed in Philadelphia chromosome positive acute lymphoblastic leukaemia.* Nature, 1987. **325**(6105): p. 635-7.

190. Clark, S.S., et al., *Unique forms of the abl tyrosine kinase distinguish Ph1-positive CML from Ph1-positive ALL.* Science, 1987. **235**(4784): p. 85-8.

191. Kurzrock, R., et al., *A novel c-abl protein product in Philadelphia-positive acute lymphoblastic leukaemia.* Nature, 1987. **325**(6105): p. 631-5.

192. Hermans, A., et al., *Unique fusion of bcr and c-abl genes in Philadelphia chromosome positive acute lymphoblastic leukemia.* Cell, 1987. **51**(1): p. 33-40.

193. Kogan, S.C., et al., *Bethesda proposals for classification of nonlymphoid hematopoietic neoplasms in mice.* Blood, 2002. **100**(1): p. 238-45.

194. Mughal, T.I., et al., *Myelofibrosis-associated complications: pathogenesis, clinical manifestations, and effects on outcomes.* Int J Gen Med, 2014. **7**: p. 89-101.

195. Bowie, M.B., et al., *Steel factor responsiveness regulates the high self-renewal phenotype of fetal hematopoietic stem cells.* Blood, 2007. **109**(11): p. 5043-8.

196. Kim, I., T.L. Saunders, and S.J. Morrison, *Sox17 dependence distinguishes the transcriptional regulation of fetal from adult hematopoietic stem cells.* Cell, 2007. **130**(3): p. 470-83.

197. Tissir, F., et al., *Lack of cadherins Celsr2 and Celsr3 impairs ependymal ciliogenesis, leading to fatal hydrocephalus.* Nat Neurosci, 2010. **13**(6): p. 700-7.

198. Yang, L., et al., *Rho GTPase Cdc42 coordinates hematopoietic stem cell quiescence and niche interaction in the bone marrow.* Proc Natl Acad Sci U S A, 2007. **104**(12): p. 5091-6.

199. Kortenjann, M., et al., *Abnormal bone marrow stroma in mice deficient for nemo-like kinase, Nlk.* Eur J Immunol, 2001. **31**(12): p. 3580-7.

200. Aliprantis, A.O., et al., *NFATc1 in mice represses osteoprotegerin during osteoclastogenesis and dissociates systemic osteopenia from inflammation in cherubism.* J Clin Invest, 2008. **118**(11): p. 3775-89.

201. Kiyohashi, K., et al., *Wnt5a signaling mediates biliary differentiation of fetal hepatic stem/progenitor cells in mice.* Hepatology, 2013. **57**(6): p. 2502-13.

202. Malhotra, S., et al., *Contrasting responses of lymphoid progenitors to canonical and noncanonical Wnt signals.* J Immunol, 2008. **181**(6): p. 3955-64.

203. Murdoch, B., et al., *Wnt-5A augments repopulating capacity and primitive hematopoietic development of human blood stem cells in vivo.* Proc Natl Acad Sci U S A, 2003. **100**(6): p. 3422-7.

204. Challen, G.A., et al., *Mouse hematopoietic stem cell identification and analysis.* Cytometry A, 2009. **75**(1): p. 14-24.

205. Thompson, B.J., et al., *Control of hematopoietic stem cell quiescence by the E3 ubiquitin ligase Fbw7.* J Exp Med, 2008. **205**(6): p. 1395-408.

206. Miao, C.G., et al., *Wnt signaling in liver fibrosis: progress, challenges and potential directions.* Biochimie, 2013. **95**(12): p. 2326-35.

207. Zhang, D.E., et al., *Absence of granulocyte colony-stimulating factor signaling and neutrophil development in CCAAT enhancer binding protein alpha-deficient mice.* Proc Natl Acad Sci U S A, 1997. **94**(2): p. 569-74.

208. Choi, Y.H., et al., *Calmodulin-dependent kinase II regulates osteoblast differentiation through regulation of Osterix.* Biochem Biophys Res Commun, 2013. **432**(2): p. 248-55.

209. Congdon, K.L., et al., *Activation of Wnt signaling in hematopoietic regeneration.* Stem Cells, 2008. **26**(5): p. 1202-10.

210. Scheller, M., et al., *Hematopoietic stem cell and multilineage defects generated by constitutive beta-catenin activation.* Nat Immunol, 2006. **7**(10): p. 1037-47.

211. Kirstetter, P., et al., *Activation of the canonical Wnt pathway leads to loss of hematopoietic stem cell repopulation and multilineage differentiation block.* Nat Immunol, 2006. **7**(10): p. 1048-56.

212. Witze, E.S., et al., *Wnt5a control of cell polarity and directional movement by polarized redistribution of adhesion receptors.* Science, 2008. **320**(5874): p. 365-9.

213. Wang, Y., et al., *IQGAP1 activates Tcf signal independent of Rac1 and Cdc42 in injury and repair of bronchial epithelial cells.* Exp Mol Pathol, 2008. **85**(2): p. 122-8.

214. Janzen, V., et al., *Stem-cell ageing modified by the cyclin-dependent kinase inhibitor p16INK4a.* Nature, 2006. **443**(7110): p. 421-6.

215. Liang, Y., G. Van Zant, and S.J. Szilvassy, *Effects of aging on the homing and engraftment of murine hematopoietic stem and progenitor cells.* Blood, 2005. **106**(4): p. 1479-87.

216. Sonomoto, K., et al., *Interleukin-1beta induces differentiation of human mesenchymal stem cells into osteoblasts via the Wnt-5a/receptor tyrosine kinase-like orphan receptor 2 pathway.* Arthritis Rheum, 2012. **64**(10): p. 3355-63.

217. Visnjic, D., et al., *Hematopoiesis is severely altered in mice with an induced osteoblast deficiency.* Blood, 2004. **103**(9): p. 3258-64.

218. Nilsson, S.K., et al., *Osteopontin, a key component of the hematopoietic stem cell niche and regulator of primitive hematopoietic progenitor cells.* Blood, 2005. **106**(4): p. 1232-9.

219. Stier, S., et al., *Osteopontin is a hematopoietic stem cell niche component that negatively regulates stem cell pool size.* J Exp Med, 2005. **201**(11): p. 1781-91.

220. Anastas, J.N. and R.T. Moon, *WNT signalling pathways as therapeutic targets in cancer.* Nat Rev Cancer, 2013. **13**(1): p. 11-26.

221. Bitler, B.G., et al., *Wnt5a suppresses epithelial ovarian cancer by promoting cellular senescence.* Cancer Res, 2011. **71**(19): p. 6184-94.

222. Kremenevskaja, N., et al., *Wnt-5a has tumor suppressor activity in thyroid carcinoma.* Oncogene, 2005. **24**(13): p. 2144-54.

223. Chang, Y.C., et al., *p210(Bcr-Abl) desensitizes Cdc42 GTPase signaling for SDF-1alpha-directed migration in chronic myeloid leukemia cells.* Oncogene, 2009. **28**(46): p. 4105-15.

224. Mian, A.A., et al., *p185(BCR/ABL) has a lower sensitivity than p210(BCR/ABL) to the allosteric inhibitor GNF-2 in Philadelphia chromosome-positive acute lymphatic leukemia.* Haematologica, 2012. **97**(2): p. 251-7.

225. Zhang, S.J., et al., *Gain-of-function mutation of GATA-2 in acute myeloid transformation of chronic myeloid leukemia.* Proc Natl Acad Sci U S A, 2008. **105**(6): p. 2076-81.

226. Huang, Y., et al., *Discovery of somatic mutations in the progression of chronic myeloid leukemia by whole-exome sequencing.* Genet Mol Res, 2014. **13**(1): p. 945-53.

227. Goldman, J.M., et al., *Chronic myeloproliferative diseases with and without the Ph chromosome: some unresolved issues.* Leukemia, 2009. **23**(10): p. 1708-15.

228. Nishimura, K., et al., *Mesenchymal stem cells provide an advantageous tumor microenvironment for the restoration of cancer stem cells.* Pathobiology, 2012. **79**(6): p. 290-306.